University of Salford MANCHESTER

Analysis on Actuator Dynamics in Active Wheelset Control

Lushan Weerasooriya

School of Computing, Science & Engineering

University of Salford

Salford, UK

Submitted in Partial Fulfilment of the Requirement of the Degree of Doctor of Philosophy

2019

LIST OF CONTENTS

LIST OF FIGURES

Chapter 1: INTRODUCTION

CHAPTER 3: MODELLING OF RAILWAY VEHICLE DYNAMIC SYSTEMS

CHAPTER 4: ACTIVE CONTROL STRATEGY

CHAPTER 5: ACTUATOR DYNAMICS AND OPTIMISATION

CHAPTER 6: SENSING WITH STATE OBSERVERS

CHAPTER 7: OVERALL SYSTEM EVALUATION

LIST OF TABLES

CHAPTER 4: ACTIVE CONTROL STRATEGY

CHAPTER 5: ACTUATOR DYNAMICS AND OPTIMISATION

CHAPTER 6: SENSING WITH STATE OBSERVERS

CHAPTER 7: OVERALL SYSTEM EVALUATION

LIST OF ABBREVIATIONS

Variable	Single Wheelset Model	Two Axle Vehicle Model		
		Front Wheelset	Rear Wheelset	Vehicle Body
Wheelset Linear (Forward) Speed	V_s	–	–	–
Angular Wheel Speed	ω	–	–	–
Left/Right Wheel Radius	$r_L,\ r_R$	–	–	–
Left/Right Conicity	λ_L, λ_R	–	–	–
Longitudinal Speeds from Linear (Forward) Motion of Left/Right wheels	V_{L_Lon}, V_{R_Lon}	–	–	–
Longitudinal Speeds from Angular (Yaw) Motion of Left/Right wheels	V_{L_Yaw}, V_{R_Yaw}	–	–	–
Effective Forward Speeds of Left/Right wheels	V_L, V_R	–	–	–
Lateral Speeds from Linear (Forward) Motion of Left/Right wheels	V_{L_Lat}, V_{R_Lat}	–	–	–
Spin Speeds from Angular (Yaw) Motion of Left/Right wheels	$\Omega_{L\_Spin}, \Omega_{R\_Spin}$	–	–	–
Longitudinal Creepage of Left/Right wheels	$\gamma_{L\_Lon}, \gamma_{R\_Lon}$	–	–	–
Lateral Creepage of Left/Right wheels	$\gamma_{L\_Lat}, \gamma_{R\_Lat}$	–	–	–

Longitudinal Creepage Coefficients of Left/Right wheels	f_{L_Lon}, f_{R_Lon}	–	–	–
Lateral Creepage Coefficients of Left/Right wheels	f_{L_Lat}, f_{R_Lat}	–	–	–
Spin Creepage Coefficients of Left/Right wheels	$f_{L_{Lat}-Spin}, f_{R_{Lat}-Spin}$	–	–	–
Lateral Creep Forces	T_{L_Lat}, T_{R_Lat}	$T_{L\_f\_Lat}, T_{R\_f\_Lat}$	$T_{L\_r\_Lat}, T_{R\_r\_Lat}$	–
Longitudinal Creep Forces	T_{L_Lon}, T_{R_Lon}	$T_{L\_f\_Lon}, T_{R\_f\_Lon}$	$T_{L\_r\_Lon}, T_{R\_r\_Lon}$	–
Lateral Suspension Forces	–	$F_{B\_f\_Lat}$	$F_{B\_r\_Lat}$	–
Half Length of the Wheelset	L_g	–	–	–
Half Length of the Vehicle	–	–	–	L_v
Gravitational Force	F_M	–	–	–
Centrifugal Force	F_C	–	–	–
Control Effort	τ	τ_{f_Yaw}	τ_{r_Yaw}	–
Yaw	ψ_w	ψ_{fw}	ψ_{rw}	ψ_v
Mass	m_w	m_w	m_w	m_v
Inertia	I_w	I_w	I_w	I_v
Curvature	$\frac{1}{R}$	$\frac{1}{R_f}$	$\frac{1}{R_r}$	–
Double of Longitudinal Passive Stiffness	k	k	k	–
Double of Lateral Passive Stiffness	–	K_S	K_S	–
Double of Lateral Passive Damping	–	C_S	C_S	–

ACKNOWLEDGEMENTS

I would like to acknowledge (with sincere appreciation and gratitude) the academic guidance, understanding and continuous encouragement provided by my supervisor, Professor T X Mei, throughout this study. His patience and inspirational guidance were extremely valuable on the successful completion of this research.

I would also like to specially thank University of Salford, UK for being the immensely propitious platform it is, such that philomathic/epistemophiliac students gets the opportunity to interact each other and to broaden their knowledge with the assistance/guidance of academic legends.

In addition, I would like to forward my deep sense of gratitude towards my family and friends for all their support and encouragement throughout this PhD study.

ABSTRACT

This thesis presents details of an investigation conducted to evaluate the applicability and requirements of actuators in the implementation of active solid–axle wheelset control systems, for primary suspensions of the railway vehicles, and the effects of actuator dynamics on the overall active control system. The research is focused on the use of electric–mechanical (EM) actuators and it addresses on two main aspects when designing active control systems for this application.

One aspect is the detailed study on actuator dynamics and parameter optimisation to improve the effectiveness/efficiency of actuator performances while the second aspect is the development of a state observer to estimate key feedback signals, for the control of actuators, which are difficult to measure using readily available sensing techniques.

The study of the actuator dynamics and its optimisation is conducted by varying key factors of the electro–mechanical (EM) actuator used in this application such as gear ratio, inertial values of the motor rotor/gear–wheel and stiffness/damping at the actuator–wheelset (load) connection, while assessing key actuator performance indicators such as output torque and power consumption. This analysis provides insight in to the task of finding optimal actuator parameter values for this particular application of active wheelset control such that the effectiveness, efficiency and robustness of the overall active wheelset control system can be improved. In order to assess the developed system comprehensively, both a two–axle vehicle model and a full bogie vehicle model are being evaluated individually in the study.

In addition, a state observer is developed in this study to estimate the output torque of the electro–mechanical (EM) actuator since feedback measurements are essential for the actuator control system developed in this case in order to ensure that actuator responds appropriately by delivering accurate and fast control efforts to maintain the stability of wheelsets. The formulation and design of the observer is done based only on the use of the actuator model such that it substantially reduces the complexity and difficult uncertainties related to the full model of a rail vehicle. Furthermore, a robustness assessment of the state observer is undertaken by conducting an assessment of its performance when key parameters of the model used to develop the state observer is varied within reasonable margins.

The performance and robustness assessments of the state estimator integrated with the full active wheelset control system and with optimised actuator parameters are carried out with the use of both two–axle vehicle model and the full bogie vehicle model with different operational track features such as curved track and straight track with lateral irregularities with various travel speeds.

Chapter 1: INTRODUCTION

1.1. Background

Trains are one of the most commonly used mass transportation methods since the 19th century and continues to be so to this date. They have evolved from horse powered to steam engines and ultimately to present day technologies of electrical motors and sophisticated electro–mechanical (EM) systems to achieve higher speeds, increased riding comfort and lower wear and fatigue of equipment. Due to high usage and passenger's dependability on trains, there have been continuous developments on many aspects of the railway vehicles. With regards to the improvements in the suspension systems of railway vehicles, active control which replaces or supplements the passive springs and dampers with actuators, sensors and controllers, has become the trend of studies recently [1].

Research in the field of railway vehicle dynamics have indicated that actively controlled suspension systems have a distinct advantage of improving dynamic performance of railway vehicles such that enhancements in riding quality, dynamic stability and effective response to track features, such as curves, can be achieved. Thus, the use advanced active control techniques provide the opportunity to address difficult trade–offs often experienced with purely passive solutions in railway vehicle suspension systems [2]. Operationally these improvements in dynamic performance can result in improvements of overall railway industry to facilitate higher travel speeds, improved passenger comfortability and reduced maintenance costs.

These continuous developments over the years have paved the way to technologically move forward, as an overall industry, towards more advanced/sophisticated systems in all key aspects of railway vehicles such as suspension systems and propulsion systems since both have a significant impact on reliability, safety and comfortability of passengers [3].

When focusing mainly on the transition from passive suspension to active control, although passive suspension systems have served well for the rail industry, with the current technological developments, potential benefits which makes active control in suspension systems more attractive/superior and an effective alternative over classical passive suspension can be summarised as below:

1. **Improved Dynamic Performances** – Active solutions in the primary suspension are capable of averting the inherent problems of classical passive suspension such as hunting effect, curving performances and higher creep forces.

2. **Reduction of Vehicle Maintenance Costs** – Although significant capital costs can be expected when active solutions are to supplement/replace passive suspension components in existing train vehicles, these costs will be complemented by the savings from lower maintenance costs resulted by improved performances of the overall railway vehicle. In addition, some weight reduction can also be achieved by supplementing/replacing conventional spring/damper suspension with active components due to the simplification of the mechanical system.

3. **Improved Riding Comfort** – Active solutions applied in the secondary suspension of railway vehicles are capable of effectively improving passenger comfortability by reducing accelerations and high frequency vibrations (caused due to track irregularities) experienced by the vehicle [4].

4. **Improved Travel Speed** – Active solutions in the secondary suspension of railway vehicle have already proven to significantly improve the overall travel speed of the railway vehicles with the tilting trains [5] (currently operating in the industry) by maintaining high travel speeds during curving.

In addition, newly proposed active solutions have the advantage of being designed in order to be readily integrated with current infrastructure of vehicle designs and track conditions such that pre–requirements will be less demanding when the transitioning from passive suspension to active control.

When discussing the broader field of railway vehicle suspension systems, it is essential to identify and distinguish the major mechanical components associated with the suspension systems of a conventional railway vehicle in order to address different sub–sections of the overall train suspension configuration and to familiarise with the terminology related with it.

1.2. Structure of Conventional Railway Vehicles

Conventional railway vehicles have several major mechanical components as shown in Figure 1.1. This suspension arrangement interconnects with seven main masses – the vehicle body, two bogies and four wheelsets. This complex vehicle system has been a result of continuous evolution of railway vehicles over the last two centuries [6].

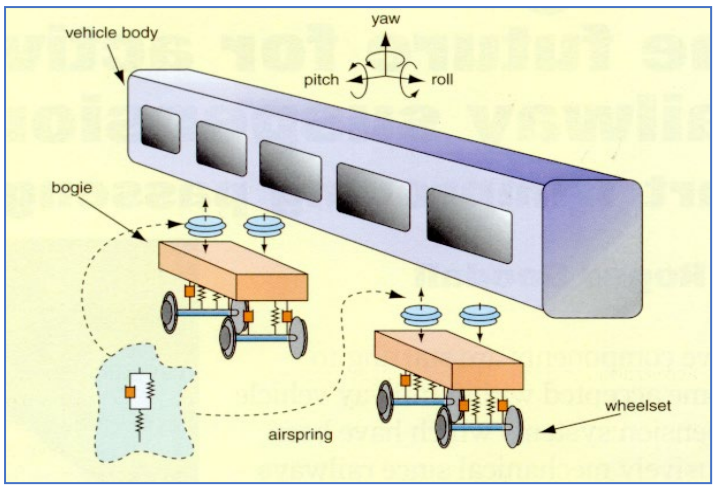

Figure 1. 1 – Railway Vehicle Structure [7]

As it can be seen in Figure 1.1, there are two bogies supporting the vehicle body and two wheelsets supporting each bogie. Each key body/mass in this system has six degrees of freedom in roll, pitch, yaw, longitudinal, vertical and lateral directions. However, some of the degree of freedoms are dynamically coupled (e.g.: lateral movement of a wheelset affects roll movement of the same wheelset) due to the nature of how these masses are connected while some degrees of freedom are constrained by track.

In a conventional train vehicle, there are suspension elements between each body to address all independent and coupled degrees of freedom. In practice, overall suspension system of the vehicle is categorised into subsections with the bogie as a reference. Firstly, the suspension system between the bogie and the vehicle body (effective for all linear and angular directions) is called the secondary suspension system and the purpose of this is mainly to improve the riding comfort by absorbing high frequency vibrations caused by track irregularities. In modern passenger railway vehicles, air–spring suspension is used in secondary suspension between the vehicle and bogies which ensure that the passengers can experience an improved riding quality.

Secondly, the suspension between the wheelset and the bogie/body is called the primary suspension system. Primary suspension is imperative to the stability of the moving railway vehicle since unconstrained conventional wheelsets are inherently unstable in the dynamic mode [2]. Therefore, it is necessary to have longitudinal and lateral constraints (usually passive stiffness/springs) to ensure the dynamic instability of wheelsets occurs at a speed higher than the vehicle's maximum design speed [7]. When focussing on a vehicle travelling on a curved (deterministic) track, these passive suspension components are affected by centrifugal forces and lateral/longitudinal creep forces acting on them. Conventional primary suspension mainly deals with low frequency movements of the wheelsets to keep the railway vehicle stabilised and passive springs and dampers are used between the bogie/vehicle and wheelset for this purpose. However, selection of these passive components is a trade–off between

curving performances and the oscillatory motion in the wheelsets called the hunting problem where high stiffness of the springs have a detrimental effect on the curving performances and lowering the stiffness causes increased oscillatory motions.

Hunting effect is the swaying motion of rail vehicle caused by the forward speed of the vehicle and by wheel–rail interactive forces due to wheel–rail contact geometry and creep characteristics [8]. Since both the lateral movement and the yaw movement in the wheelsets are coupled, these undesirable oscillations affect both dynamic modes.

When focusing on the other railway vehicle configurations, in contrary to the conventional train vehicles, the two–axle vehicle have only three key masses, namely the vehicle body and two wheelsets. Thus, a two–axle vehicle has the inherent advantage of a simpler design and lower weight compared to the full bogie vehicle since it does not have bogie units. Hence, while the full bogie vehicle has both the primary and secondary suspension systems, two–axle vehicle only has primary suspension.

However, this arrangement has poor curving performances compared to the conventional full bogie vehicle since there is more distance between the front and rear wheelsets. In addition, another disadvantage of two–axle vehicle arrangement is that they are also more susceptible to high frequency vibrations since they only have one layer of suspension to isolate the high frequency vibrations. Thus, two–axle vehicles are not the optimal choice for passenger transportation as they have low riding comfortability.

Furthermore, when focusing on wheelsets of a railway vehicle, there are two basic configurations, which have distinct characteristics, utilised in the industry.

Solid–Axle Wheelsets (SW):

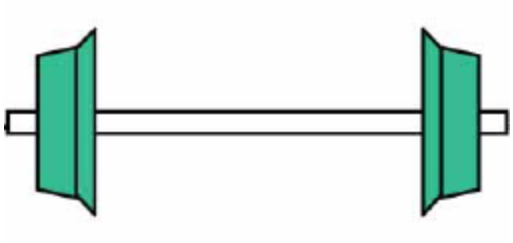

Figure 1. 2 – Solid–Axle Wheelset [22]

In this configuration (Figure 1.2), wheels are connected to each other with a solid–axle. Thus, both wheels are constrained to have the same rotation frequency. Conventional solid–axle wheelsets have been successfully used in the industry for many years in both passenger and freight trains due to their inherent ability to negotiate curves without any external guidance support. However, when traveling on

curved tracks with high stiffness passive elements in lateral/ yaw primary suspension, the constraint of having the same rotational frequency in this configuration results in undesirable wear/fatigue of contact surfaces and noise.

Independently Rotating Wheelsets (IRW):

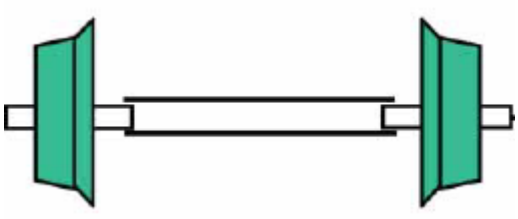

Figure 1. 3 – Independently Rotating Wheelset [22]

Contrary to the previous configuration, in this configuration two wheels on an axle are free to rotate independently as there is not a solid constraint between wheels (Figure 1.3).

Allowing the wheels to rotate independently reduces the effect of the dynamic instability and lowers longitudinal creep forces to almost zero [9]. This reduction of longitudinal creep force results in reduced control effort. However, since the natural curving is no longer present with the IRW arrangement, additional guidance is essential for the stability of the vehicle during curving.

1.3. Active Control in Primary Suspension

Although passive suspension strategy is the conventional method of control (which uses only springs and dampers) for primary lateral/yaw suspension of railway vehicles, studies focusing on full active control strategies are showing promising technological advancements which can particularly improve the curving performances of the wheelsets while the stability is not compromised [10].

When evaluating curving performances of a conventional wheelsets, this limitation with passive suspension can be clearly elaborated. An unconstrained solid–axle wheelset can travel on a curved track while adhering to the natural forces such as centrifugal forces acting on it due to the effect of coned/profiled wheels. Thus, when travelling on a curved track, wheelsets move outwards from the centre of the curve and since the wheels of a wheelsets are coned/profiled, rolling radius of the wheels in both inward and outward and wheel deflection change accordingly to have an equal rolling rate. However, since unconstrained wheelsets are unstable in the dynamic mode, generally passive suspension springs are added from the longitudinal and lateral direction. Specifications of these passive

components are selected in order to avert instabilities for the maximum design speed named as critical speed [7]. Adverse effect of the passive suspension components is that they restrict the wheelsets from having natural curving movements and result in higher creep forces. Therefore, selecting passive components for longitudinal and lateral suspension is a trade–off between better curving performances and stability [11].

However, active suspension solutions can be used to address this design issue. Main difference between the passive suspension and active control configuration can be elaborated shown in the Figure 1.4 which depicts how passive suspension components in longitudinal direction can be replaced with actuators in active control configuration.

- Passive Suspension – Only springs and dampers are used with constant stiffness values (Figure 1.4. (a))

- Actively Controlled Suspension (Active Control) – Controller operating an actuator to control the wheelsets which can emulate different stiffness/damping values accordingly (Figure 1.4. (b))

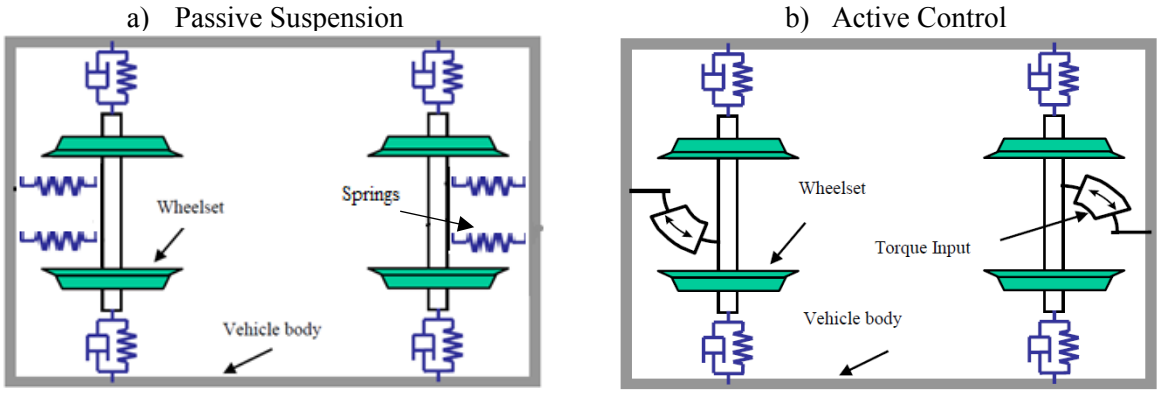

Figure 1. 4 – Passive Suspension Vs Active Control

When compared between dynamic performances of wheelsets with passive suspension and actively controlled suspension, active control in primary suspension has proven to provide enhanced dynamic performance for wheelsets [12]. Thus, in theory, full active control strategies can be applied to any or all of the degrees of freedom, but in practice, it is restricted due to practicalities.

Due to the promising nature of active control, continuous development has taken place suggesting various active control configurations for the two wheelset configurations of solid–axle and

independently rotating wheelsets over the years. Below are two of (from a total of five) the main active configurations proposed to implement active control for wheelset stability/curving.

Actuated Solid–Axle Wheelsets (ASW)

In the case of active control in solid–axle wheelsets, it is called Actuated Solid–Axle Wheelsets (ASW) and the basic concept is to apply actuators instead of passive components for stability. Actuators can be fixed in either of the arrangements shown in Figure 1.5 and Figure 1.6 where the actuation is applied in lateral direction, longitudinal (which essentially results effecting yaw direction) direction respectively, while feedback is given to the controllers to generate an accurate and rapid actuation.

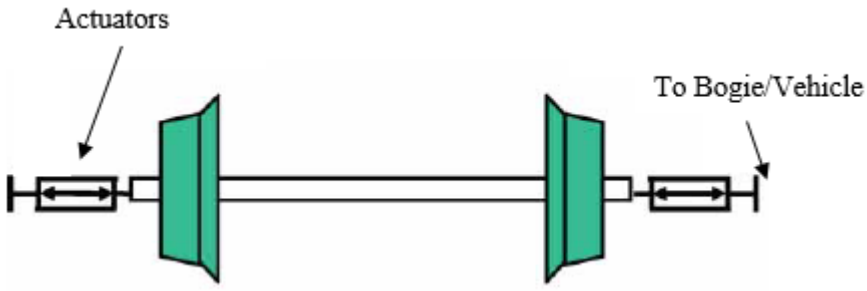

Figure 1. 5 – Lateral Force Actuator in ASW [22]

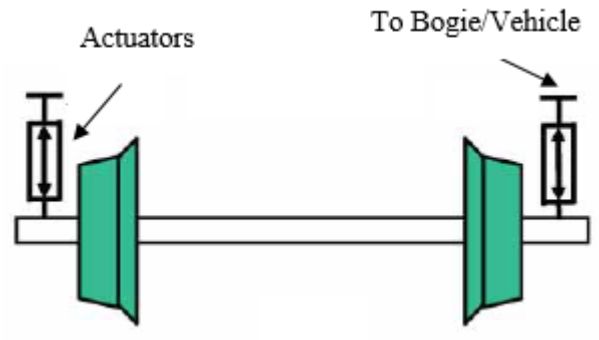

Figure 1. 6 – Toque Actuator in ASW [22]

The actuator location has a significant impact on the effectiveness of the overall active control. A comparison of both configurations has indicated that, while it is possible to stabilise the wheelsets as well as developing active steering schemes with actuators either in the yaw or in the lateral directions, the latter arrangement worsens the ride quality [2]. This is because the wheelset controlling force directly applied to the vehicle body in the lateral direction which has an adverse effect on the body/vehicle dynamic modes.

Actuated Independently Rotating Wheelsets (AIRW)

As mentioned before, external guidance is essential for the IRW configuration and there are several well–known configurations of applying the control effort for the IRW configuration. As one of the main active configurations for IRWs, Actuated Independently Rotating Wheelsets (AIRW) configuration is designed to provide the active guidance to the wheelsets by applying a control effort to the common axle as well as for the wheels themselves [13].

However, the main challenge with all active configuration for IRW is obtaining feedback for the control schemes. In AIRW, where the control effort is supplied to the wheelsets in either lateral, yaw or longitudinal directions, wheel–rail deflection is the optimum feedback which can be used to provide the necessary guidance action in order for the wheelset to follow the track. However, with this configuration, obtaining accurate feedback of wheel–rail deflections with practical sensors pose difficulties. In addition to the guidance, for stabilisation and performance optimisation, other measurements such as yaw angle may also be required. Studies have also assessed the feasibility of using relative rotational speed of the wheels in the same axle for a simplified feedback control to directly steer the wheelsets and using traction motors to address this challenge [14].

On the other hand, although model–based solutions can be proposed to estimate the feedback, it can introduce more difficulties since the control structure can be much more complex with high orders and it can be extremely challenging to make the state estimators to work effectively against parameter variations.

1.4. Active Control for Secondary Suspension

As mentioned before, secondary suspension is mainly used for improving the riding comfortability in passenger railway vehicles. In the competitive market of the passenger transportation it is highly favourable for the railway vehicles to have higher riding comforts and travel speeds. However, higher travel speeds can result in vehicle experiencing increased accelerations and vibrations which detrimentally effects the riding comfort and with conventional passive suspension, it is difficult to improve comfortability factor against a broad spectrum of vibration frequencies and accelerations.

Active control in the secondary suspension has the potential to address the trade–off between travel speed and riding comfortability even when track conditions are unfavourable [15].

One of the major commercial success of active control technology in secondary suspension for the rolling motion is the tilting train [16]. In this arrangement vehicle body is tilted by active means

such that the car body rolls inwards when travelling in curved tracks to reduce the centrifugal force/ lateral acceleration experienced by the passengers. This averts the necessity to reduce the travel speed on curves which subsequently allows the vehicle to travel on curves at enhanced speed while maintaining riding comfort [17].

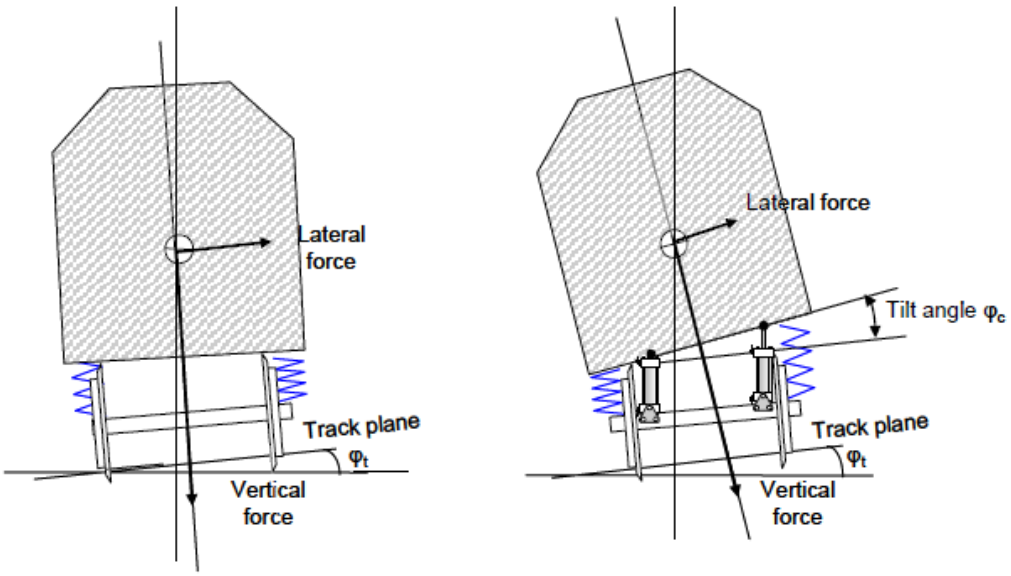

Figure 1. 7 – Tilting Trains [15]

In addition to the undesirable accelerations, active control can be used to reduce/eliminate vibrations experienced by the vehicle by providing active control effort from lateral directions [18] and well as vertical directions [19].

1.5. Actuator Technologies in Active Control of Railway Vehicles

Actuators are an important aspect of the any active control system since ultimately, they are responsible of effectively executing the control efforts as demanded by the control schemes and accuracy/efficiency of the actuators can significant affect the effectiveness of the overall control system. There are several types of actuators currently being used in railway applications while the choice of actuator is dependent on the trade–off between actuator performance (power, efficiency, bandwidth, etc.), size, and maintenance cost considerations [20].

Common actuator technologies in active control of railway vehicles are [21]:

Servo–hydraulic Actuators – These have the advantage of being able to generate higher forces from relatively low sized actuators. However, due to the inefficiencies associated with servo–valves, it is highly power consuming. In addition, another disadvantage of these actuators is that in the cases (which frequently occurs with wheelsets) where it needs to maintain lower force levels in the presence of high frequency movements, to achieve this, the lubricant/oil in the actuator needs to be inserted to and extracted at these high frequencies and this scenario cause reduction in the efficiency of the actuator.

Electro–mechanical Actuators – Common use of these actuators in active control is when the electric motor is to drive leadscrew/ball nut mechanisms to apply linear force to the load as well as directly coupled with gear boxes to apply torque. Although these are less compact when comparing with servo–hydraulic actuators, EM actuators can be operated to have high efficiency with the use of "Pulse Width Modulated" (PWM) control of the motor averting the power losses associated with a servo–valve. With high frequency movements, these actuators require the armature of the motor to accelerate rapidly. Although this does not significantly affect power consumption, motor rating is affected. However, once the controllers for these actuators are well designed, higher performance levels can be archived even with high frequency movements.

Servo–pneumatic Actuators – Although complexities associated with air compression is constraining these actuators achieve high performance levels at higher operating frequencies, pneumatic systems are widely used on railway vehicles in the cases of self–levelling air springs. Since the production of compressed air and maintenance of pressure levels are themselves inefficient processes, excessive power consumption of these actuators is a disadvantage.

Electro–magnetic Actuators – Since most of the control efforts in active control of railway vehicles demand relatively minor movements, a direct use of electro–magnetic forces is a possibility. Similar to control of electro–mechanical actuators, these can be efficiently controlled using PWM amplifiers. However, lack of compactness is a major disadvantage.

1.6. Research Overview

The study presented in this thesis is concerned with active control of solid–axle wheelsets in primary suspension in railway vehicles and has focused more on actuator dynamics in an active wheelset control system.

Multiple previous studies [22] have indicated, although active control technology is more scientifically/technically challenging to implement, it has the potential to be more efficient and effective than classical passive suspension. Furthermore, full active control configurations/schemes have also suggested solutions for the fundamental design conflicts between the vehicle stability and curving performance of passive suspension designs. Flexibility inherited in active control designs enable active solutions to provide significant reductions of wheel and rail wear, fatigue and noise when travelling on curved tracks as well as straight tracks with lateral irregularities.

Although active control has been studied for rail vehicle applications for its potential, most studies have concentrated on developing control configurations and its strategies for active control while less focus has been given on the actuator technologies [23].

Thus, this study is conducted focusing on actuator dynamics for active control in railway vehicle primary suspensions. During the study, electro–mechanical actuators are being evaluated against active control requirements while actuator optimisation is also carried out to improve performances. Furthermore, a model–based sensing technique is developed in the study to estimate feedback measurements for the actuator controller in order to avert practical challenges of accurately measuring actuator output force/torque. This thesis is written to contain eight chapters which individually address and elaborate different aspects of the research.

1.6.1. Definition of Problem

As elaborated before, with passive suspension there is a trade–off between curving performances and instability of solid–axle wheelsets. When passive springs with high stiffness values are used for better stability of the wheelsets, it restricts natural movements of the wheelsets and results in significant amount of creep forces acting on the contacts surfaces of rail and the wheel profiles. Hence, passive suspension method results in wear and fatigue of both the wheels and track due to high creep forces.

This inherent design trade–off between stability and curving performances causes significant amount of revenue to be allocated between replacing the worn components such as wheelsets and track sections and replacing components which are detrimentally affected by the hunting effect (instability).

Figure 1.8 and Figure 1.9 depict the extent of wear and fatigue that could occur on contact surfaces due to creep forces.

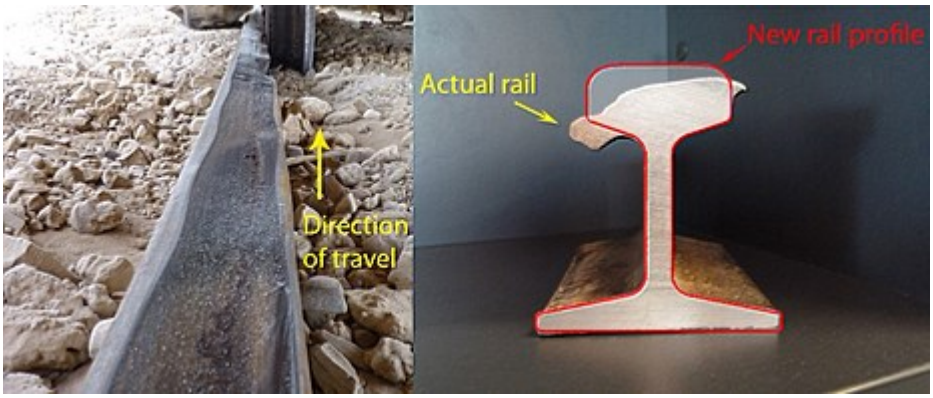

Figure 1. 8 – Wear and Fatigue of the Rail Surface

Figure 1. 9 – Wear and Fatigue of the Wheel Profile

In order to overcome these issues with the use of active control, there are a number of active control strategies proposed by experts and academics in the field over the years. Those studies have proposed both classical and model–based control strategies for both SW as well for IRW configurations which can address the trade–off issue between the curving performances and the stability of the wheelsets. Wheelset stabilisation through active control is a high bandwidth operation. Thus, actuators used for this application demands to be designed to have fast responses. However, there have not been many studies focusing on the actuator design and optimisation which can be used to realise the active control strategies in the most effective manner.

This is an important aspect of the active control system since properly designed and optimised actuators are capable producing accurate and rapid responses as demanded by the control strategy.

1.6.2. Aim of the Research

This study aims to evaluate and optimise an EM actuator for active control of railway vehicles. During the study, actuator dynamics and its behaviour with active control configurations are assessed to improve the actuator performances for the task of active wheelset control by optimising the key parameters of the actuator. This optimisation process has a significant importance to the whole active control system since when it comes to realistically implementing active control methods, a key aspect to consider is, whether the actuators are capable of generating required rapid forces or torques to stabilise and improve dynamic behaviours of the wheelsets as per demand of the control configuration. Hence, aspects such as power consumptions and response times have significant prominence when selecting actuators when implementing active wheelset control systems. Thus, the study aims to evaluate actuator systems to further optimise its performances.

In addition, when focusing on obtaining feedback of actuator output force/torque, it is essential to the actuator controller that it receives accurate measurements of the control effort provided by the actuator to the wheelsets. However, in reality, obtaining accurate actuator feedback can be extremely difficult due to harsh operating environments of railway vehicles. To address this issue, this study aims to develop a model–based control structure which can be used to operate an electro–mechanical actuator in active wheelset control based on estimated feedback measurements.

1.6.3. Objectives and Research Contributions

Objectives associated with this particular research are leading to ultimately study the actuator dynamics and its effect on the overall control system when an active wheelset control configuration (as an alternative to passive suspension with springs/dampers) is used as a means to stabilise wheelsets and reduce creep forces which will result in reduced wear and fatigue of contact surfaces when curving. These objectives can be elaborated as:

a) Conduct a background study on deriving the plan view dynamic models for a two–axle vehicle model and that for a conventional full bogie vehicle model which provides insight into lateral and yaw movements of the vehicle.

b) Implement an active wheelset control configuration in both the two–axle vehicle and the full bogie vehicle models while including electro mechanical actuator models and actuator controllers in the vehicle models.

c) Carry out a comprehensive study on the optimisation of the actuator parameters by critically analysing performances.

d) Develop a state observer as a sensing method to obtain accurate torque (applied to the wheelset) feedback.

Thus essentially the research contribution of the particular study is the evaluation of an EM actuator dynamics and actuator parameter optimisation for active wheelset control and the design of a model–based sensing technique for the actuator controller.

1.6.4. Research Methodology

As academic research, this study is conducted using the simulation tool MATLAB Simulink and dynamic models of both two–axle vehicle model and bogie vehicle model since it enables to avert the practical difficulties and investigate dynamics of the vehicle thoroughly. Several types of track data (curved and straight tracks with lateral irregularities) are used in the study to evaluate the vehicle dynamics and control configurations on both deterministic and stochastic conditions. Furthermore, analysis of the train models, control systems and actuator model are simulated under other various conditions (travel speed, parameter changes and etc.) to evaluate the dynamic behaviour and robustness of all systems. Next a state observer model for the control of actuators is incorporated for sensing purposes (with actuator controller) and its performances / robustness is assessed before a full evaluation of the overall system with both vehicle models and different track conditions.

Each of these stages are discussed in the thesis in a chronological order and steps followed in the study are depicted in Figure 1.10 as a brief sequential order in the flowchart below,

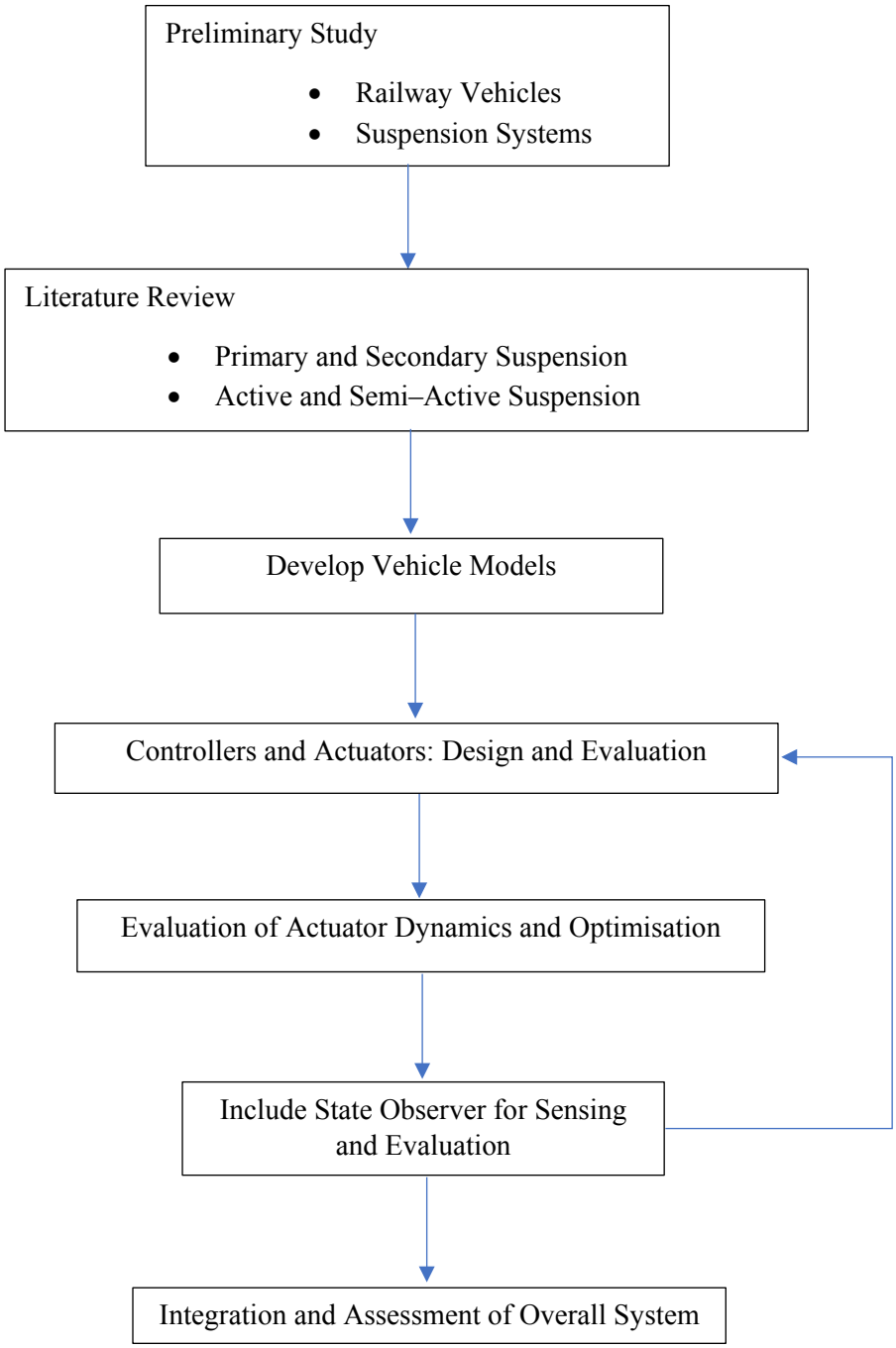

Figure 1. 10 – Flowchart of the Study

As it can be seen in Figure 1.10, at the start of the study railway vehicle suspension systems and active control solutions proposed for them is studied by conducting literature review on the field so that fundamentals can be understood. Furthermore, literature reviews also enables to identify the previous work and their limitations in order to identify aspects that can potentially be improved.

Once the background of the railway vehicle suspension systems and previous research has been studied, both two–axle vehicle and conventional full bogie vehicle models are implemented in the MATLAB Simulink platform using their dynamic equations in plan–view. An assessment of the model accuracies are conducted by comparing the results vehicle dynamics (with passive suspension) against previously published academic materials and fundamentals of railway vehicle dynamics before the implementation of actively controlled suspension systems in order to thoroughly distinguish its effects on the vehicle dynamics.

Sequentially, the assessment of dynamics is continuously done after implementing the actively controlled suspension systems and optimisation of the actuators used for this task. Optimisation of the actuator performances is done such that its energy dissipation is minimised in this application. For this task focus is given to evaluate the actuator performances when primary actuator parameters such as, gear ratio, inertial values, etc. are varied in a systematic order.

Furthermore, the investigation is extended to evaluate the performances of the both the vehicles and actuators when a model–based sensing technique is implemented to avert the practical issues related to sensing feedback measurements for the control systems and the robustness of this method is also assessed. In addition, a robustness assessment is also carried out to investigate the accuracy of the estimates and operational limits when key parameters varied since the erroneous estimation can cause significantly detrimental effects on the overall performances.

Finally an overall assessment of the overall active control system (with state observer feedback) and both the two–axle and full bogie vehicle dynamics against different track conditions are done to evaluate the performances of the systems developed in this study. This analysis is done to assess and evaluate both vehicle and actuator performances improvements which the study attempted to address at the beginning of the research.

1.7. Thesis Layout

Brief overview of the individual chapters in the thesis are as below:

Chapter 1: INTRODUCTION

This chapter discusses about the overall background of the railway vehicles, train suspension systems while elaborating primary suspension systems, secondary suspension systems individually and different control configurations of wheelset mechanisms, such as solid–axle wheelset and independently rotating wheelset. In addition, this chapter contains details of the research and the thesis layout.

Chapter 2: LITERATURE REVIEW

A thorough discussion about the previously published literature focusing on this subject is covered in this chapter. Furthermore, details of newly proposed contributions to improve vehicle dynamics, use of actuators in active control and use model–based approaches for sensing are also discussed in the chapter.

Chapter 3: BACKGROUND OF MODELLING RAILWAY VEHICLE DYNAMIC SYSTEMS

This chapter contains a brief background of the derivation of a conventional solid–axle wheelset dynamics of order extend that to vehicle models, such as two–axle wheelset model and conventional bogie vehicle, used in this research. Details regarding the assessment of vehicle models for accuracy, (by evaluating the dynamic behaviour against different track conditions) is also presented in this chapter.

Chapter 4: ACTIVE CONTROL STRATEGY

Design of both wheelset controller and actuator controller are discussed in this chapter and their effect on the dynamic behaviour of both two–axle vehicle and conventional bogie vehicle are analysed while comparing with the dynamic behaviour of same vehicles/track conditions with passive suspension.

Chapter 5: ACTUATOR DYNAMICS AND OPTIMISATION

This chapter contains details about the optimisation process of the actuator using the actuator dynamics to identify suitable values for key actuator parameters and assessing the robustness of each of those key parameters.

Chapter 6: SENSING WITH STATE OBSERVERS

This chapter is fully focused on discussing the use of state observers in this application for sensing and details from the concept, derivation to assessment are presented in the chapter while a robustness analysis is also conducted.

Chapter 7: OVERALL SYSTEM EVALUATION

This chapter presents the results of the fully integrated overall system and the behaviour of both two–axle vehicle and the full bogie vehicle when full active wheelset control systems with model–based sensing technique is used to actively stabilise wheelsets.

Chapter 8: CONCLUSIONS AND FURTHER WORK

This chapter concludes this thesis while discussing the prospects and remaining challenges of the full active wheelset control in general and gives potential directions for further research in this area.

CHAPTER 2: LITERATURE REVIEW

2.1. Introduction

The focus of this research is active primary suspension on railway vehicles, with the intention to analyse the dynamic behaviour of actuators in an active control configuration to stabilise (countering the hunting effect) the wheelsets without interfering with the natural curving of curved/deterministic tracks.

Hence, in the literature review, an extensive survey on previous studies is conducted in the field of stability control and curving of wheelsets with active primary suspension (lateral, yaw or longitudinal directions) in order to identify the various control configurations and strategies proposed by the researchers, while active secondary suspension is also briefly covered.

In addition, this particular research also investigates the use of state observers to generate feedback for the effective control of actuators and relevant studies of state observes and model–based sensing techniques for similar applications are also reviewed in this chapter.

When referring to previous studies done on the field of active wheelset control (stability and curving), a certain flow of research interests (phases) over time (last 20 years) can be readily noticed. It can be observed that at the start of research in to this particular field, main focus was on introducing and evaluating active wheelset configurations and subsequently focus is shifted to developing both classical and model-based control schemes to control the proposed active wheelset configurations [14, 53, and 57]. In addition, during last decade, adhering to the trend of continues development, more studies have been undertaken to develop and evaluate model-based sensing techniques [96] while some research have focused on evaluating fault tolerance techniques [60]. Therefore, although there haven't been many recent studies on earlier topics as introducing new configurations or new control strategies, there have been many studies on sub-topics as sensing, fault tolerance and actuator dynamics evaluation which will eventually support the main focus of active wheelset control.

2.2. Active Control Configurations for Stability and Curving:

As discussed in the previous chapter, a number of active control configurations [22] have been proposed to address the issues related to trade–offs between curving performance and stability of railway vehicles. Thus, in order to improve curving and to avert the classical hunting oscillation, the active control strategies discussed below have been introduced and assessed by researchers.

Since the scope of this research is focussed on full active control configurations directed only for primary suspension in the lateral, yaw and longitudinal directions with solid–axle wheelset configuration, greater attention has been given to the control strategies associated with those specific dynamic modes.

Active control configurations aimed at improving stability and curving performances of the railway vehicles can primarily be categorised as direct and indirect concepts since some concept suggests to apply the control effort directly to the wheelsets (primary suspension) while there is another indirect approach to do so by applying the control effort through the bogie (secondary suspension). An evaluation of all these configurations are done below while discussing their distinct characteristics.

Furthermore, when discussing active control for primary suspension in lateral and yaw directions, it is essential to identify the distinction between the terms as, steering/curving, guidance and stability control in the context of active wheelset control as there are control schemes developed for addressing these challenges individually or as a whole (depending on the respective wheelset configuration).

Steering/curving control in this case can be defined as the control of wheelset yaw angle/angle of attack, where actively external effort is applied to the wheelsets to achieve pure rolling line in order to minimise/eliminate undesirable contact forces when negotiating curves [24]. Although unconstrained solid–axle wheelsets are capable of achieving pure rolling without any external control effort, steering of the solid–axle wheelset on curves is required when the yaw stiffness in vehicle (passive) suspensions are severely interfering with natural curving.

Stability control on the other hand focuses on the stabilising of the inherently unstable wheelsets against hunting effect. This is essentially required for solid–axle wheelsets when passive yaw stiffnesses are completely replaced by active control configurations. It is also worth pointing out that it is desirable when active stability control for solid–axle is introduced, that active control efforts for stabilising the wheelsets does not interfere with natural curving abilities of the wheelsets.

Guidance control is mainly focused on independently rotating wheelsets, and it is essential to have an external control effort guiding the IRW wheelsets with both curved and straight tracks, since natural track following ability is missing in this case.

2.2.1. Concepts for Primary Suspension (Stability and Curving)

Active control for primary suspension where control effort is directly applied to the wheelsets can essentially be categorised based on wheelset configuration in terms of, concepts for conventional solid–axle wheelsets (SW) and independently rotating wheelsets (IRW) respectively [25].

Actuated Solid–axle Wheelset (ASW) – This is the active control configuration proposed for SW configurations where active control effort can be directly applied to the wheelset either in the lateral, yaw directions or in the longitudinal direction. The concept has been investigated in a study [26] where the authors have initially investigated the use of actively controlled traction rods on longitudinal to improve steering performance of SWs (with passive yaw stiffness) without compromising on stability. However further continuous research has led to the idea that both stabilisation and improved curving performance of SW wheelsets can be achieved through completely active means [2, 27].

Various studies have demonstrated with the use of two–axle vehicle model, that yaw or longitudinal actuation is preferable than lateral actuation since it requires a lower control effort to achieve the same degree of stability and curving performances. When considering the ASW concept for conventional full bogie vehicle architectures, studies [28] have shown that the yaw actuation method has the advantage of improving stability and curving performance for high–speed bogie vehicles over conventional passive suspension as well and the authors have also elaborated on the problems of sensing using readily available sensors due to the harsh operating conditions that railway vehicles are typically subject to and thus suggested the use of state estimators for a practical implementation. Another study [29] that investigated the on robustness of ASW configuration, for full bogie vehicles, focussed on the use of a yaw action method and using methodically delaying the actuation effort to assess the effects of actuator performance delays on both stability and curving performance. A full–scale realistic demonstration of ASW, where actuators have been used to provide active torque/force in the yaw/longitudinal direction, has been performed on a roller rig in Munich and provided excellent results in terms of increased vehicle stability [30].

In addition to the improvements of dynamic performances such as stability and curving performances, another study [31] has evaluated the use of ASW for the reduction of rolling contact fatigue (RCF) in rails focussing on the conventional full bogie vehicles. The authors evaluated the benefits of using this ASW method, where actuators are used between the wheelset and the bogie to steer the wheelsets when negotiating curves, which resulted in reduced curving forces and reduced rolling contact fatigue (RCF) in rail tracks.

Furthermore, to the above–mentioned studies, where the conventional ASW configuration is used to apply the control effort to the wheelset, a study [32] has investigated the possible interactions of the conventional ASW method with the traction system of a motorized wheelset, and their results have offered considerable insight into the effects of torsional flexibility in the axle on wheelset stability.

Another study has focused on actively steering the ASWs to achieve the optimal lateral displacement and pure rolling for the wheels in order to reduce the noise created by undesirable creepages [33] and proven that using yaw actuation, these noise levels can be significantly reduced.

Actuated Independently Rotating Wheelset (AIRW) – This is the basic active configuration for IRW configuration, where the control steering force/torque is applied to the common axle in either the lateral, yaw or longitudinal direction for the guidance of the wheelsets on curves. This method has been thoroughly investigated in a study [2], and authors have compared the ASW and AIRW in terms of their performance stability and curving performances. It has been found that due to the low longitudinal creep forces in the IRW configuration, control effort is significantly lower than for the ASW configuration and also that, similar to the ASW configuration, yaw or longitudinal actuation is preferred in the AIRW configuration over lateral actuation of the wheelset axle since the latter deteriorates ride comfort by directly affecting the vehicle's dynamic modes. Further research has been undertaken to control the AIRW arrangement effectively by using an initiative controller, which can be adaptive, based on the relative rotational speed of the wheel pair [34]. There have been multiple studies that have introduced model–based robust optimal controllers for active steering of the AIRWs and a study has used a robust H∞ controller which can maintain the stability and good curving performance even against rail–wheel interface parameters (such as creep coefficients and wheelset conicity) variations and the study has concluded that assessment on the robustness of the closed loop control system using μ synthesis technique has proven excellent results [35].

Driven Independently Rotating Wheel (DIRW) – As another configuration for the IRWs, this method has been investigated by studies [36, 37] as related to high–speed, long distance applications and in this configuration, driving torques for the IRWs are being applied by the servomotor connected directly to the to the wheels (independently) via a differential gearbox. From the numerical simulations performed and tests on a 1:5 scaled roller rig, this method has shown to possess the potential to obtain vehicle stability at speeds well above the maximum service speed and offers improved curving performance when compared with conventional passive vehicles. Further investigations into this method have been undertaken on this technique and authors [38] have investigated the combined use of the AIRW and DIRW concepts to improve curving performance. Active control in this case is applied using one active steering actuator for each wheelset and one traction motor for each wheel to improve both the ability

and curving performance of conventional vehicles. A study [39] has investigated the application of the DIRW concept with an articulated tramcar train to provide guidance in curved track in order to improve curving and DIRW technique is used in case to provide traction torques to the wheels to mimic a solid–axle connecting the wheels such that a steering moment is introduced for the wheelsets. Another study [40] has also discussed the use of permanent magnet motors embedded inside the wheel to implement the DIRW concept, with the idea to obtain a compact and lightweight design solution.

Directly Steered Wheels (DSW) – As another active configuration for the IRW this can be used for active guidance on curved tracks with a traction rod to steer the independently rotating wheels. Even though this method is not for the stability purposes, it is noted as being the most considered active guidance method in primary suspension. This idea was investigated by authors [41, 42] who considered vehicle architecture with the car body and two bogies equipped with DSW, guided by feedback on lateral wheel/rail displacement with the use of eddy current sensors. They have investigated the vehicle stability and dynamic response to the curved track and stated that results indicate improved curving performance in comparison with a conventional passive vehicle.

As another approach with DSW, authors have [43] to complement and improve the curving performances of independently rotating steerable wheels. Here, a DC motor acted as a passive electromagnetic damper in order to improve the damping of yaw oscillations in a tangent/curved track and a powered actuator is used to provide the compromise for curve transitions. By the numerical results and by tests on a 1/10 scaled model of a two–axle vehicle, authors have stated that this concept seemed favourable.

2.2.2. Concepts for Secondary Suspension (Stability and Curving)

In addition to above mentioned direct methods, there is also an indirect method of applying the control effort through the secondary suspension (bogie) instead of directly to the wheelsets to improve stability and curving of the railway vehicles.

Secondary Yaw Control (SYC) – Although in SYC, actuation is applied at the secondary suspension level, this concept has been developed to improve vehicle running dynamics rather than ride comfort. Applying yaw torque on the bogie is the main concept underlying secondary yaw control (SYC) and is intended to improve stability and curving performance. This configuration was investigated [44] in relation to the tilting body in some high–speed trains and an electro–mechanical actuator is used in this

case to provide the control force to the bogie. On a straight track with lateral irregularities, active control is used to mimic a passive yaw damper, taking advantage of the wide pass–band of the actuator to provide appropriate damping to the hunting motion (instability) in a frequency range (6–8 Hz) where the efficiency of hydraulic yaw dampers is reduced by internal deformability effects. Similarly, for a curved track, a yaw torque is applied as a function of cant deficiency and curve radius, to equalize lateral forces on the two–axles.

There has been a study [45] to compare the difference between yaw actuation (actuators mounted in longitudinal direction) with the combined use of lateral (actuators in lateral direction) and yaw actuation of wheelsets. It has been demonstrated that combined actuation has a much higher potential for vehicle stabilization and may lead to the use of smaller scale actuators but has a negative effect on passenger comfort.

Another similar study [46] focussed on the use of actuators mounted in the lateral direction (with no yaw actuation) but this model appears to show that this would be less effective than yaw actuation. It suggests the difference in the results is possibly due to differences in the positioning of the lateral actuators and in the control, strategy used for stabilisation.

Further evaluation of this configuration is done in a study [47] to improve the steering performance of a vehicle with car body and two bogies. Full–scale tests on an entire bogie has been performed on a roller rig test stand at the National Traffic Safety and Environment Laboratory in Tokyo and were compared with numerical calculations, demonstrating the effectiveness of the concept on the reduction of guiding forces in curves of radii varying from 150 to 400 m.

The main attraction of this configuration is that actuators can be designed readily to replace the traditional passive yaw dampers such that this configuration can be implemented without a significant redesign current vehicle configuration. However overall results indicate that, this indirect control effort approach is less effective than the direct configurations since it has been observed that during curving SYC is not able to affect the yaw angles of single wheelsets [22].

2.3. Control Strategies:

As mentioned before, there are a number of control strategies with classical feedback control approaches and model–based approaches focussing on the challenges of stability, steering/curving and guidance of railway wheelsets either individually or as a whole (integrated control). Thus, in order to thoroughly discuss the methodologies behind these control schemes, they can be categorised based on their application as follows:

- Stability Control
- Steering / Curving and Guidance Control
- Integrated Control

It should be noted that as a field which attracts a large number of researchers, over the years there have been numerous publications proposing various control schemes.

2.3.1. Control Strategies for Stability Control

Stability is an important aspect for both the SW and IRW configurations when passive suspension is to be replaced/supplemented by active means. In addition, another aspect which needs to be considered when developing active control systems for stability is that developed control schemes (for both ASW and AIRW configurations) are not detrimentally affecting the curving performances of the wheelsets since the whole purpose of the using active control is to address the trade–off between stability and curving.

Strategies for Solid–Axle Wheelsets:

Active yaw damping is a classical control strategy which is one of the main methods proposed for the ASW configuration for stability control [48]. In this method, an actuator is used to apply yaw torque to the wheelset based on the feedback of the lateral velocity of the wheelset. Active lateral damping is another similar scheme where control effort is applied along the lateral direction to the wheelsets based on the yaw angular speed feedback from the wheelsets [49, 50]. A study [2], has been done to address the hunting problem of solid–axle wheelsets (ASW), which found that active yaw damping strategy requires lower actuation forces and power than active lateral damping and provides better riding comfort. It has also been found that although the passive damping at the wheelsets cannot improve the stability of wheelsets, both active lateral/yaw damping can stabilise the wheelsets. However, active yaw damping is preferred over active lateral damping as the latter has proven to worsen the riding comfortability.

Another classical control approach proposed to improve stability of ASW configuration is the skyhook stiffness control strategy [51]. With this approach, authors suggest that applying a yaw torque proportional to the absolute yaw angle measurement of the wheelset with the ASW configuration can act as an effective stabilisation control for the dynamic mode of the wheelsets. Since this scheme requires a feedback measurement of the wheelset absolute yaw angle, authors have suggested a number of methods with which absolute yaw of the wheelsets can be obtained to generate the control signal.

One such is the use of double integration of accelerometer measurements and the other is the use of a state estimator. An additional method has also been suggested as a relatively simple method of obtaining the absolute yaw of the wheelset by exploring the characteristics of spring–mass seismic accelerometers since the output signals from this type of sensor give the yaw acceleration of the measured wheelset at frequencies below the natural frequency of the sensor, whilst at above the natural frequency the sensor output represents the absolute yaw angle.

Strategies for Independently Rotating Wheelsets:

IRW configurations, unlike SWs, can be stabilised by passive yaw damping, although active steering is essential for the guidance [52] on curved tracks. When focussing on stabilising AIRWs, a control configuration where the control effort is applied along the yaw direction based on the relative yaw velocities between the wheelset and the vehicle body/bogie. This configuration (a different form of yaw damping) can stabilise IRW wheelsets and the control effort is significantly lower compared to the SW arrangement since the longitudinal creep forces are extremely low (almost non–existent) in the IRW arrangement. The study has also found that this method is more effective as it allows for speed adaptation of the stabilising action [14].

Strategies for Bogies:

In addition to the primary suspension, active yaw damping has also been proposed for secondary yaw damping (SYC) for stabilisation. In this case, yaw torque on the bogie is based on the feedback of bogie yaw speed relative to the car body. In addition, this study indicated that additional proportional gain with the longitudinal bogie acceleration is required to compensate for actuator delays [44, 54].

2.3.2. Control Strategies for Steering and Guidance

Guidance is more essential to the IRW configuration than the SW configuration since the latter has the ability to naturally follow the track essentially when travelling on a curved track (when unconstrained). However, since usually some amount of passive stiffness is always present (unless completely replaced by active control) to maintain the stability of SWs, studies have shown that curving performances SW

wheelset arrangement can be improved using active steering to restore the self–curving ability which is hindered by passive suspensions used in railway vehicles [41].

Strategies for Solid–Axle Wheelsets:

Although unconstrained solid–axle wheelsets have the ability to allow for natural curving, extra active effort is needed in addition to the steering of the wheelsets when negotiating curved tracks in cases where high–stiffness springs are mounted in longitudinal directions. Yaw relaxation is a control configuration for ASW to improve curving performance. The authors of [55] proposed to the use of active (actuated) traction rods in conjunction with actuators so that their length could be varied by electronic means such that resultant yaw torque (from passive and active elements) is reutilised. This has a unique physical arrangement and the active traction rod has a predefined stiffness that is sufficient to ensure the stability of the railway vehicle. The authors claimed that on straight track this predefined stiffness dominates, while on curved track the length of the traction rods is varied (which suggests that the control effort is only applied at low frequencies).

Another similar study [56] investigated the use of active control to eliminate longitudinal creep forces by achieving a pure rolling rate and equalising the lateral creep forces to be sufficient to just act against the centrifugal forces whilst traversing the curve using the feedback measurements of deflection feedback from the wheelsets using yaw actuation. The authors indicated from their results that a significant curving performance improvement can be obtained from this strategy, and that this can be used even as a supplement to passive suspension although this would result in a substantial increase in the required control effort.

Furthermore, a recent study has been conducted into active solid–axle wheelsets using a Hα controller [58] as a model–based approach with the two–axle vehicle model, which inherently possess poor curving performances with passive suspension due to the larger distances between wheels. In this study, the authors designed a controller with closed–loop transfer function shaping and H∞ optimisation, while the controller is designed to improve curving performance. The authors found that this method shows a satisfactory level of improvement in both curving and the guidance of the vehicle, and that model–based controllers have more adaptability compared to more conventional feedback controllers.

Strategies for Independently Rotating Wheelsets:

Since an IRW is unable to naturally follow the track, unlike a SW, guidance control strategies are essential for this arrangement. Both classical and robust model–based controllers can be used for actuated IRW configurations such as AIRW, DIRW and DSW arrangements. However, there are challenges related to the sensing and uncertainties of the parameters, which need to addressed separately.

Although some studies have indicated that designing a feedback control system for AIRW is practically challenging, since wheel–rail contact measurements are required [2], another study [34] has investigated the use of an active steering controller for the IRW configuration which can be adaptive based on the relative rotational speed of the wheel pair, where the control efforts in the yaw direction to the wheelset are achieved.

In addition, another study has focussed on another simpler (non–model–based) approach with feedback in the DIRW concept, which sets out to control the traction torques required to achieve and maintain the rotational speed difference of the motors at zero. This action forces IRWs to act as SWs [33]. Another complex approach has been taken in a study into DIRW was where feedback of lateral displacements and of the yaw velocity of the leading wheelset [58] are used to steer the wheelsets. The authors found that this system can be demonstrated in a test rig, and stable running of the vehicle up to the maximum design speed are achievable.

A study [42] has proposed a control strategy for the DSW configuration which uses a computed tracking error from wheel position with respect to the centreline of the track. The idea behind the study is to minimise the tracking error so that the wheel flanges are not in contact with the rail. The author found a large margin of stability at high speeds of the vehicle with this method.

Strategies for Bogies:

As for the indirect method of curving/guidance control, a feed–forward control scheme has been proposed by for the SYC configuration. This curving strategy is developed based on estimating the value of track curvature from the measurements of the cant deficiency and of the bogie yaw rate. Subsequently the steering torque is applied on the bogie is obtained by the use of lookup tables, developed by simulations. Authors have stated that results have indicated that the system is capable of correctly identify the rail curvature and applying torque accordingly [44, 45].

2.3.3. Integrated Control Strategies

As mentioned before, in addition to the control strategies targeting on either stability or curving/guidance, there are control strategies proposed to address both these aspects with SW and IRW configurations respectively.

Strategies for Solid–Axle Wheelsets:

In this study, a modal–based control schemes have also been developed for wheelset stability control and curving [27] which use kalman filter based model controllers for the wheelsets using acceleration measurements of the bogies and the body such that the curving performance of the vehicle are not deteriorated. Furthermore, authors have stated that, with this scheme, which suggest to use actuators in either yaw or longitudinal directions, when compared to a passive vehicle, the vehicles with this model–based active steering is capable of improving the ride quality on straight track in addition to improving the curving performances.

Another recent study [59] has conducted a similar assessment with linear actuators with a Hα controller (model–based) for active steering of a high–speed train bogie with solid–axle wheelsets, as an integrated solution to improve stability and curving performance. In addition, this study has included a second–order polynomial extrapolation to compensate for delays relating to actuator dynamics and modified the control signal to compensate for the undesirable delays and found that both stability and curving performances while can be improved with this concept.

More studies [58, 60] have undertaken a comprehensive study on the use of active control for improving the curving of the ASW configuration using model–based optimal controllers. The authors investigated the use of yaw actuation for the primary suspension as well as the use of lateral actuation for the secondary suspension with model–based controllers via multiple measurement arrangements to prove that significant improvements to the curving performance can be achieved by optimal controllers based on active control with minimum changes to the original mechanical configuration. In addition to assessment of the control scheme, a study [60] has evaluated the use of an effective condition monitoring through fault detection and isolation (FDI) since active wheelset control is a safety–critical control system.

Another classical feedback control (with model–based sensing) approach has been suggested by a study to robustness of active wheelset control with a self–tuning linear–quadratic regulator (S–L LQR) [61]. This scheme attempts to maintain the wheelset stability at high speeds and adequate curving performance simultaneously by minimising the lateral displacement of the wheelset, relative to track

centre line and its yaw angle, on straight and curved tracks. In addition, self–tuning feature in the control design allows to main the desired performances over the whole range of the track parameters variations such as conicity and cant deficiency. Authors have stated that this scheme has been tested with two–axle vehicle model results indicate that the method performs well.

Strategies for Independently Rotating Wheelsets:

When focussing on integrated controllers for the IRW, there are model–based controllers with inherent stability control and can therefore also be used for guidance [35] for curved tracks. H_2 model–based controllers have been studied for their ability to maintain the natural curving in a solid–axle arrangement as well as to assist in curving for IRW wheelsets. The Hα modal–based controller has also been studied to address robustness issues and has been found to have the ability to adhere to certain parameter variations such as track conicity [62].

Another study [35] discussed and studied an active steering method for independently rotating wheelsets with model–based controllers using the Hα design. The authors stated that although a linearized model has been used in the development of a robust control strategy, it can be justified from the point that an active steering scheme will improve performance on curves in a manner which considerably reduces the effects of nonlinearities. The nonlinearities of a railway vehicle model are largely associated with nonlinear wheel–rail profiles and contact forces, and which become especially problematic when the wheel–rail contact point approaches the wheel flanges. However, robust active steering control proposed in this study largely overcomes this problem by steering the wheelset to operate at the linear region of the wheel tread and rail surface.

In addition, a model–based control system for steering and stability has been investigated by a study [34] which has an intuitively formulated and simple control structure and is capable of adapting to vehicle speed. This method uses speed sensors to measure the relative rotational speed of the two wheels on a same axle with sensors that are also used to measure the relative yaw velocity of the wheelset and the body. This control scheme has indicated that it can improve both the curving performance and passenger ride comfort of actively controlled AIRWs compared with typical passive suspension.

2.4. Actuator Technologies for Railway Applications

As briefly discussed in the previous chapter, there are several types of actuators currently being used in railway applications. The choice of actuator is dependent on the trade–off between actuator performance (power, efficiency, bandwidth, etc.), size, and maintenance cost considerations [20, 63] and it is essential to assess the performances of each actuator type against the demand for active wheelset control applications.

Servo–pneumatic actuators are mainly used in the secondary suspension of trains. In an active servo–pneumatic system the air pressure is controlled, which gives rise to desired suspension characteristics. Authors of a study [64] has found that in the vertical direction the air pressure in an already existing air spring system with fixed reservoir volume can be actively controlled by a reservoir with variable volume. However, due to the large air compressibility, the controllable frequency bandwidth is restricted to 2–3 Hz, and hence the operational range of the actuator is limited. Thus, this option is not suitable for the primary suspension as wheelsets for stabilisation application which have bandwidth of up to 6–8 Hz in dynamic mode.

However, in an investigation [65], servo–pneumatic actuators were tested on a roller rig in order to reduce vibrations in the vertical, lateral and roll modes and up to 50% reduction of these particular modes of vibration could be achieved with the active system. More studies [66, 67] have also found, that once passive hydraulic dampers in lateral direction are replaced by pneumatic actuators (at secondary suspension), they are capable of improving riding quality by reducing vibrations.

The general concept of hydraulic actuators is based on the idea that a control signal activates valves or a pump controlling the flow of the hydraulic fluid into and out of an actuator. Hereby, a pressure difference is created between the two chambers of the actuator cylinder which, in turn, gives rise to the actuator force. Generally, hydraulic actuators have a fast response time and they are able to maintain a demanding loading capacity indefinitely and without excessive heat generation. However, hydraulic systems are highly non–linear and subject to parameter uncertainty [68].

Hydraulic actuators are well studied and often used in railway applications for secondary suspension as they are compact and can easily be fitted in the narrow spaces between car body and bogie. In addition, their cost–effectiveness makes them favourable for implementation in vehicles to enable full–scale tests as well. An experimental analysis was performed [69], where authors chose a hydraulic actuator over a pneumatic actuator due to its ability to control up to a 12 Hz frequency range, compared to the 2–3 Hz as mentioned above and found to be performing well to minimise vibrations. However, there is a major disadvantage of hydraulic actuators are the risk of oil leakage, maintainability and maintenance costs [70].

An electro–mechanical actuator is powered by an electrical motor (preferably BLDC). This actuator type has been successfully applied in many ASW control strategies [42]. The rotational motion torque of the actuator is converted to a linear motion by a screw. Another approach is to connect the motor through a gear box to actuate the wheelset in the angular direction, and indeed this has been studied with ASW [71, 72] while with DIRW configuration EM actuators incorporated through a gearbox [73]. EM actuators have the advantages of having an operational bandwidth that is over the wheelset bandwidth, a compact design, low maintenance cost and linear behaviour for the operational torque/force range (0 – 5 kNm) required for wheelset control. A recent study had assessed the use of EM actuators with skyhook damping configuration [74] for secondary suspension and found that EM actuator is operating well with a frequency of 10 Hz [75].

The electromagnetic actuator consists of two pairs of electromagnets mounted back to back and operating in attraction mode. The magnets produce a force in both directions between two masses connected through the actuator, e.g., car body and bogie [76, 77]. Similarly a study [20] has focus on adding an electro–magnetic actuator between the centre of the car body and an auxiliary (mass of one tonne) in order to suppress the first symmetrical flexible mode, which, if unsuppressed, has a negative impact on ride comfort and found to be operating adequately. The electromagnetic actuator is often preferred due to its property of large frequency bandwidth. It is considered to show a good frequency response up to 50 Hz. Since it does not contain any moving parts it is a robust and reliable device as well [64]. However, it suffers from a relatively high unit size and weight and can be difficult to fit in the narrow places between two bodies of the vehicle. Studies have also found that [78, 79] the effect of air gap variations between the magnets results in an unstable system which, can be overcome with proper force feedback.

2.5. Sensing – State Observers

Sensing is an important aspect of active control since feedback is essential to achieve active control. However, as discussed previously, there are cases where obtaining accurate feedback with readily available sensors is not possible.

In scenarios where actual measurements are unable to be obtained for the feedback, model–based solutions can be used to estimate those states based on the measurements which can be obtained easily and the dynamic relationships between states.

There have been many previous studies conducted into the use of estimators on railway vehicles with actively controlled suspension systems to obtain feedback measurements for the controllers as well as for other applications. Research have focussed on the development of a model–based state estimator

using a two–axle railway vehicle model to estimate track feature measurements (such as creep coefficients and conicity) for an active steering control system with ASWs. In this case, to measure the observable states, eight sensors and three accelerometers are used to measure the lateral accelerations of the body and the two wheelsets, and three of the five gyros are used to measure the yaw velocities of the vehicle body and the wheelsets. A kalman filter is formulated to include the track features such as curve radius and cant angles of the track, as some of the state variables and the parameters of the railway track are directly estimated by the kalman filter so that estimated track features can be used to apply the active steering (yaw actuation) using an optimal controller [80].

In addition, a kalman–bucy filter has been investigated to estimate the creep forces in the contact area through inertial sensor measurements while the estimations are further processed to convert them into usable adhesion level information [81] via parameter identification to reduce their dependency upon track irregularity levels and produce an interpretable signal. The results of the study indicated that this has enabled the detection of low adhesion of during travel. This would have been extremely difficult to obtain using readily available sensors.

Furthermore, a study [82] has used a model of a DC motor to design a state observer to estimate the motor torque using motor speed measurement and motor current input where pole–placement method [83, 84] has been used to find observer gains to rapidly converge the estimations found estimations are accurate.

Similarly, model–based sensing techniques have been used in a semi–active control configuration to estimate the states of the vehicle suspension systems [85]. In this case, an unscented kalman filter design, as based on a two–axle vehicle model can be used to estimate states, such as vertical velocity of stiffness components, while its vertical acceleration and stroke velocity are provided as measurable states using accelerometers, which assists in developing an adaptive sliding mode controller in real time. The authors found that the UKF designed in this study is less effective with regards to uncertainties associated with track disturbances.

In addition, a study has developed state estimation techniques using state observers to provide essential feedback variables for the active control of railway vehicles with IRW [86], such that expensive sensors and complex instrumentation can be avoided for this application. This study estimating track data based with the use of full model of the vehicle and readily available measurements such as yaw velocity, lateral acceleration of wheelsets, bogie and vehicle.

In addition, another variation of a kalman filter called ensemble KF is being used in the power distribution industry to estimate certain states such as high current values in power distribution systems for condition monitoring purposes based on voltage magnitudes and angle of the grid measurements, when it is either difficult or costly to measure certain states accurately [87].

CHAPTER 3: BACKGROUND OF MODELLING RAILWAY VEHICLE DYNAMIC SYSTEMS

3.1. Introduction

A background in to the dynamic derivation of vehicle models such as the two–axle vehicle model and the conventional bogie vehicle model are discussed using Newtonian motion laws in this chapter. An established publication (text book) [24] related to railway vehicle modelling is referred for this task as these linearized vehicle models are widely regarded in the field. Subsequently, the dynamic models of vehicles are implemented in MATLAB Simulink along with the passive suspension components (active control is introduced in the next chapter) in order to assess the curving performances and stability on curved tracks and straight tracks with lateral irregularities respectively. However, this chapter only contains results with a curved track since more thorough comparison with both the tracks and passive suspension and active control is done in the next chapters, once active control is introduced. Furthermore, by the analysis of the results, model verifications and dynamic issues related curving with the passive suspension are discussed in this chapter.

3.2. Solid–Axle – Single Wheelset Model

When deriving the dynamic equations for the wheelsets it is considered here that forward velocity of the wheelset is always tangential to the centre line of the track. This direction is considered as the X axis while the Y and Z axis are defined in the Figure 3.1. All X, Y and Z planes are necessary in this case to illustrate the lateral and longitudinal forces as well as creep forces occurring due to the conicity of the rail track. First the equations are derived to a single wheelset as below, which the derivations are then extended for the vehicle models.

Regarding the abbreviations/symbols used with the equations in this chapter, key parameters are introduced in the below descriptions while full list is elaborated in the ***List of Abbreviations*** section at the start of the thesis.

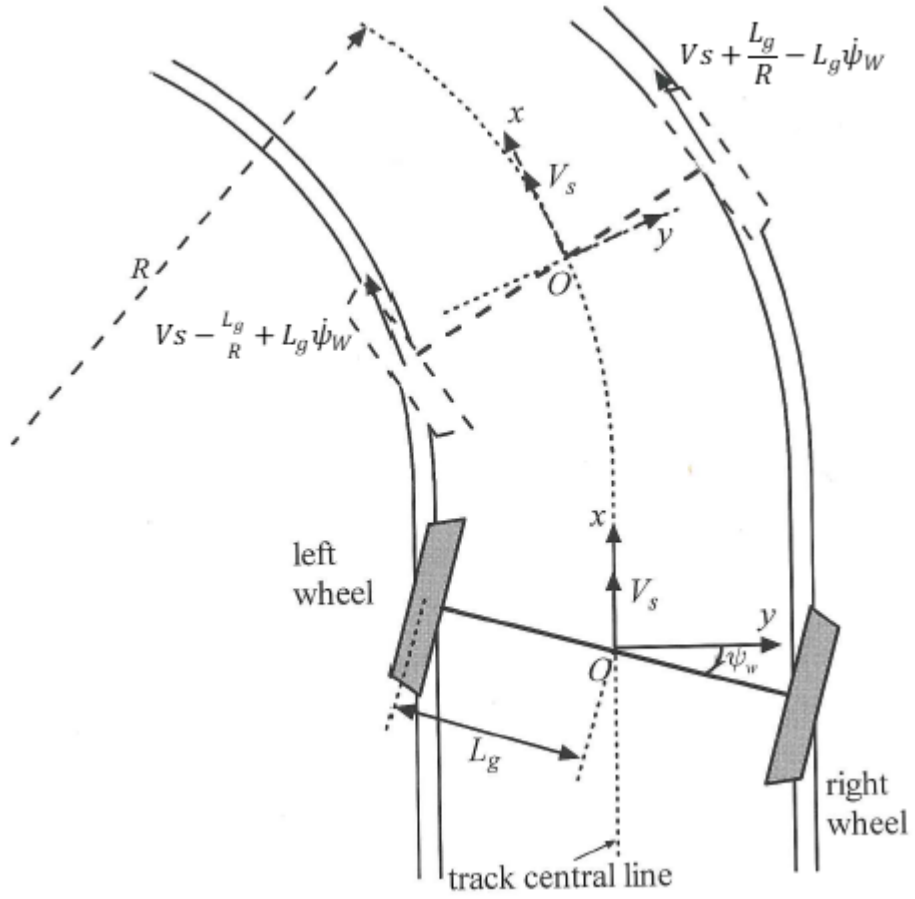

Figure 3. 1 – Plan View of Single Wheelset [24]

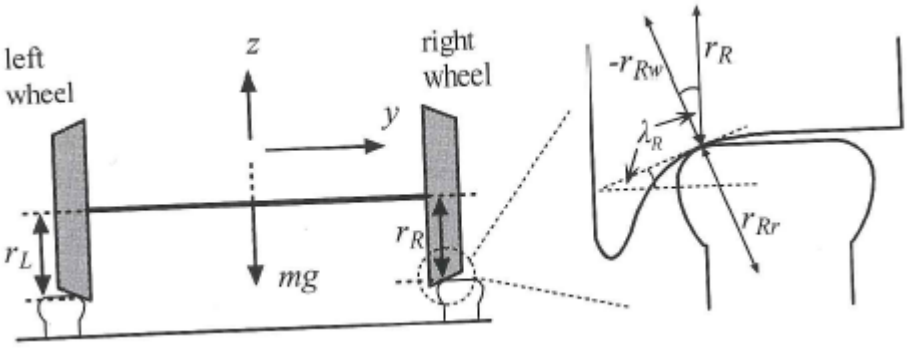

Figure 3. 2 – Sectional Cross View of Single Wheelset [24]

Although there are six degrees of freedom for these bodies in the Cartesian coordinate system defined by X, Y and Z, only the plan view of the wheelset is mainly considered and the yaw and lateral movements of the wheelset are assessed since the study is concerned with the lateral and yaw dynamic

modes of the railway vehicle, which are largely decoupled from other modes such as longitudinal and vertical modes.

In the equations, lateral displacement of the wheelset is denoted as y_W while yaw displacement is denoted as ψ_W while velocities and accelerations are denoted in derivative form of the displacement variables. In addition, radius of the curve is defined as R while the curvature is $\frac{1}{R}$ and L_g is the half length of the wheelset as illustrated.

As Figure 3.2 illustrates, wheel radius of the left and right–side wheels are denoted as r_L and r_R respectively. This is also the distance between centres of the wheel axle to the contact point of the wheels. But due to the conicity of the wheels, when the wheel moves in the lateral direction, r_L and r_R values change inversely proportionally with regards to the lateral displacement. But when the wheel centrals align with the rail centre, both $r_L = r_R = r_O$ which is a constant. On the contact point of the wheel slope angles (conicity) are considered as (λ_L and λ_R) the angle between the normal of the contact point tangent and vertical lines.

3.2.1. Contact Forces and Contact Dynamics

Dynamic behaviour of railway vehicle wheelsets (vehicle and bogie are also affected due to suspension components) are mainly influenced by the forces and dynamics occur at the contact point of the wheel and rail. In this scenario the main dominant type of contact forces are occurred due to creepages at the contact points while these creepages are generated due to minor relative velocity differences of the wheelsets in lateral and longitudinal directions and they result in elastic deformation of the material at the contact point. Creepages and the creep forces [11, 89] occurring at this application are analysed below. Figure 3.3 shows a side view of left and right wheels fixed in the same axle while it is considered that the wheelsets are travelling at a constant forward speed of V_s and the wheel radius is r_O for both the wheels. Hence wheel rotational speed can be derived as ω,

$$\omega = \frac{V_s}{r_0} \tag{1}$$

The creepage in the longitudinal direction is determined by the relative longitudinal velocity. This is being influenced by both track curvature and yaw motion of the wheelset.

Figure 3. 3 – Creepages 1 [24]

Due to the curvature of the rail track, forward speed V_s has different effects on the left and right wheels on longitudinal direction speeds as V_{L_Lon} and V_{R_Lon} respectively.

$$V_{L\_Lon} = V_s(1 - \frac{L_g}{R}) \tag{2}$$

$$V_{R\_Lon} = V_s(1 + \frac{L_g}{R}) \tag{3}$$

Similarly, yaw motion of the wheelset also has an effect on longitudinal direction speeds as V_{L_Yaw} and V_{R_Yaw} for the left and right wheels.

$$V_{L\_Yaw} = L_g\dot{\psi} \tag{4}$$

$$V_{R\_Yaw} = -L_g\dot{\psi} \tag{5}$$

Hence the effective forward speeds of the wheels are as V_L and V_R for the left and right wheels respectively,

$$V_L = V_{L\_Lon} + V_{L\_Yaw} = V_s\left(1 - \frac{L_g}{R}\right) + L_g\dot{\psi} \tag{6}$$

$$V_R = V_{R\_Lon} + V_{R\_Yaw} = V_s\left(1 + \frac{L_g}{R}\right) - L_g\dot{\psi} \tag{7}$$

Another aspect which affect the dynamic behaviour of the wheelsets are the creepages which occur due to difference of relative velocities between rail and wheel at the contact points [88]. Hence, by using the definition of creepages of the longitudinal direction is derived for the left (Υ_{L_Lon}) and right (Υ_{R_Lon}) wheels as below,

$$\Upsilon_{L\_Lon} = (-\omega . r_L + V_L)/V_s \tag{8}$$

$$\Upsilon_{R\_Lon} = (-\omega . r_R + V_R)/V_s \tag{9}$$

Similar to the longitudinal direction, lateral direction equations can be derived as below for the left and right wheels as V_{L_Lat} and V_{R_Lat} respectivly,

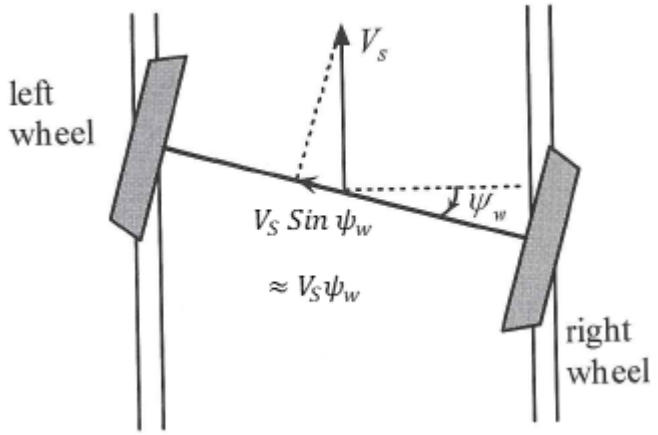

Figure 3. 4 – Creepages 2 [24]

$$V_{L\_Lat} = \dot{y}_w - V_s Sin(\psi_w) \tag{10}$$

$$V_{R\_Lat} = \dot{y}_w - V_s Sin(\psi_w) \tag{11}$$

Since yaw angle values (ψ_w) of the wheelsets are very small in value for this case, it can be considered that,

$$Sin(\psi_w) \approx \psi_w \tag{12}$$

Thus,

$$V_{L\_Lat} = \dot{y}_w - V_s \psi_w \tag{13}$$

$$V_{R\_Lat} = \dot{y}_w - V_s \psi_w \tag{14}$$

From the definition of the creepage, for creepages for lateral direction for left (Υ_{L_Lat}) and right wheels (Υ_{R_Lat}),

$$\Upsilon_{L\_Lat} = V_{L\_Lat}/V_s \tag{15}$$

$$\Upsilon_{R\_Lat} = V_{R\_Lat}/V_s \tag{16}$$

There is also a creepage in the spin direction of the wheel occurring due to relative spin velocity of the wheels as and for left (Ω_{L_Spin}) and right (Ω_{R_Spin}) wheels respectively, which also has an effect from yaw motion and the wheel rotation. Yaw motion of the wheel causes the wheel to spin on the contact patch with $\dot{\psi}_w$ angular speed. Similarly, due to longitudinal velocity, wheel angular speed ω creates a spinning in the contact patch. By taking the contact sloops (conicity) in to account as λ_L for left side and λ_R for right side,

$$\Omega_{L\_Spin} = \dot{\psi}_w + \omega.Sin(\lambda_L) \tag{17}$$

$$\Omega_{R\_Spin} = \dot{\psi}_w - \omega.Sin(\lambda_R) \tag{18}$$

Since λ_L and λ_R are miniature values,

$$Sin(\lambda_L) \approx \lambda_L \tag{19}$$

$$Sin(\lambda_R) \approx \lambda_R \tag{20}$$

$$\Omega_{L\_Spin} = \dot{\psi}_w + \frac{V_s}{r_0}.\lambda_L \tag{21}$$

$$\Omega_{R\_Spin} = \dot{\psi}_w - \frac{V_s}{r_0}.\lambda_R \tag{22}$$

From the definition of the creepage, in the spin direction creepages are as Υ_{L_Spin} and Υ_{R_Spin} for he respective wheels,

$$\Upsilon_{L\_Spin} = \Omega_{L\_Spin}/V_s \tag{23}$$

$$\Upsilon_{R\_Spin} = \Omega_{R\_Spin}/V_s \tag{24}$$

From above derivations creepages which the wheels encounter when travelling tracks can be calculated using Equations 8–9 for longitudinal direction, Equations 15–16 for lateral direction and Equations 23–24 for spin direction respectively.

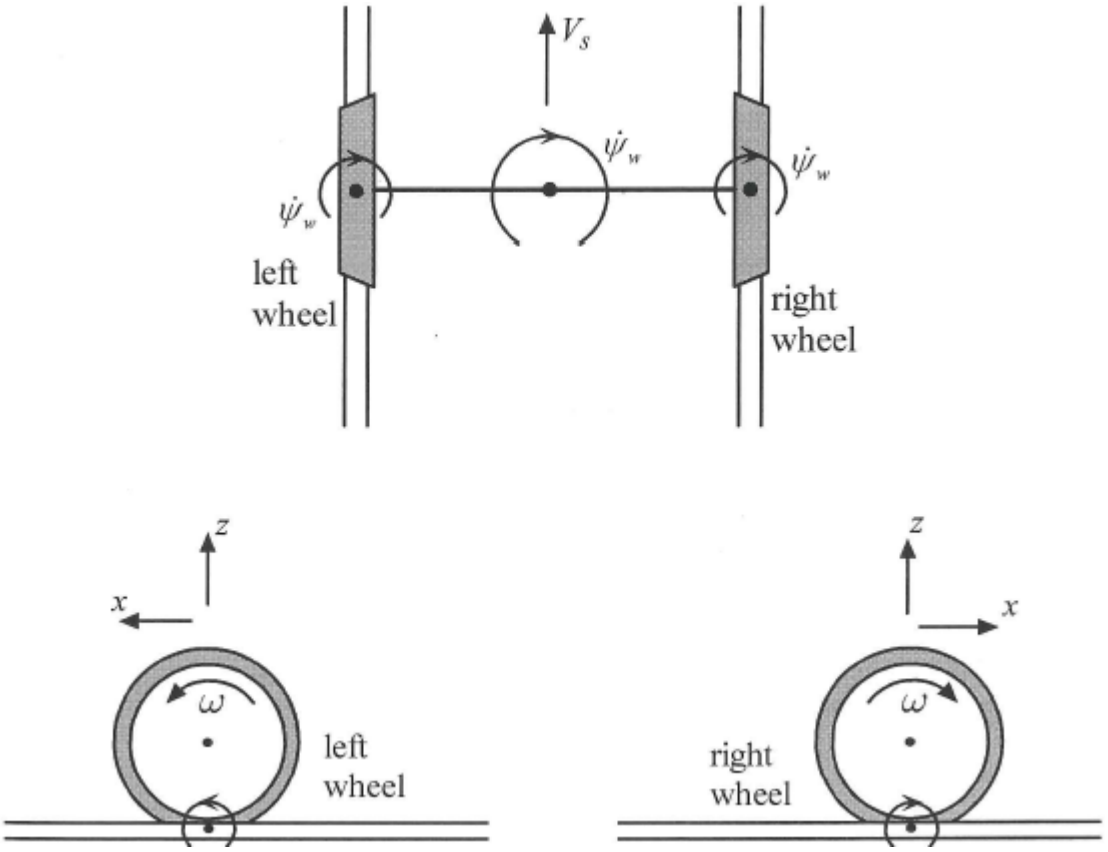

Figure 3. 5 – Creepages 3 [24]

Due to these creepages defined above, forces occur as below. These forces are functions of both lateral, longitudinal and spin creepages along with their relative differences.

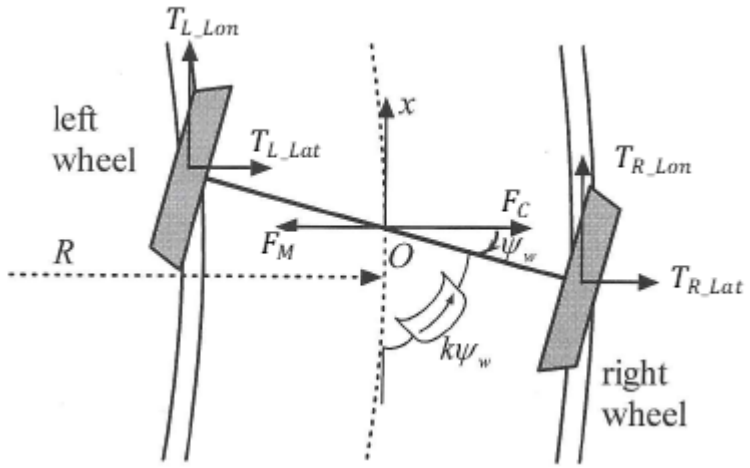

Figure 3. 6 – Forces Occurring 1 [24]

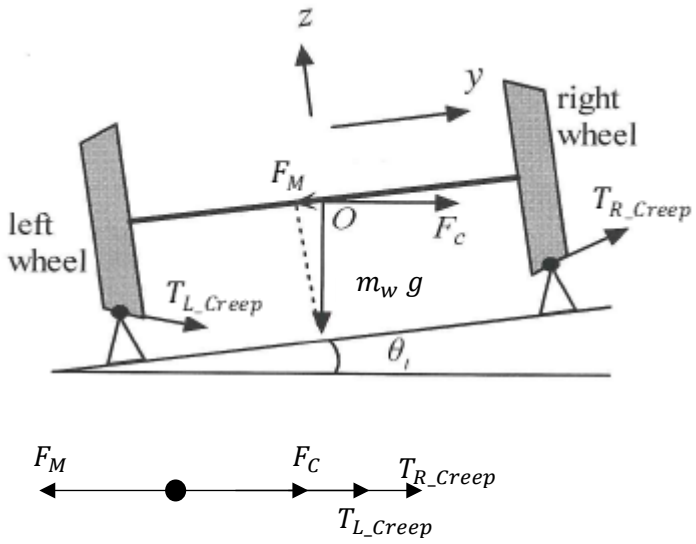

Figure 3. 7 – Forces Occurring 2 [24]

By using the linear theory of kalker [90], these forces can be defined by introducing the term creep coefficient, f_{L_Lat}, f_{R_Lat}, f_{L_Lon}, f_{R_Lon}, $f_{L_{Lat}-Spin}$, $f_{R_{Lat}-Spin}$ and the creep forces can be denoted as T_{L_Lon} and T_{R_Lon} for the longitudinal creep forces of the left and right wheels while similarly T_{L_Lat} an T_{R_Lat} for the lateral creep forces.

$$T_{L\_Lon} = -f_{L\_Lon} * \Upsilon_{L\_Lon} \tag{25}$$

$$T_{R\_Lon} = -f_{R\_Lon} * \Upsilon_{R\_Lon} \tag{26}$$

$$T_{L\_Lat} = -f_{L\_Lat} * \Upsilon_{L\_Lat} - f_{L_{Lat}-Spin} * \Upsilon_{L\_Spin} \tag{27}$$

$$T_{R\_Lat} = -f_{R\_Lat} * \Upsilon_{R\_Lat} - f_{R_{Lat}-Spin} * \Upsilon_{R\_Spin} \tag{28}$$

These creep coefficients are constants and they are based on the properties of the material and the size of the contact patches in each wheel.

For the stability, the wheelset is connected to a passive spring with a coefficient k, which will generate a torque of $\tau = k\,\psi_w$

Hence, according to the energy conservation law, dynamic motion of the wheelset can be expressed as below, where I_w is the moment of inertia in the wheels using Euler–Newton law.

$$I_w\,\ddot{\psi}_w = T_{L\_Lon}L_g - T_{R\_Lon}L_g - k\,\psi_w \tag{29}$$

When the train is moving on a cant angle θ_t, due to gravitational effect there is force (F_M) in lateral direction which can be defined as below where the mass if the wheelset is m_w and g is the acceleration due to gravity,

$$F_M = -m_w\,g\,Sin(\theta_t) \tag{30}$$

But since θ_t is always a very small value, it can be considered as

$$F_M = -m_w\,g\,\theta_t \tag{31}$$

Centrifugal force (F_C) due to a curvature also has an effect on the wheelset as below,

$$F_C = \frac{m_w {V_s}^2}{R} \tag{32}$$

With regarding the T_{L_Lon} and T_{R_Lon} , even though in reality they act on different spots of the wheelset, in this simplified model it is considered that these forces act on the centre of the wheelset where F_M and F_C are occurring. Hence, dynamic model of the wheelset in the lateral direction can be derived as below using newton laws,

$$m_w\,\ddot{y}_w = T_{L\_Lat} + T_{R\_Lat} + F_M + F_C \tag{33}$$

3.3. Two–Axle Vehicle Dynamic Model

Conventional railway vehicles are equipped with two bogies for each body, of which, each bogie has two wheelsets. Suspension system that connects train car to the bogie is called the secondary suspension, and bogie to the wheelset suspension is called as primary suspension.

In the case of two–axle vehicle, it has been considered that the vehicle body is directly connected to the wheelset via a suspension system. Since there is an increasing trend in the industry to have the vehicle body directly fixed with the wheelset through an optimal suspension system, which will make the system much more mechanically simple with lower weight [2].

In the two–axle vehicle configuration presented in the Figure 3.8, it shows sets of spring–damper passive components fixed in the lateral side of the wheelsets which has $\frac{K_S}{2}$ as spring coefficient $\frac{C_S}{2}$ as damping coefficient for each spring and damper and four spring passive components are fixed in the longitudinal direction which has $\frac{k}{2}$ as spring coefficient for each spring [27].

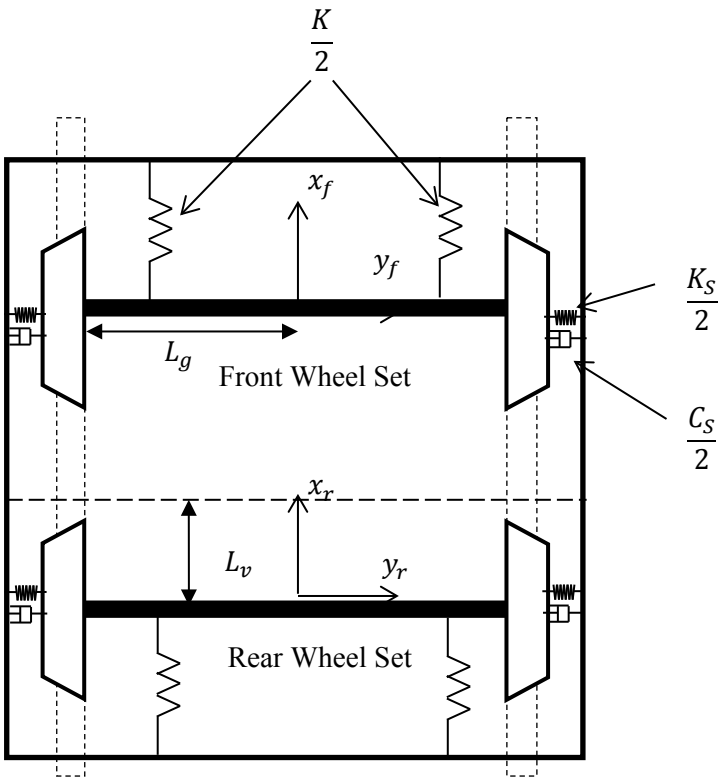

Figure 3. 8 – Two–axle Vehicle

Torque generated for the wheelsets from longitudinal stiffness (in the case of passive vehicle) can be derived by taking difference of yaw angles between the frame (ψ_v) and the wheelset (ψ_{fw} or ψ_{rw}) while it also has an effect from the curvature.

$$\tau_{f\_Yaw} = -{L_g}^2\, k \left(\psi_{fw} - \psi_v + \frac{L_v}{R_f}\right) \tag{34}$$

$$\tau_{r\_Yaw} = -{L_g}^2\, k \left(\psi_{rw} - \psi_v - \frac{L_v}{R_r}\right) \tag{35}$$

Forces generated from the front ($F_{B\_f\_Lat}$) and rear ($F_{B\_r\_Lat}$) wheelsets from lateral suspension can be derived from the difference in the displacements of the frame and the wheelsets generating force on the springs connected effects of the frame's yaw displacement and the impact of the curvature.

$$F_{B\_f\_Lat} = -K_S \left(y_{fw} - y_v - \psi_v . L_v - \frac{{L_v}^2}{R_f}\right) - C_S \left(\dot{y}_{fw} - \dot{y}_v - \dot{\psi}_v . L_v + \frac{{L_v}^2}{{R_f}^2}\right) \tag{36}$$

$$F_{B\_r\_Lat} = -K_S \left(y_{rw} - y_v + \psi_v . L_v - \frac{{L_v}^2}{R_r}\right) - C_S \left(\dot{y}_{rw} - \dot{y}_v + \dot{\psi}_v . L_v + \frac{{L_v}^2}{{R_r}^2}\right) \tag{37}$$

With all the derivations above, the dynamic motion equations of the wheelsets, car body can be concluded as below where $T_{L\_f\_Lon}$, $T_{R\_f\_Lon}$ and $T_{L\_f\_Lat}$, $T_{R\_f\_Lat}$ represents the longitudinal and lateral creep forces of the front wheelset respectively. Similar representation is done for the rear wheel as $T_{L\_r\_Lon}$, $T_{R\_r\_Lon}$ and $T_{L\_r\_Lat}$, $T_{R\_r\_Lat}$.

Front Wheelset:

Yaw Motion:

$$I_w \ddot{\psi}_{wf} = T_{L\_f\_Lon} L_g - T_{R\_f\_Lon} L_g + \tau_{f\_Yaw} \tag{38}$$

Lateral Motion:

$$m_w \ddot{y}_{wf} = T_{L\_f\_Lat} + T_{R\_f\_Lat} + F_M + F_C + F_{B\_f\_Lat} \tag{39}$$

Rear Wheelset:

Yaw Motion:

$$I_w \ddot{\psi}_{wr} = T_{L\_r\_Lon} L_g - T_{R\_r\_Lon} L_g + \tau_{r\_Yaw} \tag{40}$$

Lateral Motion:

$$m_w \ddot{y}_{wr} = T_{L\_r\_Lat} + T_{R\_r\_Lat} + F_M + F_C + F_{B\_r\_Lat} \tag{41}$$

Car Body:

Yaw Motion:

$$I_v \ddot{\psi}_v = -F_{B\_f\_Lat} L_v + F_{B\_r\_Lat} L_v - \tau_{f\_Yaw} - \tau_{r\_Yaw} \tag{42}$$

Lateral Motion:

$$m_v \ddot{y}_v = F_M + F_C - F_{B\_f\_Lat} - F_{B\_r\_Lat} \tag{43}$$

The lateral and yaw dynamic equations for the wheelsets and the vehicle body shown above can be represented as below in a generalised way. Abbreviations and the values of these variables depicting the generalised two axle vehicle model are elaborated in Appendix A.

Wheelset 1:

$$\begin{aligned} m_w \ddot{y}_{wf} + \left(\frac{2f_{22}}{V_S} + C_S\right)\dot{y}_{wf} + K_S y_{wf} - 2f_{22}\psi_f - C_S\dot{y}_v - K_S y_v - C_s L_v \dot{\psi}_v \\ - K_s L_v \psi_v = m_w \left(\frac{{V_S}^2}{R_f} - g\theta_f\right) \end{aligned} \tag{44}$$

$$\begin{aligned} I_w \ddot{\psi}_{wf} + \frac{2f_{11}{L_g}^2}{V_S}\dot{\psi}_{wf} + \frac{2f_{11}\lambda L_g}{r_0} y_{wf} \\ = \frac{2f_{11}{L_g}^2}{R_f} + \frac{2f_{11}\lambda L_g}{r_0} y_{tf} + I_w V_S \left(\dot{1/R_f}\right) + T_{wf} \end{aligned} \tag{45}$$

Wheelset 2:

$$m_w\,\ddot{y}_{wr} + \left(\frac{2f_{22}}{V_S} + C_S\right)\dot{y}_{wr} + K_S y_{wr} - 2f_{22}\psi_r - C_S\dot{y}_v - K_S y_v + C_S L_v\dot{\psi}_v + K_S L_v\psi_v = m_w\left(\frac{{V_S}^2}{R_r} - g\theta_r\right) \quad (46)$$

$$I_w\,\ddot{\psi}_{wr} + \frac{2f_{11}{L_g}^2}{V_S}\dot{\psi}_{wr} + \frac{2f_{11}\lambda L_g}{r_0}y_{wr} = \frac{2f_{11}{L_g}^2}{R_r} + \frac{2f_{11}\lambda L_g}{r_0}y_{tr} + I_w V_S\left(\dot{1/R_r}\right) + T_{wr} \quad (47)$$

Vehicle Body:

$$m_v\,\ddot{y}_v + 2C_S\dot{y}_v + 2K_S y_v - C_S\dot{y}_{wf} - K_S y_{wf} - C_S\dot{y}_{wr} - K_S y_{wr} = \frac{m_v{V_S}^2}{2}\left(\frac{1}{R_f} + \frac{1}{R_r}\right) - \frac{m_v g}{2}(\theta_f + \theta_r) \quad (48)$$

$$I_v\,\ddot{\psi}_v + 2{L_v}^2C_S\dot{y}_v + 2{L_v}^2K_S y_v - L_v C_S\dot{y}_{wf} + L_v C_S\dot{y}_{wr} - L_v K_S y_{wf} + L_v K_S y_{wr} = \frac{I_v V_S}{2}\left(\dot{1/R_f} + \dot{1/R_r}\right) - (T_{wf} + T_{wr}) \quad (49)$$

For Passive Suspension

$$T_{wf} = {L_g}^2 k\left(\psi_v - \psi_f + \frac{L_v}{R_f}\right) \quad (50)$$

$$T_{wr} = {L_g}^2 k\left(\psi_v - \psi_r - \frac{L_v}{R_r}\right) \quad (51)$$

In order to actively control the wheelset of the full bogie vehicle, the T_{wf}, T_{wr} terms in equation 45 and 47 will have to be replaced by the active control scheme.

3.4. Full Bogie Vehicle Dynamic Model

In the full bogie vehicle, which includes one vehicle body, two bogies and four wheelsets. Figure 3.9 shows sets of spring–damper passive components fixed in the lateral side of the wheelsets which has $\frac{K_{py}}{2}$ as spring coefficient $\frac{C_{py}}{2}$ as damping coefficient for each spring and damper while similarly $\frac{K_{sy}}{2}$ and $\frac{C_{sy}}{2}$ are for secondary suspension and four passive spring components are fixed in the longitudinal

direction which has $\frac{K_{px}}{2}$ as spring coefficient for each spring. In addition, $\frac{K_{px}}{2}$ is the secondary passive suspension in longitudinal direction [91].

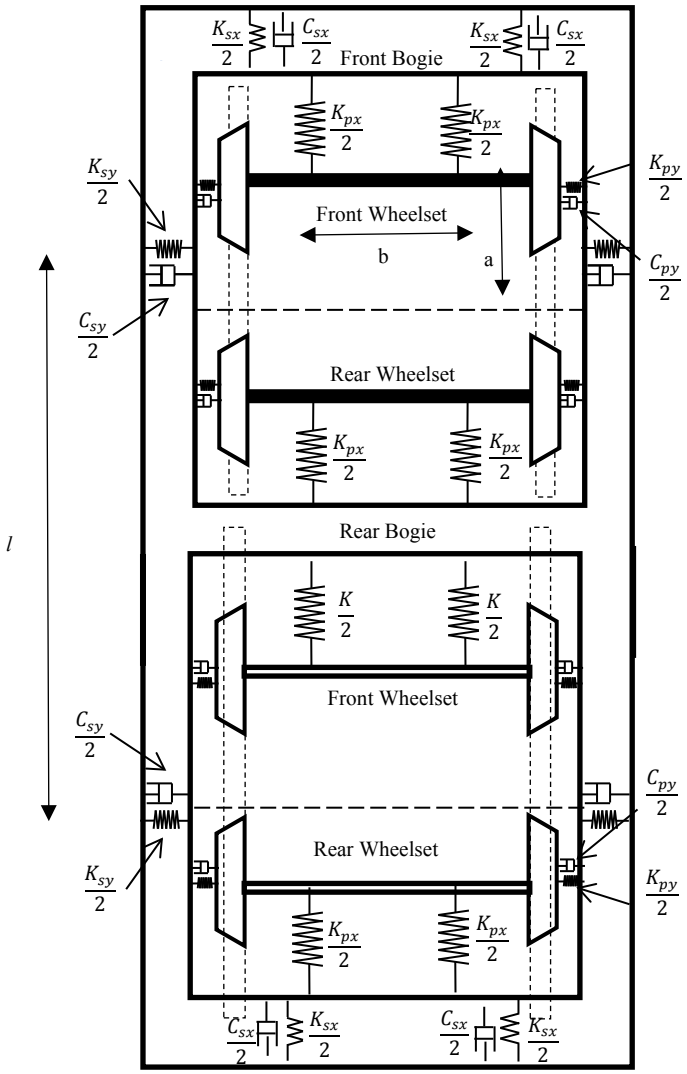

Figure 3. 9 – Full Bogie Vehicle

From including the dynamics of the two bogies and their lateral and longitudinal suspension to the two–axle vehicle model, full bogie vehicle model can be written as shown below. Significant difference from the former dynamic model and latter dynamic model is that it has an extra passive suspension in lateral direction connecting bogie to vehicle frame and an extra passive suspension in longitudinal direction between the bogie and the vehicle frame.

Abbreviations and the values of these variables depicting the conventional full bogie vehicle model are elaborated in Appendix A.

Wheelset 1:

$$M_w\ddot{y}_{w1} = K_{py}\left[y_{b1} + a\psi_{b1} - y_{w1}\right] + C_{py}\left[\dot{y}_{b1} + a\dot{\psi}_{b1} - \dot{y}_{w1}\right] - \frac{2f_{22}}{v}\dot{y}_{w1} + 2f_{22}\psi_{w1} + M_w\left(\frac{v^2}{R_1} - g\theta_1\right) \quad (52)$$

$$I_w\ddot{\psi}_{w1} = T_{w1} - \frac{2f_{11}b^2}{v}\dot{\psi}_{w1} - \frac{2f_{11}\lambda b}{r_0}\left(y_{w1} - y_{r1}\right) + \frac{2f_{11}b^2}{R_1} + I_w\, v\left(1/R_1\right)^{\cdot} \quad (53)$$

Wheelset 2:

$$M_w\ddot{y}_{w2} = K_{py}\left[y_{b1} - a\psi_{b1} - y_{w1}\right] + C_{py}\left[\dot{y}_{b1} - a\dot{\psi}_{b1} - \dot{y}_{w1}\right] - \frac{2f_{22}}{v}\dot{y}_{w2} + 2f_{22}\psi_{w2} - M_w\left(\frac{v^2}{R_2} - g\theta_2\right) \quad (54)$$

$$I_w\ddot{\psi}_{w2} = T_{w2} - \frac{2f_{11}b^2}{v}\dot{\psi}_{w2} - \frac{2f_{11}\lambda b}{r_0}\left(y_{w2} - y_{r2}\right) + \frac{2f_{11}b^2}{R_2} + I_w\, v\left(1/R_2\right)^{\cdot} \quad (55)$$

Wheelset 3:

$$M_w\ddot{y}_{w3} = K_{py}\left[y_{b2} + a\psi_{b2} - y_{w3}\right] + C_{py}\left[\dot{y}_{b2} + a\dot{\psi}_{b2} - \dot{y}_{w3}\right] - \frac{2f_{22}}{v}\dot{y}_{w3} + 2f_{22}\psi_{w3} - M_w\left(\frac{v^2}{R_3} - g\theta_3\right) \quad (56)$$

$$I_w\ddot{\psi}_{w3} = T_{w3} - \frac{2f_{11}b^2}{v}\dot{\psi}_{w3} - \frac{2f_{11}\lambda b}{r_0}\left(y_{w3} - y_{r3}\right) + \frac{2f_{11}b^2}{R_3} + I_w\, v\left(1/R_3\right)^{\cdot} \quad (57)$$

Wheelset 4:

$$M_w\ddot{y}_{w4} = K_{py}\left[y_{b2} - a\psi_{b2} - y_{w4}\right] + C_{py}\left[\dot{y}_{b2} - a\dot{\psi}_{b2} - \dot{y}_{w4}\right] - \frac{2f_{22}}{v}\dot{y}_{w4} + 2f_{22}\psi_{w4} - M_w\left(\frac{v^2}{R_4} - g\theta_4\right) \quad (58)$$

$$I_w\ddot{\psi}_{w2} = T_{w4} - \frac{2f_{11}b^2}{v}\dot{\psi}_{w4} - \frac{2f_{11}\lambda b}{r_0}\left(y_{w4} - y_{r4}\right) + \frac{2f_{11}b^2}{R_4} + I_w\, v\left(1/R_4\right)^{\cdot} \quad (59)$$

Bogie 1:

$$\begin{aligned} M_b\ddot{y}_{b1} = {} & K_{sy}\left[y_c + l\psi_c - y_{bi}\right] + C_{sy}\left[\dot{y}_c + l\dot{\psi}_c - \dot{y}_{b1}\right] - K_{py}\left[y_{b1} + a\psi_{bi} - y_{w1}\right] \\ & - C_{py}\left[\dot{y}_{bi} + a\dot{\psi}_{b1} - \dot{y}_{w1}\right] - K_{py}\left[y_{b1} - a\psi_{b1} - y_{w2}\right] \\ & - C_{py}\left[\dot{y}_{b1} - a\dot{\psi}_{b1} - \dot{y}_{w2}\right] + \frac{M_b v^2}{2}\left(\frac{1}{R_1} + \frac{1}{R_2}\right) - \frac{M_b g}{2}(\theta_1 + \theta_2) \end{aligned} \tag{60}$$

$$\begin{aligned} I_b\ddot{\psi}_{b1} = {} & K_{sx}{b_1}^2\left(\psi_c - \psi_{b1}\right) + C_{sx}{b_1}^2\left(\dot{\psi}_c - \dot{\psi}_{b1}\right) - K_{py}a\left[y_{b1} + a\psi_{b1} - y_{w1}\right] \\ & - C_{py}a\left[\dot{y}_{b1} + a\dot{\psi}_{b1} - \dot{y}_{w1}\right] + K_{py}a\left[y_{b1} - a\psi_{bi} - y_{w2}\right] \\ & + C_{py}a\left[\dot{y}_{b1} - a\dot{\psi}_{bi} - \dot{y}_{w2}\right] + \frac{I_b v}{2}\left(\dot{1/R_1} + \dot{1/R_2}\right) - (T_{w1} + T_{w2}) \end{aligned} \tag{61}$$

Bogie 2:

$$\begin{aligned} M_b\ddot{y}_{b2} = {} & K_{sy}\left[y_c - l\psi_c - y_{b2}\right] + C_{sy}\left[\dot{y}_c - l\dot{\psi}_c - \dot{y}_{b2}\right] - K_{py}\left[y_{b2} + a\psi_{b2} - y_{w3}\right] \\ & - C_{py}\left[\dot{y}_{b2} + a\dot{\psi}_{b2} - \dot{y}_{w3}\right] - K_{py}\left[y_{b2} - a\psi_{b2} - y_{w4}\right] \\ & - C_{py}\left[\dot{y}_{b2} - a\dot{\psi}_{b2} - \dot{y}_{w4}\right] + \frac{M_b v^2}{2}\left(\frac{1}{R_3} + \frac{1}{R_4}\right) - \frac{M_b g}{2}(\theta_3 + \theta_4) \end{aligned} \tag{62}$$

$$\begin{aligned} I_b\ddot{\psi}_{b2} = {} & K_{sx}{b_1}^2\left(\psi_c - \psi_{b2}\right) + C_{sx}{b_1}^2\left(\dot{\psi}_c - \dot{\psi}_{b2}\right) - K_{py}a\left[y_{b2} + a\psi_{b2} - y_{w3}\right] \\ & - C_{py}a\left[\dot{y}_{b2} + a\dot{\psi}_{b2} - \dot{y}_{w3}\right] + K_{py}a\left[y_{b2} - a\psi_{b2} - y_{w4}\right] \\ & + C_{py}a\left[\dot{y}_{b2} - a\dot{\psi}_{b2} - \dot{y}_{w4}\right] + \frac{I_b v}{2}\left(\dot{1/R_3} + \dot{1/R_4}\right) \\ & - (T_{w3} + T_{w4}) \end{aligned} \tag{63}$$

Vehicle Body:

$$\begin{aligned} M_c\ddot{y}_c = {} & -K_{sy}\left[y_c + l\psi_c - y_{b1}\right] - K_{sy}\left[y_c - l\psi_c - y_{b2}\right] - C_{sy}\left[\dot{y}_c + l\dot{\psi}_c - \dot{y}_{b1}\right] \\ & - C_{sy}\left[\dot{y}_c - l\dot{\psi}_c - \dot{y}_{b2}\right] + \frac{M_c v^2}{4}\left(\frac{1}{R_1} + \frac{1}{R_2} + \frac{1}{R_3} + \frac{1}{R_4}\right) \\ & - \frac{M_c g}{4}(\theta_1 + \theta_2 + \theta_3 + \theta_4) \end{aligned} \tag{64}$$

$$\begin{aligned} I_c\ddot{\psi}_c = {} & -K_{sy}l\left[y_c + l\psi_c - y_{b1}\right] + K_{sy}l\left[y_c - l\psi_c - y_{b2}\right] - C_{sy}l\left[\dot{y}_c + l\dot{\psi}_c - \dot{y}_{b1}\right] \\ & + C_{sy}l\left[\dot{y}_c - l\dot{\psi}_c - \dot{y}_{b2}\right] + \frac{I_c v}{4}\left(\dot{1/R_1} + \dot{1/R_2} + \dot{1/R_3} + \dot{1/R_4}\right) \\ & - K_{sx}{b_1}^2\left(\psi_c - \psi_{b1}\right) - C_{sx}{b_1}^2\left(\dot{\psi}_c - \dot{\psi_{b1}}\right) - K_{sx}{b_1}^2\left(\psi_c - \psi_{b2}\right) \\ & - C_{sx}{b_1}^2\left(\dot{\psi}_c - \dot{\psi_{b2}}\right) \end{aligned} \tag{65}$$

To actively control the wheelset of the full bogie, the T_{w1} to T_{w4} terms in above equations 53, 55, 57, 59, 61 and 63 will have to be replaced by the active control scheme. Passive suspension torques for the wheelsets are as below,

For Passive Suspension:

$$T_{w1} = K_{px} b^2 \left(\psi_{b1} - \psi_{w1} + \frac{l + a}{R_1} \right) \tag{66}$$

$$T_{w2} = K_{px} b^2 \left(\psi_{b1} - \psi_{w2} - \frac{l - a}{R_2} \right) \tag{67}$$

$$T_{w3} = K_{px} b^2 \left(\psi_{b2} - \psi_{w3} + \frac{l - a}{R_3} \right) \tag{68}$$

$$T_{w4} = K_{px} b^2 \left(\psi_{b2} - \psi_{w4} - \frac{l + a}{R_4} \right) \tag{69}$$

3.5. Track Inputs

It is important to evaluate the vehicles on both generic straight track with lateral irregularities and as well as curved tracks. There are seven different track data sets used in the research. One is a computer–generated lateral irregularity track representing a more generic case of track irregularity with a broad spectrum of lateral irregularity frequencies which is used for the optimisation of the actuator parameters, while the other four measured straight tracks sets with lateral irregularity [92] which are from measured data from four different sections of tracks between Paddington and Bristol stations in the UK which are used to assess the overall performances as depicted in the later part of the paper. During the analysis with computer generated generic straight track with lateral irregularities, vehicle travels at a high–speed of 300 km/h while mid–speed of 180 km/h is used for the measured tracks.

In addition, three curved tracks are used to assess the curving dynamics and the tracks are defined as tight–curvature track radius of 300 m, mid– curvature of 1500 m and a high–curvature of 3500 m with a cant angle of 6^0 [93]. Speeds for these curved tracks are considered as low–speed (90 kmh^{-1}), mid–speed (180 kmh^{-1}) and high–speed (300 kmh^{-1}) respectively. In order to evaluate the system in the worst possible case, transition period (at both ends) in the deterministic/curved track are kept for 2 seconds duration (since generic curved tracks have 2–3 seconds transition time). As mention before, this chapter only contains results with the curved track since more thorough comparison with both generic straight track and curved track are conducted in the next chapter once active control is introduced.

3.5. Performance Evaluation with Passive Suspension (Model Verification)

In order to proceed further in the study, these derived dynamics equations for the two–axle vehicle model and full bogie vehicle model are implemented in the simulation platform MATLAB Simulink for analysing purposes with the passive suspension.

Curvature and Cant angle used in these validation simulations are 300 m and 6^0 as shown below and these are given as inputs as $^1/_R$ and θ as shown in Figure 3.10 and Figure 3.11.

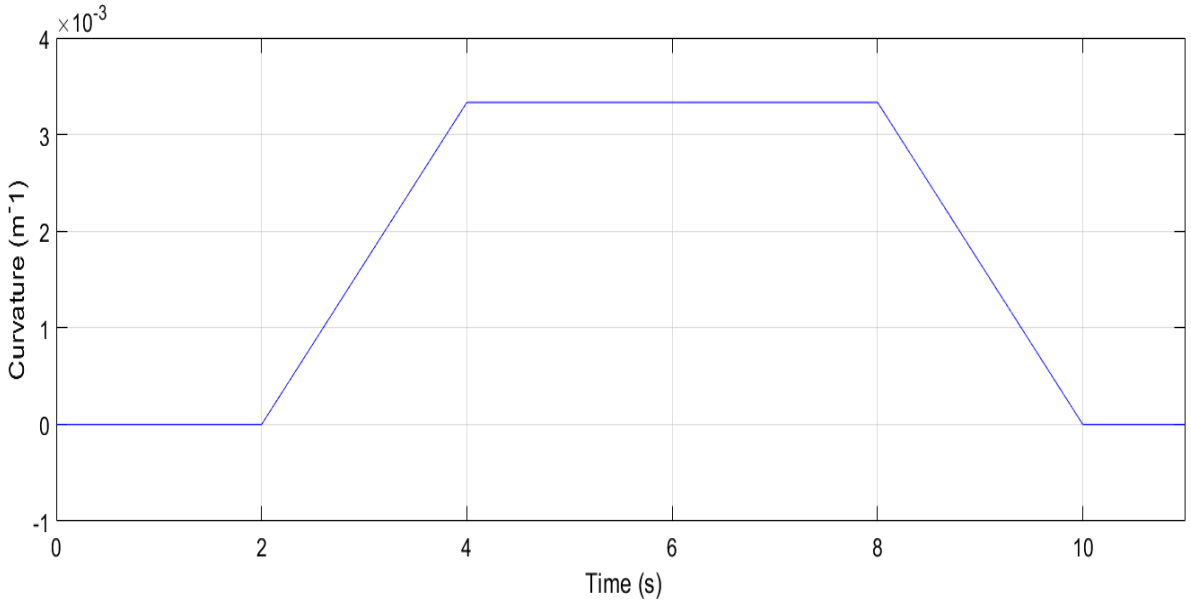

Figure 3. 10 – Curvature Input

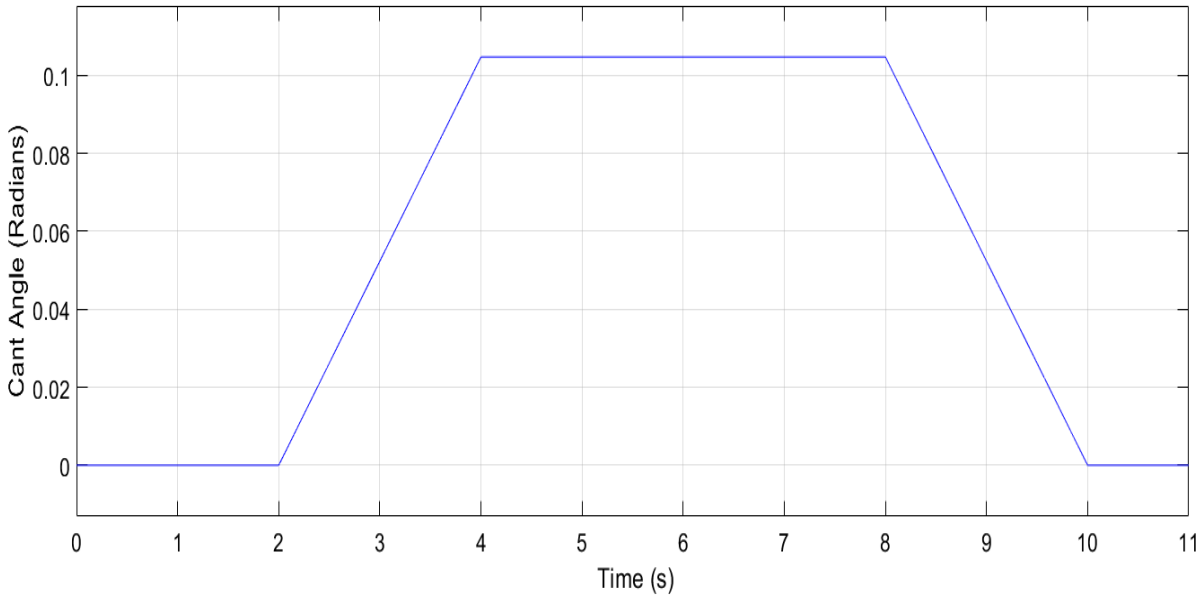

Figure 3. 11 – Cant Angle Input

3.5.1. Two–Axle Wheelset Vehicle

Below Figure 3.12 to 3.17 show the lateral displacement, yaw angle displacement and creep forces of the two–axle vehicle wheelsets/vehicle during the slow speed curved track.

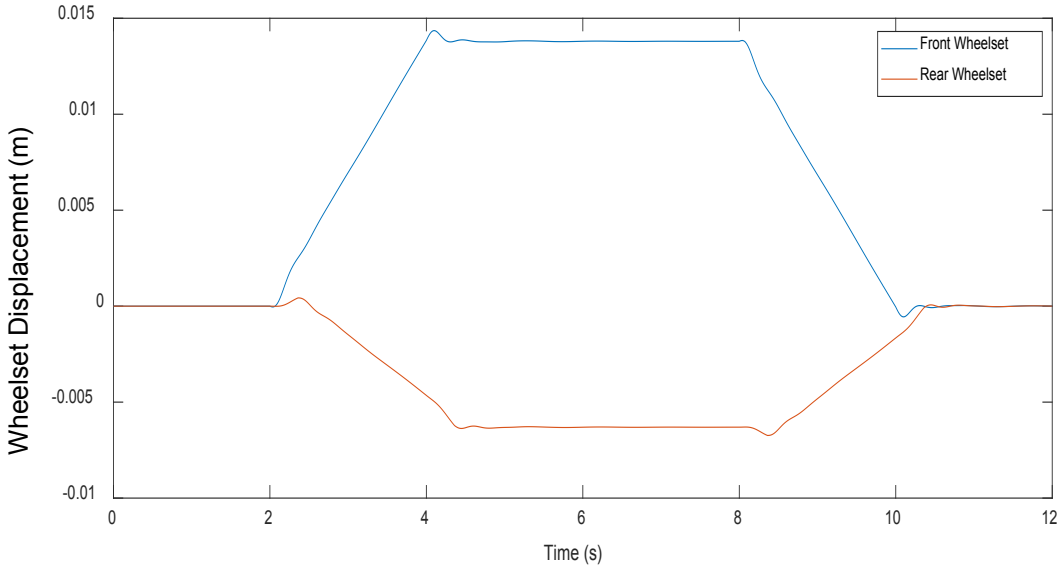

Figure 3. 12 – Two–axle Vehicle – Wheelset Displacement

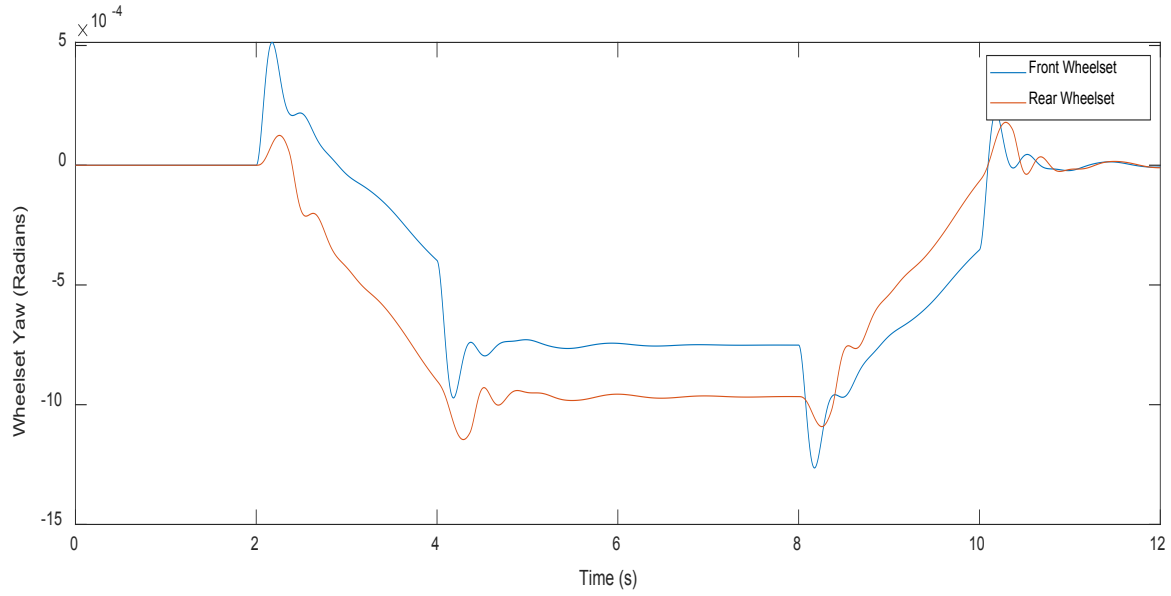

Figure 3. 13 – Two–axle Vehicle – Wheelset Yaw

As expected, it can be seen that the front wheelset (Figure 3.12) has a large variation in displacement when approaching the curve. This occurs due to the centrifugal force caused by the curvature and it is a necessity to have a displacement in the wheelset so that the outer wheel has a higher contact wheel radius while the inner wheel has a smaller contact radius. Conventional wheelsets (solid–axle) are capable of varying the contact radius due their coned profiles [7] and this configuration allow the vehicle to have variable angular speeds in wheels, (without using a differential such as ones used in road vehicles) so that sliding/slipping does not occur. Rear wheelset is having a displacement in the opposite direction, since the vehicle body is already aligned to the curve and primary passive suspension causes the rear wheelsets to be pushed inward towards the curve. Same wheelset behaviour has been encountered by prior studies on this topic and authors have stated that this occurrence is due to the high longitudinal stiffness adversely affecting the natural movement of the rear wheelset when travelling on tight curves [2, 7]. In addition, there is approximately 15 mm displacement in the front rail while there is approximately 5 mm displacement in the real wheelset on the opposite direction. In the real case, having a 15 mm displacement is not possible due to the restrictions of wheel flanges (not modelled here). Yaw angles of the both wheelsets (Figure 3.13) have same direction and approximately similar values. This dynamic behaviour is can be expected since both wheelsets are travelling in the same curvature while there is more distance between the wheelsets and these similar yaw angles results is similar lateral creep forces which acts against centrifugal forces on the curved track.

It can be seen that lateral creep forces (Figure 3.14) are in the same direction for both wheelsets while longitudinal creep forces (Figure 3.15) have opposite directions. These lateral creep forces occur as a reaction force to the centrifugal force which the vehicle is experiencing during the curved track and the total of lateral creep forces in the wheelsets are equal to the centrifugal force. On the other hand,

longitudinal creepage with different directions occur due the difference in the direction of displacements, where front wheelsets experience the creep force as negative while the rear wheelset as positive.

These phenomena can be intuitively understood using the reference frame considered for the dynamic equations (Figure 3.1) and Figure 3.13 which depicts wheelset displacement. Since the front wheelset has a positive displacement, it moves outwards of the curvature and it results in outward wheel having larger rolling radius than the inner wheel. On the rear wheel, opposite phenomenon takes place since it has negative displacement. With high longitudinal passive suspension, wheelsets are restricted to achieve pure rolling rates and these high creep forces occur. In addition, it can be seen that the creep forces generated during travel on the curved track on both longitudinal and lateral directions (approximately 20 kN and 80 kN respectively) are significantly high. Especially the high longitudinal creep forces result in wear and fatigue of both the wheelsets as well as the track and this can be eliminated/reduced using active control [2].

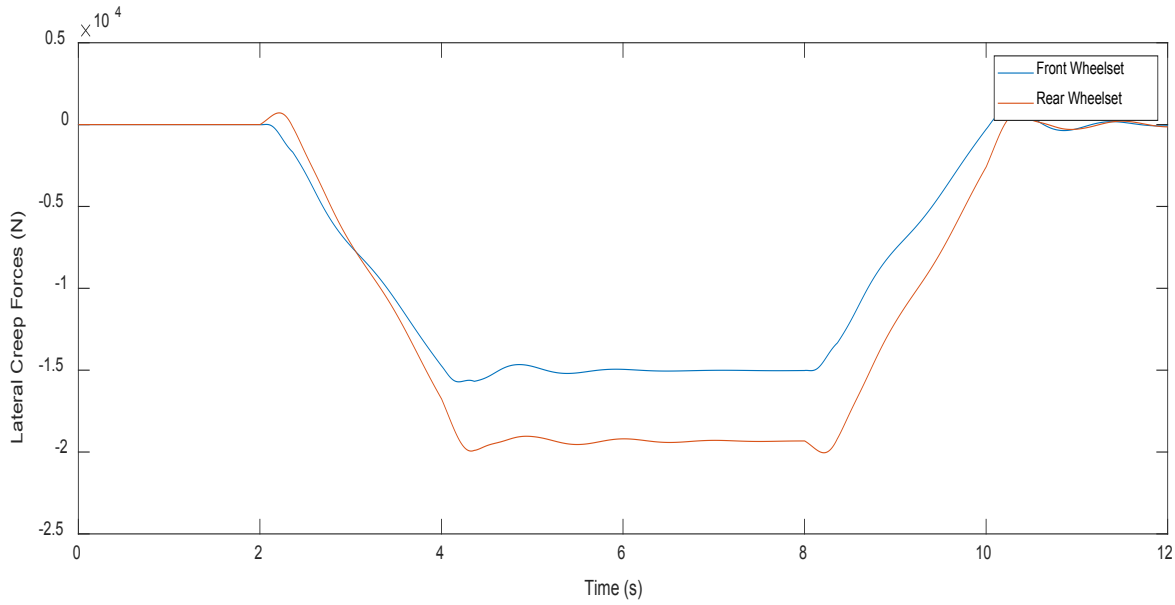

Figure 3. 14 – Two–axle Vehicle – Lateral Creep Forces

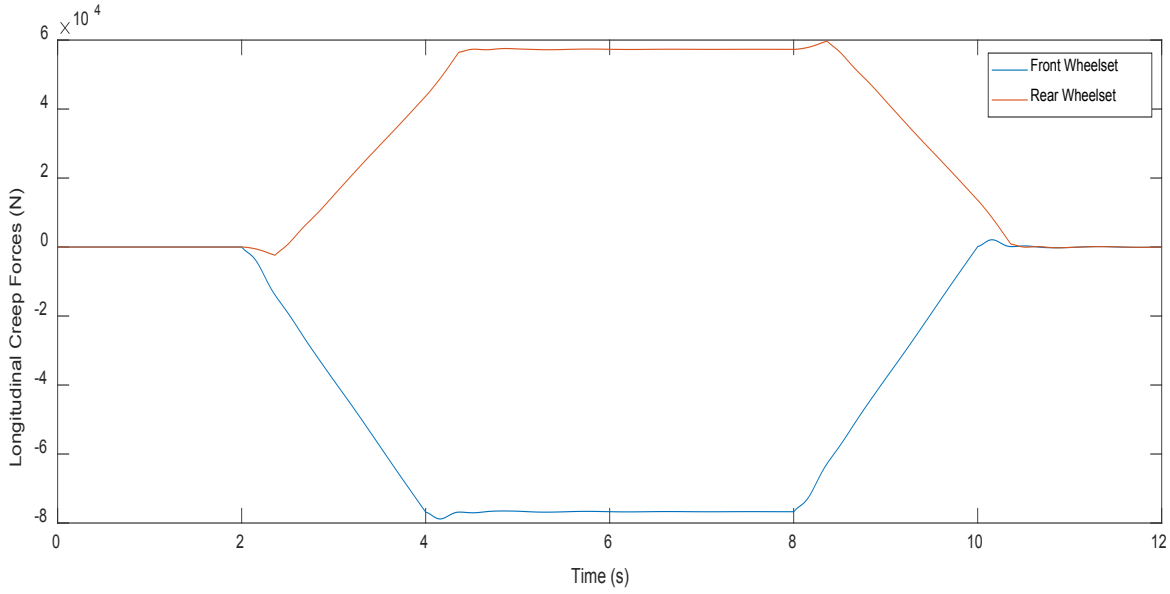

Figure 3. 15 – Two–axle Vehicle – Longitudinal Creep Forces

When analysisng the dynamic behavior of the vehicle body, from the Figure 3.16 and 3.17, it can be seen that the curve transistions are relativly smooth in both lateral and yaw direcitions.

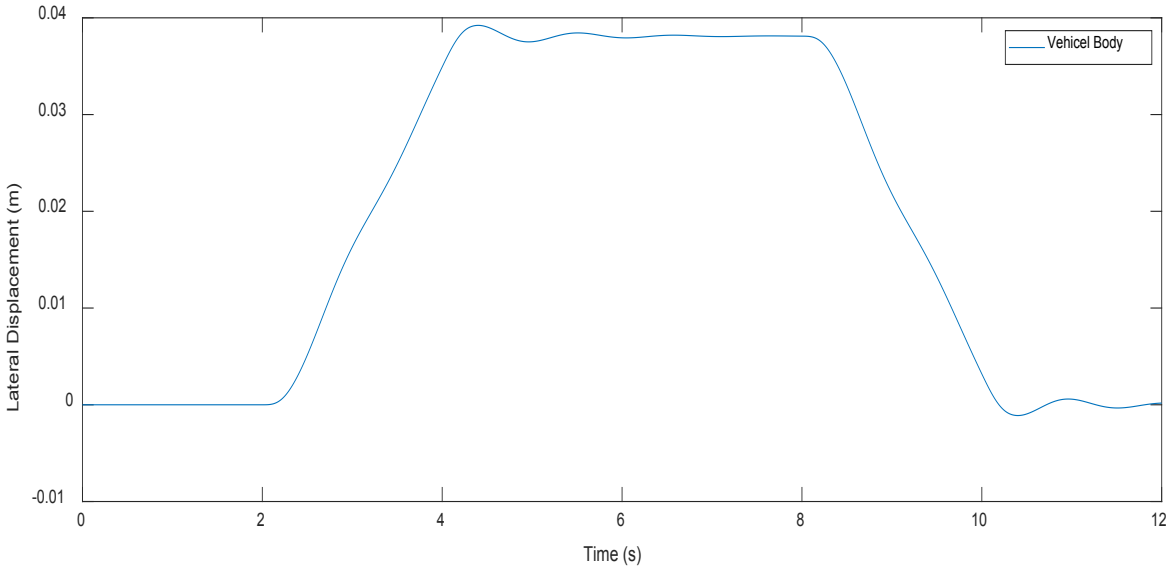

Figure 3. 16 – Two–axle Vehicle – Vehicle Body Lateral Displacement

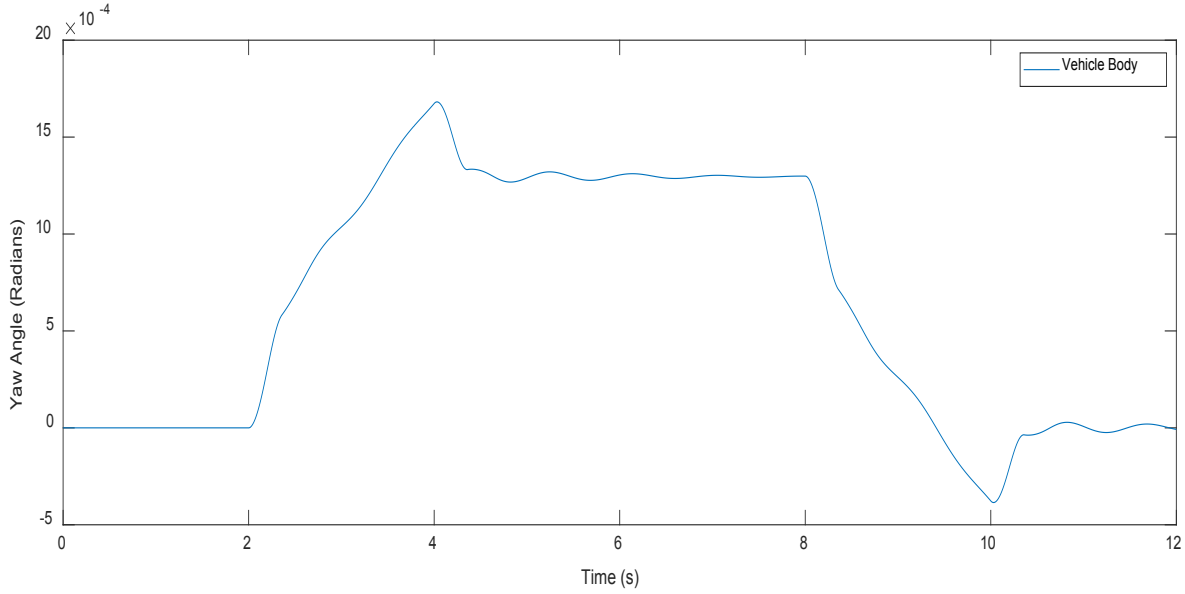

Figure 3. 17 – Two–axle Vehicle – Vehicle Body Yaw

Since the dynamic behaviours of the wheelsets of the two–axle vehicle on the curved track are initiative and follow the same pattern depicted by prior studies [94], it is feasible to accept the simplified model of the two–axle vehicle as accurate.

3.5.2. Full Bogie Vehicle

Similer to the two–axle vehicle, below figure 3.18 to 3.28 shows the lateral displacement, yaw angle displacement and creep forces of the bogie vehicle wheelsets during the curved track.

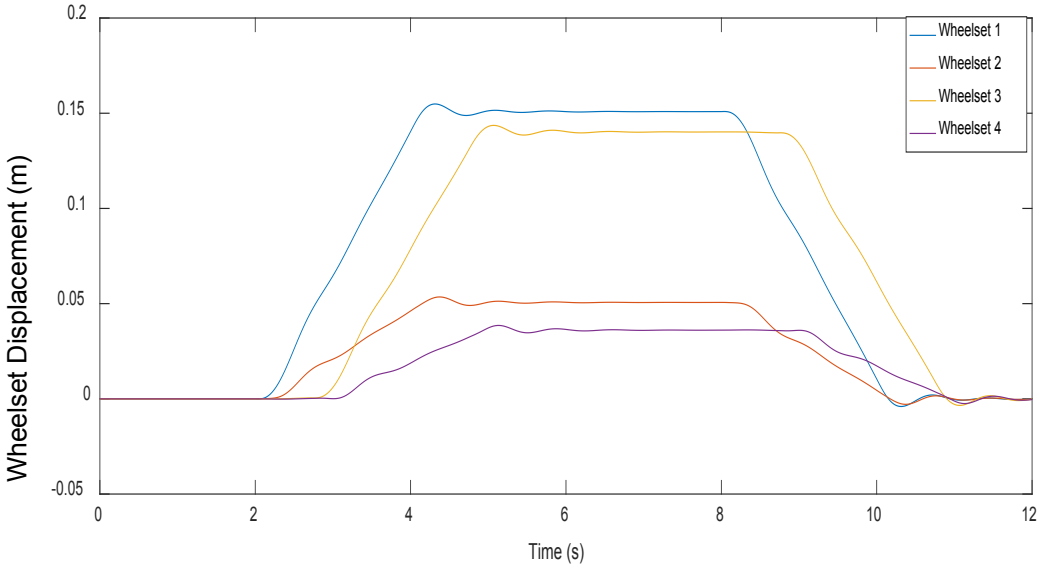

Figure 3. 18 – Full Bogie Vehicle – Wheelset Displacement

It can be seen from the above Figures 3.18 that there is a significant amount of displacement in the front wheelsets of the bogies (approximatly 15 mm) during the slow speed curved track (In a real senario, wheel flanges will be contacted before these significantly high displacements occure for safety of the vehicle) while the rear wheelsets of the bogies are having a relativly low displacment (approximatly 5 mm). Similar to the two–axle vehicle, this phenomenon occures due to the centrifugal force due to the curvature and once the first weelsets enter the curve, it affect the lateral displacment of the bogie and passive springs between bogie and the wheelsets are pushing the rear wheelsets to be allighned with the curve, so that they have a lower displacement. However, when compared with the two–axle vehicle dynamics, even with passive suspension, bogie vehicle has better displacment since the wheelsts are having displacment in the same direction unilike the two–axle vehicle which has opposite direction difflections of front and rear wheelsets due to high stiffness of passive suspension (Figure 3.12). This can be expected since the distance between the wheelsets are lower in the bogie vehicle than the two–axle vehicle.

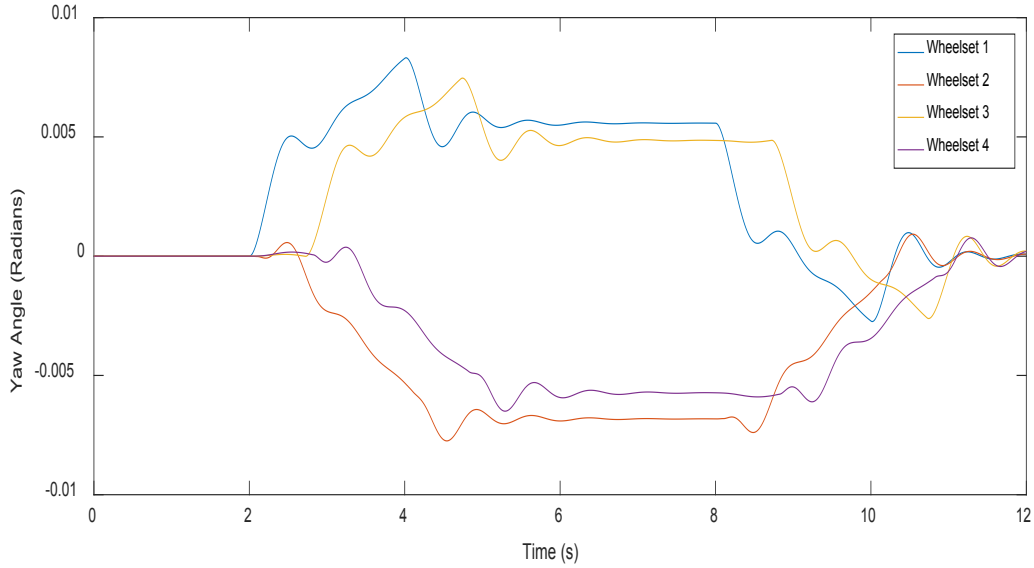

Figure 3. 19 – Full Bogie Vehicle – Wheelset Yaw

Yaw angles of the wheelsets are also intuative since the front and rear wheelsets of the bogie are having different oriantations. This is expected due the tight curve and unlike the two–axle vehicle, the distance between the wheelsets are low. So the passive stiffness is causing the front and rear wheelsets to have yaw angles in opposite direction for the wheelsets when negotiating the curved track.

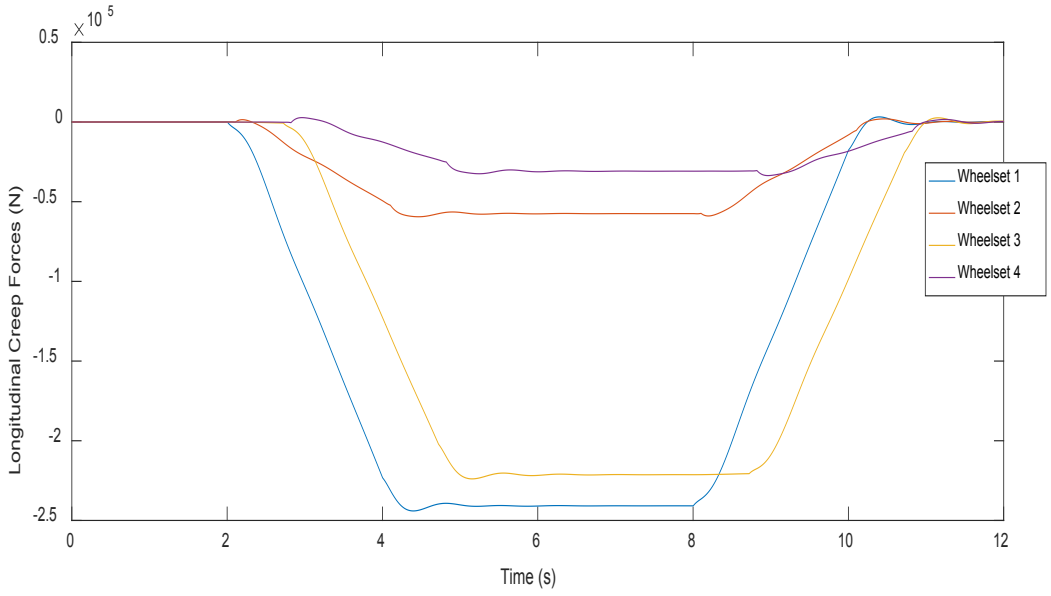

Figure 3. 20 – Full Bogie Vehicle – Longitudinal Creep Forces

From assessing Figure 3.20 and Figure 3.21, it can be seen that these creep forces rear wheelsets have a lower creep force compared to the front wheelsets and from further analysis it is found that this

caused by the creep lower lateral displacements of the rear wheelsets. Thus, the creep forces of a bogie vehicle, when travelling on a curved track, is different than that of a two–axle vehicle since the wheelset lateral displacement and yaw behaviour is deferent.

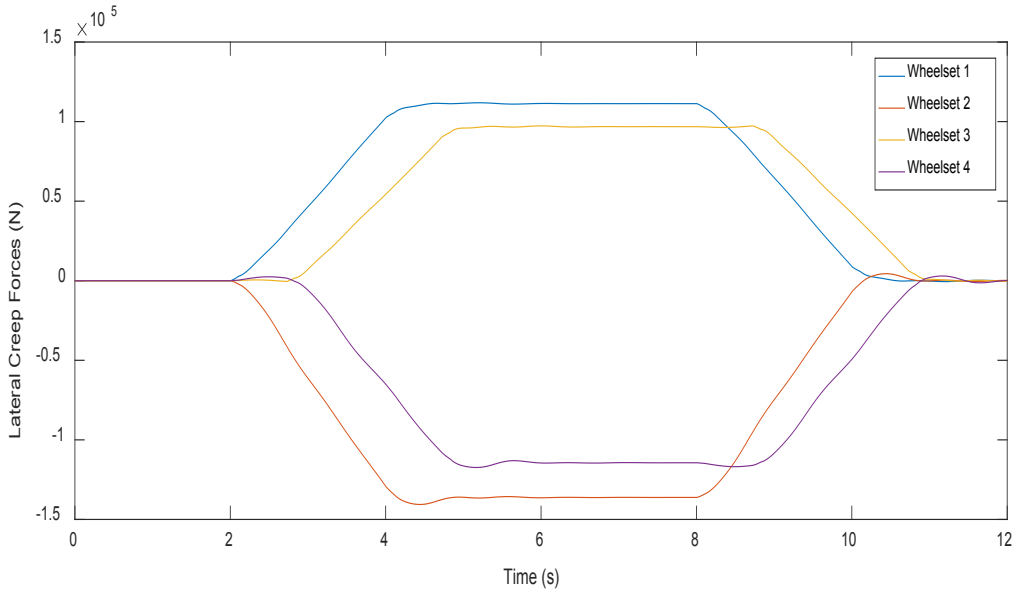

Figure 3. 21 – Full Bogie Vehicle – Lateral Creep Forces

As elaborated above these lateral creep forces occur as a reaction force to the centrifugal force of the curved track. However, in this case reaction forces are not equally distributed among the front and rear wheelsets like the two–axle vehicle results since the passive suspension is not allowing the wheelsets to have same angle of attack. Thus, due to the opposite yaw, lateral creep forces have occurred similar to the yaw behaviour which has almost the same value with opposite direction.

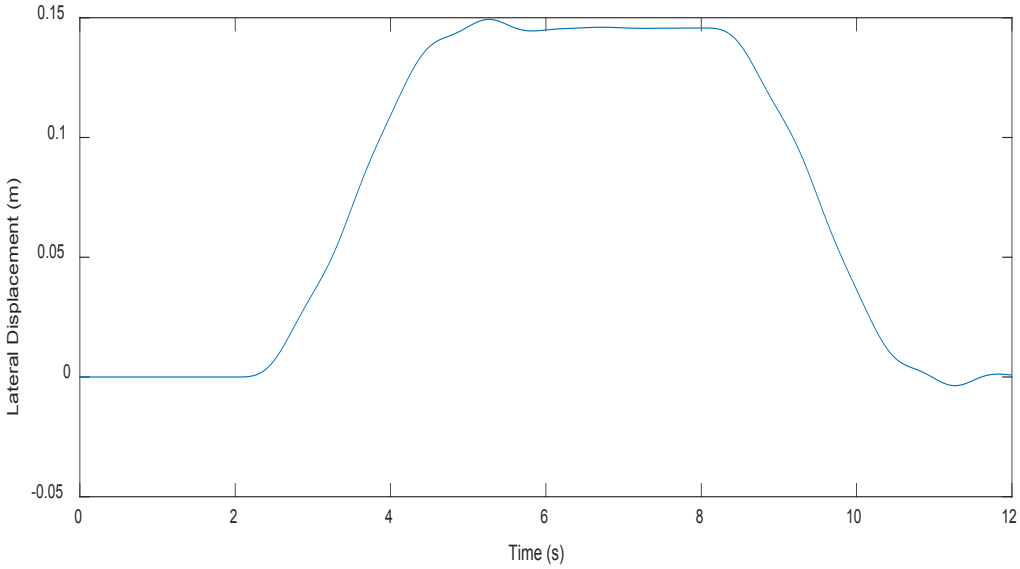

Figure 3. 22 – Full Bogie Vehicle – Vehicle Body Lateral Displacement

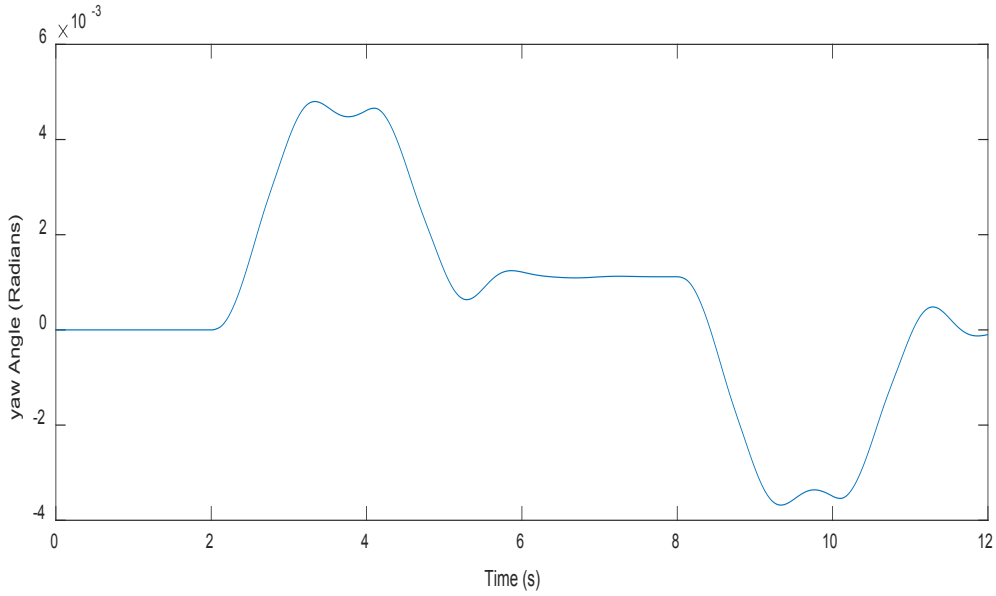

Figure 3. 23 – Full Bogie Vehicle – Vehicle Body Yaw

It can be seen from the above Figures 3.22 and 3.23 that vehicle body is experiencing relatively smooth transition from both lateral and yaw aspects.

Since the dynamic behaviours of the wheelsets of the full bogie vehicle on the curved track can be explained as per the model equations and intuitiveness, it is possible to accept the simplified model of the bogie vehicle as accurate.

CHAPTER 4: ACTIVE CONTROL STRATEGY

4.1. Introduction

At the literature review stage of this research, a number of active control configurations and schemes for full active primary suspension are assessed thoroughly to identify a suitable configuration and scheme for this particular research while a thorough review on suitable actuator technologies is also conducted in order to select a suitable actuator technology (such as electro–mechanical, hydraulic, etc.) for this application of active wheelset control in primary suspension.

Thus, based on the findings from previous literature, overall active control system is designed as per control architecture shown in Figure 4.1 with actuated solid–axle wheelsets (ASW) configuration for both two–axle vehicle and the full bogie vehicle with absolute stiffness control scheme where EM actuators are being used to deliver the actuation.

Two–axle vehicle is assessed in the study due to its mechanical simplicity and low weight while full bogie vehicle is evaluated since it is a conventional vehicle arrangement widely used in the industry. In addition, by analysing/comparing the effects of the active controller and the actuator (developed in this research) having on both vehicle arrangements, further insight in to dynamics between the vehicle and the active wheelset control can also be examined.

ASW configuration is selected for the study in this case since it is commonly used and more acceptable in the rail industry compared to the other methods such as AIRW, DIRW, etc. Hence it is thought that this method holds more potential to be realistically implemented in the industry due to its simplicity and good track record in previous studies [2].

As it can be seen from the Figure 4.1, there are two feedback loops for controlling the wheelsets and actuators, respectively, when the vehicle is excited with lateral track inputs. Feedback is obtained from the wheelset to control the wheelset stability and curving performances while a local actuator controller is used to effectively control the actuator performances. Since the aim of this research is to design and optimise an actuator for active wheelset control, the main focus here is on the actuator controller and the actuator model.

Although Figure 4.1 depicts the system only for two–axle vehicle, same arrangement can be extended for the full bogie vehicle.

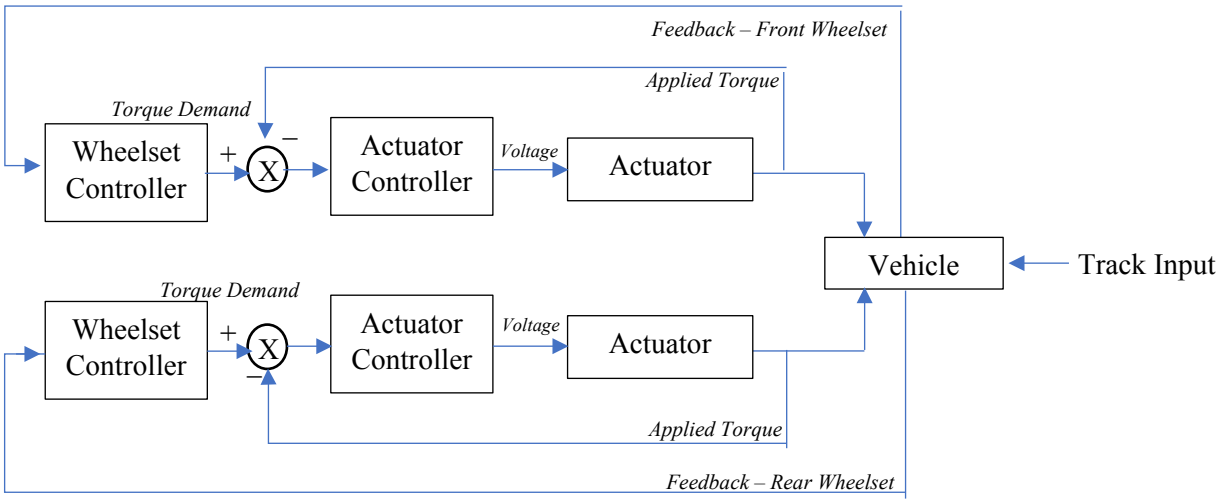

Figure 4. 1 – Overall Control Architecture

4.2. Wheelset Controller

The selection of a control scheme for active wheelset control can be achieved by focussing on the control mission of stability, curving and guidance. Since ASW has been selected for the research, classical control strategies, such as active damping and absolute stiffness can provide controllability for both the stability and curving while model–based control strategies such as H∞ and optimal control can also be used for these purposes [66] as an integrated solution.

However, the absolute stiffness–skyhook approach is selected for this research due to its simplicity of implementation and this research is targeted toward full active solutions where wheelsets do not have any passive stabilisation in yaw mode (which will require active steering for better curving). In this method control effort is produced for each wheelset using absolute yaw angle feedback from the wheelsets. The absolute yaw angle measurement required for this strategy can be obtained using several methods, such as (as thoroughly discussed in the literature review), double integration of the yaw acceleration measurement, or obtained through the use of state estimation which may be based on measurements from sensors mounted on the bogie/body frames [2]. However, the most convenient way is to obtain the measurement is by exploring the characteristics of spring–mass seismic accelerometers since output signals from this type of sensor represent the yaw acceleration of the measured wheelsets at frequencies below the natural frequency of the sensor, while measurements above the natural frequency of the sensor output represent the absolute yaw angle. Thus, by selecting a sensor with a lower natural frequency than the frequency of the wheelsets in dynamic mode (approximately 6–7 Hz), feedback measurements can be easily obtained [51].

Furthermore, this study particular focuses on the actuation task of the control system and thus assumes that accurate absolute yaw angles are obtained using one of the above methods and measurements are readily available for the system.

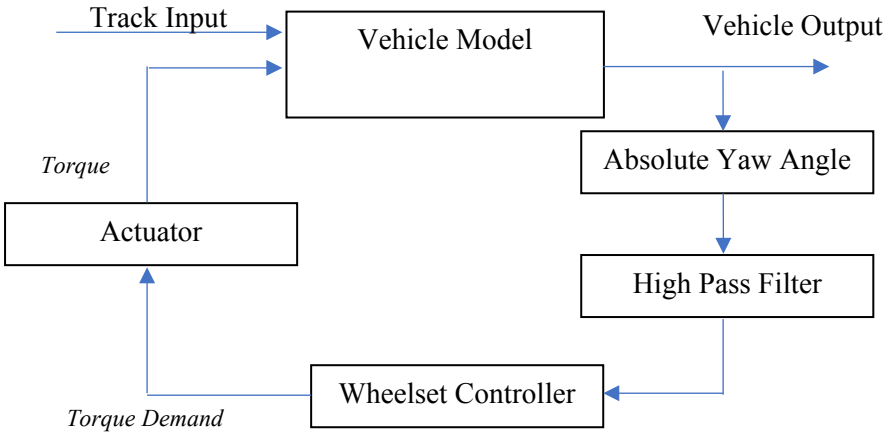

Figure 4. 2 – Wheelset Controller

With all full active stability control configuration for wheelsets, it is essential that natural of curving of wheelsets with curved tracks are not hindered. This is achieved in this case by filtering the feedback of the absolute yaw angle such that controller is not acting against the natural curving dynamics of the wheelsets. Hence, as shown in the Figure 4.2, it is crucial to filter the yaw absolute yaw measurement ($\psi_{Absolute}$) of the wheelsets to remove any low frequency components (which are from natural movements of the wheelsets) from that feedback prior being processed in the control scheme as depicted in Equation 70 in the continuous (S) domain. Unless filtered, active control system acts against the wheelset's natural yaw movements for curving and it will result in undesirable creep forces to those seen with the passive suspension.

$$\psi_{Absolute} \times \left(\frac{S}{S+\omega_c}\right) \tag{70}$$

Bode Plot of the High-Pass Filter:

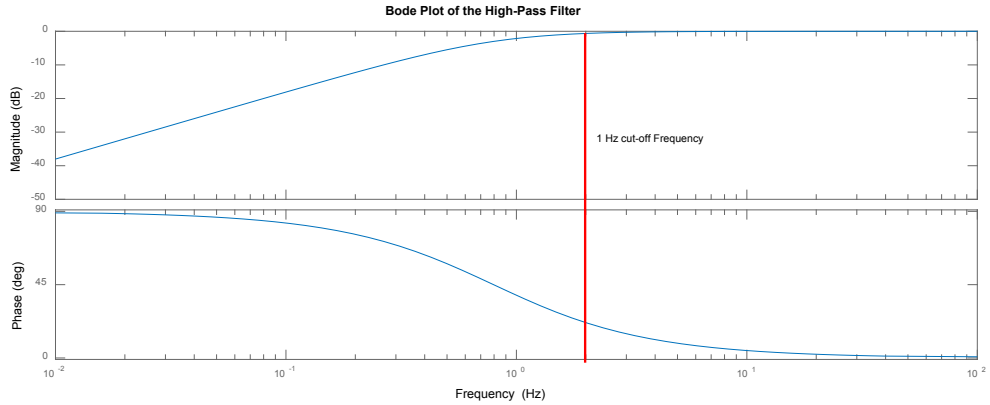

Figure 4. 3 - Bode Plot of the High-Pass Filter

Since the absolute yaw angle is the feedback in this wheelset control scheme which uses to compute the control effort, a first order high pass filter with a cut-off frequency (ω_c) as shown in equation 70, is used in this case to remove the low frequency signals ($< 1\ Hz$) of the absolute yaw angle measurement such that the controller is only reacting to the high frequency components while the wheelsets are unconstrained for curving motion. Effect of this high pass filter can also be seen from the bode plot of the filter as depicted in Figure 4.3. It is evident from the gain and phase plots that low frequency signals ($< 1\ Hz$) are attenuated while gain of the signals with higher frequency is 0 dB (equal magnitudes of input-output signals).

As shown in Figure 4.2, in this control scheme, only the absolute yaw angles of the wheelsets are considered instead of the relative yaw angle of the wheelset and train body, and this angle is fed back to the controller with a negative gain to generate the required control effort demand. Although the basic idea behind the absolute stiffness control strategy only uses proportional gain, in this study a derivative term is also included to increase the stability margin by increasing the damping in the system. This enables a trade–off between the gains for the controller to allow rapid responses with lower oscillations (frequency) and greater stability.

$$Control\ Effort\ (T_w) \quad = -\left[k_P\ \psi_w + k_D\ \dot{\psi}_w\right] \tag{71}$$

In order to find suitable control gains (proportional – k_P and derivative – k_D) for the wheelset controllers, such that stability and desired damping (approximately 25%) can be attainted for the wheelsets, poles of the closed–loop multiple–input multiple–output (MIMO) system can be assessed against the variation of control gains. Thus for this analysis, both the two–axle vehicle (order of 21) and the conventional bogie vehicle (order of 32) are evaluated since the wheelsets are dynamically coupled with the vehicle or bogie + vehicle depending the arrangement and it is necessary to evaluate the system

as a whole (as shown in Figure 4.1) during this assessment while focusing on the of the wheelsets. Essence of this process is to evaluate the poles of the closed–loop transfer function (representing the relationship between the control effort ($T_w(s)$) and the yaw angle ($\psi_w(s)$)) shown in Equation 74 [50] for each wheelset, which is derived from individual open–loop transfer functions of the wheelset (Equation 72) and the controller (Equation 73).

$$\left[\frac{\psi_w(s)}{T_w(s)}\right]_{\text{Open–Loop}} = \left[\frac{\left(\frac{m_w}{2f_{22}}s + \frac{1}{v_s}\right)s}{\frac{2f_{11}{L_g}^2}{{v_s}^2}s^2 + \frac{2f_{11}L_g}{r_0}}\right] \tag{72}$$

$$Controller = [k_D s + k_P] \tag{73}$$

By close closed–looping the system:

$$\left[\frac{\psi_w(s)}{T_w(s)}\right]_{\text{Closed–Loop}} = \frac{[k_D s + k_P]\left[\frac{\left(\frac{m_w}{2f_{22}}s + \frac{1}{v_s}\right)s}{\frac{2f_{11}{L_g}^2}{{v_s}^2}s^2 + \frac{2f_{11}L_g}{r_0}}\right]}{1 + [k_D s + k_P]\left[\frac{\left(\frac{m_w}{2f_{22}}s + \frac{1}{v_s}\right)s}{\frac{2f_{11}{L_g}^2}{{v_s}^2}s^2 + \frac{2f_{11}L_g}{r_0}}\right]} \tag{74}$$

By rearranging the denominator polynomial of the transfer function poles can be found be as shown in Equation 75 and Equation 76,

$$\left(\frac{2f_{11}{L_g}^2}{{v_s}^2} + \frac{k_D m_w}{2f_{22}}\right)s^2 + \left(\frac{k_D}{v_s} + \frac{k_P m_w}{2f_{22}}\right)s + \left(\frac{2f_{11}L_g}{r_0} + \frac{k_P}{v_s}\right) = 0 \tag{75}$$

$$Poles = \frac{-\left(\frac{k_D}{v_s} + \frac{k_P m_w}{2f_{22}}\right) \pm \sqrt{\left(\frac{k_D}{v_s} + \frac{k_P m_w}{2f_{22}}\right)^2 - 4\left(\frac{2f_{11}{L_g}^2}{{v_s}^2} + \frac{k_D m_w}{2f_{22}}\right)\left(\frac{2f_{11}L_g}{r_0} + \frac{k_P}{v_s}\right)}}{2\left(\frac{2f_{11}{L_g}^2}{{v_s}^2} + \frac{k_D m_w}{2f_{22}}\right)} \tag{76}$$

It can be seen from the Figure 4.4 and Table 4.1 results that how the conjugate poles of the two wheelsets moves in such a way that, when the controller is only having the proportional term, higher gain values enable the poles to shift towards stability while damping decreases. On the other hand, when only having the derivative term, although increasing the gain value can improve the damping, it is

unable to shift the poles in to the stable region. It is clear from the results that gain values needs to be selected such that they can stabilise the wheelsets and to have adequate damping (approximately 25%) in order to avoid oscillations and to maintain robustness.

Thus, by selecting $k_P = 1 \times 10^7$ and $k_D = 5 \times 10^5$ gains to the wheelset controller of the two–axle vehicle, low oscillations and rapid response can be expected.

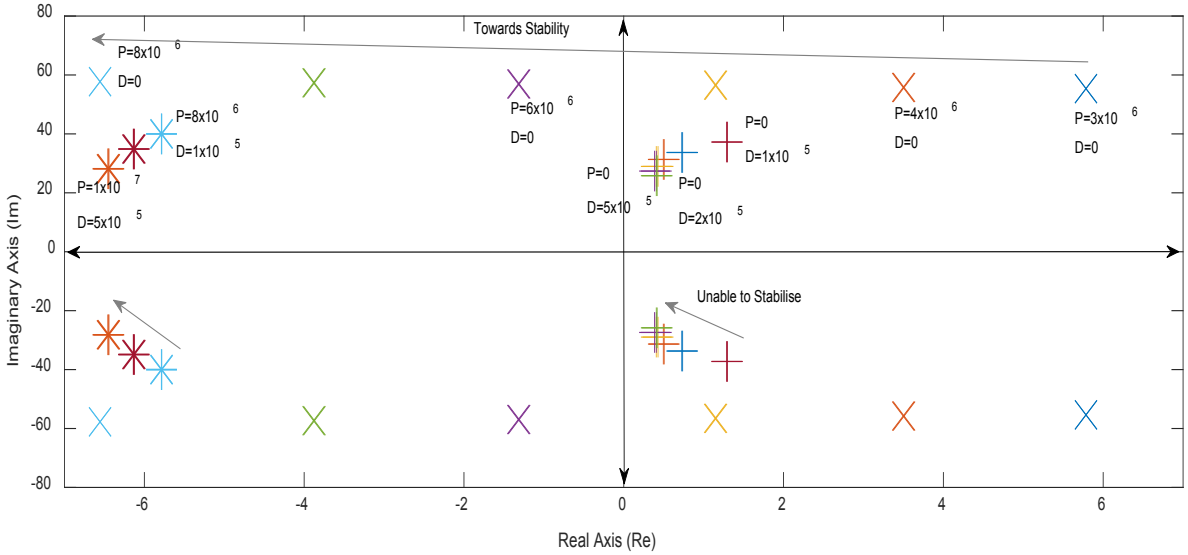

Figure 4. 4 – Pole Movement of the Wheelset Controller – TAV

Table 4. 1 – Wheelset Eigenvalues Movement of Two–Axle Vehicle

Wheelset	Eigenvalues	Damping	Gains
Wheelset 1 Wheelset 2	5.78e+00 + 5.53e+01i 5.78e+00 – 5.53e+01i 5.78e+00 + 5.53e+01i 5.78e+00 – 5.53e+01i	–0.104	$k_P = 3 \times 10^6$ $k_D = 0$
Wheelset 1 Wheelset 2	3.50e+00 + 5.59e+01i 3.50e+00 – 5.59e+01i 3.50e+00 + 5.59e+01i 3.50e+00 – 5.59e+01i	–0.0625	$k_P = 4 \times 10^6$ $k_D = 0$
Wheelset 1 Wheelset 2	1.14e+00 + 5.64e+01i 1.14e+00 – 5.64e+01i 1.14e+00 + 5.64e+01i 1.14e+00 – 5.64e+01i	–0.02	$k_P = 5 \times 10^6$ $k_D = 0$
Wheelset 1	–2.03e+00 + 5.18e+01i –2.03e+00 – 5.18e+01i	0.0393	$k_P = 5 \times 10^6$ $k_D = 1 \times 10^4$

Wheelset 2	–2.03e+00 + 5.18e+01i –2.03e+00 – 5.18e+01i		
Wheelset 1 Wheelset 2	–3.68e+00 + 4.73e+01i –3.68e+00 – 4.73e+01i –3.68e+00 + 4.73e+01i –3.68e+00 – 4.73e+01i	0.0775	$k_P = 5 \times 10^6$ $k_D = 1 \times 10^5$
Wheelset 1 Wheelset 2	–5.60e+00 + 4.70e+01i –5.60e+00 – 4.70e+01i –5.59e+00 + 4.70e+01 –5.59e+00 – 4.70e+01	0.118	$k_P = 6 \times 10^6$ $k_D = 1 \times 10^5$
Wheelset 1 Wheelset 2	–5.79e+00 + 4.00e+01 –5.79e+00 – 4.00e+01 –5.78e+00 + 3.99e+01i –5.78e+00 – 3.99e+01i	0.143	$k_P = 6 \times 10^6$ $k_D = 2 \times 10^5$
Wheelset 1 Wheelset 2	–6.46e+00 + 2.83e+01i –6.46e+00 – 2.83e+01i –6.45e+00 + 2.83e+01i –6.45e+00 – 2.83e+01i	0.223	$k_P = 1 \times 10^7$ $k_D = 5 \times 10^5$

Similarly, it can be seen from Figure 4.5 and Table 4.2 that the conjugate poles of the four wheelsets shift towards stability when increasing the proportional term gain while the increase in derivative term improves damping.

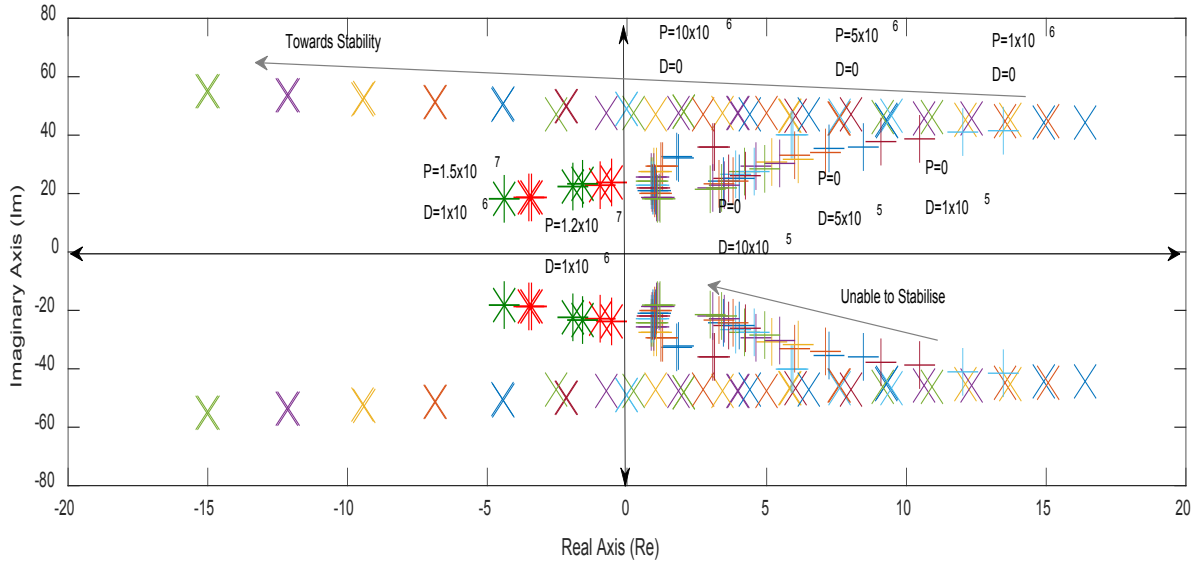

Figure 4. 5 – Pole Movement of the Wheelset Controller – FBV

Thus, gain values are selected in order to stabilise the wheelsets and to have an adequate damping for the wheelsets.

Table 4. 2 – Wheelset Eigenvalues Movement of Full Bogie Vehicle

Wheelset	Eigenvalues	Damping	Gains
Wheelset 1	1.37e+01 + 4.55e+01i 1.37e+01 – 4.55e+01i	–0.289	$k_P = 3 \times 10^6$ $k_D = 0$
Wheelset 2	1.21e+01 + 4.53e+01i 1.21e+01 – 4.53e+01i	–0.258	
Wheelset 3	5.83e+00 + 4.66e+01i 5.83e+00 – 4.66e+01i	–0.124	
Wheelset 4	5.81e+00 + 4.66e+01i 5.81e+00 – 4.66e+01i	–0.124	
Wheelset 1	9.48e+00 + 4.67e+01i 9.48e+00 – 4.67e+01i	–0.199	$k_P = 6 \times 10^6$ $k_D = 0$
Wheelset 2	7.60e+00 + 4.65e+01i 7.60e+00 – 4.65e+01i	–0.169	
Wheelset 3	–2.26e–02 + 4.89e+01i –2.26e–02 – 4.89e+01i	0.0004	
Wheelset 4	–2.08e–02 + 4.90e+01i –2.08e–02 – 4.90e+01i	0.0004	
Wheelset 1	4.99e+00 + 4.74e+01i 4.99e+00 – 4.74e+01i	–0.0682	$k_P = 9 \times 10^6$ $k_D = 0$
Wheelset 2	2.73e+00 + 4.72e+01i 2.73e+00 – 4.72e+01i	–0.0576	
Wheelset 3	–6.85e+00 + 5.15e+01i –6.85e+00 – 5.15e+01i	0.132	
Wheelset 4	–6.88e+00 + 5.14e+01i –6.88e+00 – 5.14e+01i	0.133	
Wheelset 1	2.53e–01 + 4.76e+01i 2.53e–01 – 4.76e+01i	–0.0514	$k_P = 12 \times 10^6$ $k_D = 0$
Wheelset 2	–2.52e+00 + 4.73e+01i –2.52e+00 – 4.73e+01i	0.0523	
Wheelset 3	–1.51e+01 + 5.49e+01i –1.51e+01 – 5.49e+01i	0.265	
Wheelset 4	–1.50e+01 + 5.49e+01i	0.263	

	–1.50e+01 – 5.49e+01i		
Wheelset 1	1.35e+01 + 4.14e+01i 1.35e+01 – 4.14e+01i	–0.309	$k_P = 0$ $k_D = 1 \times 10^5$
Wheelset 2	1.20e+01 + 4.09e+01i 1.20e+01 – 4.09e+01i	–0.281	
Wheelset 3	5.93e+00 + 4.03e+01i 5.93e+00 – 4.03e+01i	–0.146	
Wheelset 4	5.88e+00 + 4.03e+01i 5.88e+00 – 4.03e+01i	–0.144	
Wheelset 1	1.05e+01 + 3.87e+01i 1.05e+01 – 3.87e+01i	–0.261	$k_P = 0$ $k_D = 2 \times 10^5$
Wheelset 2	9.10e+00 + 3.80e+01i 9.10e+00 – 3.80e+01i	–0.233	
Wheelset 3	3.13e+00 + 3.60e+01i 3.13e+00 – 3.60e+01i	–0.0866	
Wheelset 4	3.07e+00 + 3.60e+01i 3.07e+00 – 3.60e+01i	–0.0849	
Wheelset 1	8.47e+00 + 3.61e+01i 8.47e+00 – 3.61e+01i	0.218	$k_P = 0$ $k_D = 3 \times 10^5$
Wheelset 2	7.23e+00 + 3.52e+01i 7.23e+00 – 3.52e+01i	0.201	
Wheelset 3	1.85e+00 + 3.24e+01i 1.85e+00 – 3.24e+01i	0.0569	
Wheelset 4	1.78e+00 + 3.24e+01i 1.78e+00 – 3.24e+01i	0.0548	
Wheelset 1	7.10e+00 + 3.38e+01i 7.10e+00 – 3.38e+01i	–0.205	$k_P = 0$ $k_D = 4 \times 10^5$
Wheelset 2	6.01e+00 + 3.29e+01i 6.01e+00 – 3.29e+01i	–0.18	
Wheelset 3	1.29e+00 + 2.95e+01i 1.29e+00 – 2.95e+01i	–0.0485	
Wheelset 4	1.21e+00 + 2.96e+01i 1.21e+00 – 2.96e+01i	–0.0415	
Wheelset 1	–5.62e–01 + 2.39e+01i –5.62e–01 – 2.39e+01i	0.0235	$k_P = 1.2 \times 10^7$ $k_D = 1 \times 10^6$
Wheelset 2	–9.45e–01 + 2.30e+01i –9.45e–01 – 2.30e+01i	0.0411	
Wheelset 3	–3.52e+00 + 1.88e+01i –3.52e+00 – 1.88e+01i	0.184	
Wheelset 4	–3.42e+00 + 1.87e+01i –3.42e+00 – 1.87e+01i	0.18	
Wheelset 1	–1.60e+00 + 2.35e+01i –1.60e+00 – 2.35e+01i	0.0618	$k_P = 1.5 \times 10^7$ $k_D = 1 \times 10^6$
Wheelset 2	–1.94e+00 + 2.25e+01i –1.94e+00 – 2.25e+01i	0.0858	
Wheelset 3	–4.40e+00 + 1.80e+01i –4.40e+00 – 1.80e+01i	0.238	

Wheelset 4	–4.51e+00 + 1.81e+01i –4.51e+00 – 1.81e+01i	0.242	

From the above analysis, gains for the wheelset controller in both vehicle configurations can be concluded as shown below:

Two–axle Vehicle: $k_P = 1 \times 10^7;\ k_D = 5 \times 10^5$

Full Bogie Vehicle: $k_P = 1.5 \times 10^7;\ k_D = 1 \times 10^6$

4.2. Actuator Model

Selecting a suitable actuator for the active control of wheelsets is critical to the actual implementation of active primary suspension concepts. As far as actuators are concerned, performance, cost and reliability issues have a significant impact on the choice of suitable actuators.

Electromechanical (EM) actuators are selected in this study, since they represent a new trend in the industry, has good dynamic performances and using EM actuators omit the necessity to use additional power sources as well. In addition, they have evolved to possess features such as low noise, low temperature and small sizes and while requiring less maintenance compared to hydraulic or pneumatic actuators [75]. Therefore, selected actuator configuration is as shown below in Figure 4.6 where they can be fitted between the wheelset and the bogie/vehicle frame from the longitudinal or yaw direction to apply either force or torque.

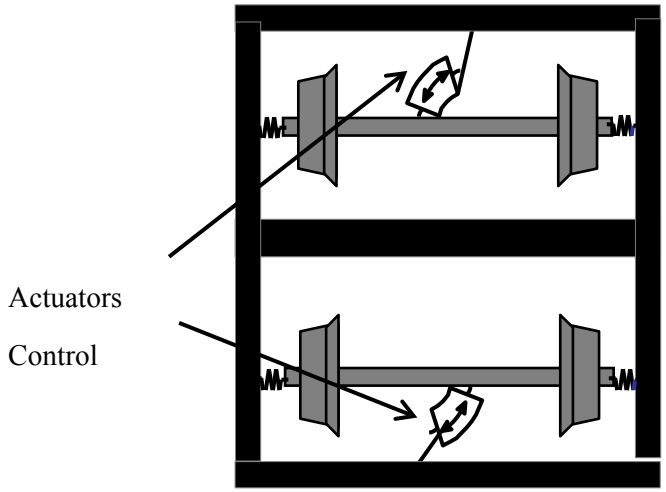

Figure 4. 6 – Actuator Configuration

4.2.1. Torque Actuator

Actuator model used in this study [14] consists of a DC motor coupled with a simple gearbox for the purpose of providing the necessary torque to control the wheelset. A model of a basic DC motor is used for the analysis in this case is due to the simplicity and due to the fact, that in an implementation stage, a brush–less DC motor (BLDC) can be used for this specific task since it has the advantage of being controlled as a simple DC motor, despite being operated by AC power. Having a gearbox for the motors is essential since electrical motors are more efficient at high speed. Thus, in order reduce the speed and increase the torque, the gear wheel is required to have a relatively higher gear ratio than the motor rotor. Since the two wheels are directly coupled, their effective inertia of the whole actuator can be calculated as $I_{motor} + I_{gear}n^2$. Motor internal damping is denoted as C_m, while damping and stiffness at the connection between the wheelset and the actuator are denoted C_g and K_g respectively. Torque applied to the wheelset is represented as T_L, while V_a and i_a are the supply voltage and current of the motor, respectively. In addition, the gear ratio is $\frac{1}{n}$ and the motor angular displacement is denoted as θ_m.

Further abbreviations and the values of these variables depicting the actuator model are elaborated in Appendix A.

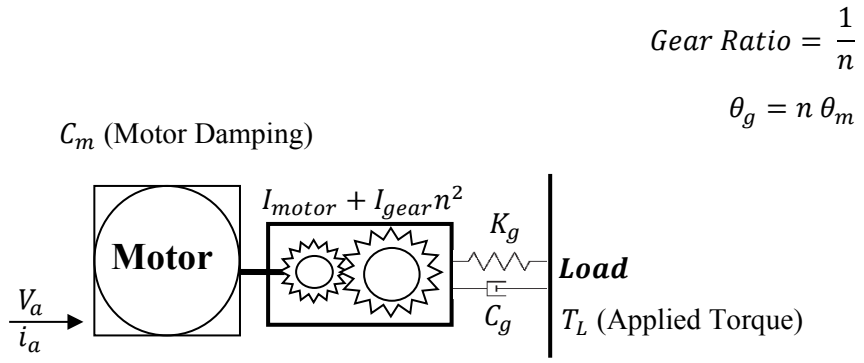

Figure 4. 7 – Torque Actuator Configuration

$$\dot{i_a} = -\frac{r_{arm}}{l_{arm}} i_a - \frac{k_e}{l_{arm}} \dot{\theta_m} + \frac{1}{l_{arm}} v_a \tag{77}$$

$$(I_m + I_g n^2)\ddot{\theta_m} = k_t i_a - c_m \dot{\theta_m} - nT_L \tag{78}$$

$$\left(I_m + I_g n^2\right)\ddot{\theta_m} = k_t i_a - c_m \dot{\theta_m} - C_g n^2 \dot{\theta_m} - K_g n^2\, \theta_m + n K_g\, \psi_m + n C_g \dot{\psi_m} \tag{79}$$

$$Torque\ (T_L)\ = K_g n\, \theta_m + C_g n\, \dot{\theta_m} - K_g\, \psi_m - C_g \dot{\psi_m} \tag{80}$$

Above equations 77 – 79 [95] depict the dynamic behaviour of the actuator from both the electrical and mechanical aspects of a DC motor with a gearbox.

4.3. Actuator Controller

It is essential that actuators in this application (active wheelset control of stability) are capable of proving rapid and accurate control efforts based on the feedback. As the kinematic mode of a solid–axle wheelset has a bandwidth of 6–7 Hz, actuator is required to have a bandwidth of at least 15 Hz. Therefore, local controllers for the actuators (for each wheelset) are necessary in order to effectively operate the actuator as demanded by the wheelset controller.

In this case, a PI controller is used to control the voltage of the motor to drive the actuator and provide the control effort as demanded by the wheelset controller.

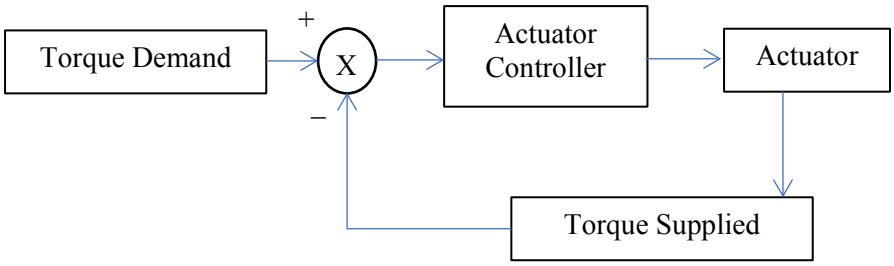

Figure 4. 8 – Actuator Controller

As shown in Figure 4.8, the actuator controller operates on the reference torque demand from the wheelset controller and the feedback from the output (applied at the wheelset) torque.

Table 4.3 provides in insight into the bandwidth of the actuator without the controller and with the controller, respectively.

Table 4. 3 – Actuator Eigenvalues

	Actuator Eigenvalues	Damping	Frequency (Hz)
Without the Controller	–7.88	1	1.27
	–7.19 + 6.15e+02i	0.16	98.52
	–7.19 – 6.15e+02i	0.16	98.52
With the Controller	–5.13e+01 + 2.19e+02i	0.21	35.81
	–5.13e+01 – 2.19e+02i	0.21	35.81
	–2.46e+01 + 5.86e+02i	0.053	93.26
	–2.46e+01 – 5.86e+02i	0.053	93.26

With Table 4.3, it is evident that the actuator without a local controller has a slow pole with a frequency of 1.27 Hz. This is clearly not sufficient for the application of an active wheelset control which demands a minimum frequency of 15 Hz. However, the above results also show that once the tuned local controller is integrated, the slow pole is replaced with poles with frequency of 35.8 Hz. Thus, it is clear that a local actuator controller is essential in order to use an EM actuator for active wheelset control applications.

When the PI controller is well tuned, the actuator functions at a rapid and high level of precision (lower steady–state errors) since the controller acts based on the current error as well as accumulative error over time.

4.4. Comparison of the Passive and Active Control Dynamic Performances

In order to compare the differences in dynamic performances between passive suspension and active control (including actuator dynamics), computer simulations are carried out while key performance indicators are analysed. Key vehicle dynamic performance indicators such as lateral displacement with curved track, lateral deflection with straight track with lateral irregularities, wheelset yaw and creep forces are evaluated to compare the dynamic performances between the two (active and passive) configurations. These tests are conducted with both the two–axle vehicle and full bogie vehicle using a low–speed curved track with 300 m curvature and 6^0 of cant angle (same condition used to evaluate the vehicle models in the previous chapter) at the vehicle speed of 25 ms^{-1} and the generic straight track with lateral irregularities at high speed (83 ms^{-1}) to distinctively compare the dynamics of the vehicles with the passive and active (actuated) systems for the different track conditions.

As mentioned above wheelset lateral displacements are analysed with the curved track in this case (active control) to assess curving performances of the vehicles with this particular control scheme such that wheelsets of both the two–axle vehicle and the bogie vehicle are achieving the pure rolling

rate (where longitudinal creep forces are completely eliminated) by reaching optimal lateral displacement. In order to identify the optimum curving case for pure rolling, the lateral wheelset displacement of each vehicle configuration can be derived using below Equation 81 [35] and it is found that for the two–axle vehicle model, optimal lateral displacement is $5.625 \times 10^{-3}\, m$ while it is $5.685 \times 10^{-3}\, m$ for the full bogie vehicle. Optimal values are different between the two vehicle configurations due to the minor variation with wheelset half gauge distance and wheel radius values.

$$Ideal\ Lateral\ Displacement = \frac{er_0}{\lambda R} \tag{81}$$

In the above Equation 81: $e,\ r_0,\ \lambda$ represent the wheelset half gauge, wheel radius and conicity, respectively, while R represents the curve radius of the curved track.

4.4.1. Two–Axle Wheelset Vehicle

The results below show the different dynamic performances for both passive and active (actuated) to the same deterministic/curved track (DT) conditions and the same two–axle vehicle (TAV).

Wheelset Dynamics Assessment (Deterministic/Curved Track):

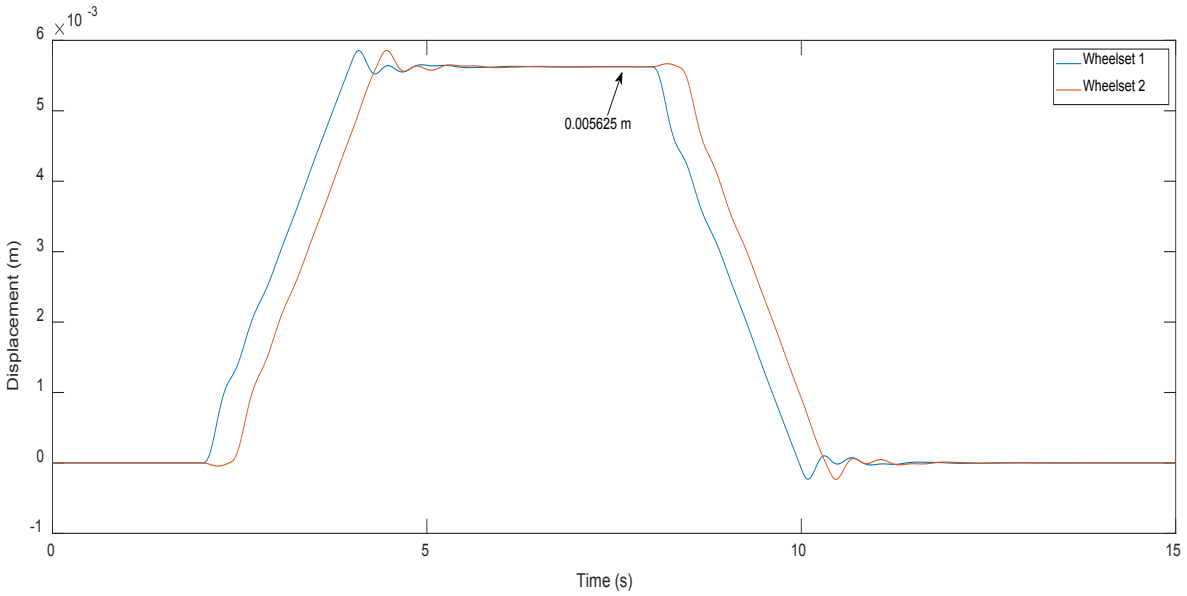

Figure 4. 9 – Wheelsets Displacement TAV–DT – Active

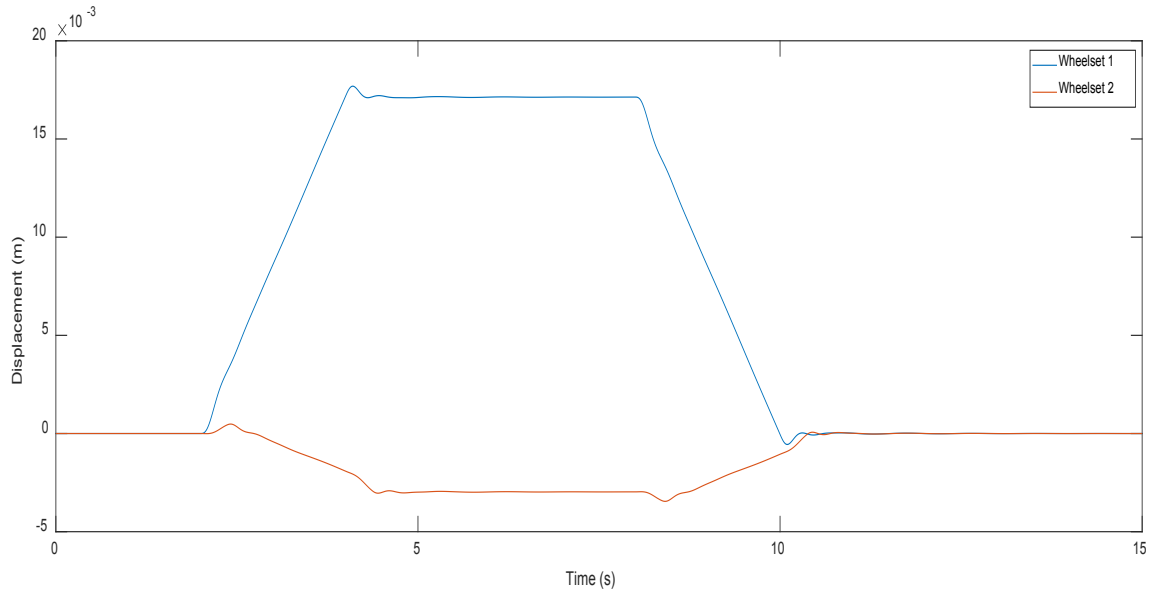

Figure 4. 10 – Wheelsets Displacement TAV–DT – Passive

Above Figure 4.9 depicts the displacement of the wheelsets travelling on the curved track and it can be seen that wheelsets are achieving the optimal displacement calculated with Equation 81 as mentioned above. Thus, it is evident that the active wheelset control in this case is not restricting the wheelsets to have natural curving movements and achieving this optimal displacement will allow the wheelsets to attain pure rolling as desired. This subsequently will result in reduced/eliminated longitudinal creep forces at contact points.

On the other hand, it can be seen with Figure 4.10 that natural curving is hindered with passive suspension due to the high yaw stiffness at the primary suspension. Thus, introducing active wheelset control can considerably reduce the control effort by averting to act against longitudinal creep forces.

Similarly, it can be seen that the as desired wheelsets are maintaining the same yaw angle with the active control [49], unlike the passive suspension, when travelling on the curved track. Having the same angle of attack for both wheelsets is advantageous since it results in equal/balanced, lateral creep forces which act against the centrifugal force in a uniform manner.

Furthermore, since Figure 4.9 and Figure 4.10 depict lateral displacements and yaw angles of actively controlled wheelsets when travelling on a widely used deterministic track (300 m curvature, 6^0 of cant angle and vehicle speed of 25 ms^{-1}), which is used in many research focused on evaluating curving performances of actively controlled wheelsets, it provide an opportunity to readily compare the results between different active wheelset control strategies used in the field by comparing the results with previously published material. Therefore, it can be seen from comparing the lateral displacements and yaw angles values of the wheelsets published in a study [2] which use an optimal control strategy,

a modal control strategy, active yaw damping control strategy and active lateral damping control strategy in comparison, (oppose to the absolute stiffness control strategy used in this particular study), results depicts almost similar values (approximately 0.005 m of lateral displacement and –0.001 rad angle of attack during the steady curve section) in the results depicted in Figure 4.9 and Figure 4.10. Thus, it is evident that absolute stiffness control strategy used in this study is as effective as model–based optimal control strategy and other classical control strategies.

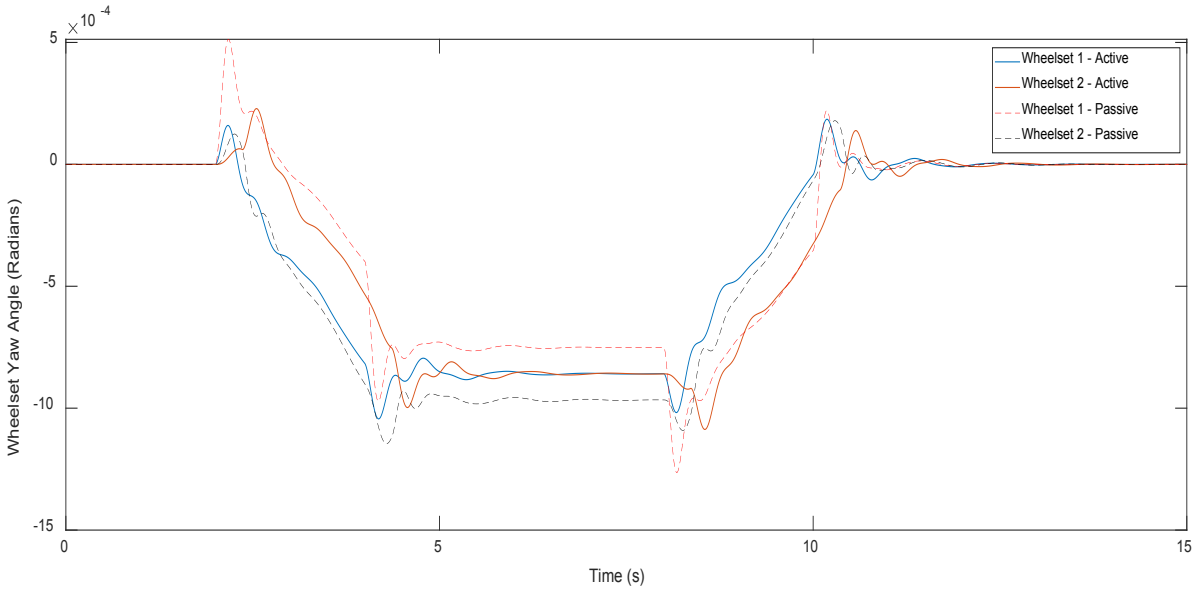

Figure 4. 11 – Wheelsets Yaw Comparison TAV–DT – Active/Passive

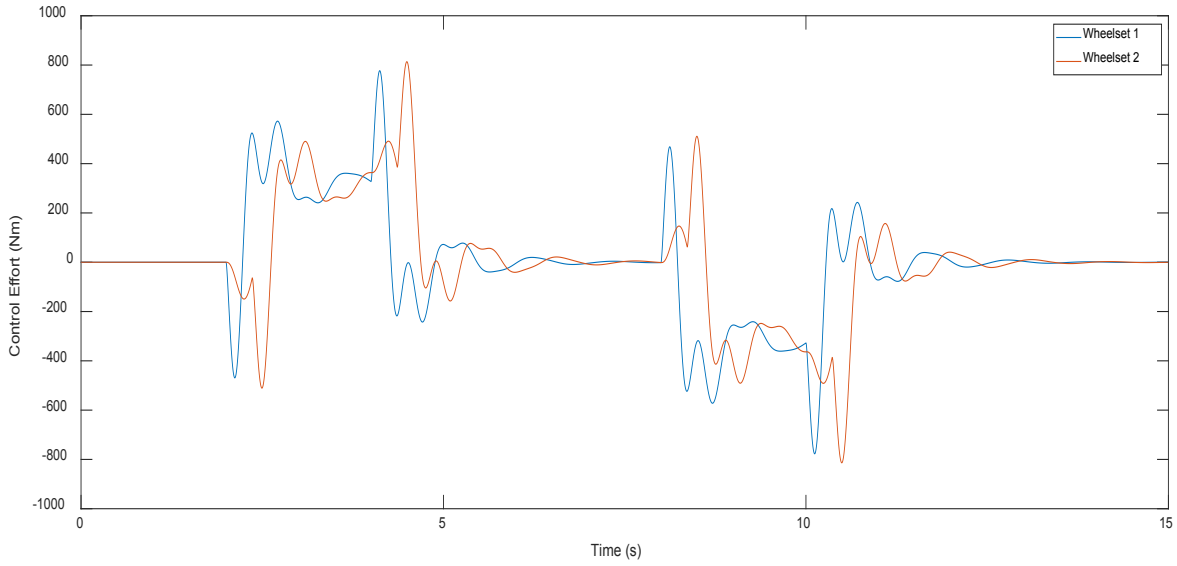

Figure 4. 12 – Control Torque Comparison TAV–DT – Active

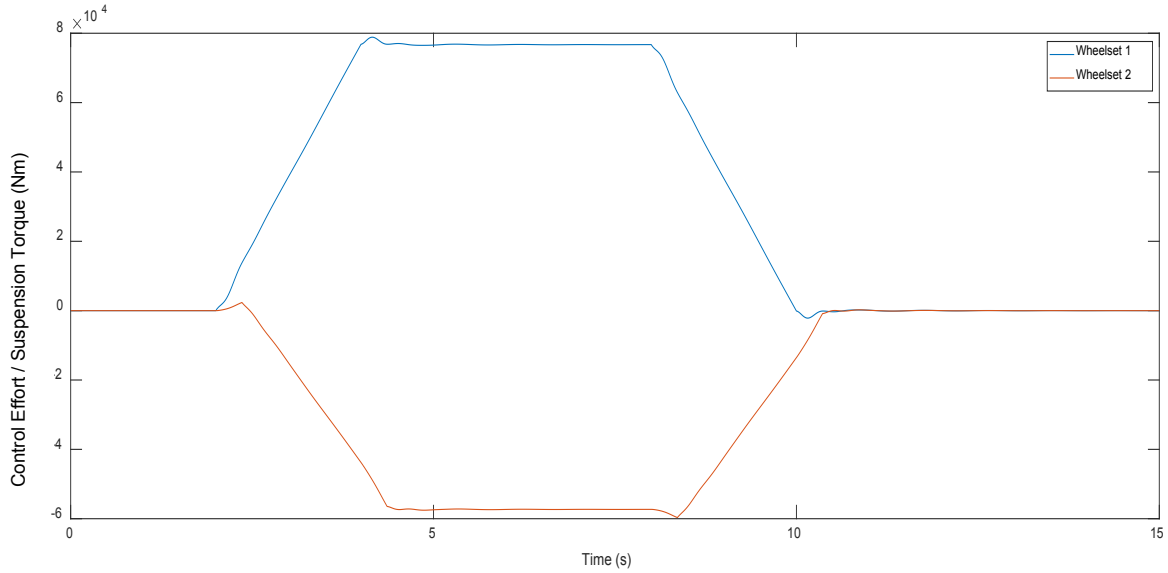

Figure 4. 13 – Suspension Torque/Force TAV–DT – Passive

As expected, Figure 4.12 above indicates a significant reduction in the control effort between the passive suspension (Figure 4.13) and active control. In addition, it shows particularly that during the curvature, control effort is not required at all. This is an important performance indicator since lower control efforts indicates lower demands for actuators and that can result in reduced energy consumption and losses. In addition, above results depicts that there is a variation in the direction of the suspension force in the passive suspension case which is a result of the difference in the direction of lateral displacement between wheelsets 1 and 2.

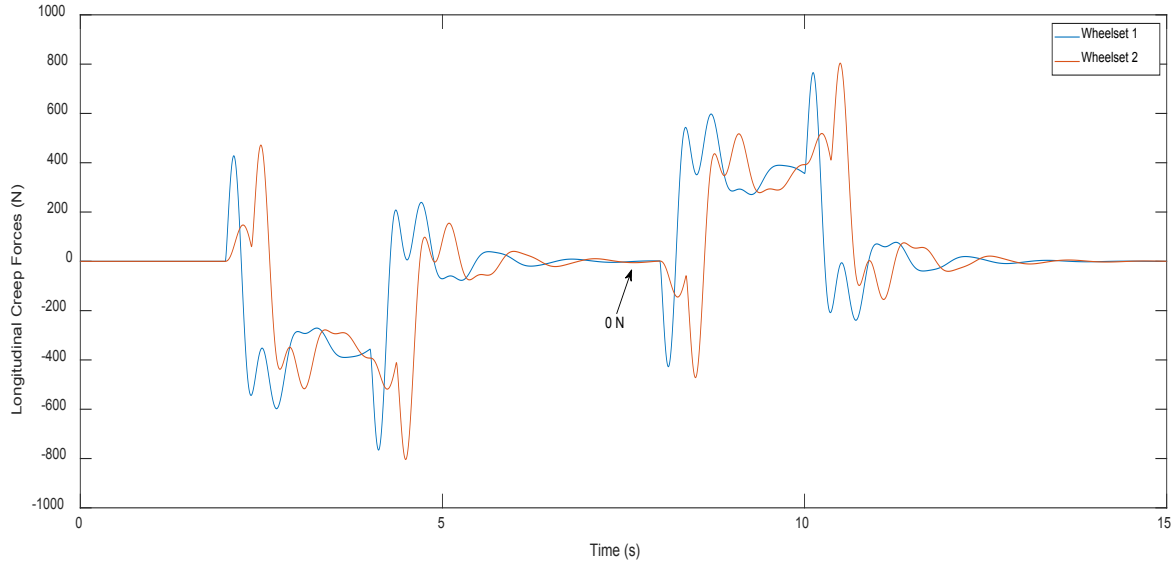

Figure 4. 14 – Longitudinal Creep Force Comparison TAV–DT – Active

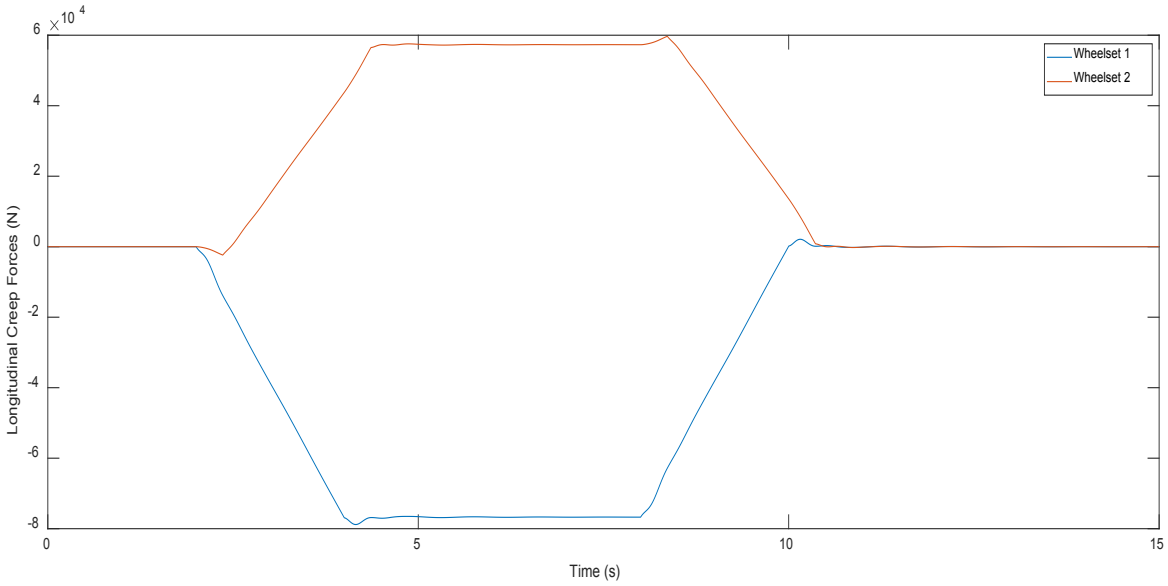

Figure 4. 15 – Longitudinal Creep Force Comparison TAV–DT – Passive

As mentioned above, it can be seen that from Figure 4.14 that lower control effort is the result of the almost eliminated creep forces in the longitudinal direction. This is possible with active control since it allows the wheelsets to move naturally on a curved track allowing pure rolling for the wheelsets which would be otherwise hindered through the use of passive suspension. This improvement can significantly reduce wear and fatigue of the associated components as well. As shown above, when evaluating the maximum magnitude of the longitudinal creep forces with passive suspension (Figure 4.15), it is a relatively significant value of approximately 0.7 x 10^5 Nm.

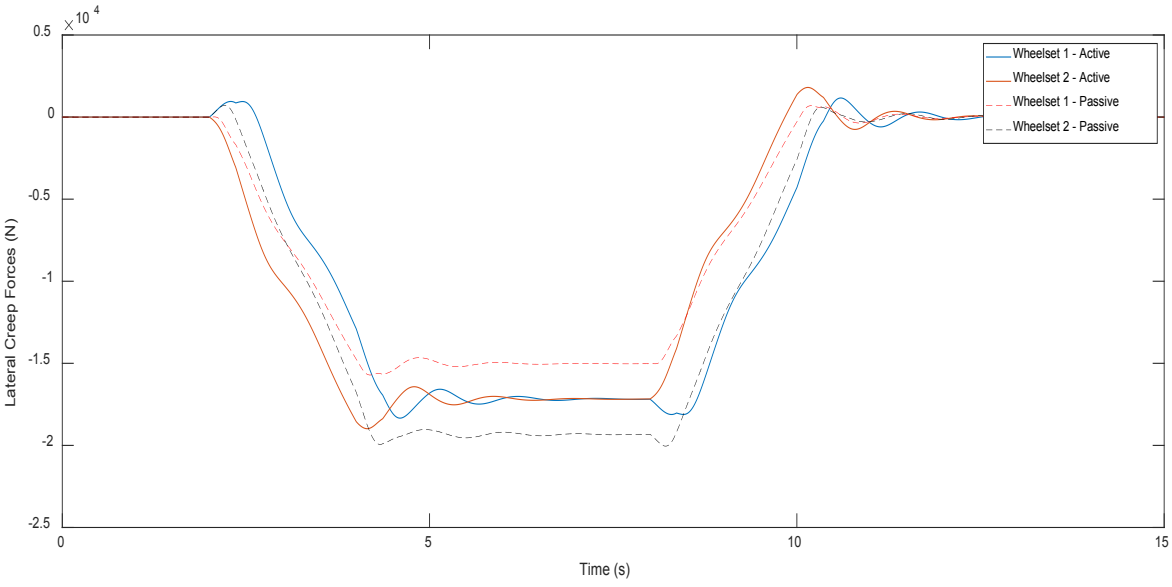

Figure 4. 16 – Lateral Creep Force Comparison TAV–DT – Active/Passive

Balanced/equal lateral creep forces between the front and rear wheelsets are desirable when negotiating curves since they counter balances the centrifugal force in order to stabilise the wheelsets. It is evident from the Figure 4.16 that active wheelset control scheme evaluated in this case is achieving that condition.

From all the above results and their comparisons, it can be seen that the curving performance of the vehicle is considerably improved through the use of active control as it has allowed the wheelsets move through the curve without hindrance.

Wheelset Dynamics Assessment (Straight Track with Lateral Irregularities):

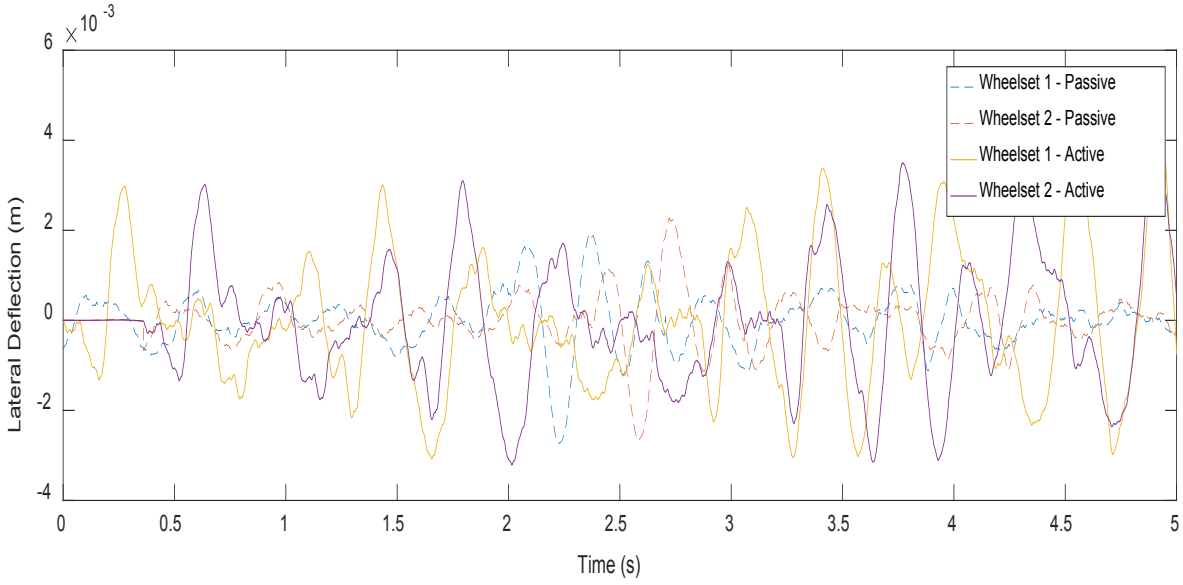

Figure 4. 17 – Deflection Comparison TAV–IT – Active/Passive

It can be seen from Figure 4.17 that active control system is capable of stabilising the wheelsets in a similar manner to the high stiffness passive suspension since the maximum difference of deflections between two configurations is < 0.002 m. In addition, it can be seen that that wheelsets flanges are not contacted by the rail since the deflections are < 0.01 m. Furthermore, when focusing on the bandwidth of the control configuration, these results indicate that the active control system is capable of operating at the frequency of wheelsets.

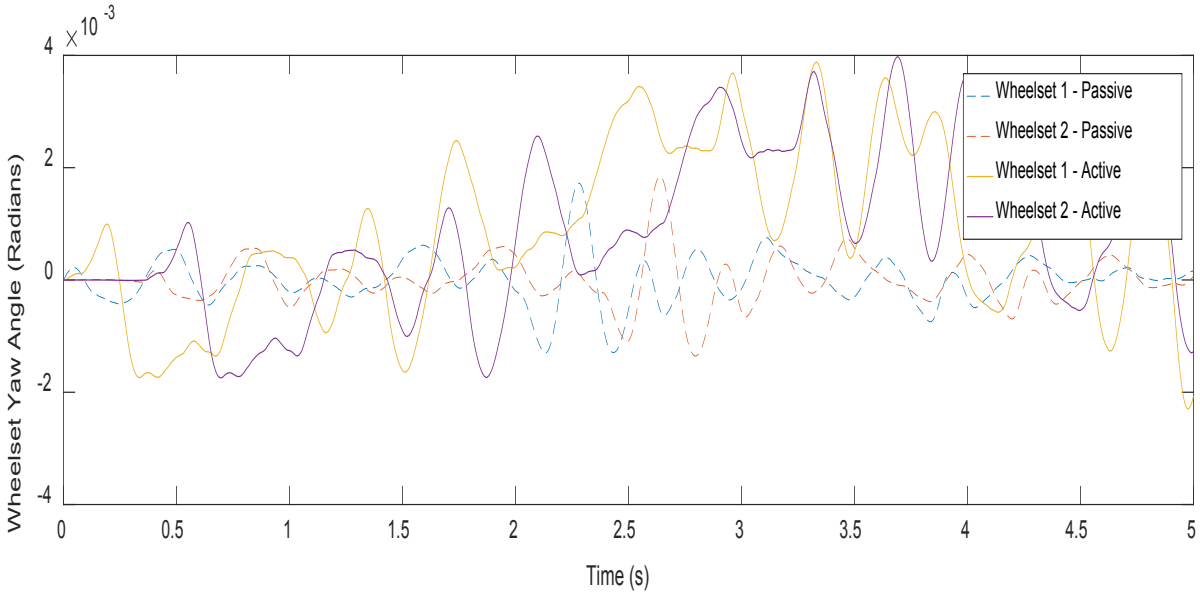

Figure 4. 18 –Yaw Comparison TAV–IT – Active/Passive

Figure 4.18 shows that, similar to the deflection results, yaw angles are slightly higher than the passive suspension arrangement, which certainly be further improved by retuning the wheelset controller.

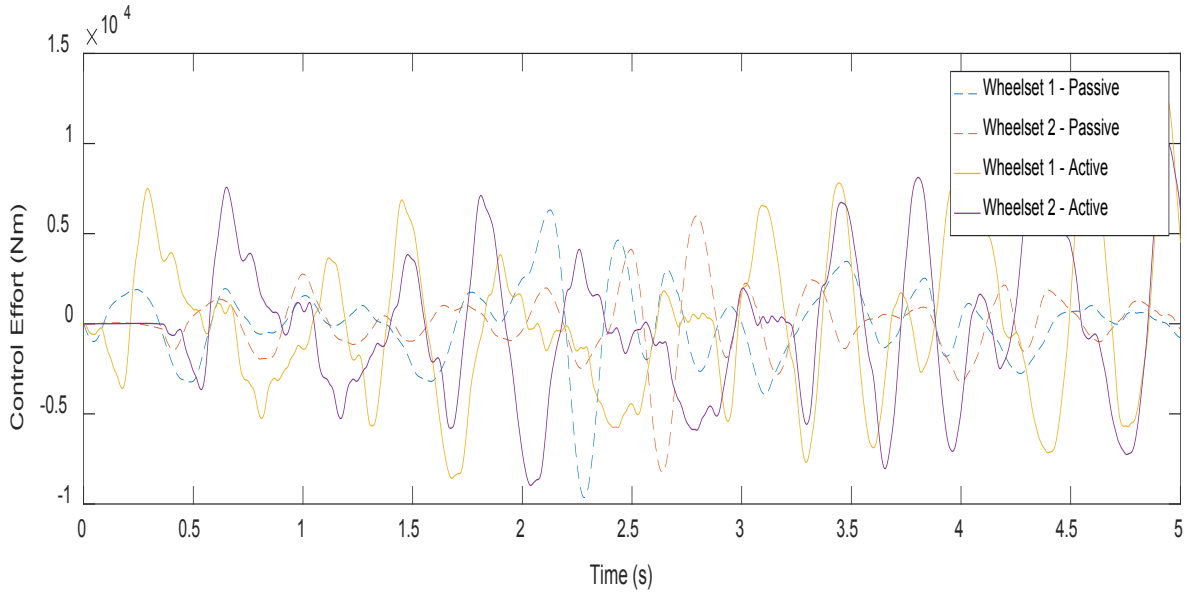

Figure 4. 19 – Control Effort TAV–IT – Active/Passive

Although the performances are almost identical for the active and passive configurations, the difference in control effort between the curved track and straight track and straight track with lateral irregularities can be seen by comparing Figure 4.12 and Figure 4.19. This indicates that the control effort required for the straight track is significantly higher than that required for the curved track. Thus,

for further optimisation of the actuator, the straight track with lateral irregularities can be used since it is more demanding on active control system.

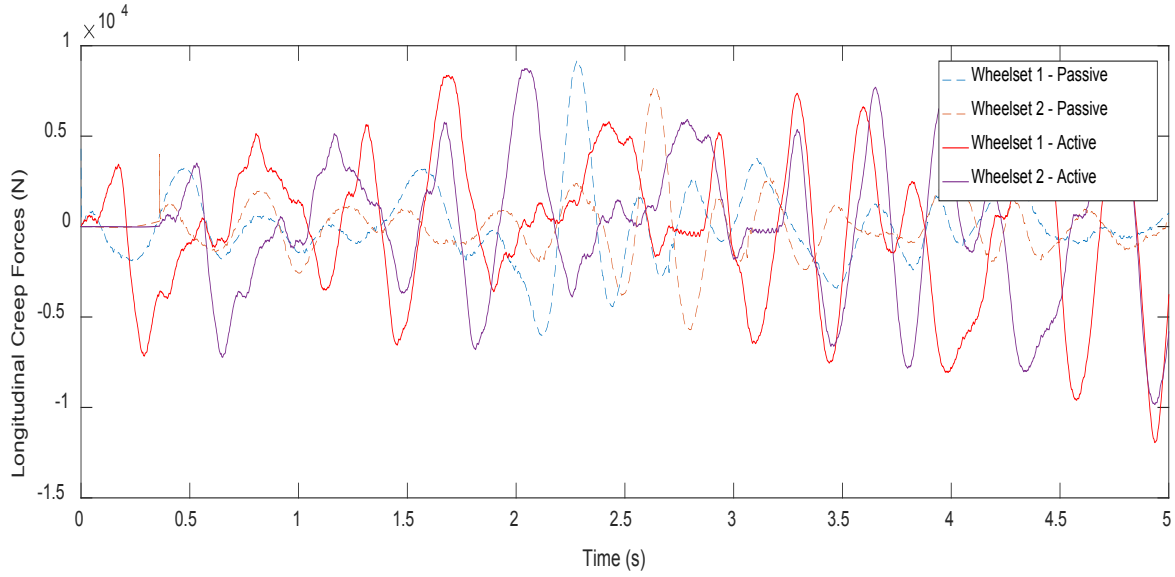

Figure 4. 20 – Longitudinal Creep Force Comparison TAV–IT – Active/Passive

Although the active control improved the longitudinal creep forces in the curved track, in the straight track with lateral irregularities, longitudinal and lateral creep forces are almost the same as the passive suspension system. This should be expected since the active control and passive suspension result in similar lateral deflections and yaw angles in the wheelsets.

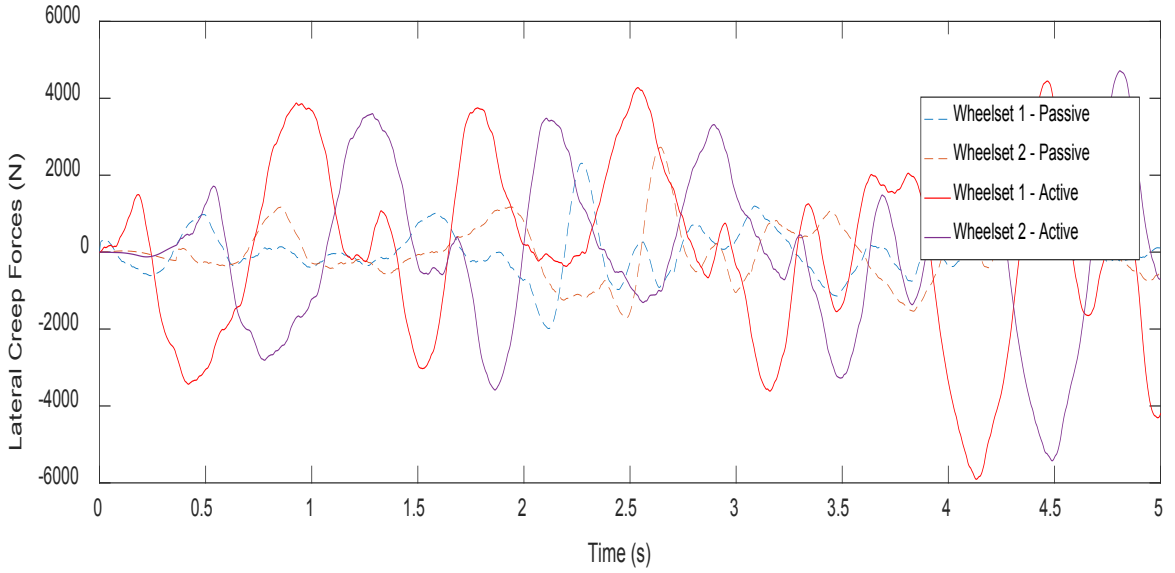

Figure 4. 21 – Lateral Creep Force Comparison TAV–IT – Active/Passive

It can be seen from Figure 4.21 above that lateral creep forces with active control are having similar values as the passive suspension.

It can be seen from the results that although active control does not improve dynamic performances, neither has it worsened them when compared with the passive suspension. Thus, it is evident that active control is capable of successfully addressing the trade–off between curving performance and wheelset stability of two–axle vehicle.

4.4.2. Full Bogie Vehicle

In parallel to the above analysis for the two–axle vehicle, same comparison is carried out for the full bogie vehicle to evaluate the different effects of the passive and active (actuated) control on the vehicle dynamics on curved tracks and straight track with lateral irregularities.

Below Figure 4.22 shows that with active control, wheelsets are able to have the optimal lateral displacement in order to have pure rolling while Figure 4.23 shows that passive suspension is restricting that.

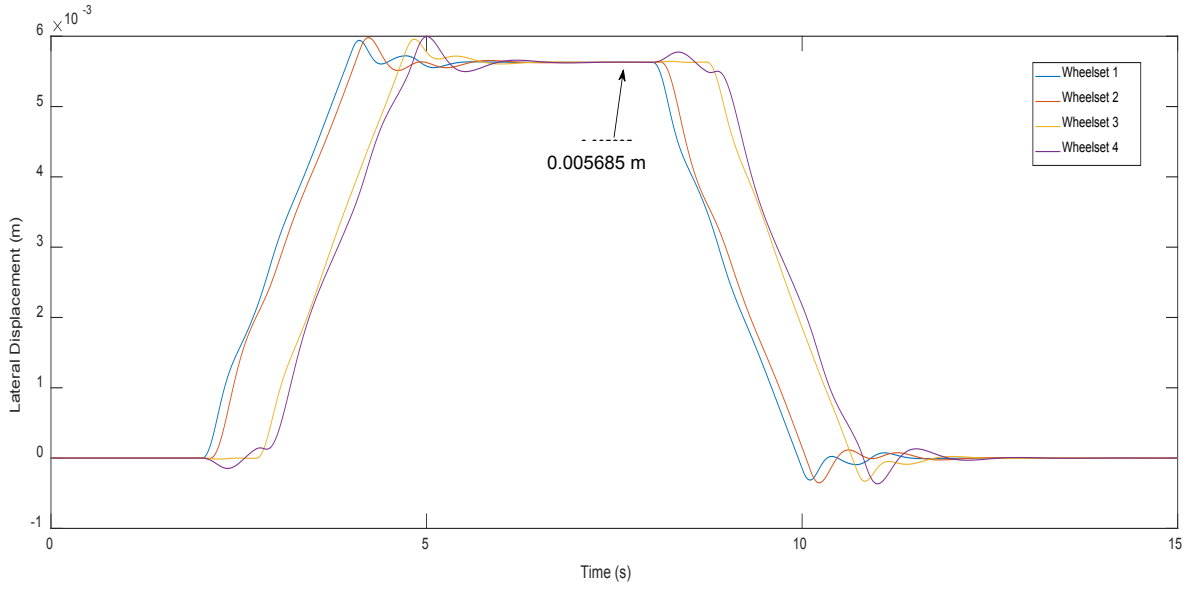

Figure 4. 22 – Wheelsets Displacement Comparison FBV – DT – Active

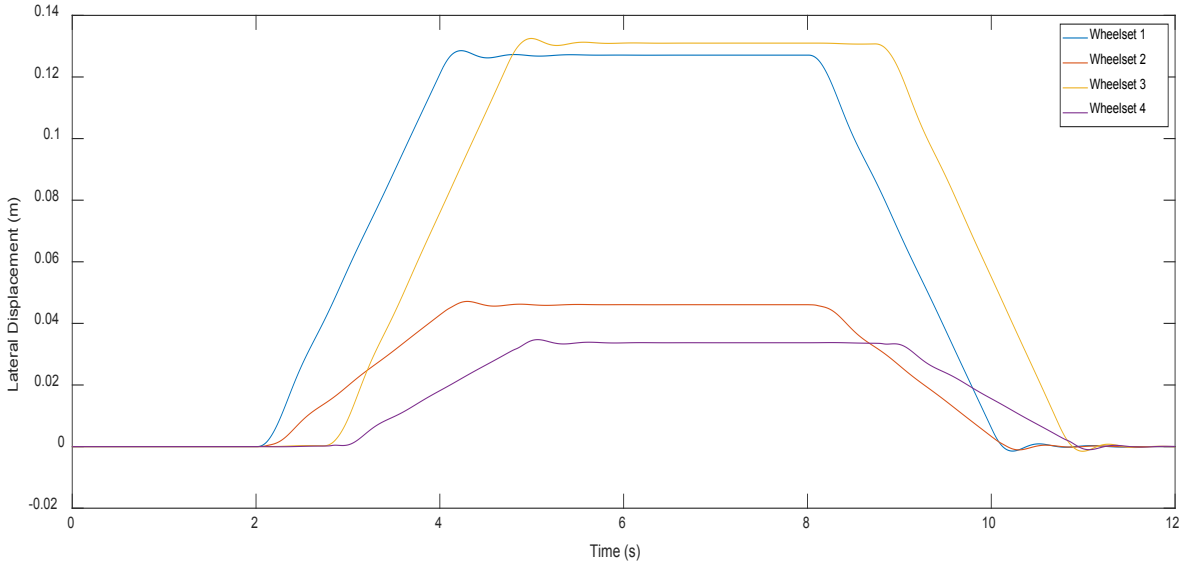

Figure 4. 23 – Wheelsets Displacement Comparison FBV – DT – Passive

From analysing the result (Figure 4.22 and Figure 4.23), it can be seen that the wheelsets with active control are achieving the optimal lateral displacement required for the pure rolling of wheelsets, where the passive suspension caused the wheelsets to displaced by approximately 0.012 m, which will cause flange contact. Thus, it is clear that the active control significantly improves the wheelset displacement.

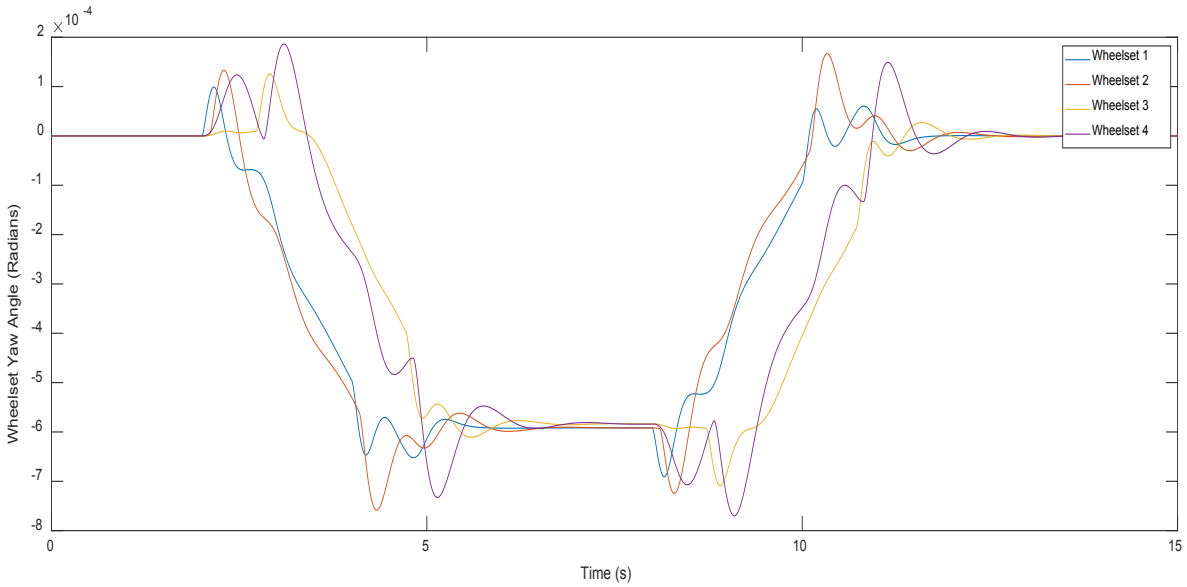

Figure 4. 24 – Wheelsets Yaw Comparison FBV – DT – Active

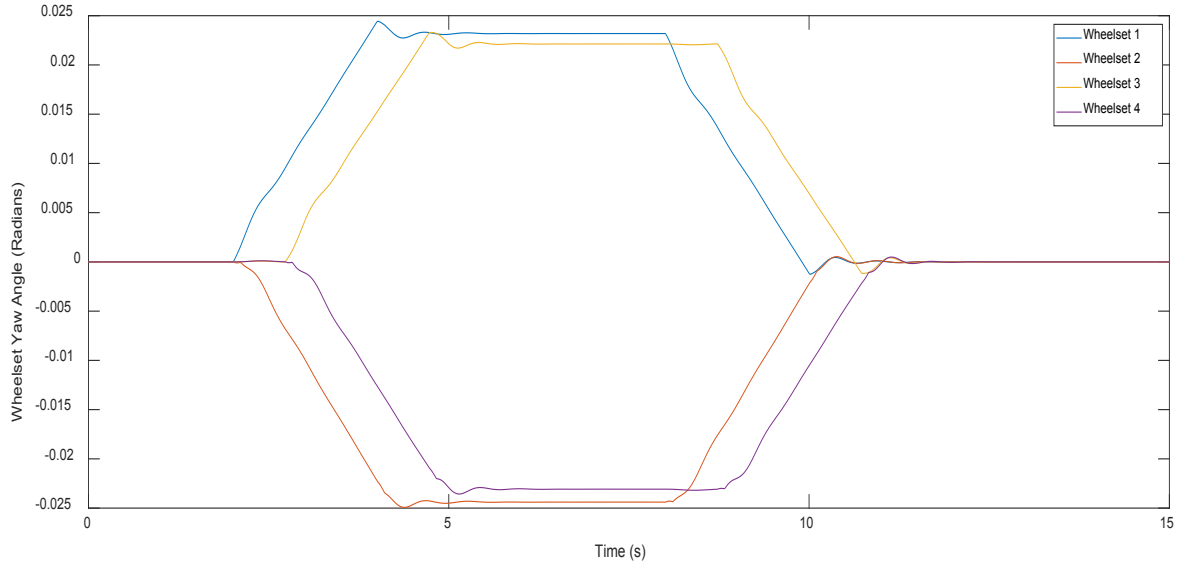

Figure 4. 25 – Wheelsets Yaw Comparison FBV – DT – Passive

From the comparison of Figure 4.24 and Figure 4.25, which show yaw angle of the wheelsets with the active control and passive suspension, respectively, it is clear that the active control improves the dynamic behaviour significantly, since all the four wheelsets show almost the same yaw angle when traversing the curve while results with passive suspension shows otherwise. Achieving the same angle of attack by the wheelsets will results in almost the same (equally distributed) lateral creep forces that acts against the centrifugal force experienced on the curve.

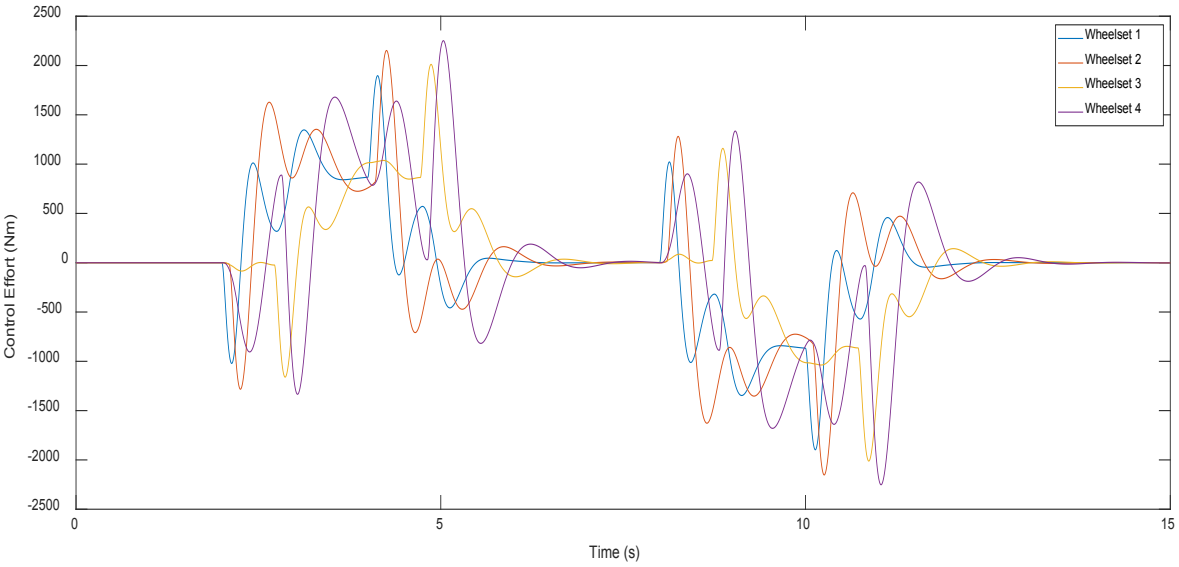

Figure 4. 26 – Control Torque Comparison FBV – DT – Active

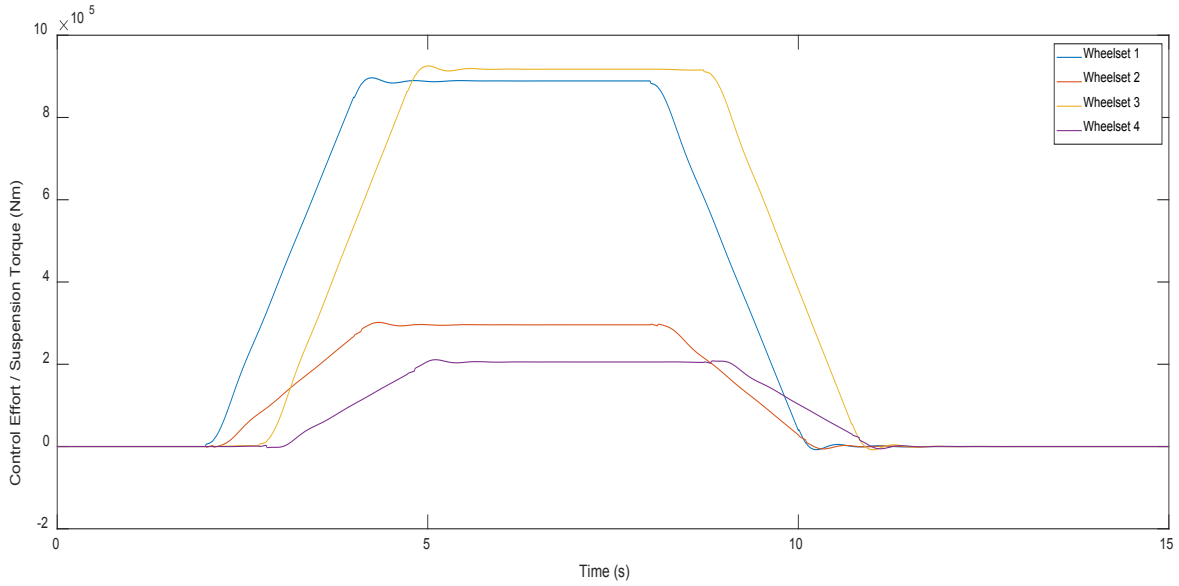

Figure 4. 27 – Suspension Torque/Force FBV – DT – Passive

It is evident from Figure 4.26 that with the active control, control effort has been almost eliminated during the steady curve part and is evenly distributed when compared with the passive suspension, which demands approximately 9 x 10^5 Nm for the front wheelsets (Figure 4.27). This reduction is a result of reduced/eliminated longitudinal creep forces due to the use of active control, as shown below in Figure 4.28.

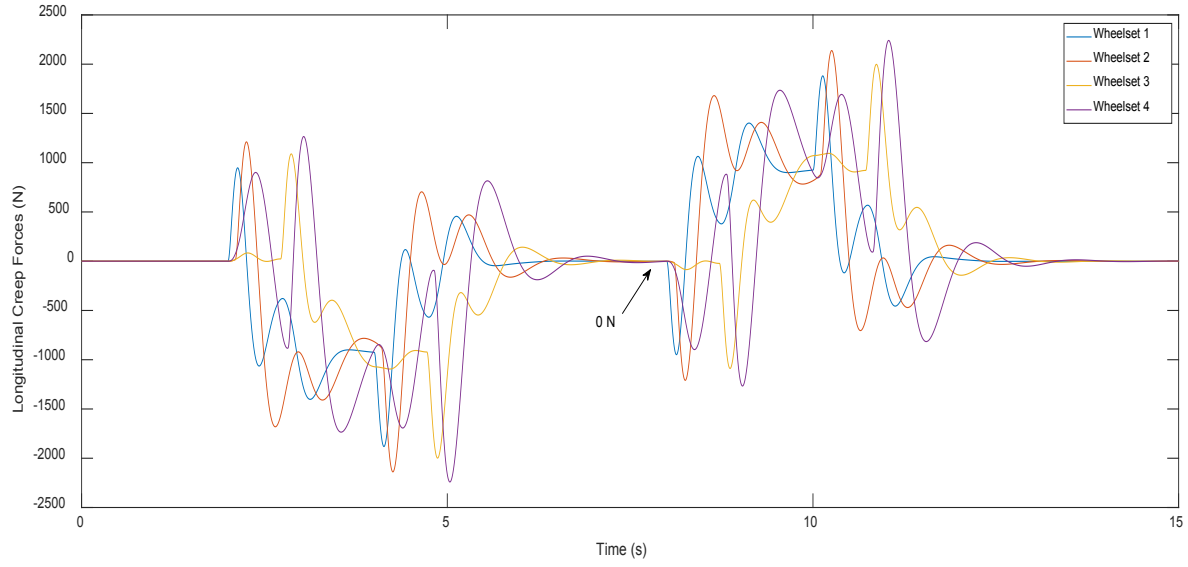

Figure 4. 28 – Longitudinal Creep Force Comparison FBV – DT– Active

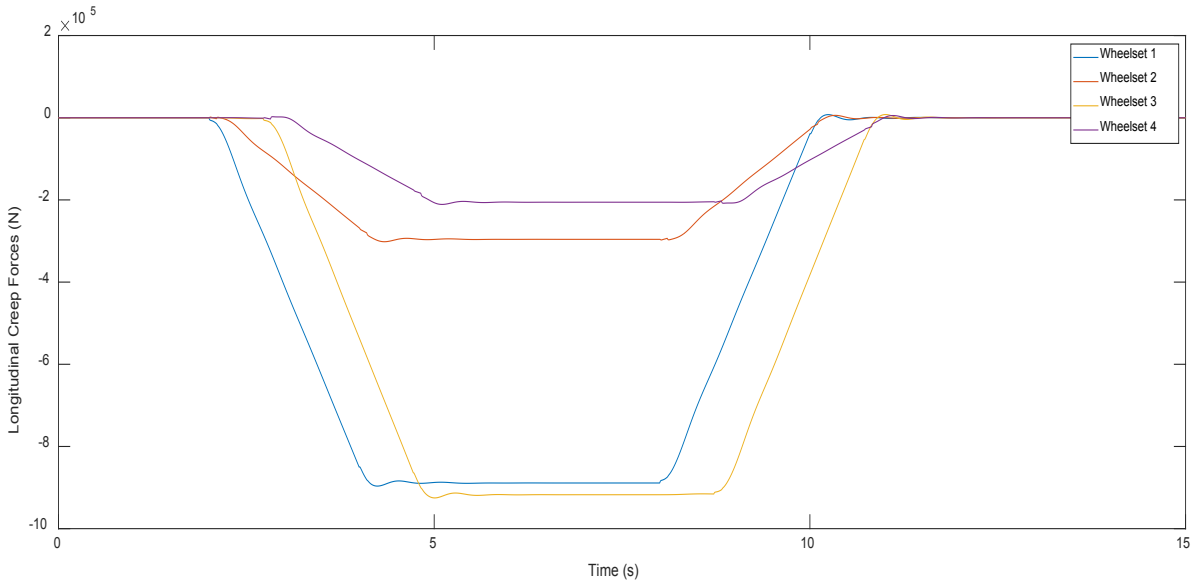

Figure 4. 29 – Longitudinal Creep Force Comparison FBV – DT– Passive

Similar to the two–axle vehicle, when further evaluating the longitudinal creep forces with active control and passive suspension, it can be seen that that the longitudinal creep forces are educed/eliminated with active control. This is a significant improvement over the 8.8 x 10^5 N with the passive suspension (Figure 4.29).

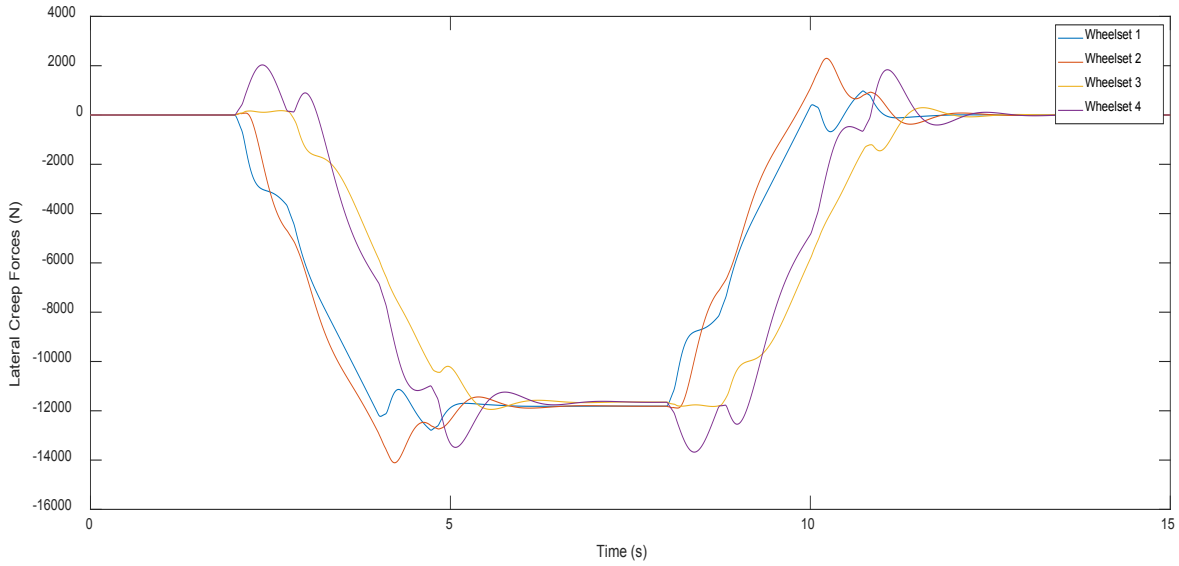

Figure 4. 30 – Lateral Creep Force Comparison FBV – DT – Active

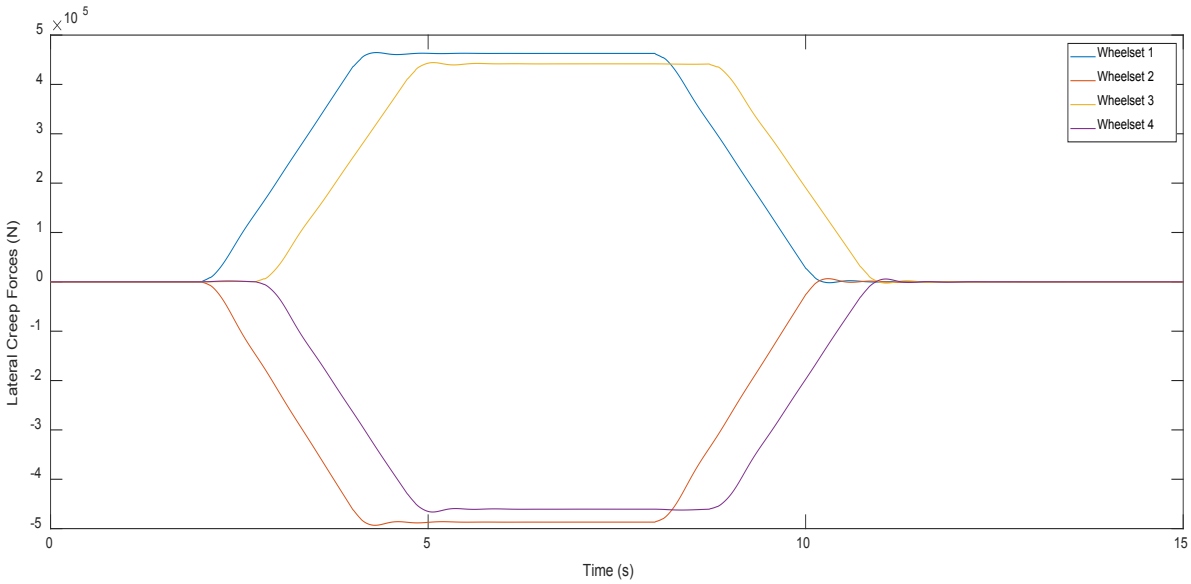

Figure 4. 31 – Lateral Creep Force Comparison FBV – DT – Passive

As expected, Figure 4.30 depicts balanced lateral creep forces which acts against to balance centrifugal forces caused by the curvature. When further evaluating the values, it is found that maximum lateral forces exerted in the wheelset approximately 1.2 x 10^4 N, where passive suspension resulted in magnitudes of approximately 8.8 x 10^5 N.

From the analysis of the above results, it is evident that active control with the skyhook absolute stiffness can result in a significant improvement in the wheelset dynamics when curving of the full bogie vehicle.

Wheelset Assessment (Straight Track with Lateral Irregularities):

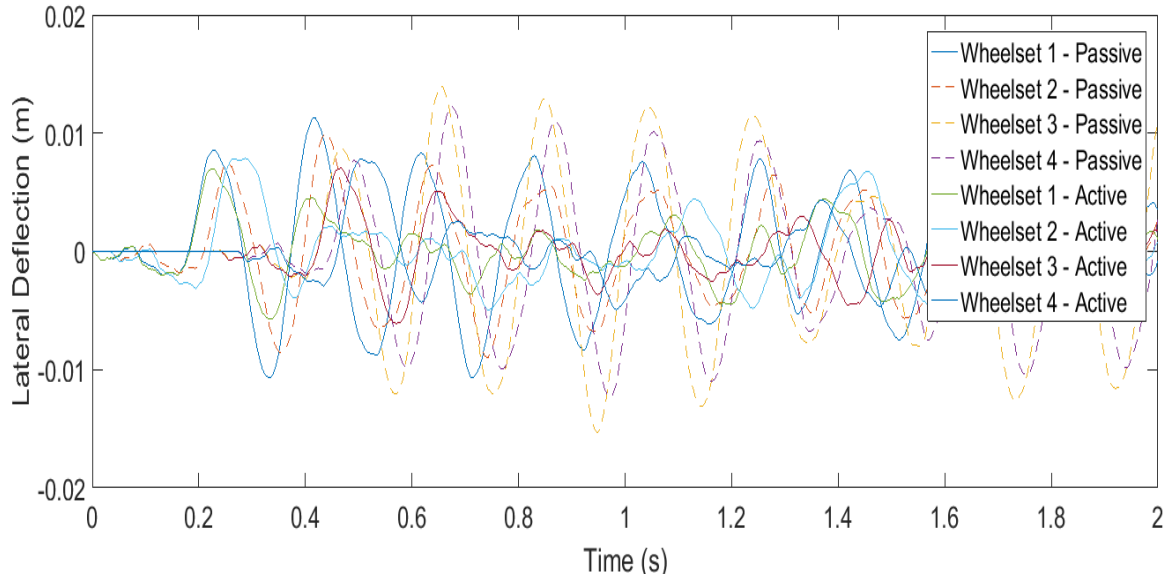

Figure 4. 32 – Wheelset Deflection Comparison FBV – IT

Similar to the behaviour of the two–axle vehicle, from the evaluation of the full bogie vehicle dynamics with the straight track with lateral irregularities, it can be seen that the active control scheme is maintaining the stability of the wheelset in the same manner as the passive suspension while not restricting the wheelset from natural curving.

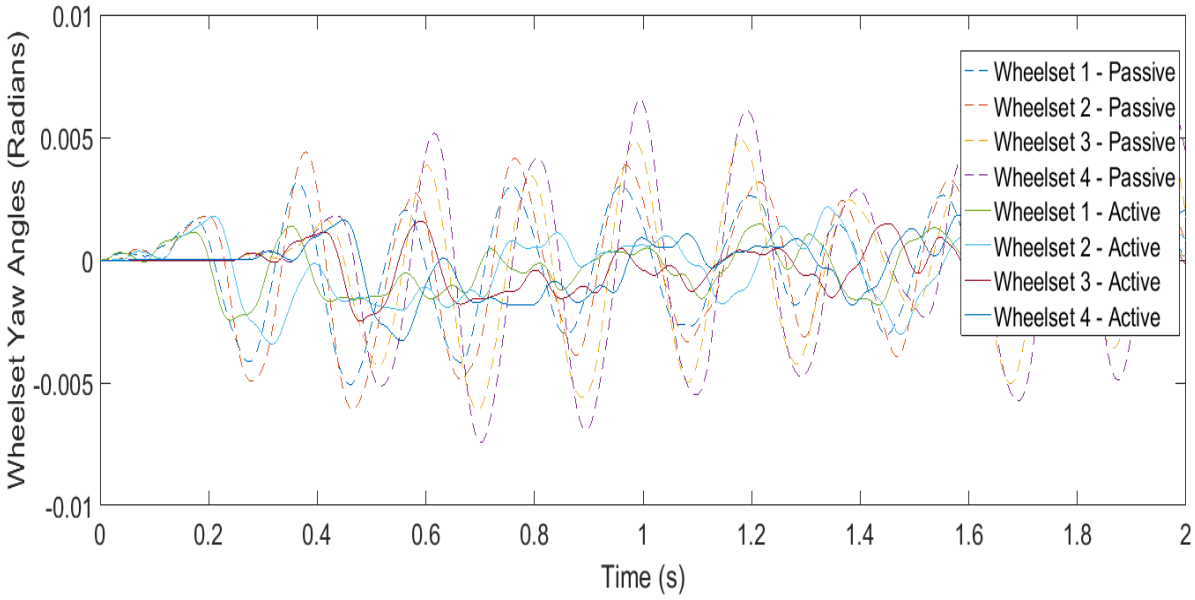

Figure 4. 33 – Wheelset Yaw Comparison FBV – IT

Similar to the deflection, wheelset yaw is almost identical for both control configurations. However, the main point is that active control maintains wheelset stability in the same manner as the passive suspension.

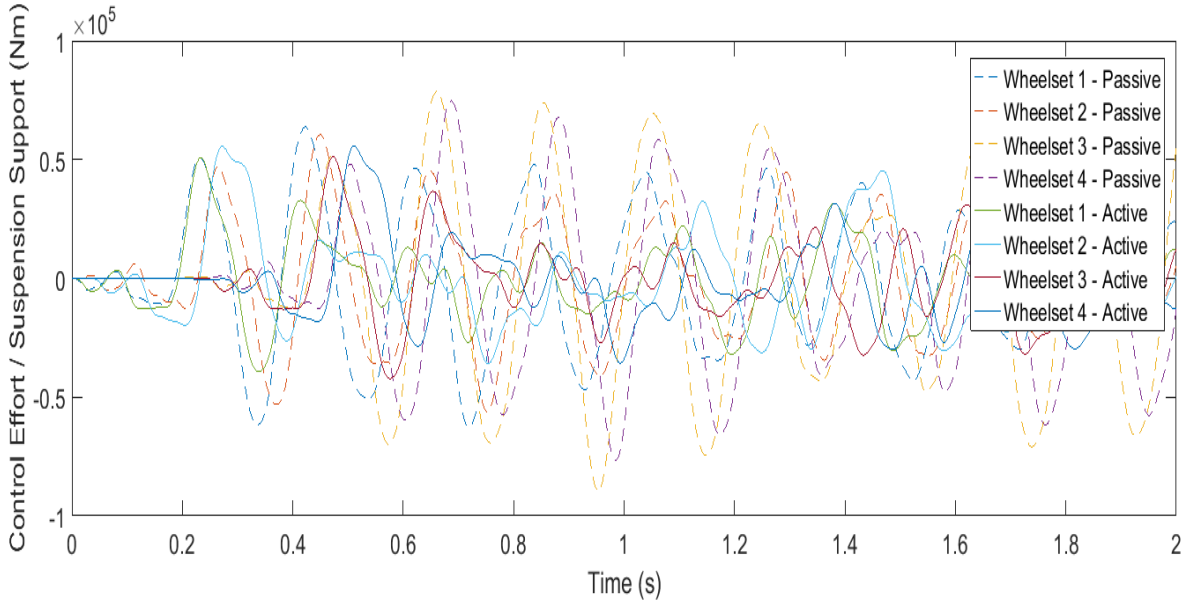

Figure 4. 34 – Wheelset Control Torque Comparison FBV – IT

Control torques between the passive suspension and active control is are almost identical, which might be expected since the active control acts in a similar manner to the passive suspension on the straight track with lateral irregularities to maintain stability.

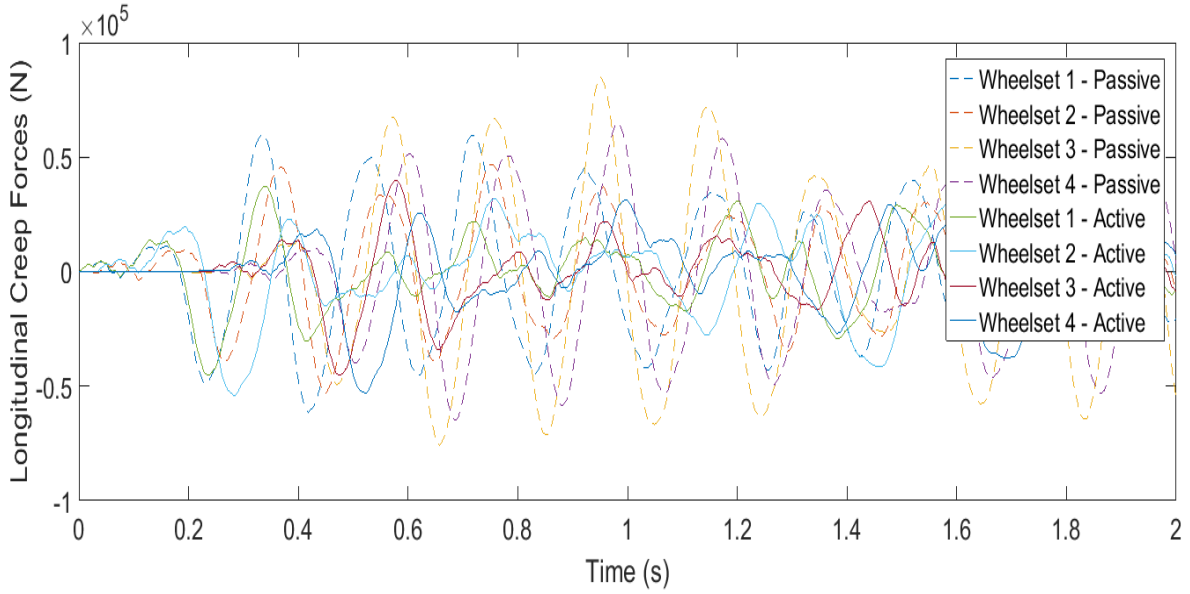

Figure 4. 35 – Longitudinal Creep Force Comparison FBV – IT

As explained in Figure 4.21, similar to the behaviour of the two–axle vehicle, longitudinal creep forces do not significantly change when actively controlled compared to the use of passive suspension.

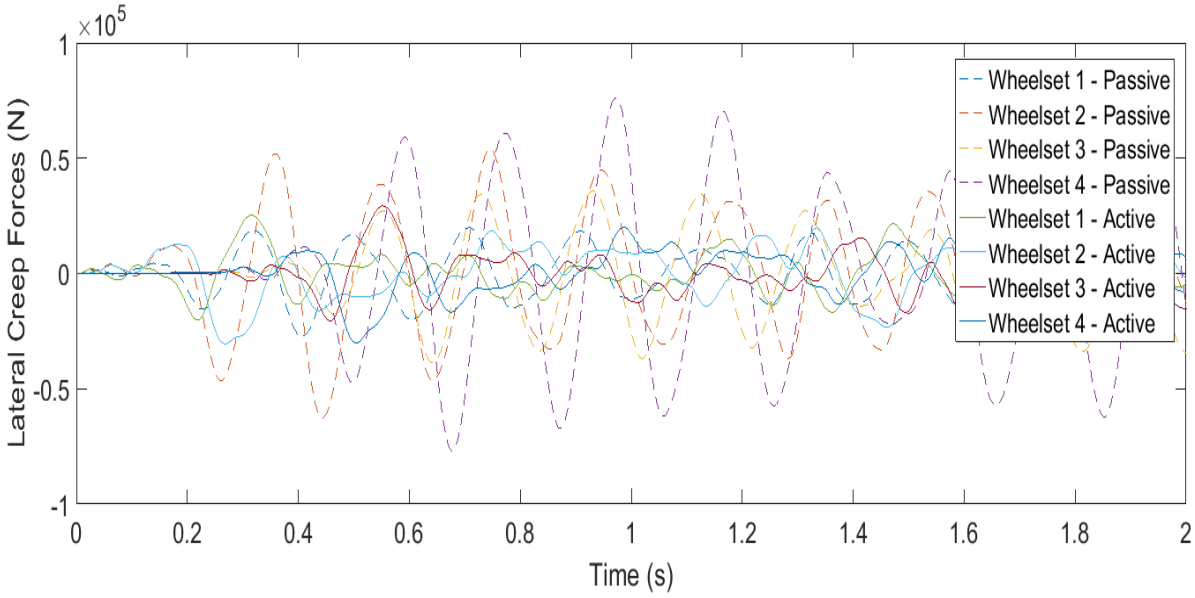

Figure 4. 36 – Lateral Creep Force Comparison FBV – IT

It can be seen from an evaluation of the above results that although active control does not improve the dynamics of the wheelsets with active on the straight track with lateral irregularities, it has not worsened the associated performance when compared to the passive suspension. Thus, it is evident that active control is capable of successfully addressing the trade–off between curving performance and the stability of the wheelsets of full bogie vehicle.

CHAPTER 5: ACTUATOR DYNAMICS AND OPTIMISATION

5.1. Introduction

As evident from the results in the previous chapter, active control systems (including the actuator dynamics) are capable of stabilising the wheelsets without compromising the curving performances. This chapter focusses on the actuators used in active wheelset control and investigates how optimising the electro–mechanical actuator parameters for this specific application of railway wheelset control would result in both improved actuator efficiency and effectiveness.

Thus for this task, a cost function based on actuator energy dissipation is considered as shown below in equation 82 [101] (where V_a and i_a are the supply voltage and current of the motor) which evaluates root-mean-square of power consumption of the actuator over the operational time since the objective is to optimise the actuator parameters to attain optimum performances with lower energy consumption.

$$Cost\ Function = \int_0^T \left\{ \sqrt{\frac{|V_a \times i_a|^2}{T}} \right\} dt \tag{82}$$

Actuator optimisation is achieved in this study by taking the values published in a previous publication [28] in to account (which uses an EM actuator for wheelset control) as the starting point and by varying the values in an analytical order to observe/evaluate how the root–mean–squared (rms) values of key actuator performance indicators behave with respect to these variations as shown below in Figure 5. 1. Considering the dynamics of the actuator design, the most readily changeable parameters are the gear ratio (n), inertial values of the motor rotor (I_m) and gear wheel (I_g), material stiffness (k_g) and material damping (c_g) at the connection (actuator–load). By analysing key performance indicators of the actuators, such as current, voltage, power consumption and losses with these variations, optimal parameter values can be found for this specific task of the active wheelset control.

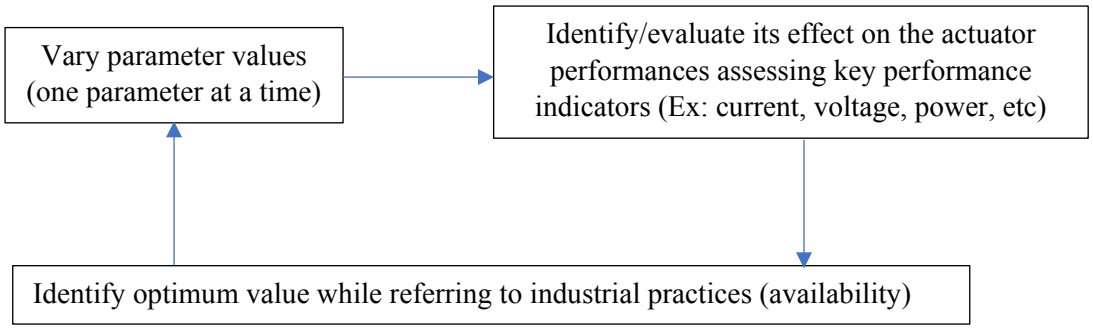

Figure 5. 1 – Parameter Optimisation Methodology

Only one actuator parameter is changed at any given time to identify its direct effect on the performance of the actuator. Other aspects such as vehicle model, wheelset controller, travel speed and track conditions are also kept the some in each case.

In addition to internal actuator parameters, in order to assess the performance of the actuator in a realistic setting, it is important to examine on the wheelset–actuator connection link (rod, etc.) since this is the physical contact point between the actuator and the wheelset, and where the control torque from the actuator is transferred to the wheelset.

Thus, as it can be seen in Figure 5.2, there are certain material stiffness and damping properties associated with the model to represent the connection between the actuator and the wheelset, where the values of these properties are based on the material used for the application. Hence, as considered in the actuator dynamic equations (Equation 77–79), stiffness (Kg) and damping (Cg) are also varied to assess their effects on the dynamics and power transmission in order to evaluate its effect and to select optimal values for parameters. Thus, all key components/elements in the electro–mechanical actuators are evaluated for optimisation.

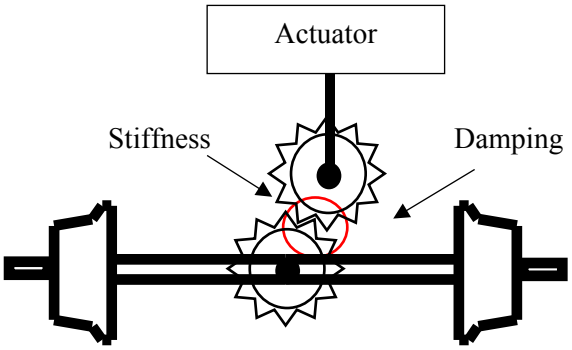

Figure 5. 2 – Actuator Connection

When focussing on the track conditions used for the optimisation study, the generic straight track with lateral irregularities is used to excite the vehicle models instead of the curved track. The reason for using the high–speed straight track instead of the low–speed curved track is based on the fact that the former demands a higher active control effort, as elaborated in the previous chapter (Chapter

4). Thus, the actuator optimisation is undertaken based on the high demand track, so the optimised values can be readily used for the curved track conditions with a low demand.

During this analysis, the optimisation of both the two–axle vehicle and the full bogie vehicle is performed separately since the difference in vehicle configuration such as mass/inertia of components, distance between the wheelsets, etc. can lead to difference in active control effort demand.

As an academic research, in this study, the initial selection of the parameter variation range is not done based on common industrial practices (market availability) of components in order to fully observe/evaluate actuator dynamic trends with respect to a wider variation range. Thus, larger ranges for parameters such as gear ratio, inertia and stiffness/damping are assessed from an academic perspective to identify their individual influences on actuator performance. However, when concluding optimal parameter values for the actuator (based on its performance) practical limitations are considered in order to maintain a more practical/realistic aspect to the study.

This study on the optimisation of the dynamics of the actuator can prove to be extremely valuable to the implementation of active wheelset control for both the two–axle vehicle and the full bogie vehicle in two main ways:

1) Identifying the boundaries of the actuator performance
2) Identifying parameters for optimal performance

5.2. Parameter Analysis

5.2.1. Gear Ratio

As elaborated above, although it is practically/mechanically challenging to achieve gear ratios high as 1:2000, in this study these larger ranges (1:100 to 1:2000) are used purely from the academic perspective to observe the dynamic effect they have on the actuator performance. Although practical limitations are neglected in this stage of the study, they are taken into account when concluding optimal values for each of the vehicle configurations.

As it can be seen from Figure 5.3 (two–axle vehicle) and Figure 5.4 (bogie vehicle), motor current significantly decreases as the gear ratio increases. This is a result of effective torque increasing with gear ratio, and thus torque generated from the motor is reduced since the control effort demand

from the wheelset controller remains almost identical. This enables the actuator control signal to be lowered and the motor to generate a reduced torque that results in a lowering of the required current.

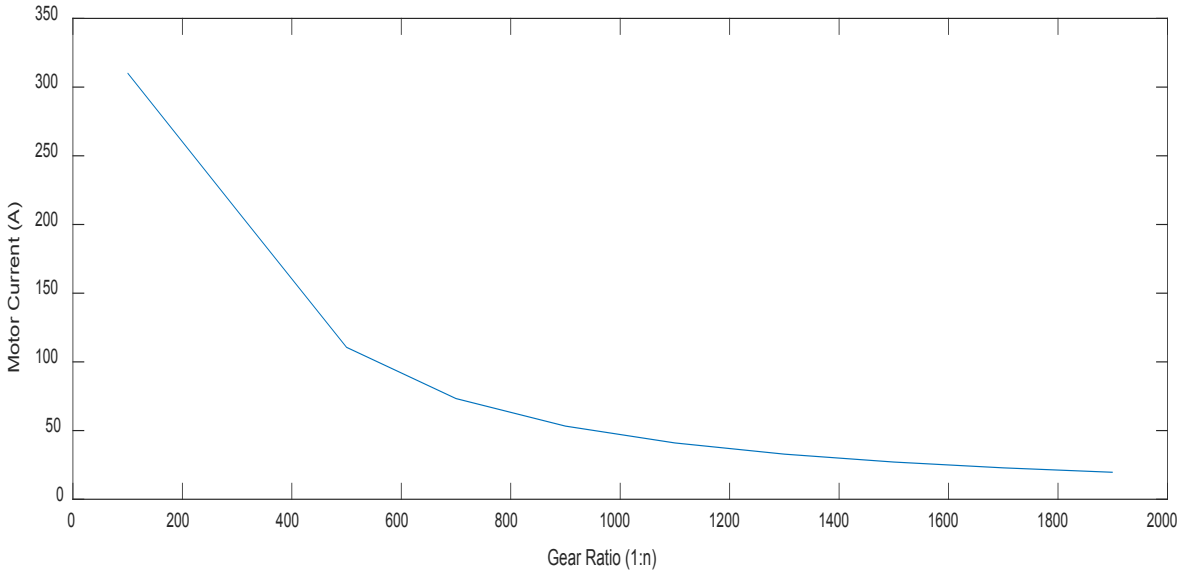

Figure 5. 3 – Gear Ratio vs. Motor Current – TAV

However, despite of the same trend, there is a slight variation in the current values due to differences (approximately 100 Nm) in the control effort demand from the wheelset controllers. This is a result from the difference between the respective vehicle configurations and it can be seen by comparing the results that full bogie vehicle has slightly lower current values compared to the two–axle vehicle. This can be expected due to the lower control effort required for the full bogie vehicle since it has features such as two stage suspension and lower wheel base.

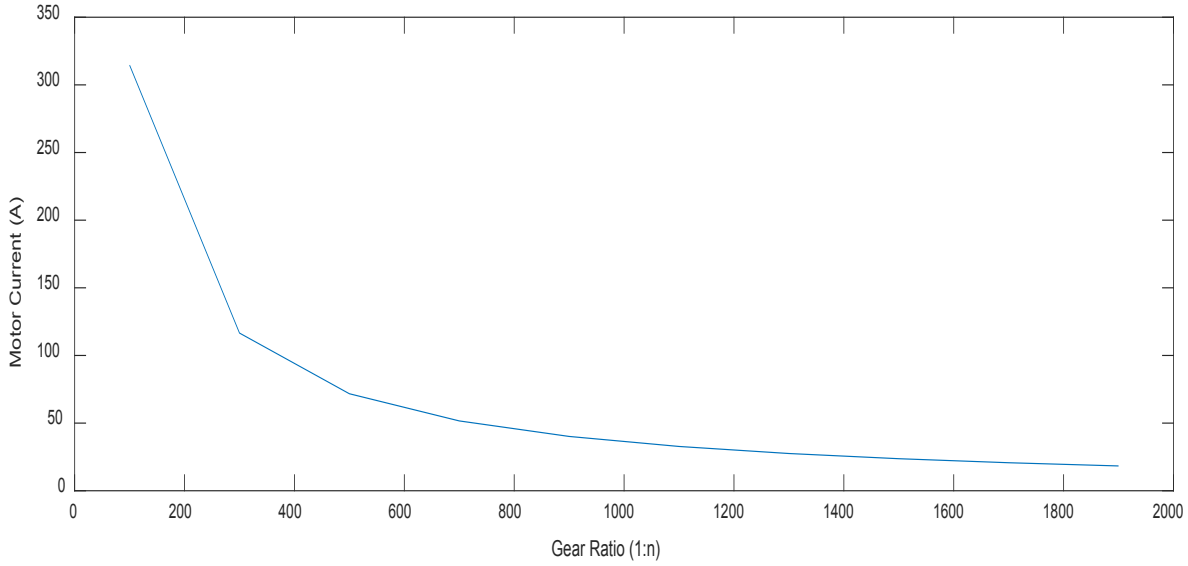

Figure 5. 4 – Gear Ratio vs. Motor Current – FBV

As explained above, due to the increase of the effective torque it can be seen from Figure 5.4 that the current consumed by the motor decreases with increasing gear ratio since the torque generation is decreasing.

In contrast to current, as shown in the Figure 5.5 (with two–axle vehicle), motor voltage shows a decreasing trend until a gear ratio of around 1:500, after which it linearly increases. The analysis shows that this phenomenon occurs due to the relationship between motor back–emf (electromagnetic force) and motor speed (in conjunction with the gear ratio). The study shows that at low gear ratios, such as 1:100, both motor voltage and current are high whilst back–emf is considerably low due to the associated low motor speeds. This behaviour can be expected since, torque demand from the motor increases with lower gear ratios due to the lower effective torque (on the load). Thus, voltage has to increase to provide the higher current, which results in higher torque, as the back–emf is not high enough to produce the current required due to the low speeds involved. Therefore, with gear ratio values less than 1:500, the motor operates in the motoring (supplying energy) mode.

In contrast, when the gear ratio is increased, it subsequently increases motor speed. This results in an increased back–emf that generates a potential that opposes the supply voltage and reduces the net voltage in the system. Therefore, when continuously increasing the gear ratio (subsequently motor speed), after a given point (a gear ratio of 1:500 in this case), the potential (back–emf) generated completely overcomes the supply voltage and the motor operates on a net potential by acting as a generator. Thus, after the 1:500 gear ratio, the motor is removing energy from the system by acting as a generator instead of supplying energy and thus the net voltage continues to increase with increasing gear ratio.

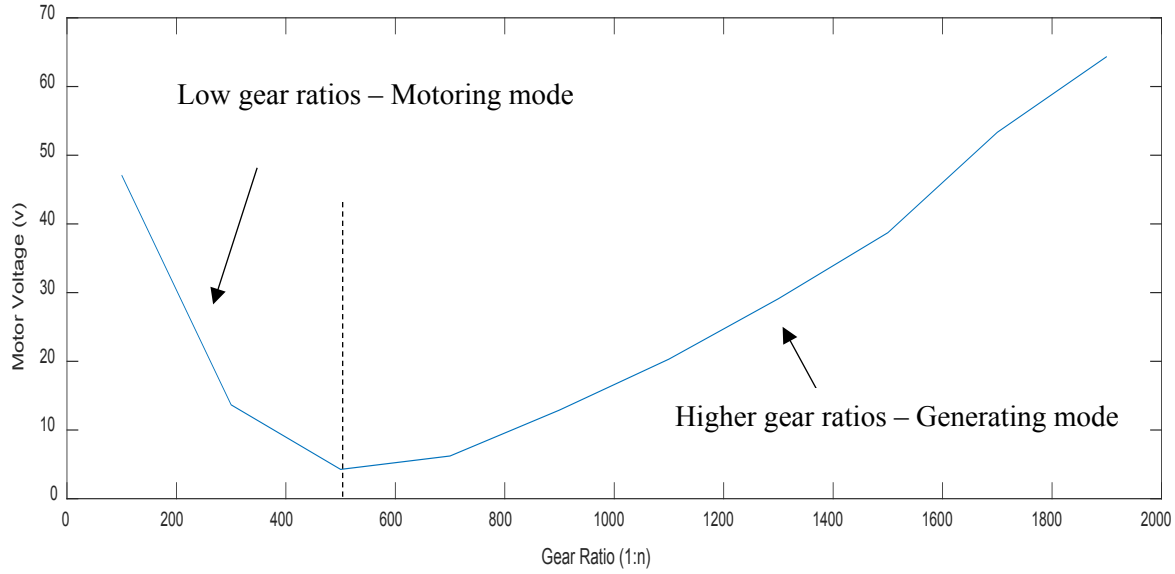

Figure 5. 5 – Gear Ratio vs. Motor Voltage – TAV

Similar behaviour can be seen for the full bogie vehicle in Figure 5.6. With the increase of gear ratio/speed of the motor, the voltage decreases up to a particular gear ratio after which it increases for the reasons explained above. Thus, after the 1:500 gear ratio, the motor stabilising the wheelsets begins to act as a generator by removing energy from the wheelsets. Regarding the values, it is found the voltage values seen in the full bogie vehicle are slightly lower than the values seen with two–axle vehicle due to the reasons elaborated above.

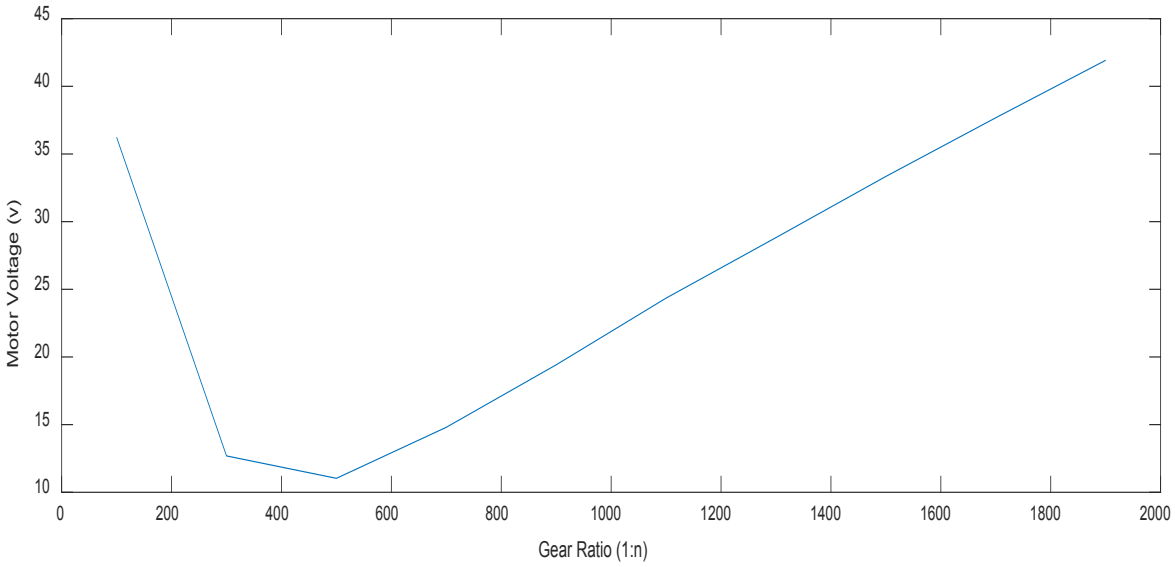

Figure 5. 6 – Gear Ratio vs. Motor Voltage – FBV

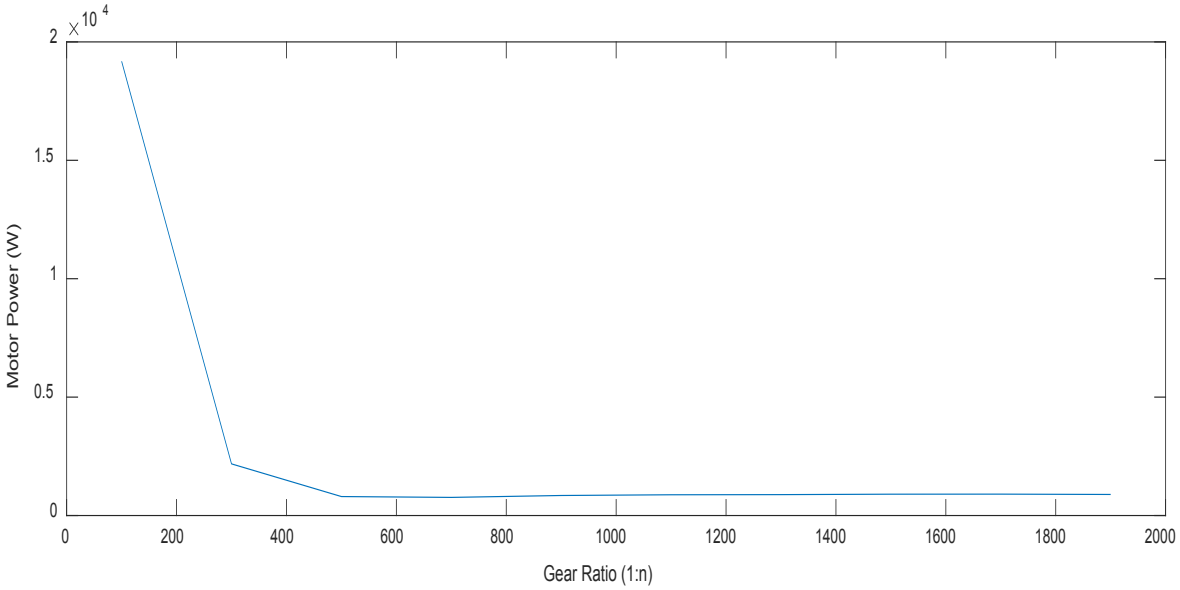

Figure 5. 7 – Gear Ratio vs. Motor Power – TAV

Figure 5.7 depicts the variations in motor power with changes in gear ratio for the two–axle vehicle. It can be seen that the gear ratio has a significant effect on the power of the motor. At low gear ratios/low motor speeds, motor power is considerably high, whilst then subsequently decreases with increasing gear ratio. This is expected due to the decrease of mainly the motor current with respect to increasing gear ratio, since the motor power is directly associated with the voltage and current of the motor. As explained above, the motor acts as a power source at high gear ratios (>1:500) and motor power follows a decreasing trend (when increasing the gear ratio) as the current during the phase when the motor is operating in generation mode. Although once the back–emf is more dominant than the supply voltage source and net voltage increases in proportion to the gear ratio, since the motor current continuous to reduce (due to increasing effective torque), motor power also continues to reduce with increasing gear ratio following the trend of the current. The directional change of the power from motoring to generator mode cannot be seen for with these results since these data represents rms values instead of instantaneous values.

With the full bogie vehicle (Figure 5.8), motor power decreases with respect to increasing gear ratio due to the effects of current (primarily) and voltage.

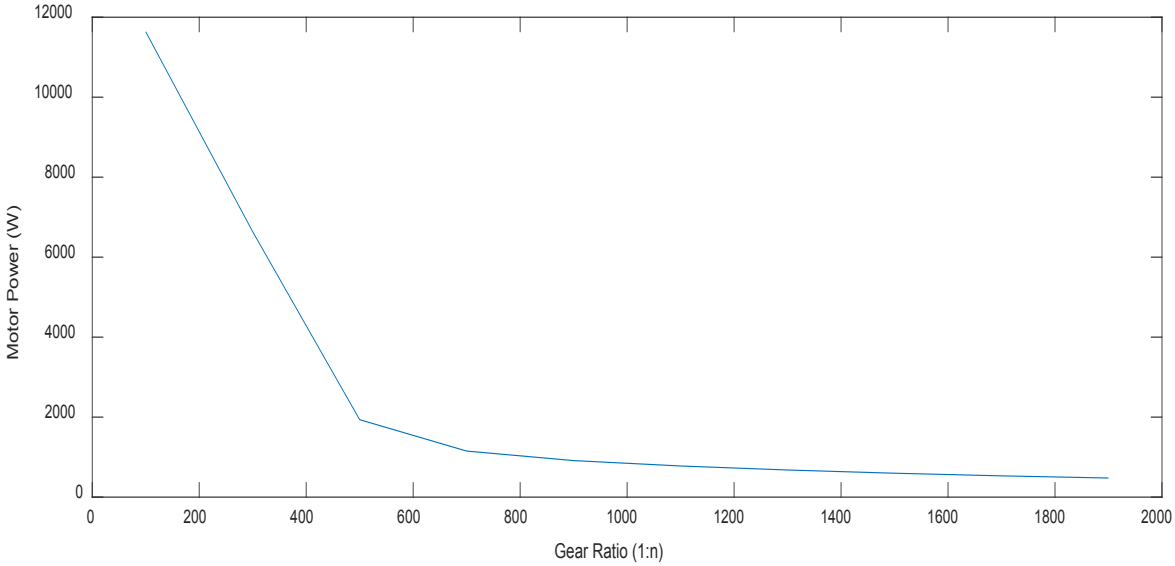

Figure 5. 8 – Gear Ratio vs. Motor Power – FBV

When focusing on the torque applied to the wheelsets, as Figure 5.9 illustrates, the gear ratio has approximately 23% effect on the torque applied to the wheelset by the actuator between the gear ratios of 1:100 to 1:2000 due to the increase in effective torque as the gear ratio increases.

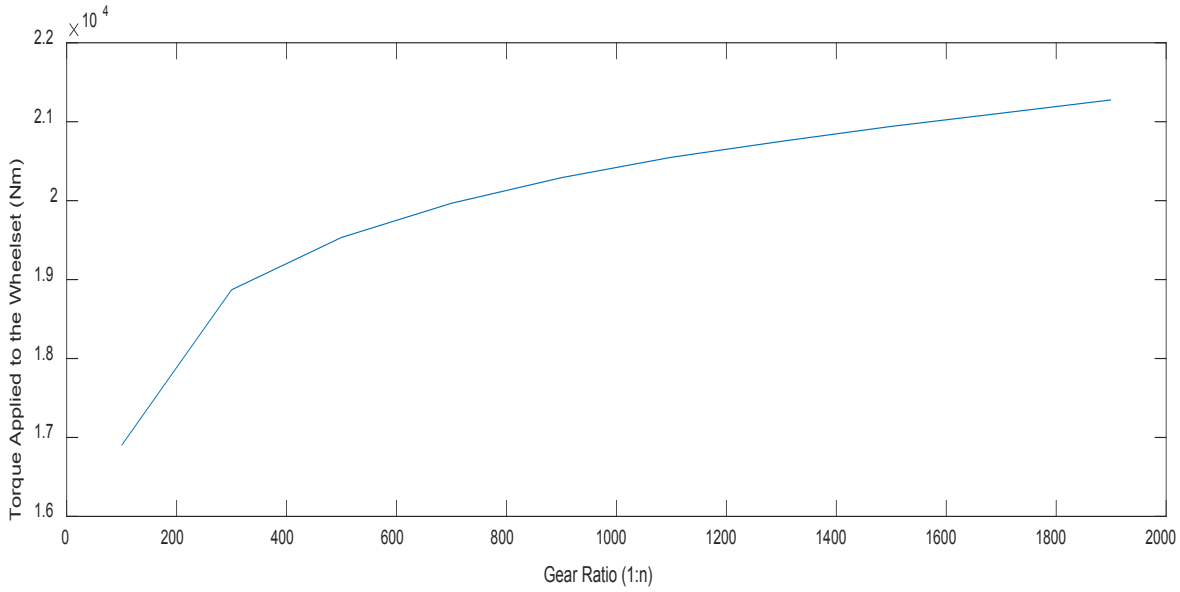

Figure 5. 9 – Gear Ratio vs. Applied Torque – TAV

Similarly, the torque applied to the wheelset in the full bogie vehicle has more of an effect than the two–axle vehicle when the gear ratio is increased. When analysing the results further, it is seen that this effect is a result of effective torque and higher inertia values in the full bogie vehicle (compared to

two–axle vehicle). This has been further analysed by re–evaluating the behaviour of full bogie vehicle when gear ratio is varied while the inertia and mass values of the wheelsets, bogie and vehicle is reduced match with the two–axle vehicle. Results showed that with lower inertia/mass, the torque variation lowers similar to the behaviour seen with two–axle vehicle. Thus, a significant change in torque values can be seen in Figure 5.10, when comparing the lowest and highest gear ratios, as expected due to higher inertia/mass of the components in the full bogie vehicle configuration.

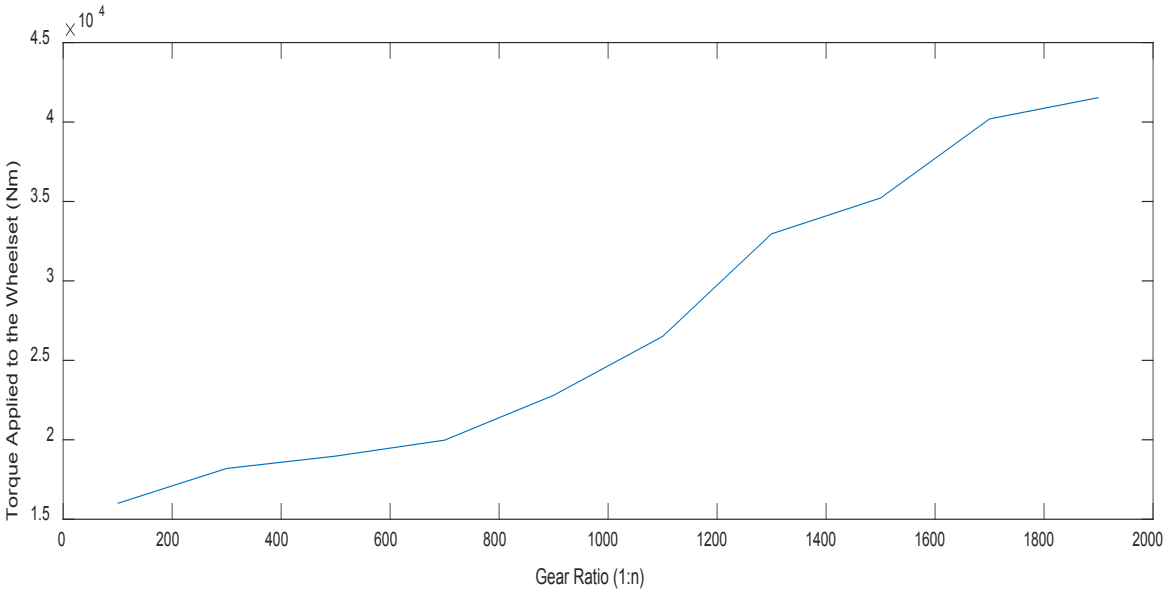

Figure 5. 10 – Gear Ratio vs. Applied Torque – FBV

As expected, due to the relationship between motor current (I) and internal loss ($Power\ Loss = I^2R$), it can be seen in Figure 5.11 that since current decrease with increasing gear ratio, internal power loss shows the same trend with increasing gear ratio.

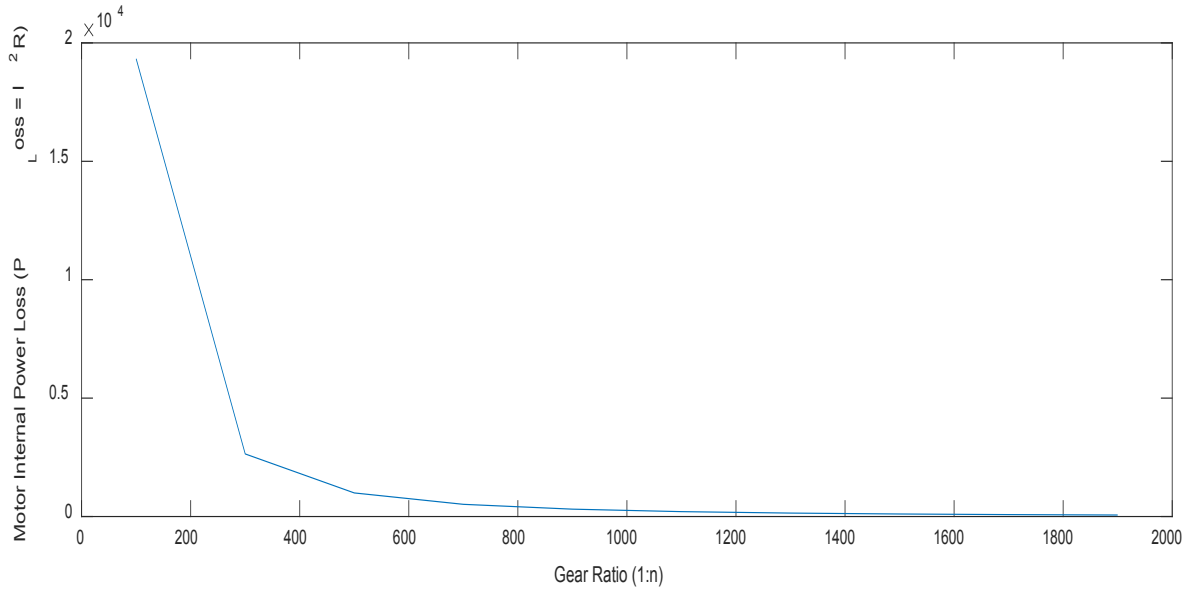

Figure 5. 11 – Gear Ratio vs. Internal Power Loss – TAV

It can also be deduced that since internal power loss decreases as the current decreases, a low current is desirable when optimising and current is inversely proportional to gear ratio.

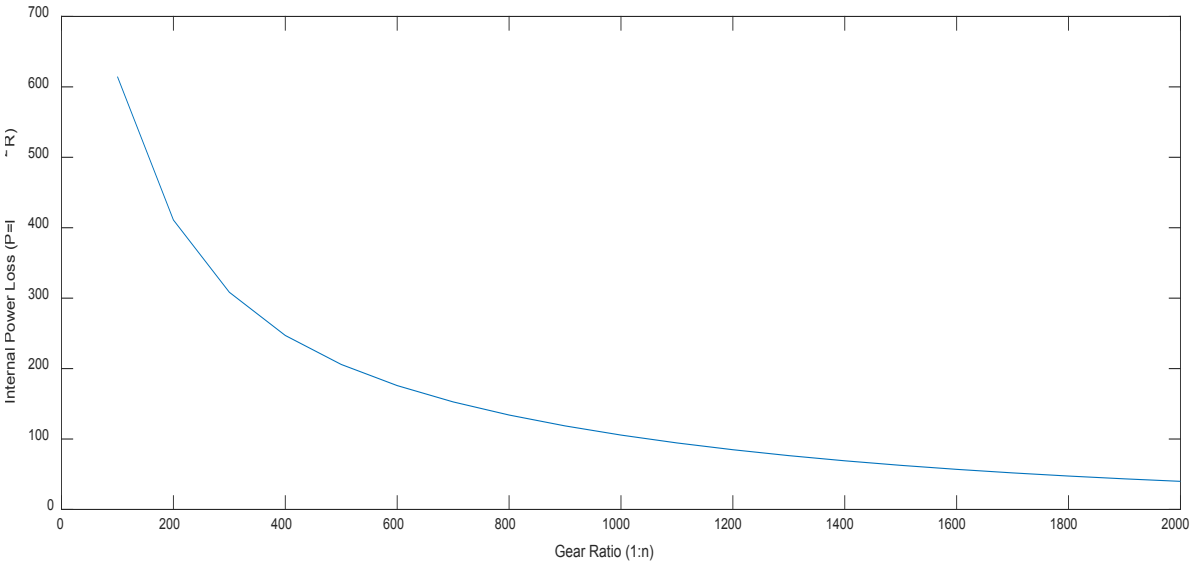

Figure 5. 12 – Gear Ratio vs. Motor Internal–Loss – FBV

Similarly, with the full bogie vehicle it can be seen that internal loss in the motor decreases with the increasing gear ratio, as seen from the actuator with the two–axle vehicle, and it reduces since motor current reduces with the increasing gear ratio.

When analysing the above results for both vehicle configurations, it is clear that the higher the gear ratio – better the performance is. This is due to the increase of effective motor torque with

increasing gear ratio, which results in lower current/internal power losses while above a certain gear ratio, the motor acts in the generator mode instead motoring mode.

However, when selecting an optimal gear ratio for this particular requirement of the railway wheelset control, it should be noted that selecting an extremely high ratio is not realistic due to practical/mechanical limitations. Thus, after some brief market research, a gear ratio of 1:700 is selected (for both vehicle configurations) since gear boxes with this ratio are currently widely available in the market [97], and it is in the region where motor can act as a generator in this application.

5.2.2. Stiffness at the Connection

Similar to the gear ratio, practical limitations to stiffness values are neglected for this analysis phase in order to observe the associated effect on the actuator performance from an academic prospective. However, when selecting appropriate values, practical limitations are ultimately taken into account.

From Figure 5.13, it is evident that stiffness of the actuator–wheelset connection/interface for the two–axle vehicle has a significant effect on the actuator dynamics since the power generated in the actuator is being transferred to the wheelset through the stiffness.

Figure 5.12 indicates that motor current starts to decrease after stiffness reaches10^5 kNm^{-1} and will substantially lower after stiffness reaches10^6 kNm^{-1}.

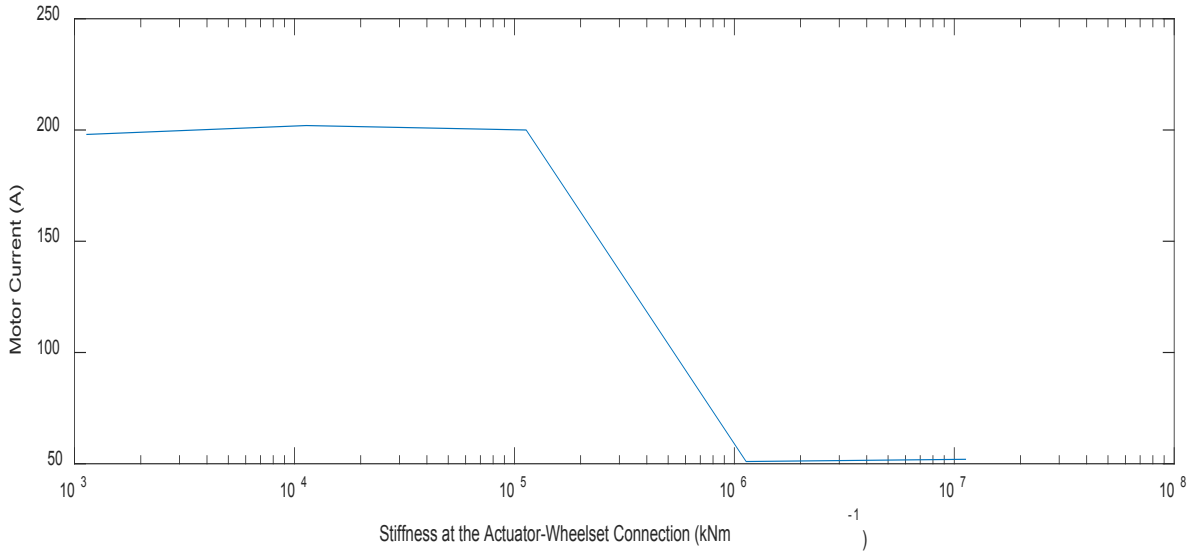

Figure 5. 13 – Stiffness vs. Motor Current – TAV

This occurs since lower stiffness values in the connection is not adequately stiffened to transfer the power in an effective manner. Thus, the motor needs to provide higher torque to compensate to the losses and it results in higher current values.

Similar analysis (Table 5.1) has been undertaken for the full bogie vehicle by varying the stiffness value of the actuator–wheelset connection/interface, and it is found from the study that the stiffness value range is very limited with current actuator controller gains with respect to the stability of the full bogie vehicle wheelsets and is stable for any value in 10^7 kNm^{-1}. This limited range could be extended through the variation of actuator controller gains while it is again a trade–off between the performance of the actuator and the robustness.

However, although the dynamic behaviour is the full bogie vehicle cannot be assessed over a wider range of stiffness at the actuator–wheelset with the controller current gains, since it is clear from the gear ratio variation assessment that despite of the difference of values, both two–axle vehicle and full bogie vehicle follows the same trends when varying the parameters. Thus, in this case, observation/deductions made about the trends with two–vehicle, with variation of the stiffness at the actuator–wheelset value, can be followed to the full bogie vehicle as well.

Table 5. 1 – Actuator Performance vs. Stiffness of the Connection – FBV

Actuated Torque (kNm)	Current (A)	Voltage (v)	Motor Power (W)	Stiffness at the Connection (kNm^{-1})
19.88	41.23	8.09	363.84	Any value in 10^7

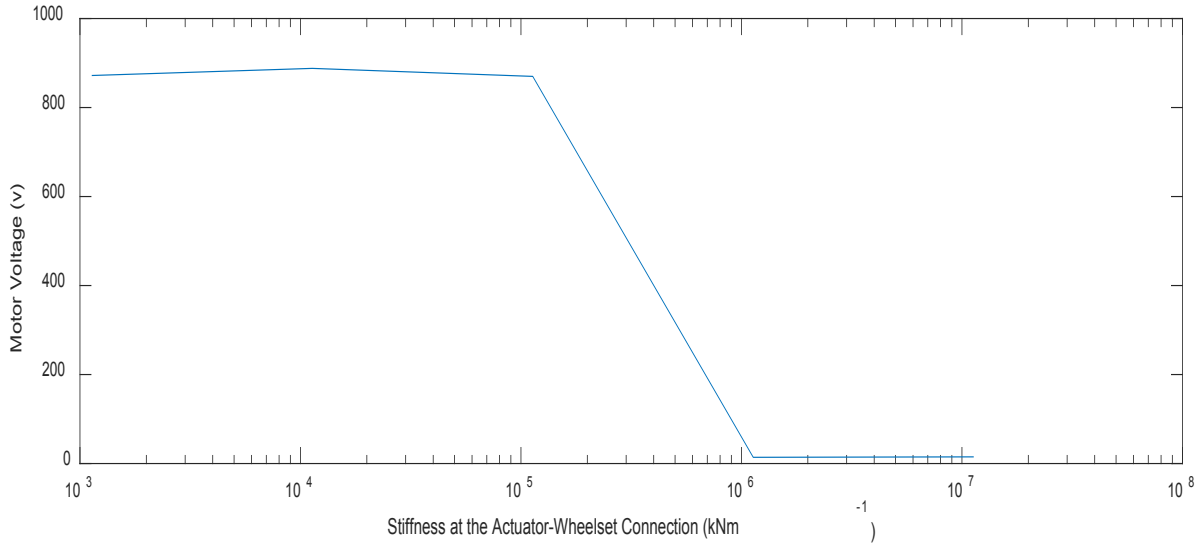

Figure 5. 14 – Stiffness vs. Motor Voltage – TAV

A similar response of the current can be observed with the voltage since the power transfer is not effective at lower stiffness's and thus the control command to the motor (voltage) is higher at lower

stiffness's since the actuator controller needs to supply more control effort based on the torque feedback and the torque demand from the wheelset controller (almost identical in all stiffness cases). Similarly, the opposite scenario occurs when increasing the stiffness, where the power is transferred to the wheelsets in an adequate manner and the control effort from the actuator controller is reduced when the error between demand and supplied torque is low.

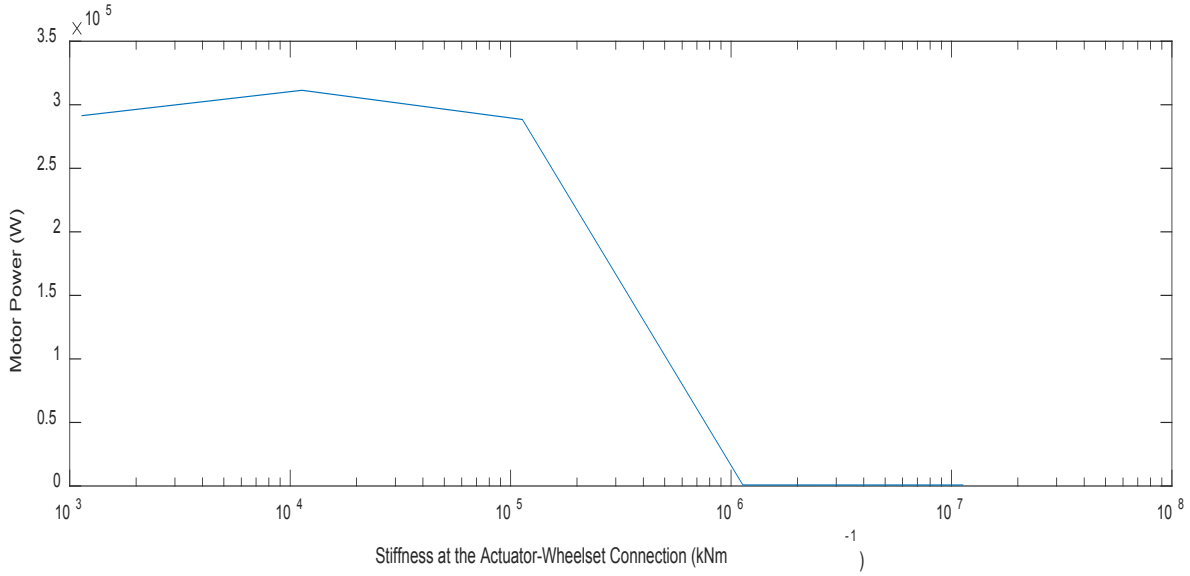

Figure 5. 15 – Stiffness vs. Motor Power – TAV

As elaborated above, the power requirements of the actuator for the two–axle vehicle decrease as the connection is stiffened since the power transfer in this circumstance is more efficient.

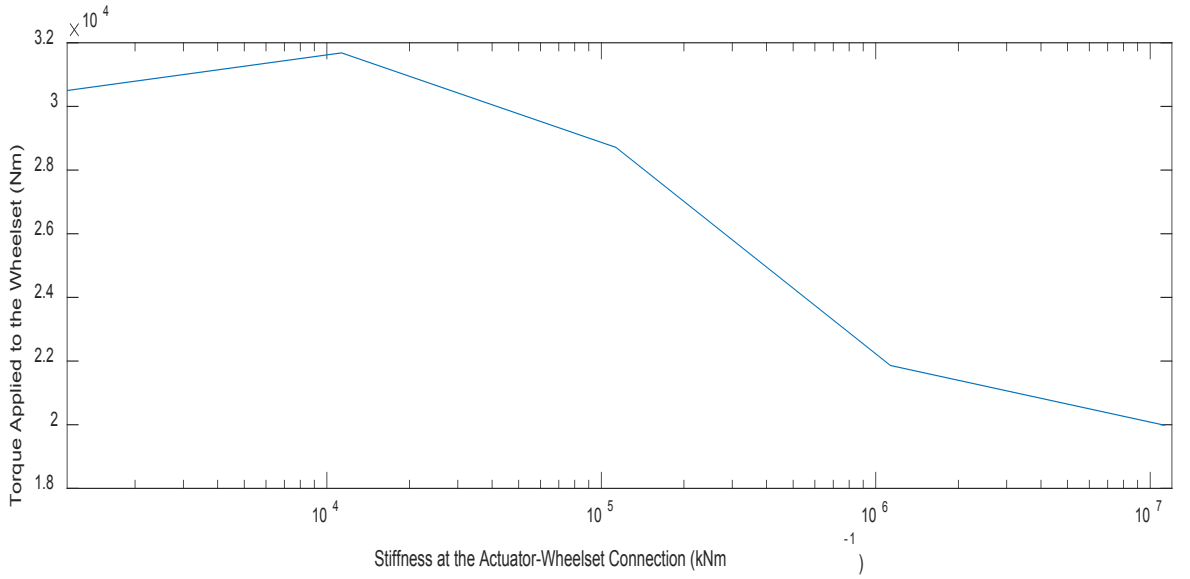

Figure 5. 16 – Stiffness vs. Applied Torque – TAV

In contrast to the trends of the motor current, voltage and power, torque applied to the wheelset have an approximately 30% of decrease in the value when the stiffness is increased. This can be expected since the control effort decreases with stiffened connection due to the increase in effectiveness of the torque transfer.

As per the above results, it is evident that a certain level of stiffness at the actuator–wheelset connection is necessary to ensure effectiveness in transferring power to the wheelsets. Thus, stiffness value of 10^7 kNm^{-1}can be used in the study since it represents an almost a rigid connection [98].

5.2.3. Gear Wheel Inertia

In order to assess the system using a larger range of values, the power/order of the inertia value of the gear wheel was varied and, as it can be seen from the results of Table 5.2, gear wheel inertia does not cause any obvious effects on actuator performance, since the effective inertia of the coupled gear wheel is $I_{gear}\, n^2$, and its value is effected by the determinant value (z) of the gear ratio (n). Since $z > 1$ and $n = \frac{1}{z} (< 0)$, which is relatively a minor value, while its squared value becomes further insignificant.

Table 5. 2 – Actuator Performance vs. Inertia of the Gear–Wheel – TAV

Output Torque (Nm)	Current (A)	Voltage (v)	Motor Power (W)	Inertia of the Gear–Wheel (kgm^2)
1.99×10^4	51.61	14.80	765.21	3.84×10^{-2}
1.99×10^4	51.61	14.80	765.21	3.84×10^{-3}
1.99×10^4	51.61	14.80	765.21	3.84×10^{-4}
1.99×10^4	51.61	14.80	765.21	3.84×10^{-5}
1.99×10^4	51.61	14.80	765.21	3.84×10^{-6}

Similarly, when varying the gear wheel inertia for full bogie vehicle, it was found from the results depicted in Table 5.3 that gear wheel inertia does not affect performance over a large range of values.

Table 5. 3 – Actuator Performance vs. Inertia of the Gear–Wheel – FBV

Output Torque (Nm)	Current (A)	Voltage (v)	Motor Power (W)	Inertia of the Gear–Wheel (kgm^2)
1.98×10^4	41.23	8.08	363.83	3.84×10^{-1}
1.98×10^4	41.23	8.08	363.83	3.84×10^{-2}
1.98×10^4	41.23	8.08	363.83	3.84×10^{-3}
1.98×10^4	41.23	8.08	363.83	3.84×10^{-4}
1.98×10^4	41.23	8.08	363.83	3.84×10^{-5}
1.98×10^4	41.23	8.08	363.83	3.84×10^{-6}
1.98×10^4	41.23	8.08	363.83	3.84×10^{-7}
1.98×10^4	41.23	8.08	363.83	3.84×10^{-8}

As elaborated above, values are changed over a larger range to observe the effects purely from an academic prospective. However, since gear wheel inertia does not seem to cause any noticeable effect, the original value mentioned in the source study [28] is used unchanged in this instance for each of the vehicles.

5.2.3. Motor Rotor/Wheel Inertia

The motor wheel/rotor inertia has some effect on the system, as indicated below. This is due to the fact that unlike the gear wheel inertia, from the wheelset's prospective, effective motor rotor inertia is $I_{rotor}\frac{1}{n^2}$. Thus since $n = \frac{1}{z}$ and when $z > 1$, value of $I_{rotor}\frac{1}{n^2}$ becomes more significant. Therefore, motor rotor inertia has a higher affect to the actuator dynamics than gear wheel inertia.

Common industrial practises (market availability) are referred in this case since this is a parameter associated with the internal structure of motor and it is not practical to change this value between large ranges as with the other parameters. From analysing the motor power results depicted in Figure 5.9 and Figure 5.10, motor power requirements are between 1 kW to 5 kW. Thus, in order to find a realistic/suitable value range for the motor rotor inertia, specification if 1 kW to 5 kW motors are referred. Thus, it is found that range is between 2×10^{-6} kgm^2 to 2×10^{-3} kgm^2.

Table 5. 4 – Actuator Performance vs. Inertia of the Motor Rotor/Wheel – TAV

Output Torque (Nm)	Current (A)	Voltage (v)	Motor Power (W)	Inertia of the Motor Rotor (kgm^2)
2.01×10^4	52.50	15.44	782.42	1.15×10^{-3}
1.99×10^4	52.46	14.29	756.76	1.15×10^{-4}
1.98×10^4	52.36	14.22	749.33	1.15×10^{-5}
1.97×10^4	52.32	14.18	743.81	1.15×10^{-6}

From the results of the analysis of the two–axle vehicle (Table 5.4), it is evident that although this parameter has more effect on the actuator performance than the gear wheel inertia, it does not have a significant effect on the actuator performance over a large range of values.

Same trend can be seen with Table 5.5 which depicts the results of motor rotor inertia variation with the full bogie vehicle and the results indicate that this parameter does not affect the performances of the actuator (within the operational range) significantly.

Table 5. 5 – Actuator Performance vs. Inertia of the Motor Rotor/Wheel – FBV

Output Torque (Nm)	Current (A)	Voltage (v)	Motor Power (W)	Inertia of the Motor Rotor (kgm^2)
1.98×10^4	41.88	8.14	377.95	1.15×10^{-3}
1.98×10^4	41.76	8.13	373.52	1.15×10^{-4}
1.97×10^4	41.76	8.11	372.96	1.15×10^{-5}
1.97×10^4	41.67	8.08	369.80	1.15×10^{-6}

5.2.4. Damping at the Connection

The study shows that unlike the effect of the stiffness, the damping effect of the actuator–wheelset connection has a lesser impact on the actuator dynamics.

It is clearly evident from the key performance indicators of current, voltage, torque and power, shown below (for the two–axle vehicle) that the effect of damping at the connection on the actuator performance is minor.

Table 5. 6 – Actuator Performance vs. Damping of the Connection – TAV

Output Torque (Nm)	Current (A)	Voltage (v)	Motor Power (W)	Damping of the Connection (at actuator and wheelset) ($kNsm^{-1}$)
2.05×10^4	51.95	22.79	1164.88	1000
2.03×10^4	51.84	20.15	1032.08	2000
2.02×10^4	51.77	18.50	947.94	3000
2.01×10^4	51.72	17.37	890.42	4000
2.01×10^4	51.69	16.54	848.83	5000
2.00×10^4	51.66	15.89	817.46	6000
2.00×10^4	51.64	15.38	792.82	7000
1.99×10^4	51.63	14.96	772.88	8000
1.99×10^4	51.61	14.62	756.23	9000
1.99×10^4	51.59	14.32	742.08	10000

It is evident from the results that increase in material damping reduces actuator performances slightly. However, since the effect is minor, the original value stated in reference [28] is considered acceptable in this case.

Similarly, it can be observed with Table 5.7 that during variation of the damping, at the connection, for the full bogie vehicle that this parameter did not have a significant effect to the performances of the actuator performance as with the case with two–axle vehicle. Thus, the value selected for the two–axle vehicle can be used for the bogie vehicle as well.

Table 5. 7 – Actuator Performance vs. Damping of the Connection – FBV

Output Torque (Nm)	Current (A)	Voltage (v)	Motor Power (W)	Damping of the Connection (at actuator and wheelset) ($kNsm^{-1}$)
2.02×10^4	41.18	7.94	339.82	1000
2.02×10^4	41.18	7.95	343.00	2000
2.01×10^4	41.19	7.97	346.37	3000
2.01×10^4	41.20	7.99	349.92	4000
2.00×10^4	41.21	8.02	353.65	5000
1.99×10^4	41.22	8.04	357.54	6000
1.98×10^4	41.23	8.07	361.59	7000
1.98×10^4	41.24	8.10	365.78	8000
1.97×10^4	41.25	8.13	370.11	9000
1.97×10^4	41.26	8.17	374.56	10000

It is evident from Table 5.1 and Table 5.7 that although the stiffness value of the connection has a low range of operation with the current controller gains, the damping value of the connection has a large range of operation.

5.3. Parameter Analysis – Summary

From the parameter analysis of the actuator in the two–axle vehicle (TAV) and full bogie vehicle (FBV), it is evident from the results that key influential parameters for the actuator, in this case, are the gear ratio and stiffness of the connection at the wheelset–actuator, while the inertial values and the damping at the connection do not affect actuator performances. Thus, selecting a gear ratio and a stiffness for the actuator–wheelset connection is essential to the effectiveness/efficiency of the actuators used in active wheelset control, where the results indicate that using higher values as possible for these parameters is desirable. However, as explained previously, due to practical limitations (as per industrial practices) the gear ratio cannot be realistically increased indefinitely, and 1:700 can be selected as an optimal realistic value. High stiffness, values of the on the other hand, can be practically achieved by making the connection between wheelset and the actuator as rigid as possible.

In addition, from evaluating the results obtained using the two–axle vehicle and the full bogie vehicle, it is evident that actuators, in both configurations show the similar pattern of results for each of the vehicle configurations when varying the above parameters. This enables the use of the same set of optimal actuator parameters for both vehicle configurations.

From analysing the variations in gear ratio, gear wheel inertia, motor rotor/wheel inertia and the stiffness/damping at the connection, it is clear that the optimal values for this particular application for both vehicle configurations are as reported below. These parameters enable the actuator to be more robust and efficient in operation.

Gear Ratio : $^{1}/_{700}$

Gear Wheel Inertia : 3.84×10^{-4} kgm^2

Motor Rotor/Wheel Inertia : $1.15 \times 10^{-3.2}$ kgm^2

Stiffness at the Connection : 1.132×10^{7} Nm^{-1}

Damping at the Connection : 7540.7 Nsm^{-1}

CHAPTER 6: SENSING WITH STATE OBSERVERS

6.1. Introduction

As mentioned previously, another important issue pertaining to the actuator controller in this application is to obtain measurements/feedback of the output torque of the actuator in order to compare and match with the torque demanded by the wheelset controller. However, a problem arises in this particular application since it is very difficult to measure the torque applied to the wheelset reliably due to the harsh operating environment of the wheelsets. Hence, to overcome the difficulties associated with obtaining reliable feedback, this chapter examines the use of a model–based solution by developing a state observer for this task.

The conventional way of using entire vehicle model to incorporate the complete model for the observer, as discussed in a previous study [7], is not followed in this case since it would be too complex (due to the larger number of sensors required for the larger number of measurements) and difficult to implement due to the uncertain and unpredictable nature of the wheel–rail contact conditions, such as changes in conicity (due to the profiled wheels) and creep coefficients. In order to avoid these complexities, a simplified model is proposed that uses an actuator model which treats the interactions between the wheelset and actuator as a dynamic load. The use of a simplified model is possible in this case since the complete dynamic model of the actuator (up to the wheelset) is available, and current/torque measurements are readily available.

A state observer with two states (as described by Equations 77–80) is designed using the actuator dynamic equation (Equation 78), as shown earlier. In this case, motor rotor speed measurement ($\dot{\theta_m}$) is considered to be a state due to the fact that the sensors required to measure rotational speeds to a high degree of accuracy are readily available. Motor rotor speed is the state that maintains the interaction between the wheelset (load) and the actuator due to the fact that they are coupled through a gearwheel connection. In addition, torque at the wheelset (T_L) is formulated as a state in such a manner that it can be reasonably estimated.

Since the motor current is proportionally correlated to the torque of the actuator, when it is set as an input to the model and because the estimated state of the motor rotor speed is corrected using the observer gains with the measured motor rotor speed, the relationship between the motor current and speed can be used to obtain the toque applied to wheelset.

As described above, in this application the motor rotor angular velocity ($\dot{\theta_m}$) and output torque (T_L) are considered to be states, while the motor current (i_a) is the input to the observer model. Since

the other parameters, namely inertial values, motor torque constant, gear ratio and motor internal damping, are all known and both the motor rotor angular speed and current consumption can be measured to high accuracy using simple measurement techniques, estimations for the state of the torque generated (T_L) can be effectively recorded while avoiding the difficulties associated with torque measurements, as mentioned above.

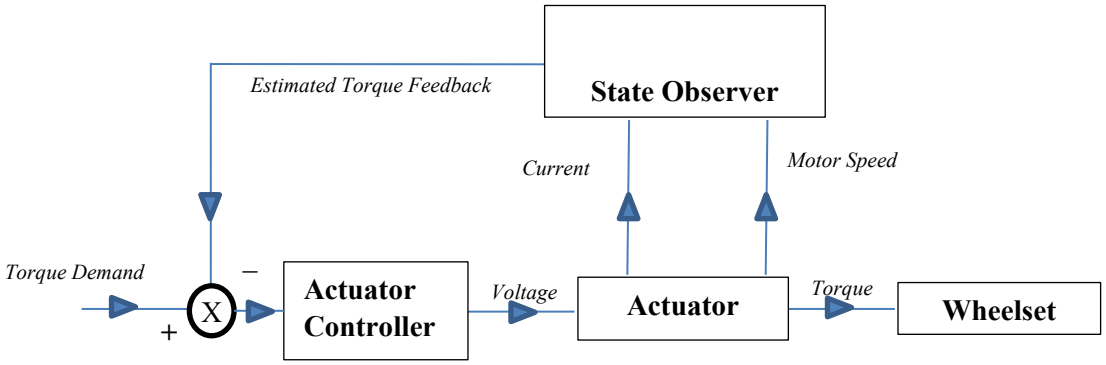

Figure 6. 1 – State Observer Model

6.2. State Space Derivation

The derivation of the observer is based on the dynamic equation of the motor. In this application, only the motor speed state has feedback to the observer.

$$(I_m + I_g n^2)\ddot{\theta_m} = k_t i_a - c_m \dot{\theta_m} - nT_L \tag{78}$$

The term nT_L (where n is the gear ratio) is considered to be T_L.

$$(I_m + I_g n^2)\ddot{\theta_m} = k_t i_a - c_m \dot{\theta_m} - T_L \tag{83}$$

$$\ddot{\theta_m} = \frac{k_t i_a}{(I_m + I_g n^2)} - \frac{c_m \dot{\theta_m}}{(I_m + I_g n^2)} - \frac{T_L}{(I_m + I_g n^2)} \tag{84}$$

$$\dot{T_L} = \beta T_L + \dot{T_L} \tag{85}$$

In addition, x is defined to be the two states given by the motor speed ($\dot{\theta_m}$) and the torque applied to the wheelset (T_L), while u is considered to be the input (i_a) and y is defined as the system

output, while matrices A, B, C, D, G and H represent the dynamics of the system. Furthermore, w is considered to be the process noise associated with the system, where w is represented as $\dot{T_L}$, while v represents the noise associated with measurements.

In addition, L is represents the observer gains and β is a parameter (a small constant) which is added to the state space to maintain the full rank of the A matrix such that the system is observable. ($I_m - motor\ rotor\ inertia, I_m - gear\ wheel\ inertia, n - gear\ ratio, k_t - motor\ torque\ constant.$)

$$x = \begin{bmatrix} \dot{\theta_m} \\ T_L \end{bmatrix} \tag{86}$$

$$\dot{x} = \begin{bmatrix} \frac{-c_m}{I_m + I_g n^2} & \frac{-1}{I_m + I_g n^2} \\ 0 & \beta \end{bmatrix} \begin{bmatrix} \dot{\theta}_m \\ T_L \end{bmatrix} + \begin{bmatrix} \frac{k_t}{I_m + I_g n^2} \\ 0 \end{bmatrix} [i_a] + \begin{bmatrix} 0 \\ 1 \end{bmatrix} [\dot{T_L}] \tag{87}$$

$$\dot{x} = Ax + Bu + Gw \tag{88}$$

$$y = Cx + Du + Hv \tag{89}$$

$$A = \begin{bmatrix} \frac{-c_m}{I_m + I_g n^2} & \frac{-1}{I_m + I_g n^2} \\ 0 & \beta \end{bmatrix} \tag{90}$$

$$B = \begin{bmatrix} \frac{k_t}{I_m + I_g n^2} \\ 0 \end{bmatrix} \tag{91}$$

$$C = [1 \quad 0] \tag{92}$$

If estimated states are defined as being $\hat{x}$,

$$\dot{\hat{x}} = A\hat{x} + Bu + Gw + L(y - \hat{y}) \tag{93}$$

$$\hat{y} = C\hat{x} + +Du + Hv \tag{94}$$

If the error in the estimation is defined to be $e_{Obs} = x - \hat{x}$,

$$\dot{e}_{Obs} = \dot{x} - \dot{\hat{x}} \tag{95}$$

$$\dot{e}_{Obs} = Ax + Bu - A\hat{x} - Bu - L(y - \hat{y}) \tag{96}$$

$$\dot{e}_{Obs} = (A - LC)e_{Obs} \tag{97}$$

It is evident from Equation 91 that for the convergence of this Luenberger (identity) observer, the condition of $(A - LC) < 0$ needs to be fulfilled [99]. Observer poles in this case are selected such that the system has a time constant of 0.0016 in order to match the actuator (with its local controller) frequency of approximately 98 Hz. Thus, by using Ackerman's formula [100] as the pole placement technique, the desired poles of $[-625, -625]$ can be used to calculate the observer gains as shown in Equation 98, which in turn allows the observer to achieve an adequate convergence speed.

$$det|sI - [A - LC]| = (s + 625)(s + 625) \tag{98}$$

$$\det\left| s\begin{bmatrix}1 & 0\\ 0 & 1\end{bmatrix} - \left[\begin{bmatrix} \frac{-c_m}{I_m + I_g n^2} & \frac{-1}{I_m + I_g n^2} \\ 0 & \beta \end{bmatrix} - [L][1 \quad 0]\right]\right| \tag{99}$$

$$= s^2 + 1250s + 390625$$

$$Observer\ gain\ (L) = \begin{bmatrix}1516.43\\ -287.93\end{bmatrix} \tag{100}$$

In order to emulate more practical measurements, 1% measurement noise is included in both the current (i) and motor speed ($\dot{\theta}_m$) measurements when conducting the study.

6.3. Observer Performance Evaluation

An analysis is performed as shown in Figure 6.2 – Figure 6.5, which depict a comparison of the actual and estimated output torques of the actuator in order to assess the accuracy of the estimations of using both the two–axle and full bogie vehicles when simulated using both curved track (with 300 m curvature radius) with low travel speed and generic straight track with lateral irregularities with high travel speed. However, only the behaviour of the first wheelset of the vehicle models is shown as the other wheelsets show very similar behaviour.

It can be seen from Figure 6.2 and Figure 6.3 that there is an approximately 10% error between the measured and estimated torque feedbacks. This can be clearly seen when the torque is zero at the steady curved section as slight differences which can be expected due to the noise included in the measurement signals.

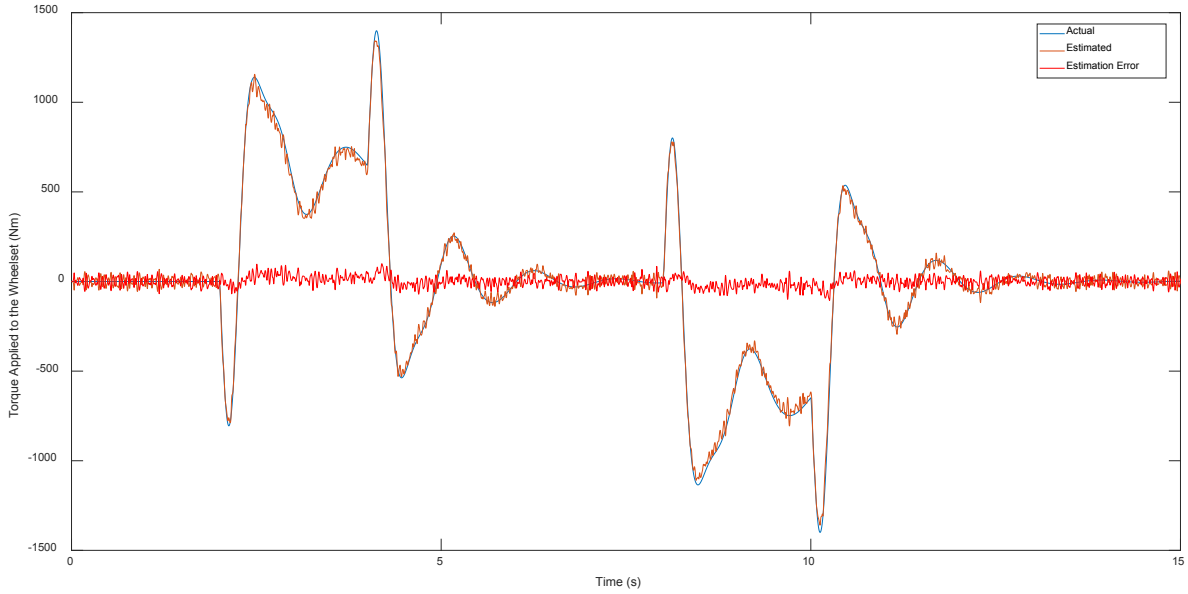

Figure 6. 2 – Torque Analysis for the Curved Track – Two–axle Vehicle

Similarly, it can be seen from Figure 6.3 that there is an approximately 10% estimation error between the actual and estimated torques, which is again expected due to the noise included in the measurement signals.

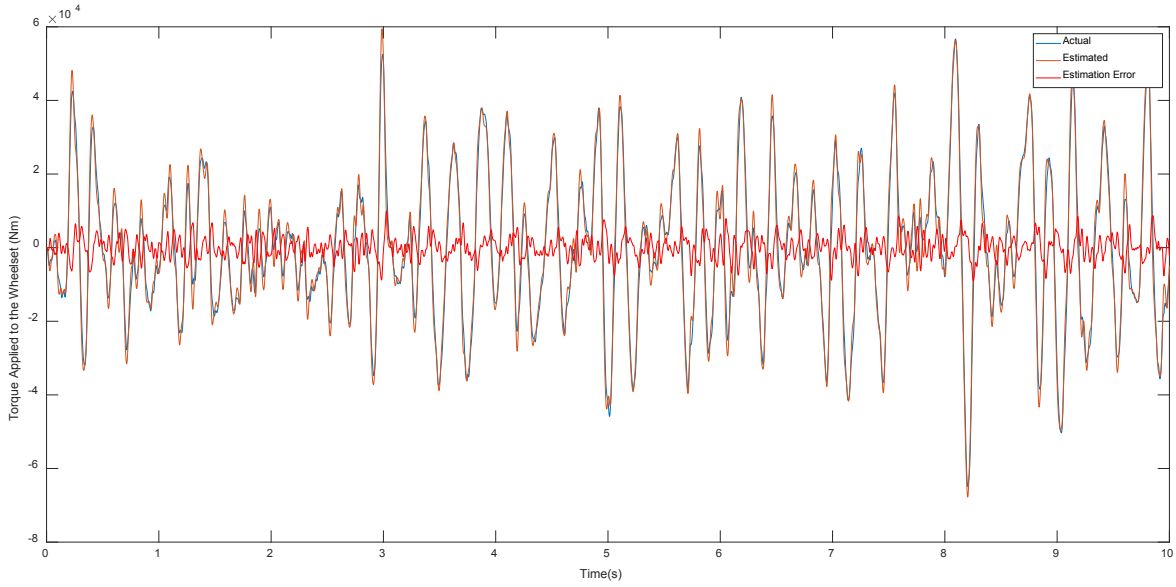

Figure 6. 3 – Torque Analysis for the Straight Track with Lateral Irregularities – Two–axle Vehicle

Similar to the behaviour observed for the two–axle vehicle, Figure 6.4 and Figure 6.5 show that there is minor error between the actual and estimated torques when the full bogie vehicle is assessed. This can be clearly seen at the times where the torque is zero (the steady curved section) as slight differences can be expected due to the noise included in the measurement signals.

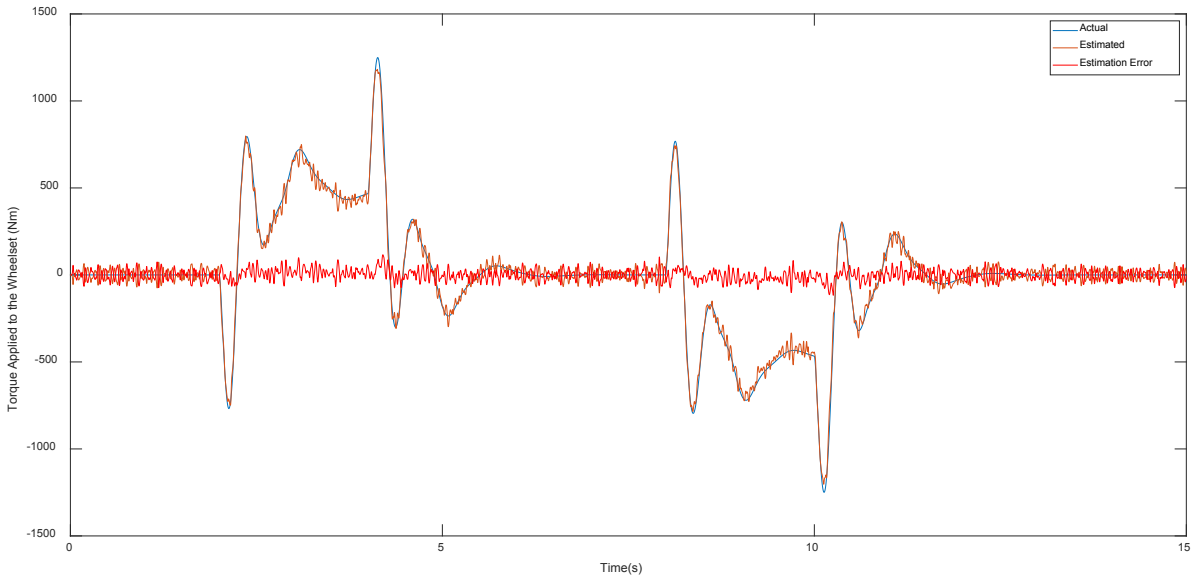

Figure 6. 4 – Torque Analysis for the Curved Track – Full Bogie Vehicle

The same analysis can be performed with the generic straight track with lateral irregularities and full bogie vehicle in order to examine the observer performance.

In a similar manner to the behaviour observed for the two–axle vehicle and generic straight track with lateral irregularities, when analysing the observer behaviour with the straight track and the full bogie vehicle, there is an approximate 10% error between the actual and estimated torques, as seen in Figure 6.3 and Figure 6.5.

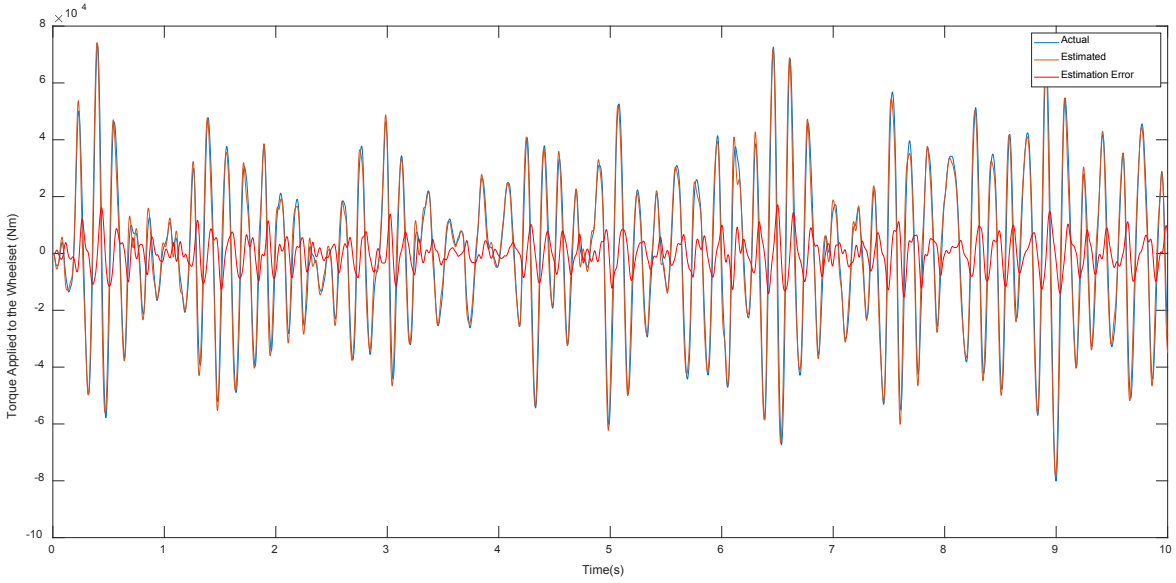

Figure 6. 5 – Torque Analysis for the Straight Track with Lateral Irregularities – Full Bogie Vehicle

6.4. Observer Robustness Analysis – Two–axle Vehicle

In order to assess the robustness of the observer, key parameters of the observer model (which are difficult to obtain accurately in a practical environment) are varied by a reasonable margin while observing the performance of the observer with the two–axle vehicle. Thus, the internal damping of the motor (c_m), motor constant (k_t) and inertial values such as gear wheel inertia (I_g) and motor rotor inertia (I_m) are varied within by a margin of ± 20% in order to evaluate the associated observer performance in each case. For this analysis, both two–axle vehicle and full bogie vehicle are considered with the straight track with lateral irregularities at a speed of 83 ms^{-1} as it can emulate a more challenging track to the vehicles than the curved track at low speeds.

Variation of Motor Internal Damping $\pm$ 20% $of\ c_m$

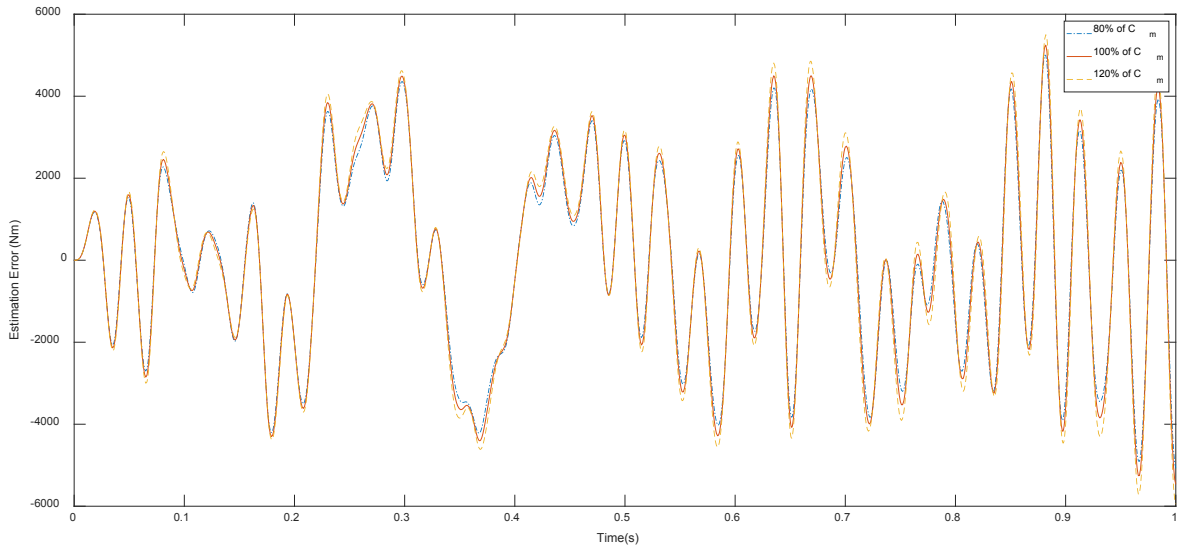

Figure 6. 6 – Assessment of Estimation Error vs. Robustness – Motor Damping 1 – TAV

It is evident from Figure 6.6 that the internal damping of the motor does not significantly affect the performance of the observer since change of estimation error is minor. Furthermore, Table 6.1 shows the effect of this variation having on the torque applied to the wheelset by this estimation error in the feedback signal, compared against the torque demand from the wheelset controller by assessing the rms values.

Table 6. 1 – Actuator Torque Analysis with Motor Damping Variation 1 – TAV

	$80\%\ of\ c_m$	$100\%\ of\ c_m$	$120\%\ of\ c_m$
Torque Demand (rms)	21.089 kNm	21.225 kNm	21.363 kNm
Torque Supplied (rms)	21.218 kNm	21.285 kNm	21.374 kNm
Error Percentage	0.611%	0.28%	0.05%

From the results depicted in Table 6.1 it can be stated that actuator performance is excellent against variation of the estimated feedback signal caused by motor damping value variation since the error percentage between demanded and supplied torques is <1%.

Variation of Gear Wheel Inertia $\pm\ 20\%\ of\ I_g$

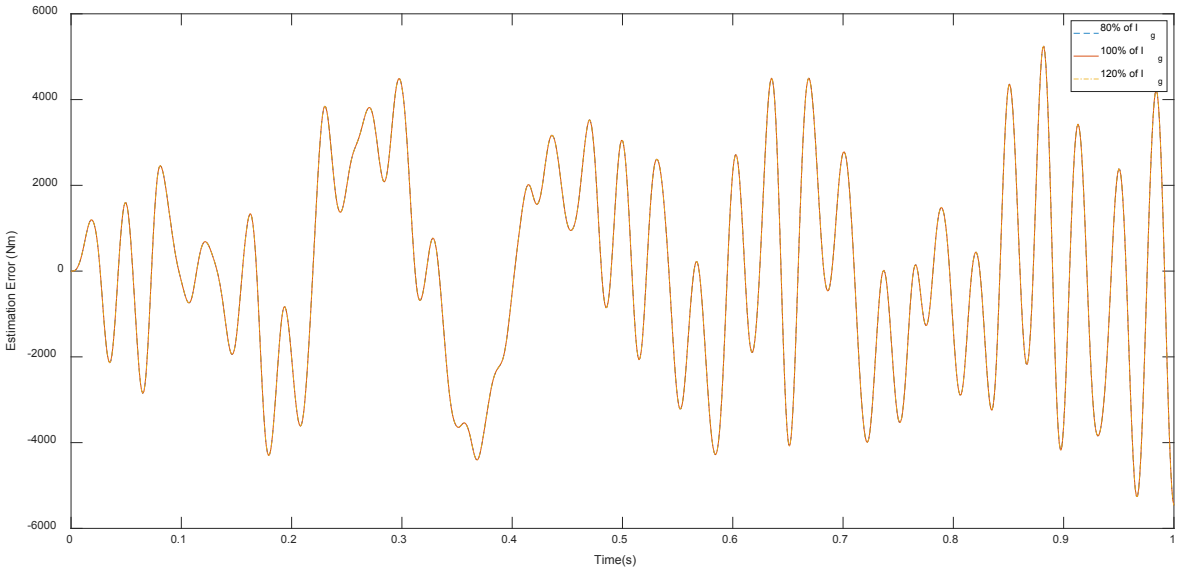

Figure 6. 7 – Assessment of Estimation Error vs. Robustness – Gear Wheel Inertia – TAV

Similarly, when the gear wheel inertia is varied by $\pm\ 20\%$ of its value, it is found that the observer performance remained unaffected. This can be expected since gear wheel inertia is being multiplied by the square of the gear ratio and that results in gear wheel inertia's influence being very minor.

Table 6. 2 – Actuator Torque Analysis with Gear Wheel Inertia Variation – TAV

	$80\%\ of\ I_g$	$100\%\ of\ I_g$	$120\%\ of\ I_g$
Torque Demand (rms)	21.224 kNm	21.225 kNm	21.225 kNm
Torque Supplied (rms)	21.284 kNm	21.285 kNm	21.285 kNm
Error Percentage	0.28%	0.28%	0.28%

Variation of Motor Rotor Inertia $\pm\ 20\%\ of\ I_m$

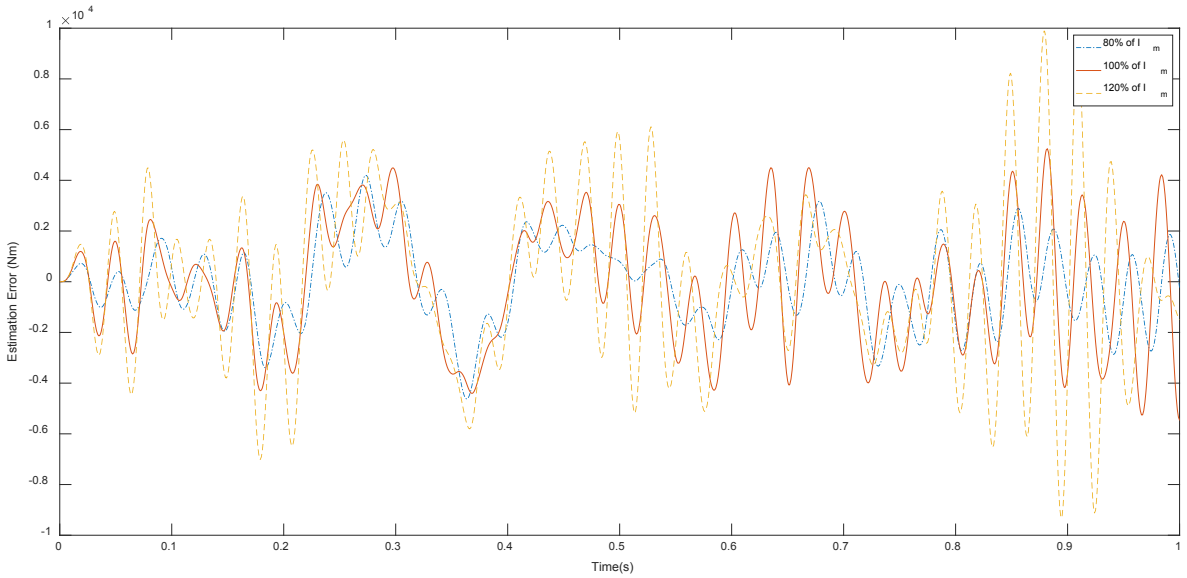

Figure 6. 8 – Assessment of Estimation Error vs. Robustness – Motor Rotor Inertia – TAV

However, as can be seen from Figure 6.8, the motor rotor inertia variation does have an effect on the estimation error. However, from the results in Table 6.3 it is evident that this does not ultimately result in a significantly detrimental performance of the actuator within the operational range since the error percentage of the actuator output torque is <1%.

Table 6. 3 – Actuator Torque Analysis with Motor Rotor Inertia Variation – TAV

	$80\%\ of\ I_m$	$100\%\ of\ I_m$	$120\%\ of\ I_m$
Torque Demand (rms)	20. 911 kNm	21.225 kNm	21.483 kNm
Torque Supplied (rms)	21.088 kNm	21.285 kNm	21.522 kNm
Error Percentage	0.844%	0.28%	0.18%

Variation of Gear Wheel Inertia $\pm$ 20% $of\ k_t$

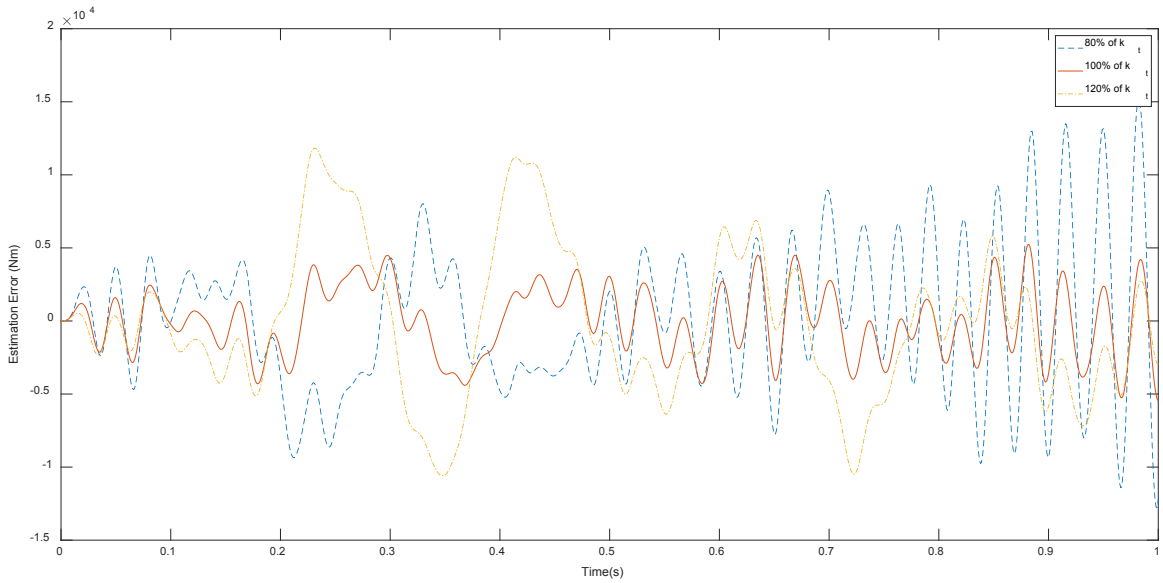

Figure 6. 9 – Assessment of Estimation Error vs. Robustness – Motor Constant – TAV

It is evident from Figure 6.9 that changing the motor constant does result in relatively higher effect on the observer performance as the error has increased. In addition, from the results depicted in Table 6.4 shows that approximately 20% of error in the actuator output torque when the motor constant is varied to its higher limit. However, a positive indication from these results can be observed as although the accuracy of the system has been compromised in this case, the system is maintaining its stability.

Table 6. 4 – Actuator Torque Analysis with Motor Constant Variation – TAV

	80% $of\ k_t$	100% $of\ k_t$	120% $of\ k_t$
Torque Demand (rms)	21.588 kNm	21.225 kNm	20.715 kNm
Torque Supplied (rms)	25.006 kNm	21.285 kNm	24.757 kNm
Error Percentage	15.83%	0.28%	19.51%

Furthermore, on further analysis of the above parameter variations, it is believed that motor internal damping (c_m) is the most difficult parameter to measure, while inertial values such as gear wheel inertia (I_g).motor rotor inertia (I_m) and motor constant (k_t) can be measured to high accurately in a straightforward manner.

Hence, the system response across a larger range of motor internal damping (c_m) values is assessed. It can be seen from Figure 6.10 and Table 6.5 that even for the wider range, (in this instance

where $\pm$ 50%, of initial motor internal damping values are being used) the observer's performance is not significantly affected since the actuator accuracy is approximately 99%.

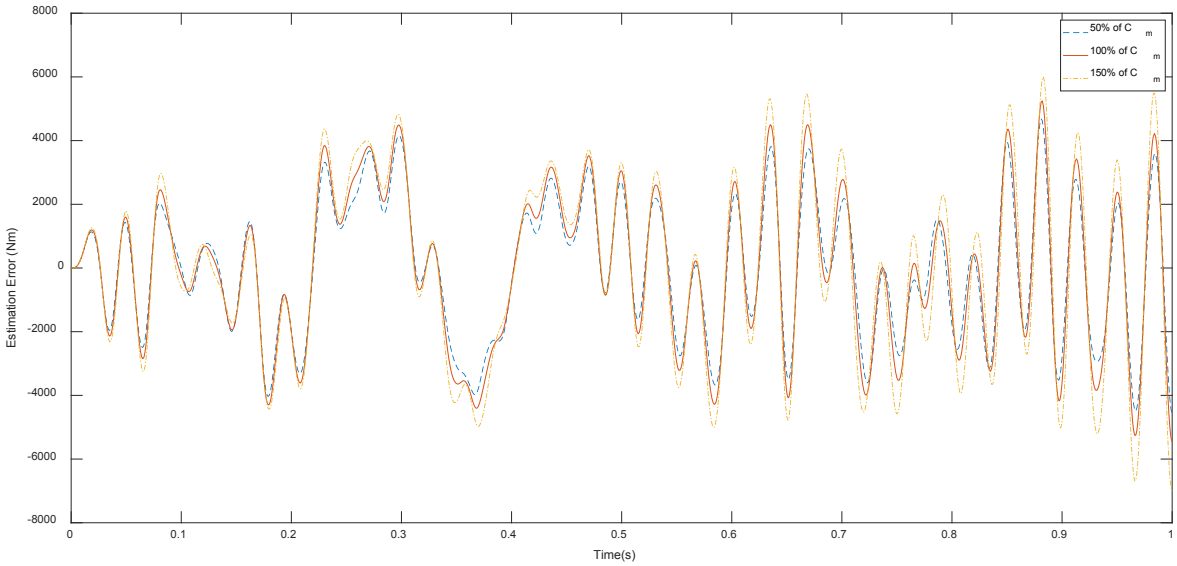

Figure 6. 10 – Assessment of Estimation Error vs. Robustness – Motor Damping 2 – TAV

Table 6. 5 – Actuator Torque Analysis with Motor Damping Variation 2 – TAV

	$50\%\ of\ c_m$	$100\%\ of\ c_m$	$150\%\ of\ c_m$
Torque Demand (rms)	20.905 kNm	21.225 kNm	21.529 kNm
Torque Supplied (rms)	21.134 kNm	21.285 kNm	21.654 kNm
Error Percentage	1.09%	0.28%	0.58%

These robustness assessments provide valuable insights into the state observer performance, since, in a realistic environment, it is highly plausible that actuator parameters will be slightly different to the values used to actually design the state observer. This could lead to inaccurate estimations and, subsequent instability in the system. However, the results of the tests conducted indicate that the observer is capable of producing accurate estimations within a reasonable range of parameter variations since parameter variation can be expected to some greater or lesser extent in a real–world situation.

In addition to the insight into the robustness of the observer, results also indicate that when all the parameters are as defined, actuator is operating at an accuracy of 99.98% since when all the parameters are at their specified values, error percentage is 0.28% with the two–axle vehicle.

6.5. Observer Robustness Analysis – Full Bogie Vehicle

In order to assess the behaviour of the observer and the actuator operated with estimated feedback measurements, with full bogie vehicle, same analysis conducted above with the two–axle vehicle is undertaken. Thus, same robustness assessment is done with the first wheelset of the front bogie.

Variation of Motor Internal Damping $\pm$ 20% $of\ c_m$

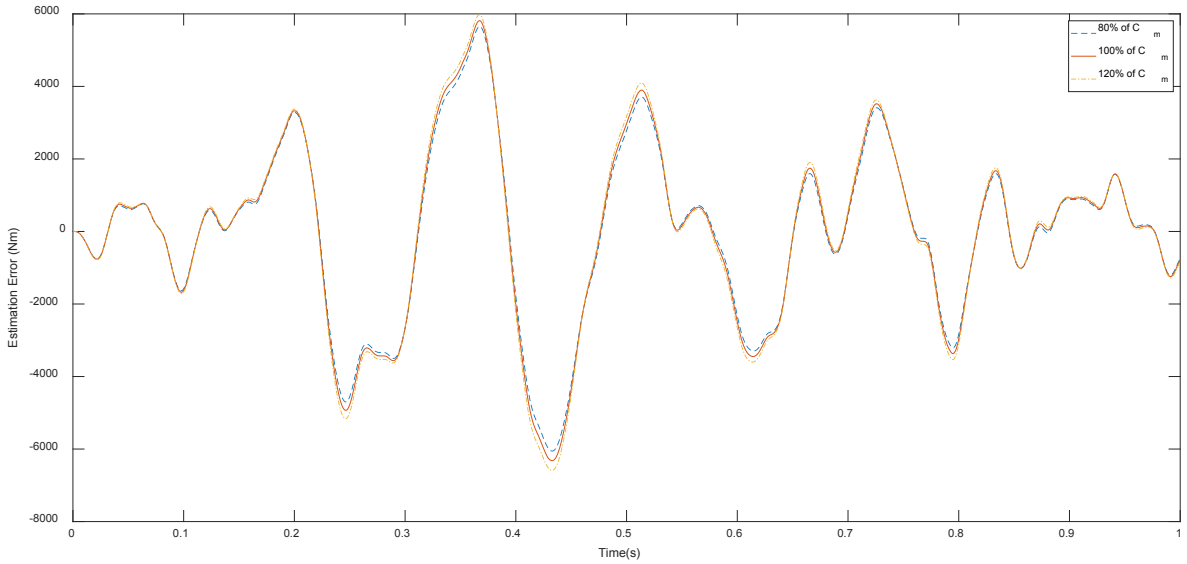

Figure 6. 11 – Assessment of Estimation Error vs. Robustness – Motor Damping 1 – FBV

It is evident from the Figure 6.11 and Table 6.6 that for ±20% variation of motor damping value, observer is capable of maintaining the accuracy reasonably well since it is generating feedback estimations adequately for the actuator to have an accuracy of approximately 98%.

Table 6. 6 – Actuator Torque Analysis with Motor Damping Variation 1 – FBV

	80% $of\ c_m$	100% $of\ c_m$	120% $of\ c_m$
Torque Demand (rms)	25.254 kNm	25.365 kNm	25.478 kNm
Torque Supplied (rms)	25.469 kNm	25.679kNm	25.894 kNm
Error Percentage	0.85%	1.23%	1.68%

Variation of Gear Wheel Inertia $\pm$ 20% $of\ I_g$

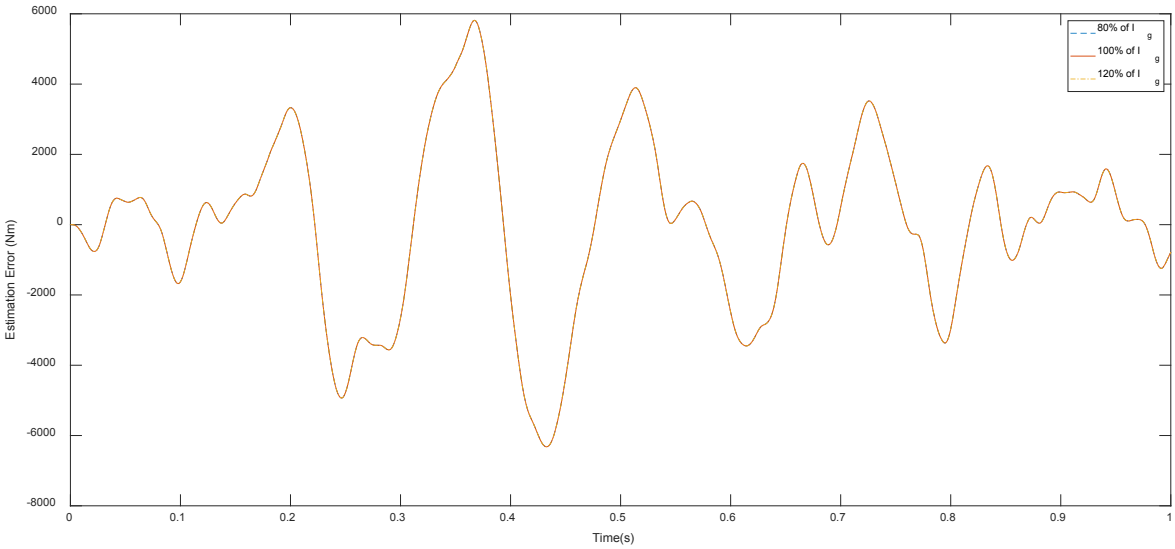

Figure 6. 12 – Assessment of Estimation Error vs. Robustness – Gear Wheel Inertia – FBV

As with the two–axle vehicle, gear wheel inertia does not affect the accuracy of the estimations and the actuator accuracy.

Table 6. 7 – Assessment of Estimation Error vs. Robustness – Gear Wheel Inertia – FBV

	80% $of\ I_g$	100% $of\ I_g$	120% $of\ I_g$
Torque Demand (rms)	25.365 kNm	25.365 kNm	25.365 kNm
Torque Supplied (rms)	25.679 kNm	25.679 kNm	25.679 kNm
Error Percentage	1.23%	1.23%	1.23%

Variation of Motor Rotor Inertia $\pm 20\%\ of\ I_m$

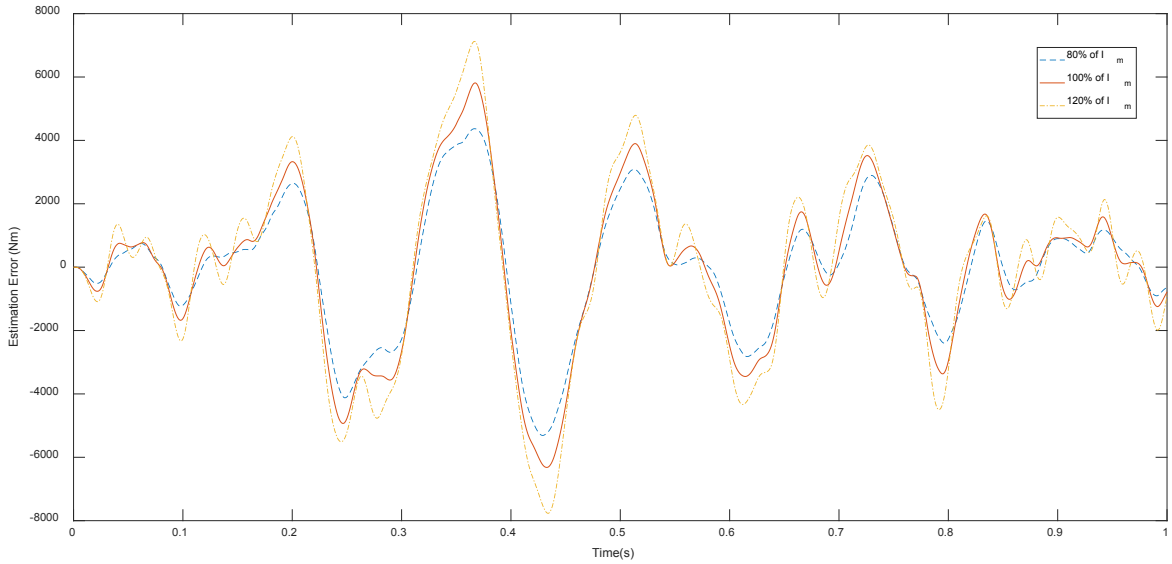

Figure 6. 13 – Assessment of Estimation Error vs. Robustness – Motor Rotor Inertia – FBV

It can be seen from the comparison of the Figure 6.13 and Table 6.8 that motor rotor inertia does affect the accuracy of the estimations and actuator more than the gear wheel inertia value. However, results indicate the effect to the accuracy of the actuator is minor since these variations have only caused a maximum error of 2.4% in the torque applied to the wheelset.

Table 6. 8 – Actuator Torque Analysis with Motor Rotor Inertia Variation – FBV

	$80\%\ of\ I_m$	$100\%\ of\ I_m$	$120\%\ of\ I_m$
Torque Demand (rms)	24.839 kNm	25.365 kNm	25.945 kNm
Torque Supplied (rms)	24.856 kNm	25.679 kNm	26.570 kNm
Error Percentage	0.06%	1.23%	2.4%

Variation of Gear Wheel Inertia $\pm$ 20% $of\ k_t$

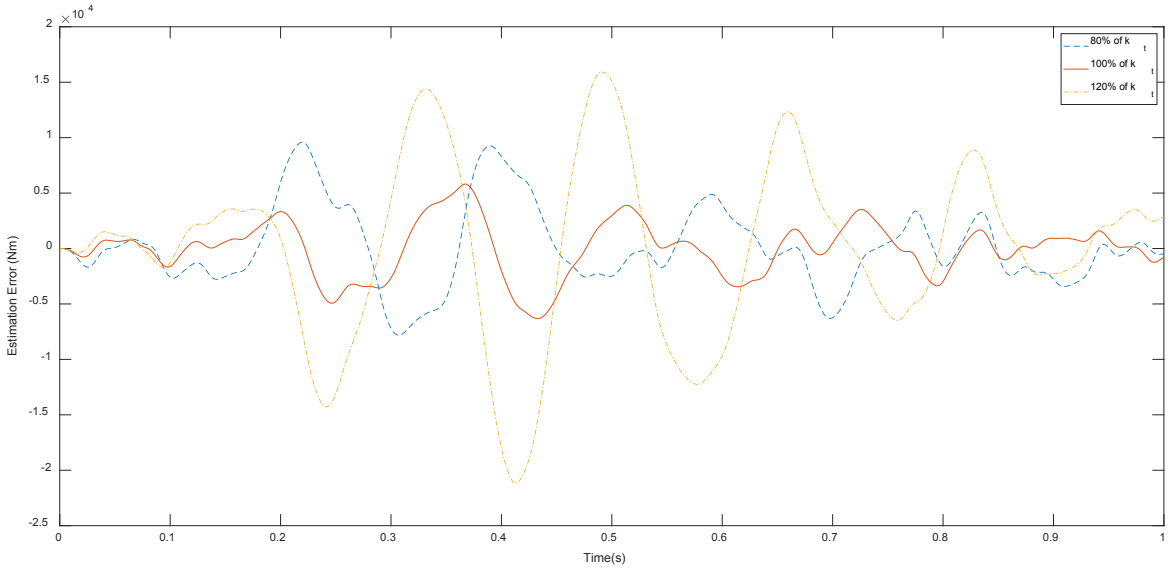

Figure 6. 14 – Assessment of Estimation Error vs. Robustness – Motor Constant – FBV

As expected, results indicate that motor constant value can cause significant effect to the accuracy of the estimations and subsequently to the actuator accuracy. However, control system has maintained its stability while compromising on the accuracy by approximately 25% when the value of motor constant is varied by ±20%.

Table 6. 9 – Actuator Torque Analysis with Motor Constant Variation – FBV

	80% $of\ k_t$	100% $of\ k_t$	120% $of\ k_t$
Torque Demand (rms)	18.946 kNm	25.365 kNm	29.258 kNm
Torque Supplied (rms)	23.870 kNm	25.679 kNm	36.270 kNm
Error Percentage	25.98%	1.23%	23.96%

Variation of Motor Internal Damping $\pm$ 50% $of\ c_m$

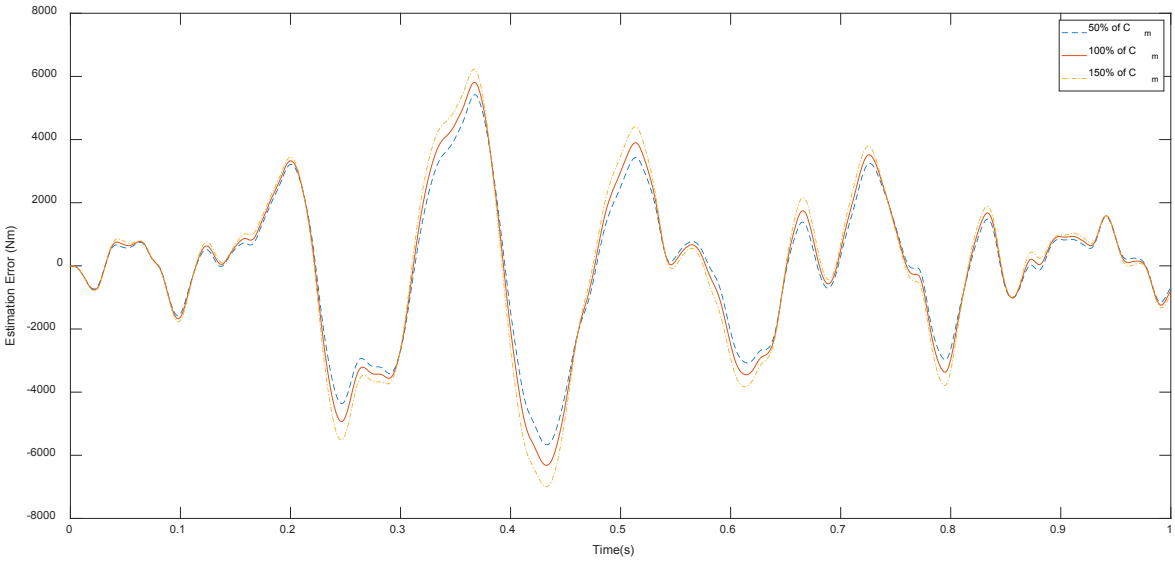

Figure 6. 15 – Assessment of Estimation Error vs. Robustness – Motor Damping 2 – FBV

As elaborated above, due to difficulties of accurately measuring the motor damping value, a wider range is used to further assess the robustness of the state observer and the actuator.

It is evident from the results that even with ±50% of the defined motor damping value, accuracy of the estimations has not been affected significantly while assessment of the actuator accuracy indicates that maximum error percentage which can occur (when the motor damping value is 50% over the defined value) is 2.22%.

Table 6. 10 – Actuator Torque Analysis with Motor Damping Variation 2 – FBV

	50% $of\ c_m$	100% $of\ c_m$	150% $of\ c_m$
Torque Demand (rms)	25.095 kNm	25.365 kNm	25.655 kNm
Torque Supplied (rms)	25.166 kNm	25.679kNm	26.227 kNm
Error Percentage	0.28%	1.23%	2.22%

CHAPTER 7: OVERALL SYSTEM EVALUATION

7.1. Introduction

Once the active wheelset controller, actuator controller and state observer (for sensing) have been thoroughly assessed through the discussions of previous chapters, the overall control configuration can be further evaluated with both the two–axle and full bogie vehicle while different measured straight tracks with lateral irregularities and curved tracks can be used for this analysis in order to evaluate the performances and robustness of the developed active control system in a more realistic/practical operational environment for the vehicles.

Since these measured straight tracks with lateral irregularities have a lower operating speed of 50 ms^{-1} (180 kmh^{-1}) and relatively smother lateral irregularities than the generic straight track with lateral irregularities (with a higher operating speed of 83 ms^{-1} [300 kmh^{-1}]) used in previous chapters, relatively lower control effort demand and improved vehicle dynamic behaviour can be expected.

Furthermore, in order to further evaluate the system with curved tracks, three track conditions to represent high, mid and low curvatures with different travel speeds such as 300 m curvature radius with 25 ms^{-1} (90 kmh^{-1}) travel speed, 1250 m curvature radius with 50 ms^{-1} (180 kmh^{-1}) travel speed and 3500 m curvature radius with 83 ms^{-1} (300 kmh^{-1}) travel speed are used. Since active control is capable of reducing/eliminating longitudinal creep forces on curved tracks, lower control efforts can be expected on curves compared to straight tracks with lateral irregularities.

During these final assessments, the focus is mainly given to investigate the overall actuator performances and vehicle dynamics since those aspects provide indications on the effectiveness of the optimised actuator and model–based sensing technique developed in the study.

Mainly the front wheelset is evaluated for the actuator performance analysis of root–mean–square (rms) values since other wheelsets show similar behaviour. This assessment of rms values provide more insight in to the internal dynamics of the motor as well as the accuracy which the actuator can perform against the control effort demand from the wheelset controller. Thus, performance indicators such as torque demand of the wheelset controller and actuator output torque are evaluated to assess the effectiveness of the actuator controller and actuator while motor current, voltage and power are also evaluated since it provides insight to the internal actuator performances.

In addition to the actuator performances, vehicle dynamics such as wheelset deflection, yaw, contact forces are also evaluated with the overall system for the both two–axle vehicle and full bogie vehicle to evaluate the improvements of vehicle dynamics with overall active wheelset control.

7.2. Two–axle Vehicle

Actuator Performances – TAV

Below Tables, 7.1 to Table 7.7 depict the performances of the actuator developed in the study with four measured straight tracks with lateral irregularities and three curved tracks with the two–axle vehicle model. Lateral irregularity levels of these measured track conditions are such that Track 1 is a relatively smooth track while Track 3 and Track 4 are mildly rough and Track 2 represents relatively roughest track with more lateral irregularities.

Table 7. 1 – Performance Analysis of Measured Straight Track with Lateral Irregularities 1 – Wheelset 1 (TAV)

Measured Straight Track with Lateral Irregularities 1 – Wheelset 1	
Performance Indictor	RMS Value
Torque Demand (Nm)	3.869×10^3
Actuator Output Torque (Nm)	3.922×10^3
Difference Percentage (%)	1.36%
Motor Current (A)	10.09
Motor Voltage (v)	2.30
Motor Power (W)	28.55

It can be seen from the above table that with the Track 1, torque demand and motor power are relatively low (motor power = 28.55 W) compared to the other measured tracks. In addition, it is clear that actuator and the controllers are performing well to match with the demand since the difference (approximately 1%) is negligible. RMS value of motor power and voltage are depicting relatively significantly low values in Table 7.1 and this can be expected since the track is relatively smoother, which subsequently results lower control effort demands and actuator operations. In addition, another reason for low motor power values is the fact that motor velocities are low [2] in this application.

Table 7. 2 – Performance Analysis of Measured Straight Track with Lateral Irregularities 2 – Wheelset 1 (TAV)

Measured Straight Track with Lateral Irregularities 2 – Wheelset 1	
Performance Indictor	RMS Value
Torque Demand (Nm)	1.032×10^4
Actuator Output Torque (Nm)	1.055×10^4
Difference Percentage (%)	2.22%
Motor Current (A)	27.08
Motor Voltage (v)	4.14
Motor Power (W)	376.36

Track 2 is relatively the roughest among the measured tracks as motor is generating (removing energy from wheelsets) the highest amount of power (376.36 W) with Track 2. Thus, it can be stated Track 2 causes the actuator to dissipate most (relatively) energy from wheelsets to maintain stability due to its higher lateral irregularities. In addition, by comparing the values between the torque demand and actuator output torque, it is evident that actuator is performing well with an accuracy of approximately 98%.

Table 7. 3 – Performance Analysis of Measured Straight Track with Lateral Irregularities 3 – Wheelset 1 (TAV)

Measured Straight Track with Lateral Irregularities 3 – Wheelset 1	
Performance Indictor	RMS Value
Torque Demand (Nm)	4.951×10^3
Actuator Output Torque (Nm)	5.032×10^3
Difference Percentage (%)	1.63%
Motor Current (A)	12.94
Motor Voltage (v)	2.58
Motor Power (W)	43.88

Similar behaviour can be seen from the results depicted in Table 7.3 and table 7.4 which indicates that the actuator is performing well to maintain the stability of wheelsets with a control effort accuracy of approximately 98% for measured Track 3 and Track 4.

Table 7. 4 – Performance Analysis of Measured Straight Track with Lateral Irregularities 4 – Wheelset 1 (TAV)

Measured Straight Track with Lateral Irregularities 4 – Wheelset 1	
Performance Indictor	RMS Value
Torque Demand (Nm)	9.697×10^3
Actuator Output Torque (Nm)	9.927×10^3
Difference Percentage (%)	2.37%
Motor Current (A)	25.44
Motor Voltage (v)	3.84
Motor Power (W)	126.45

Similar analysis is done with the curved tracks as well as with straight track with lateral irregularities to assess the actuator performances. As discussed in Chapter 4, due to improved vehicle dynamics with active control, it can be seen from analysing the torque values, vehicle travelling on the curved tracks requires much less amount of effort than when travelling on the straight track with lateral irregularities.

Table 7. 5 – Performance Analysis of Curved Track 1 – Wheelset 1 (TAV)

Curved Track with 300 m Radius and 25 ms^{-1} Travel Speed – Wheelset 1	
Performance Indictor	RMS Value
Torque Demand (Nm)	438.81
Actuator Output Torque (Nm)	457.47
Difference Percentage (%)	4.25%
Motor Current (A)	1.163
Motor Voltage (v)	0.0908
Motor Power (W)	0.1215

It is clear from the Table 7.5 that with higher curvature and low speed, actuator operation is low since the motor current, voltage and power (0.09 W) are significantly low. This can be expected since the control effort demand and motor velocities are very low with active control as it allows wheelset natural curving movements which results in reduced eliminated creep forces. In addition, actuator is performing well with approximately 95% of accuracy in this case.

Table 7. 6 – Performance Analysis of Curved Track 2 – Wheelset 1 (TAV)

Curved Track with 1250 m Radius and 50 ms^{-1} Travel Speed – Wheelset 1	
Performance Indictor	RMS Value
Torque Demand (Nm)	335.41
Actuator Output Torque (Nm)	349.93
Difference Percentage (%)	4.32%
Motor Current (A)	0.8892
Motor Voltage (v)	0.1125
Motor Power (W)	0.1114

Results from the Table 7.6 shows that (as it can be expected) once the curvature has decreased, although the travel speed has increased, control effort has become less demanding. In addition, due to low actuator velocities with the curve track, motor power value is also very low compared to straight track.

Following the same trend, it can be seen from the Table 7.7 that when the curvature is further decreased, even with high speed, control effort demand decrease compared to case in Table 7.6. This can be expected since the curvature is smoother and the longitudinal/lateral creep forces are further deceased. However, it is evident from the results that actuator is performing well since the difference percentage between demand and supply is less than 5%.

Table 7. 7 – Performance Analysis of Curved Track 3 – Wheelset 1 (TAV)

Curved Track with 3500 m Radius and 83 ms^{-1} Travel Speed – Wheelset 1	
Performance Indictor	RMS Value
Torque Demand (Nm)	311.91
Actuator Output Torque (Nm)	324.88
Difference Percentage (%)	4.15%
Motor Current (A)	0.83
Motor Voltage (v)	0.086
Motor Power (W)	0.081

From summarising the results from the Table 7.1 to Table 7.7, RMS values of wheelset controller torque demand, actuator output torque and motor power indicates that the actuator is performing well with the integrated state observer to obtain the feedback since the actuator output torque values are closely matching the torque demand from the wheelset controllers.

In addition to the analysis of RMS values, below Figure 7.1 to Figure 7.7 depicts the instantaneous behaviour of the output torques of the actuator and the torque demand from the wheelset controller. This provides further insight, into the accuracy of the actuator as well as into control effort values for different track conditions. It can be seen from the results that output torque of the actuator has a close correlation with the demand, which indicates higher performance accuracy from the actuator with estimated torque feedback.

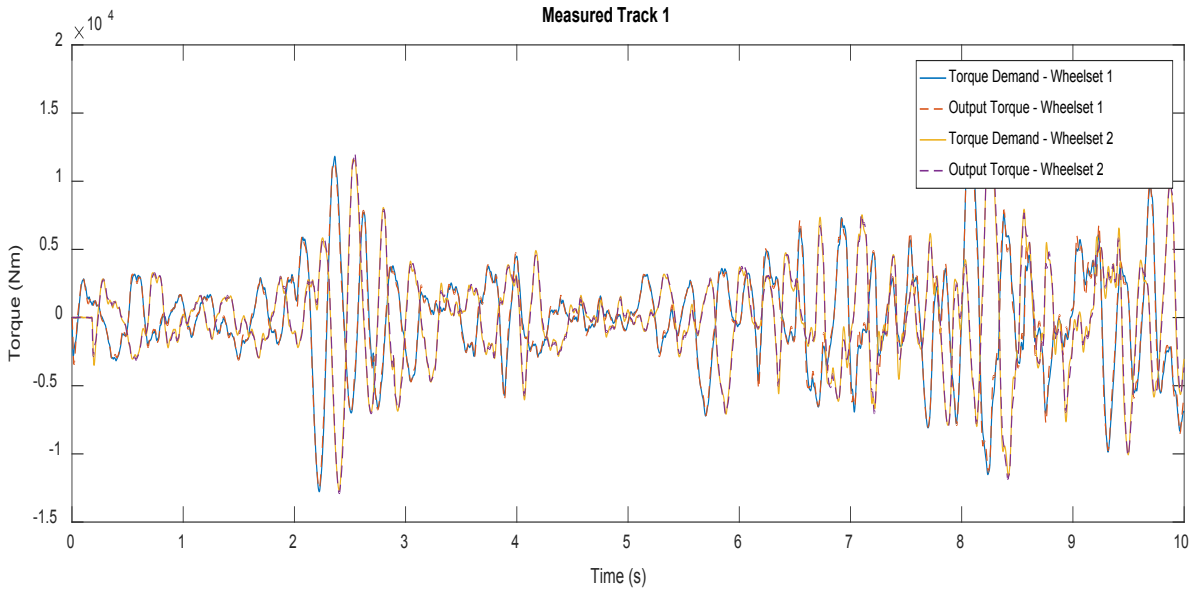

Figure 7. 1 – Torque Demand vs Output Torque – Measured Track 1 (TAV)

It is evident from the results of Figure 7.1 that both front wheelset and rear wheelset have similar control efforts applied on them and this is a positive indication wheelset controllers are performing well to stabilise the wheelsets based on absolute yaw angle of the wheelsets and wheelsets are experiencing similar/balanced contact forces. Due to the similar behavior of the control effort, same pattern can be expected with both lateral and logitudinal contact forces. In additon, correlating with the values observed in Table 7.1, when comparing maximum (approximatly 10 kNm) and minimum (approximatly –10 kNm) of the instantenous values, it can be seen that Track 1 has the lowest control demand from other measured straight tracks with lateral irregulariries.

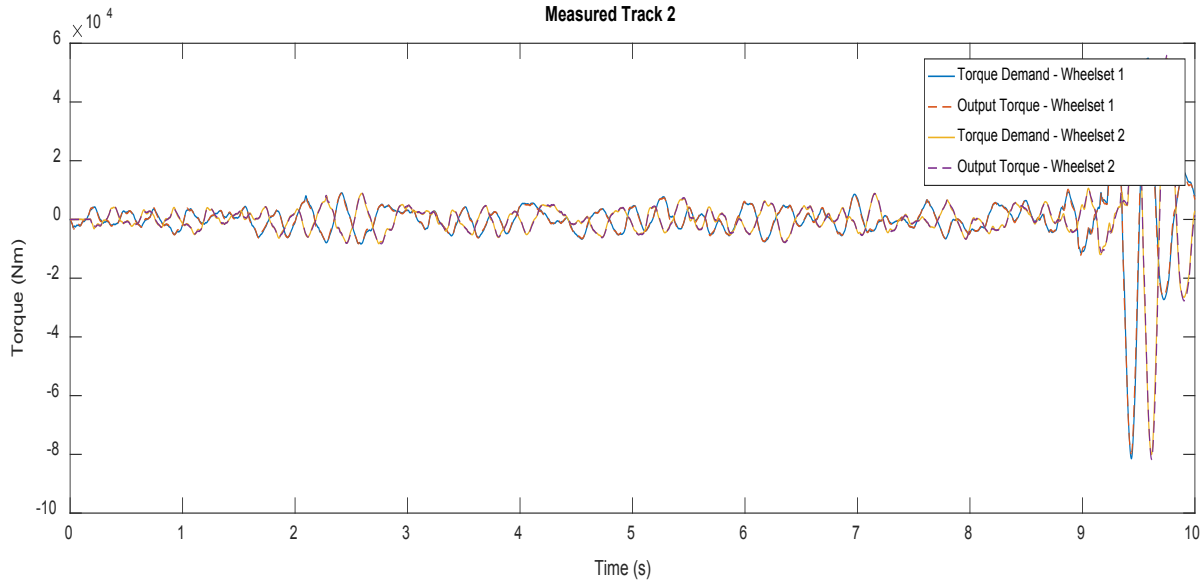

Figure 7. 2 – Torque Demand vs Output Torque – Measured Track 2 (TAV)

It can be seen that from Figure 7.2 that it has a relatively rougher irregularity pattern than the other tracks and thus results of Table 7.2 indicating higher dynamics occurs due to the fact that wheelsets need more control effort during 9^{th} to 10^{th} seconds of the track due to sudden increase in irregularities.

Same higher actuator accuracy can be seen with measured track 3 and track 4.

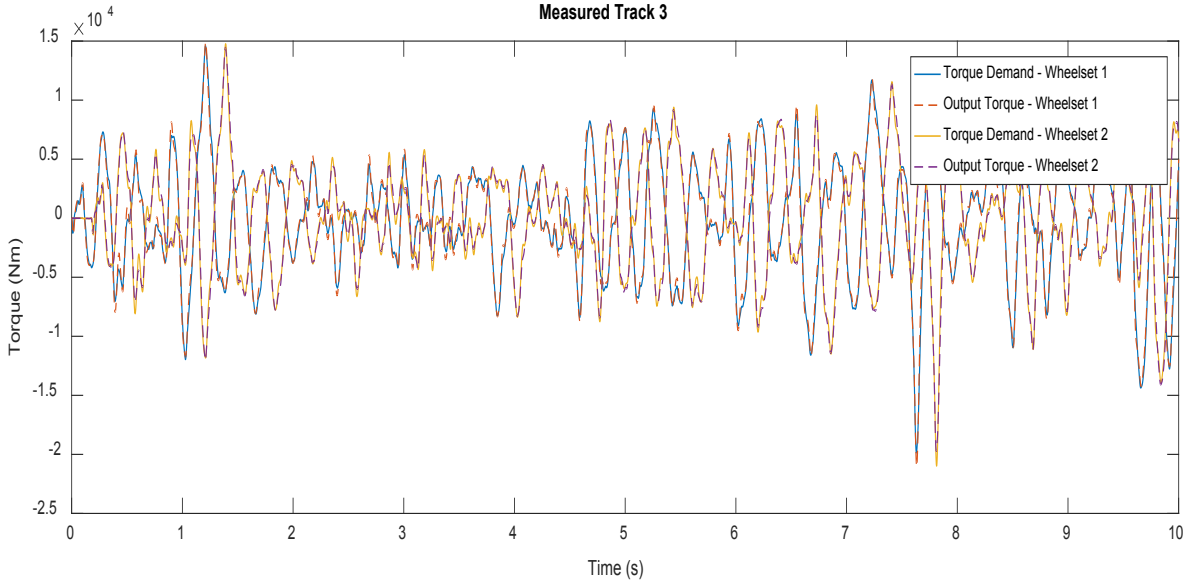

Figure 7. 3 – Torque Demand vs Output Torque – Measured Track 3 (TAV)

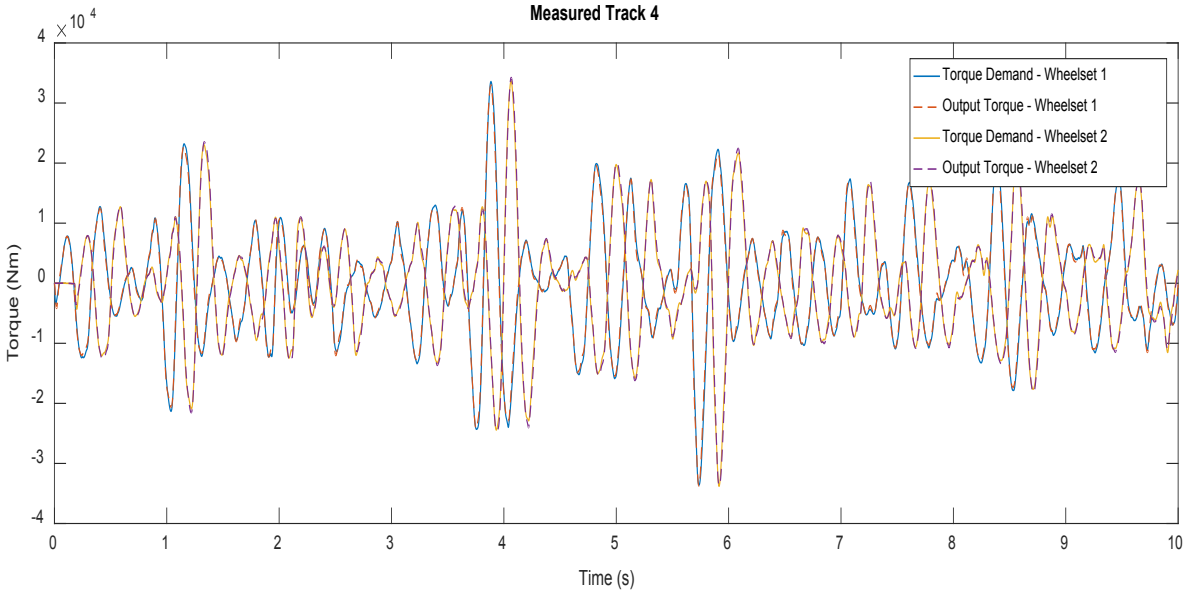

Figure 7. 4 – Torque Demand vs Output Torque – Measured Track 4 (TAV)

From observing the Figure 7.1 to Figure 7.4, it is clear that the developed actuator is performing well since the actuator output torque is approximately identical to the torque demand from the wheelset controller.

In addition to the straight tracks with lateral irregularities, same analysis is done to the curved tracks to assess the accuracy and improvements of actuator developed in the study.

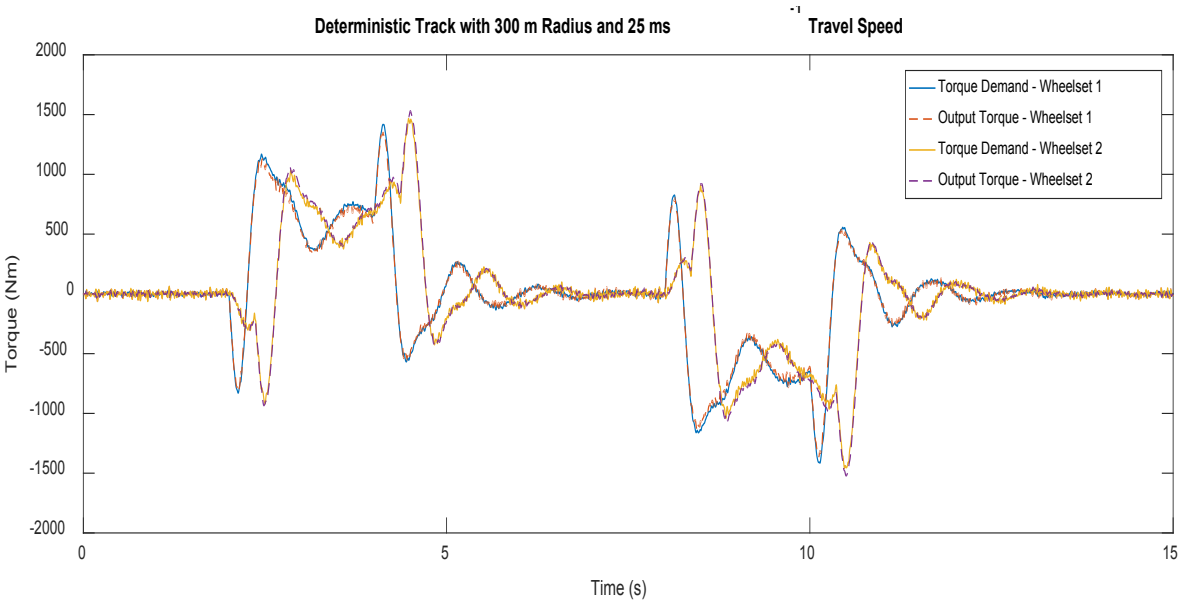

Figure 7. 5 – Torque Demand vs Output Torque – Curved Track (300m / 25 ms–1) (TAV)

It is clear from the control torque shown in the Figure 7.5 that as expected, control effort almost eliminated when the vehicle in travelling on the steady curved section of the track and overall control efforts are significantly lower, when traversing (approaching/leaving) the curved section of the track, compared to the straight tracks with lateral irregularities.

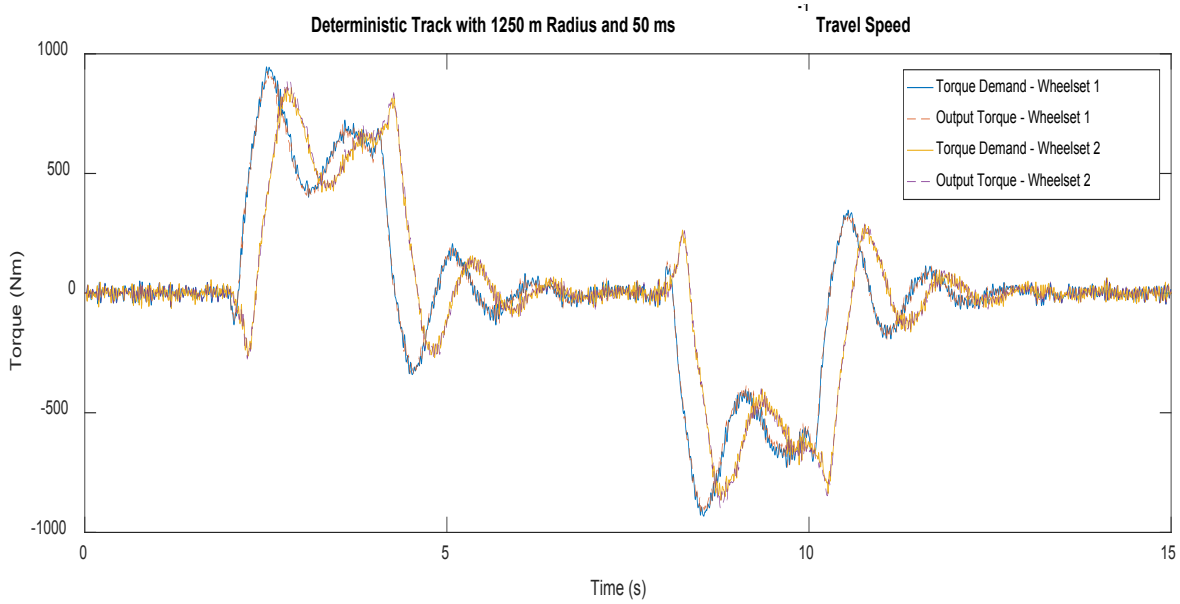

Figure 7. 6 – Torque Demand vs Output Torque – Curved Track (1250m / 50 ms^{-1}) (TAV)

Figure 7.6 depicts that once travel speed is increased from 25 ms^{-1} to 50 ms^{-1}, and curvature radius has increased from 300 m to 1250 m control effort to stabilise the wheelsets has decreased when traversing the curve and this can be expected due to decreased creep forces with lower curvature. However, as desired, when travelling on the curved section, wheelset control efforts are completely eliminated by the active control.

In addition, due to lower overall values, minor errors/noise introduced to the system by the state observer when generating estimations are more visible in this case than the irregularity track. But it is clear from the vehicle dynamics assessment (Table 7.6), these minor variations are not high enough for any significant detrimental influence.

Figure 7.7 depicts the control efforts when the wheelsets are travelling on smoother curve with high travel speed. Due to the decrease in the curvature radius (despite higher travel speed), it can be seen that traversing control effort is at its lowest with this track. However, due to low values, high frequency noise associated with estimations of the state observer are more visible in this case than others.

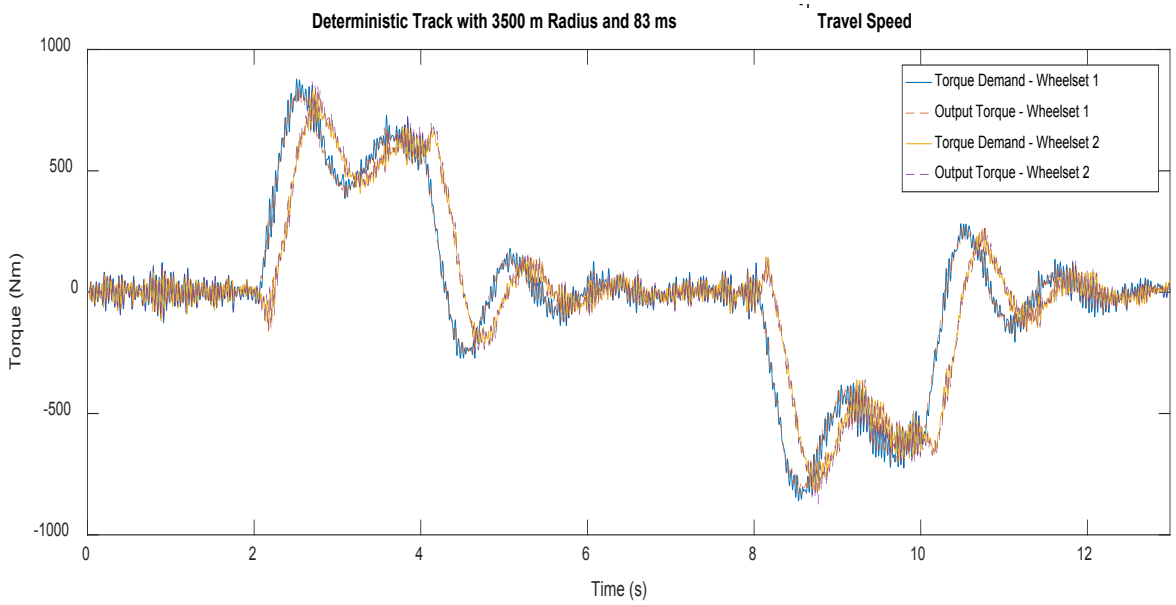

Figure 7. 7 – Torque Demand vs Output Torque – Curved Track (3500m / 83 ms^{-1}) (TAV)

In addition, above results indicate that overall actuator developed (with model–based feedback) in the study are performing well to provide output torque as demanded by the wheelset controller.

Vehicle Dynamics Evaluation – TAV

In order to further evaluate the vehicle dynamics with overall full active control system, key performance indicators, such as, wheelset lateral deflection, wheelset yaw and contact forces can be observed. Through this analysis, it is possible to assess essential dynamic conditions such as whether the wheelset flanges are not contacted by having lateral deflection values < 10 mm and whether ideal lateral displacements are achieved by the wheelsets when negotiating curved tracks. During this analysis with all the four measured straight tracks with lateral irregularities are used as well as three curved tracks mentioned earlier.

Wheelset Deflection

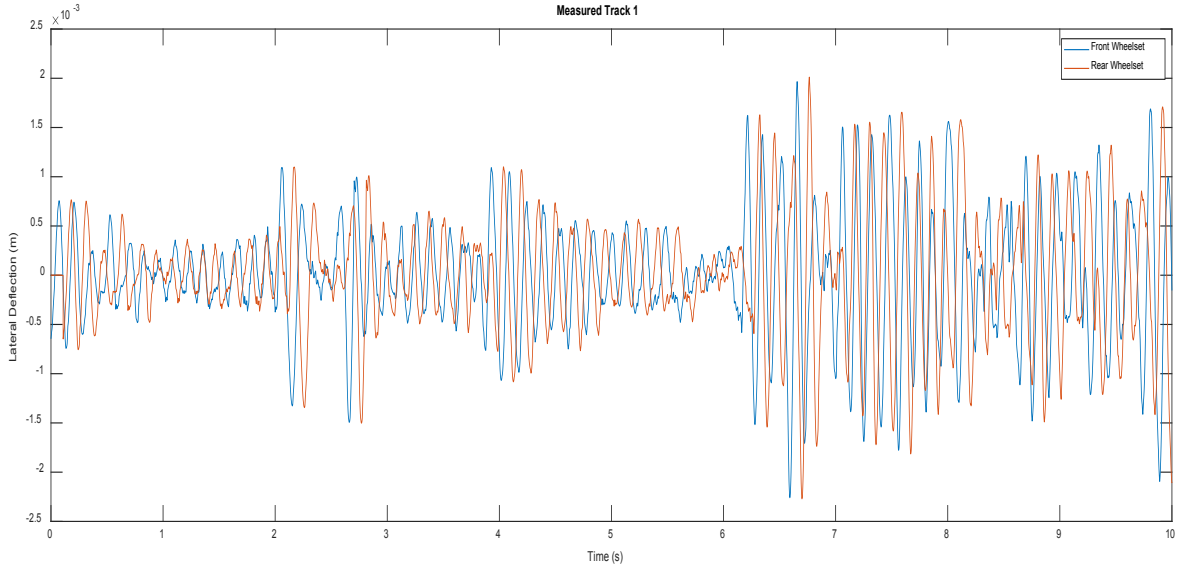

Figure 7. 8 – Wheelset Deflection – Measured Track 1 (TAV)

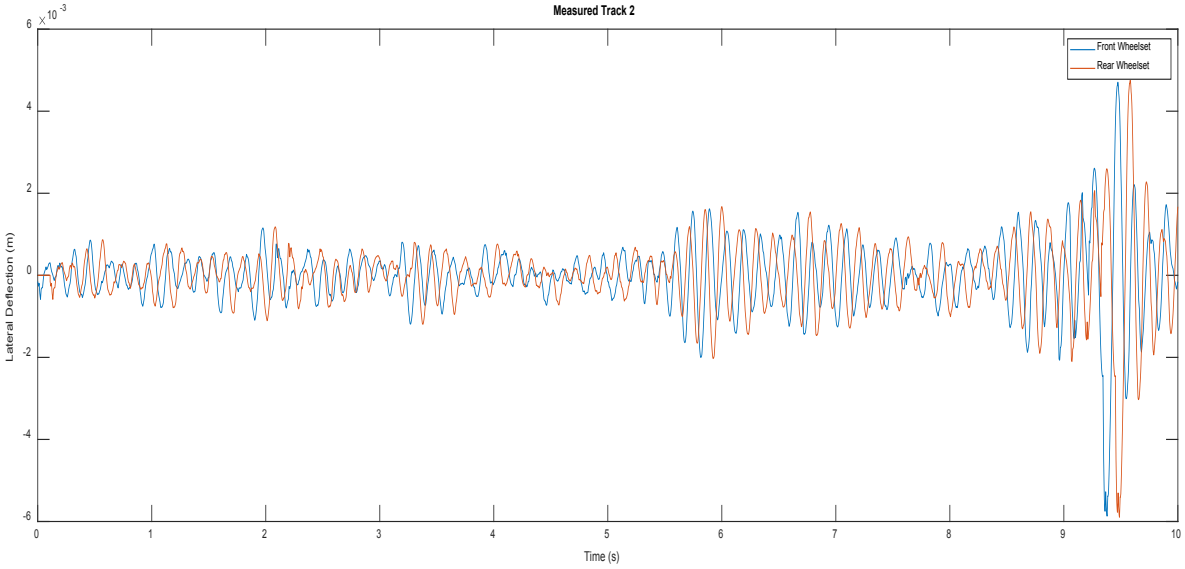

Figure 7. 9 – Wheelset Deflection – Measured Track 2 (TAV)

Figure 7.8 shows that with the full active control system, both front and rear wheelsets have almost identical lateral deflection with the time delay between the wheelsets and has a maximum deflection of approximately 2 mm (<10 mm).

Similarly Figure 7.9 is having a maximum lateral deflection of approximately 6 mm (<10 mm) and although Track 2 is relatively rougher than the other measured tracks, its deflections does not cause the wheelset flanges to be contacted.

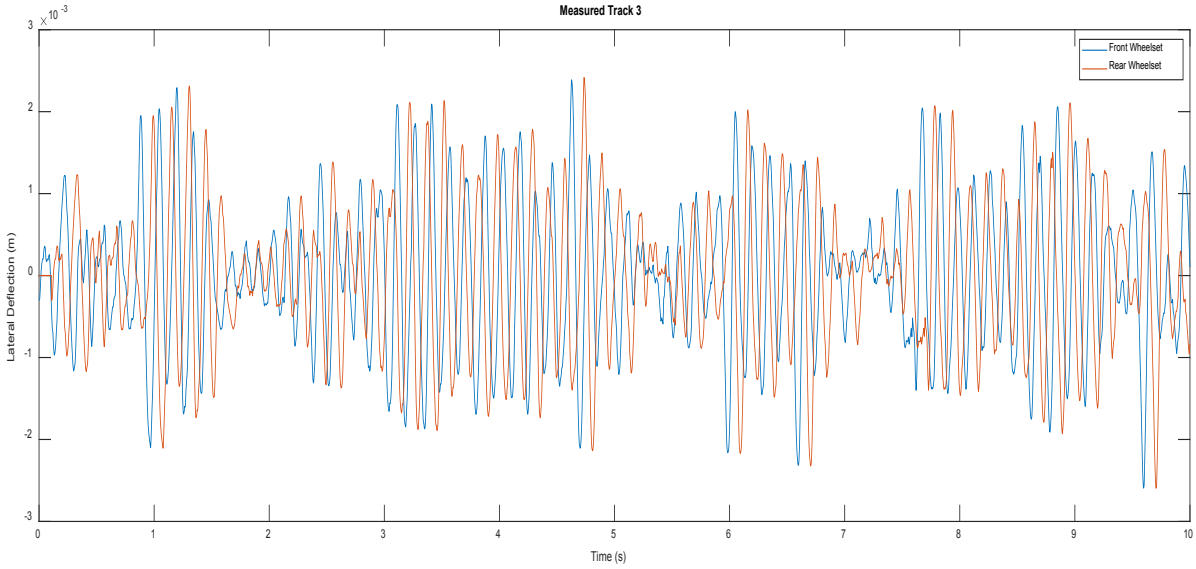

Figure 7. 10 – Wheelset Deflection – Measured Track 3 (TAV)

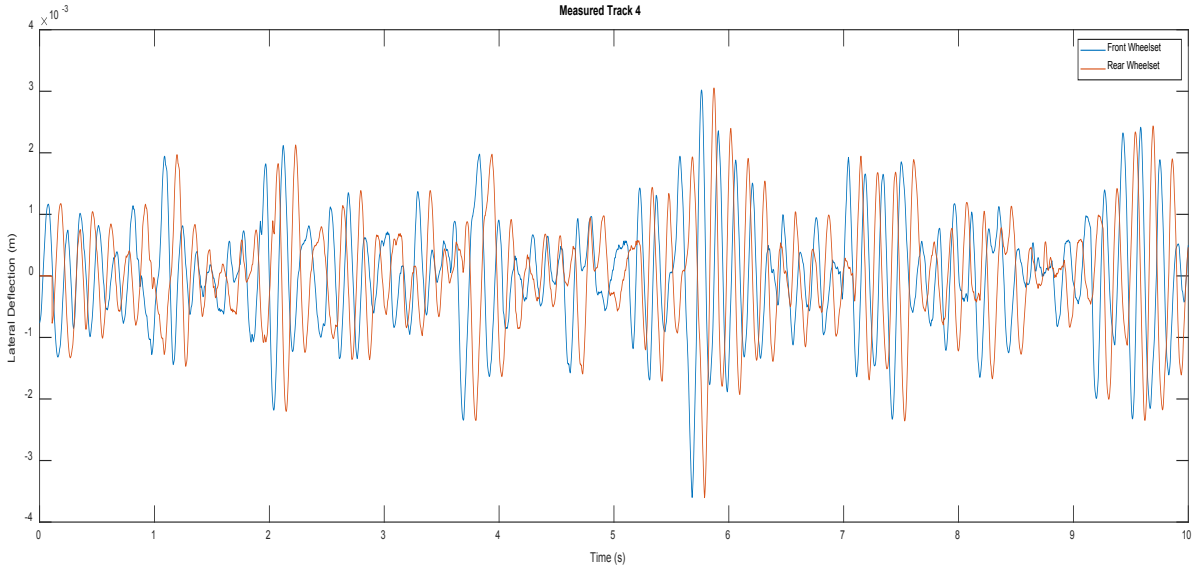

Figure 7. 11 – Wheelset Deflection – Measured Track 4 (TAV)

Figure 7.10 and Figure 7.11 depicts similar behaviour which the active controller allows the front and rear wheelsets to have identical lateral deflections with peaks less than 10 mm. This is an indication of the safety and proves that wheelset is not running on the flanges.

In addition to the straight tracks with lateral irregularities, curved tracks are also used for the analysis and ideal displacement for each curved track is calculated with the Equation 76 in Chapter 4.

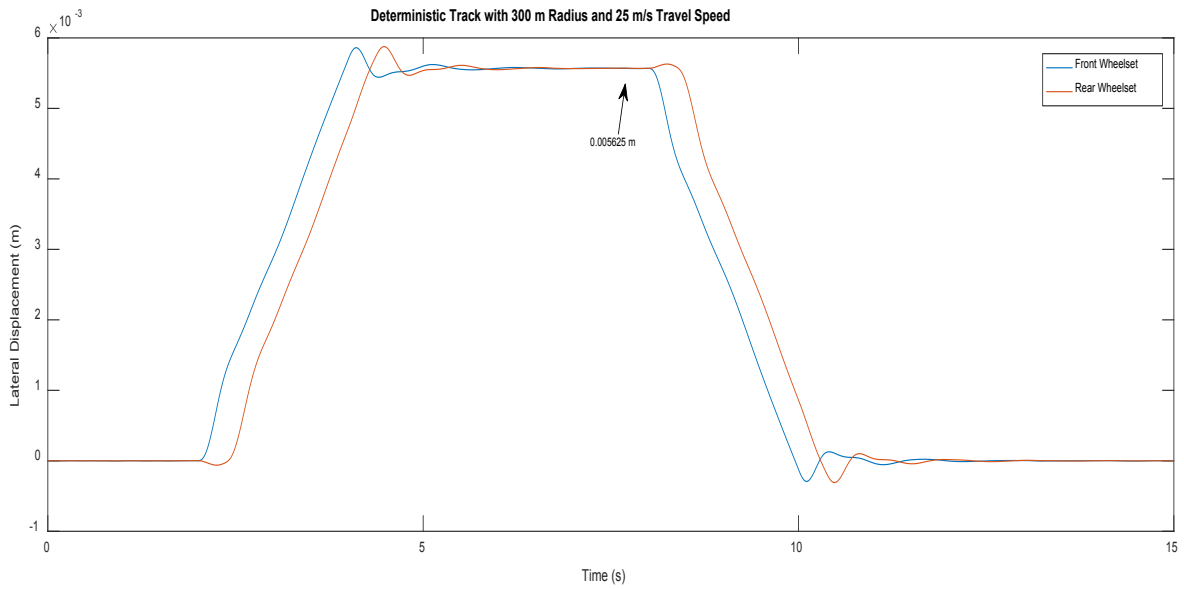

Figure 7. 12 – Wheelset Displacement – Curved Track (300 m / 25 ms^{-1}) (TAV)

It is evident from the Figure 7.12 to Figure 7.14 that overall active control system is enabling the wheelsets have natural curing movements on curved track such that the ideal displacement of 0.005625 m, 0.0014 m and 0.000482 m are achieved for each curvature radii of all 300 m, 1250 m and 3500 m respectively.

Since active controller with the actuator is allowing the wheelsets to achieve ideal displacement during curved tracks, eliminated longitudinal creep forces can be expected.

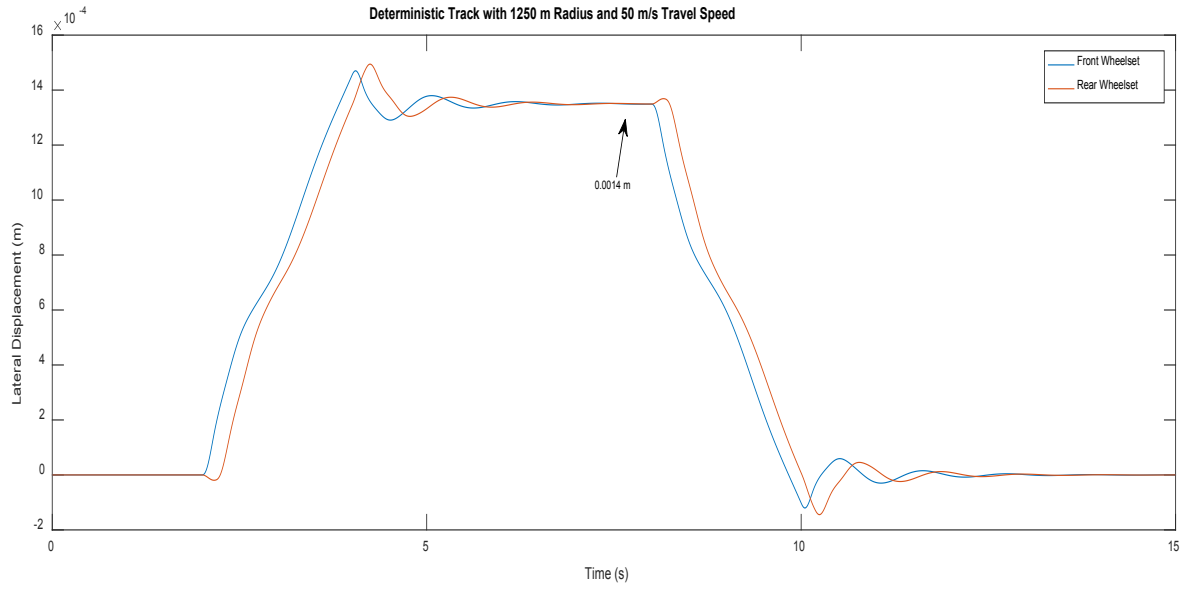

Figure 7. 13 – Wheelset Displacement – Curved Track (1250 m / 50 ms^{-1}) (TAV)

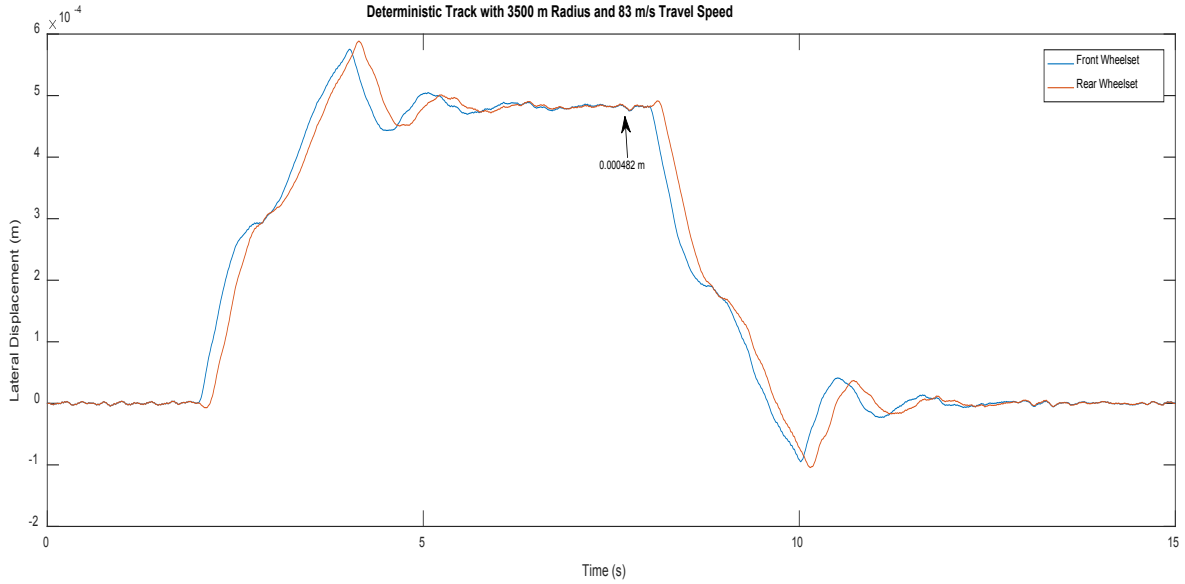

Figure 7. 14 – Wheelset Displacement – Curved Track (3500 m / 83 ms^{-1}) (TAV)

Yaw Angles

In addition, wheelset lateral deflections/displacements, wheelset yaw angle provides further insight to the wheelset dynamics and below Figure 7.15 – 7.21 depicts the yaw angles of the front and rear wheelsets with active wheelset control system when traveling on both measured tracks and curved tracks. It can be seen from the results that both front and rear wheelset yaw angles are almost identical with the time delay between wheelsets.

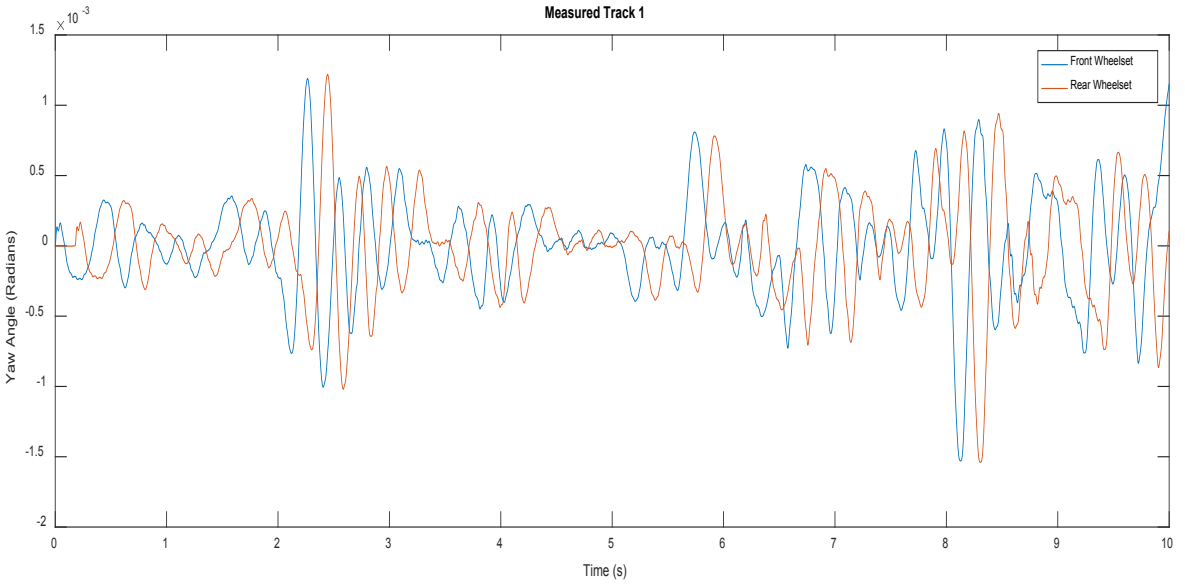

Figure 7. 15 – Wheelset Yaw Angle – Measured Track 1 (TAV)

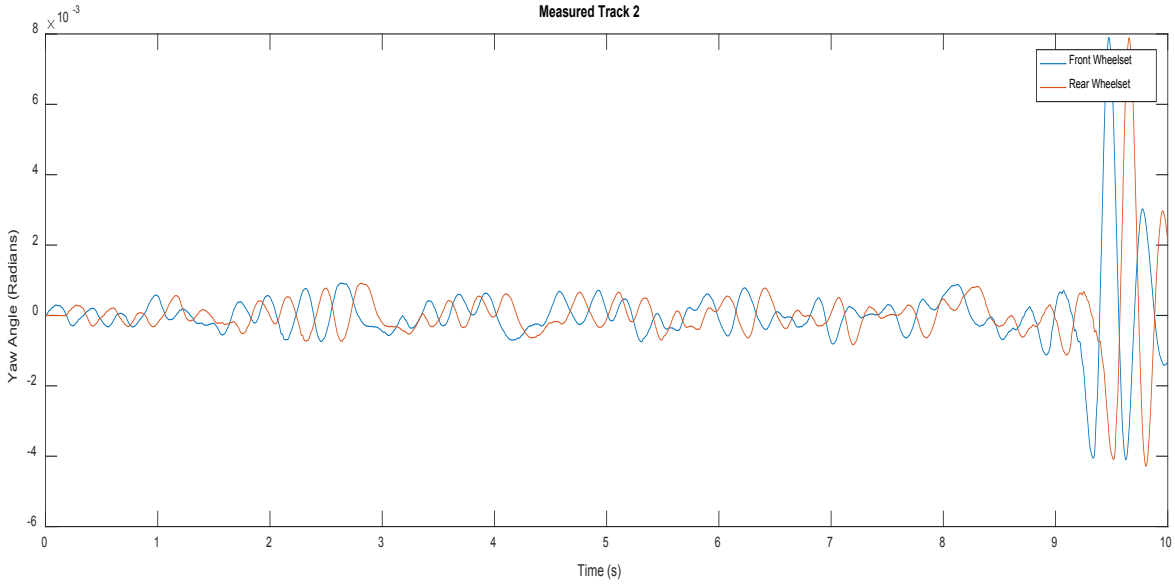

Figure 7. 16 – Wheelset Yaw Angle – Measured Track 2 (TAV)

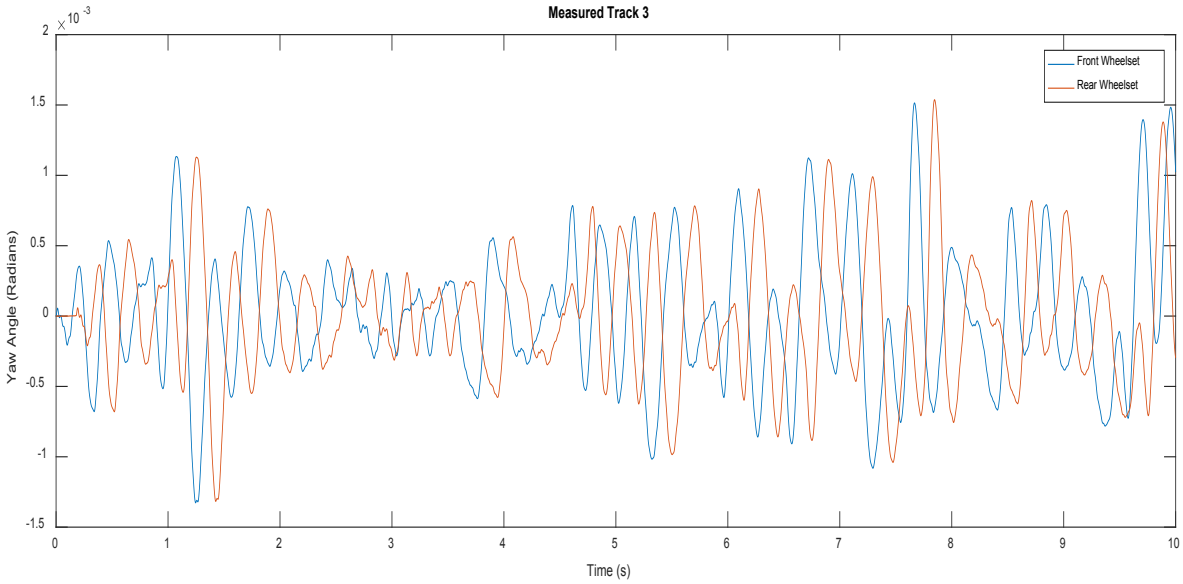

Figure 7. 17 – Wheelset Yaw Angle – Measured Track 3 (TAV)

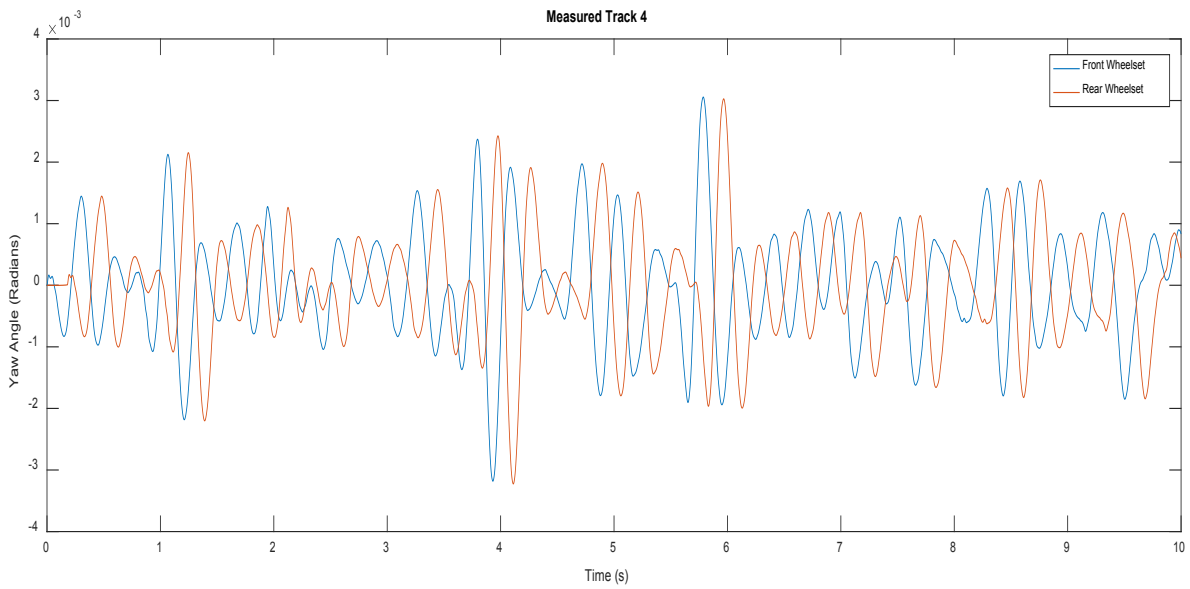

Figure 7. 18 – Wheelset Yaw Angle – Measured Track 4 (TAV)

Above Figure 7.15 to Figure 7.18 depicts that active wheelset controllers are maintaining yaw variations of wheelsets at low levels (less than 1^0 in the worst case). Since yaw angles (also called as angle of attack when curving) has an impact on the lateral creep forces, low yaw angles indicate low creep forces for the wheelsets during measured tracks. In addition, since the yaw angles of both the wheelsets are having similar patterns in the, similar/balanced creep forces can be expected in wheelsets.

When assessing the angle of attack of the wheelsets with the all the curved tracks, it is evident from the Figure 7.19 to Figure 7.21 that, as desired the wheelsets are having similar values as yaw of the wheelsets.

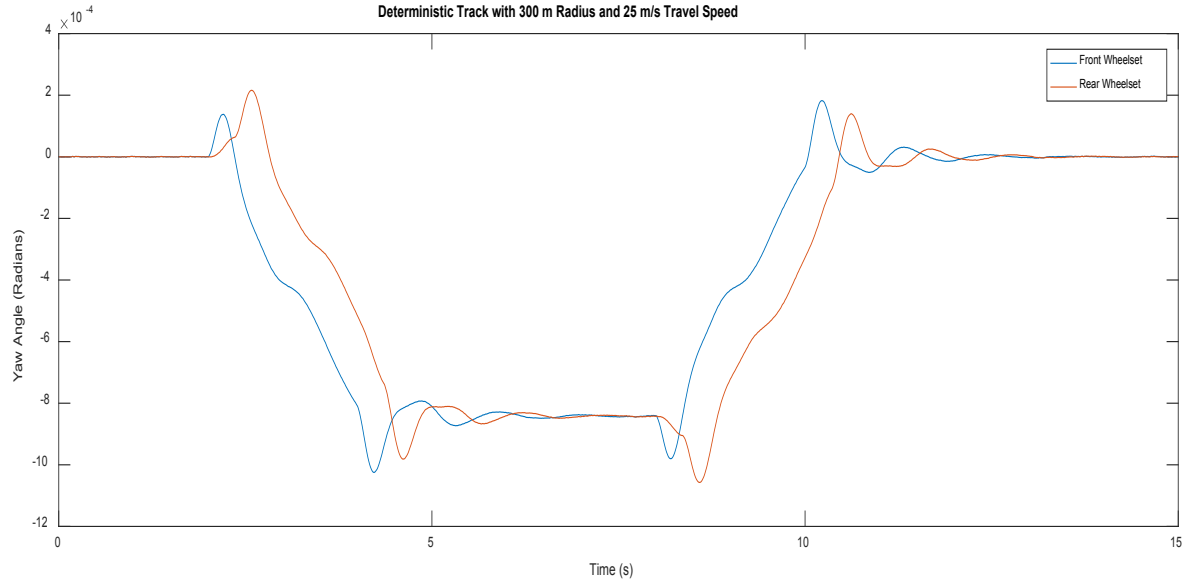

Figure 7. 19 – Wheelset Yaw Angle – Curved Track (300 m / 25 ms^{-1}) (TAV)

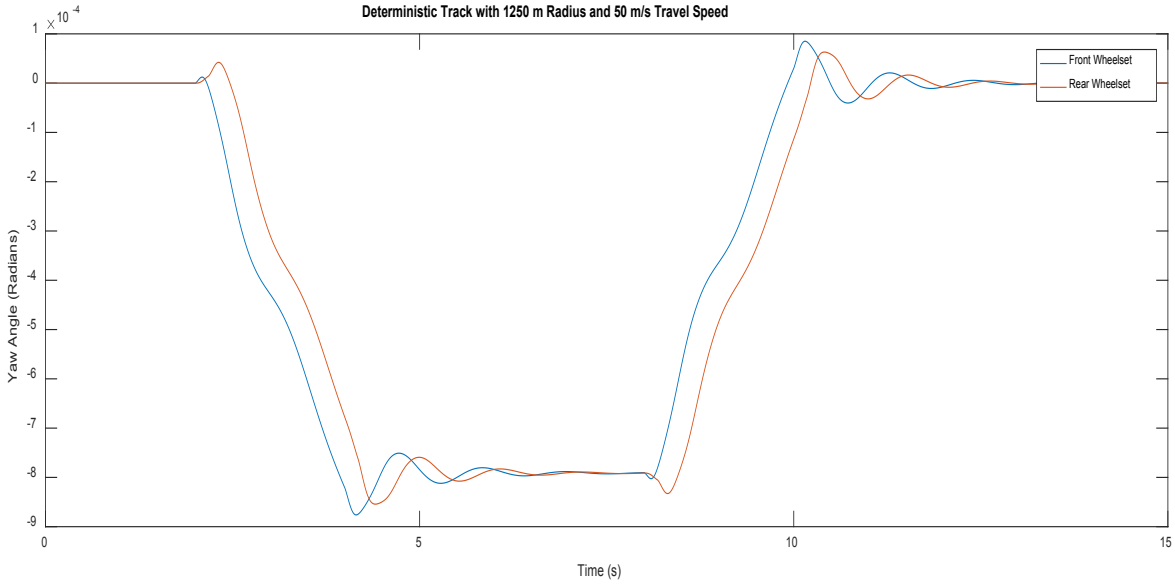

Figure 7. 20 – Wheelset Yaw Angle – Curved Track (1250 m / 50 ms–1) (TAV)

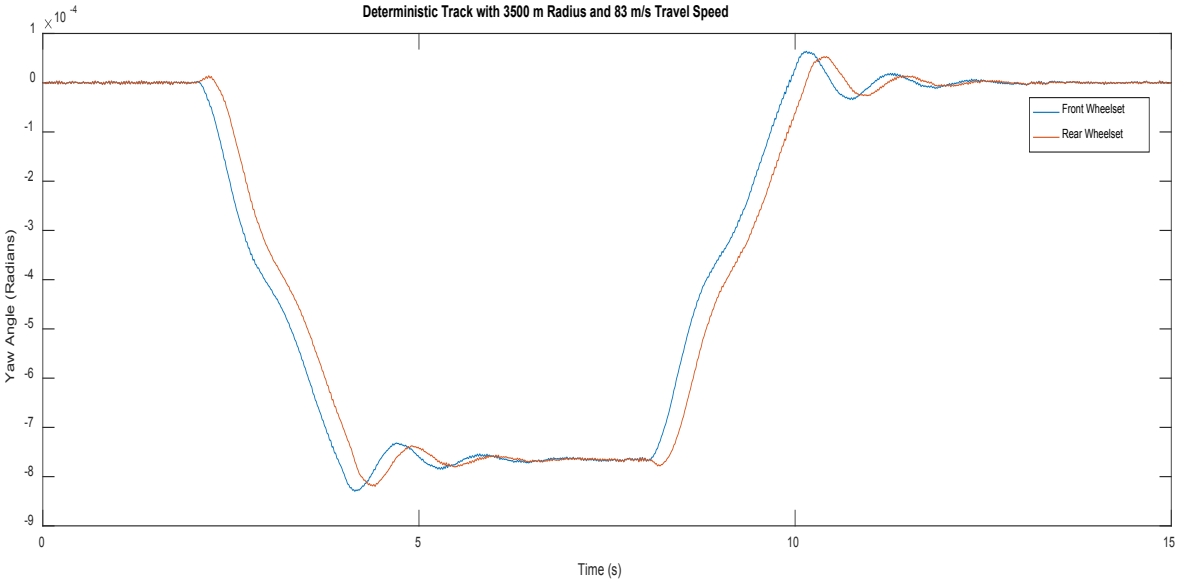

Figure 7. 21 – Wheelset Yaw Angle – Curved Track (3500 m / 83 ms^{-1}) (TAV)

Longitudinal Creep Forces

When evaluating improvements in wheelset dynamics when controlled with active control system developed in the study, assessment of the creep forces is essential since both lateral and longitudinal creep forces affects the control torque demand and generally higher creep forces are undesirable (except

lateral creep forces on curved track which counters the centrifugal forces) as they also cause wheel fatigue.

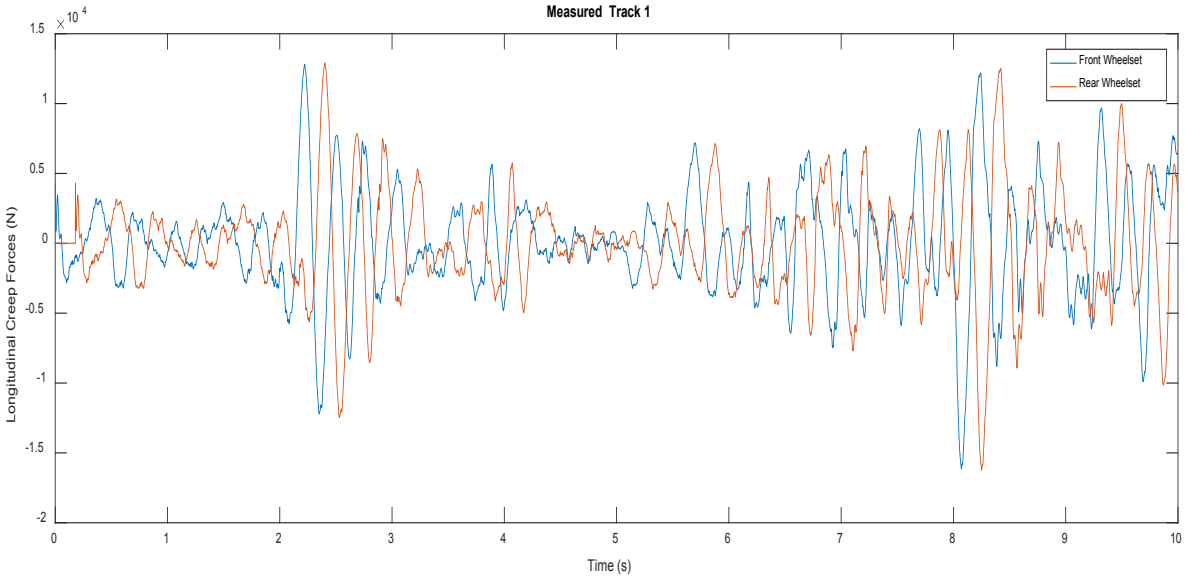

Figure 7. 22 – Longitudinal Creep Forces – Measured Track 1 (TAV)

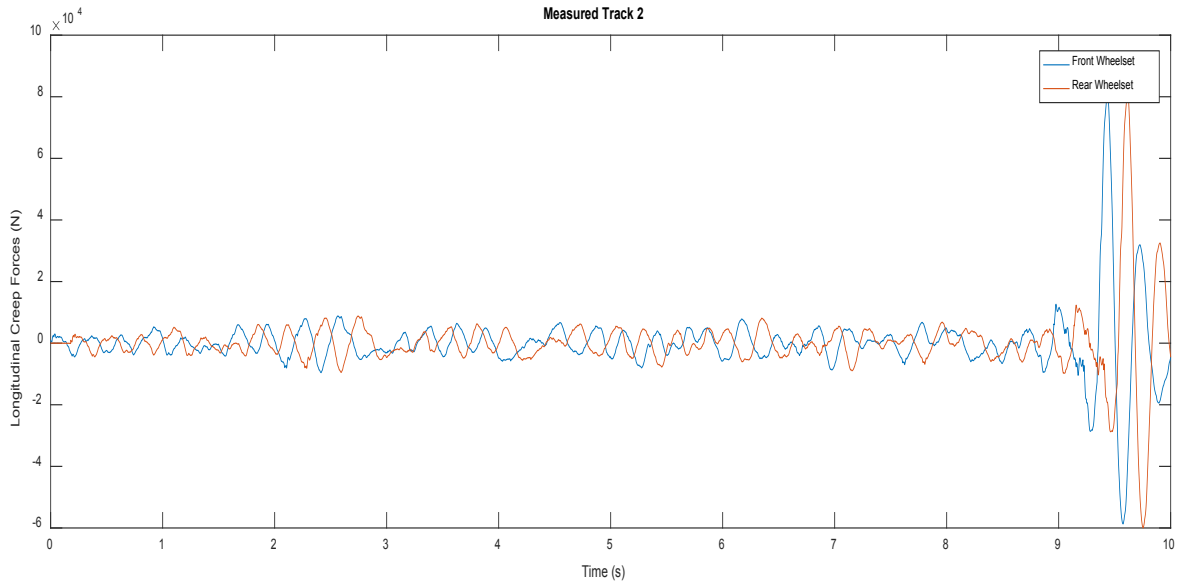

Figure 7. 23 – Longitudinal Creep Forces – Measured Track 2 (TAV)

It is clear from the Figure 7.22 to Figure 7.25 that longitudinal creep forces experienced by both wheelsets are similar in pattern, which indicates that longitudinal creep forces are balanced between the wheelsets.

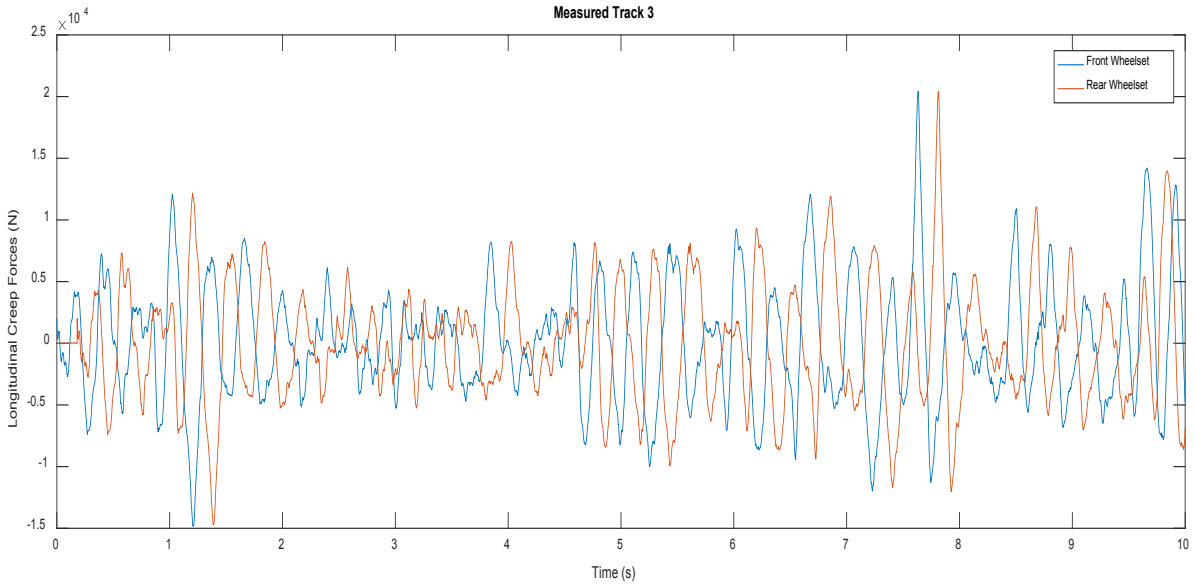

Figure 7. 24 – Longitudinal Creep Forces – Measured Track 3 (TAV)

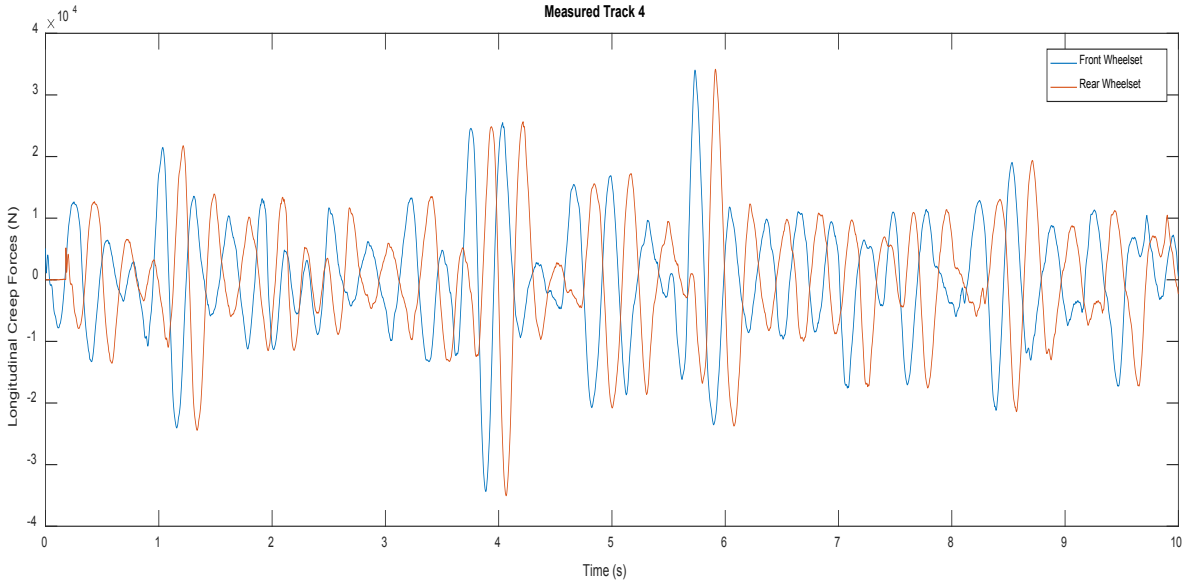

Figure 7. 25 – Longitudinal Creep Forces – Measured Track 4 (TAV)

Unlike with the straight track with lateral irregularities, Figure 7.26 to Figure 7.28 shows that active control can significantly reduce/eliminate longitudinal creep forces of the wheelsets travelling on the curved tracks. This is achieved by reaching the ideal lateral displacement of wheelsets such that wheelsets achieve ideal angle of attack, which enable the wheelsets to negotiate the curve effectively with pure rolling.

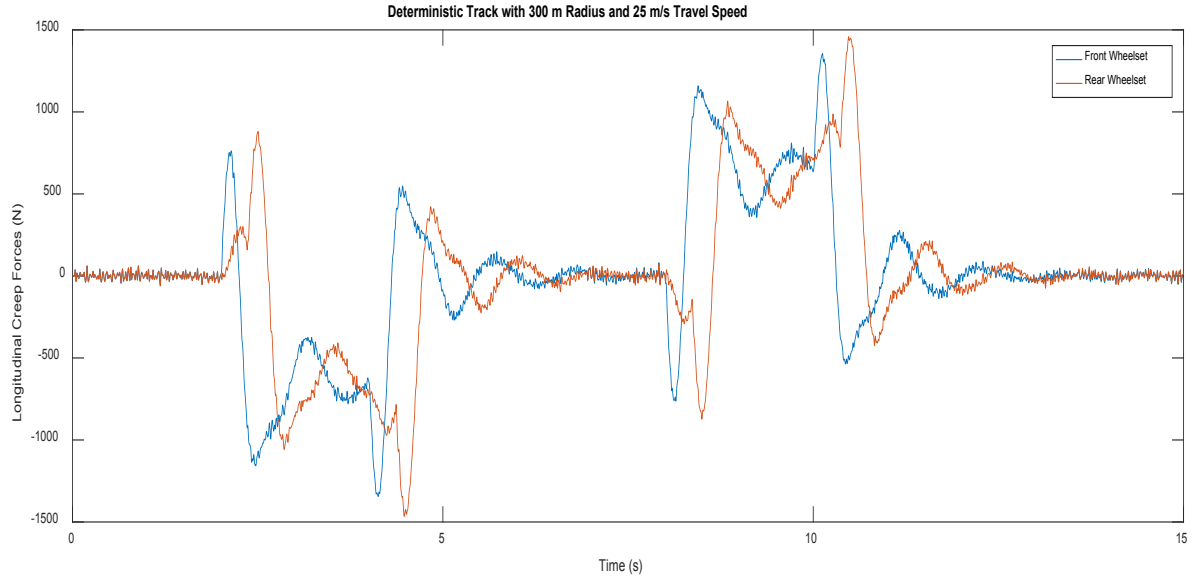

Figure 7. 26 – Longitudinal Creep Forces – Curved Track (300 m / 25 ms^{-1}) (TAV)

It is evident from the results between Figure 7.26 and Figure 7.27 that at high curvature radius, creep forces occurred when approaching/leaving the curved section (curve transition) of the track also increases while lower curvature radius, longitudinal creep forces decreases.

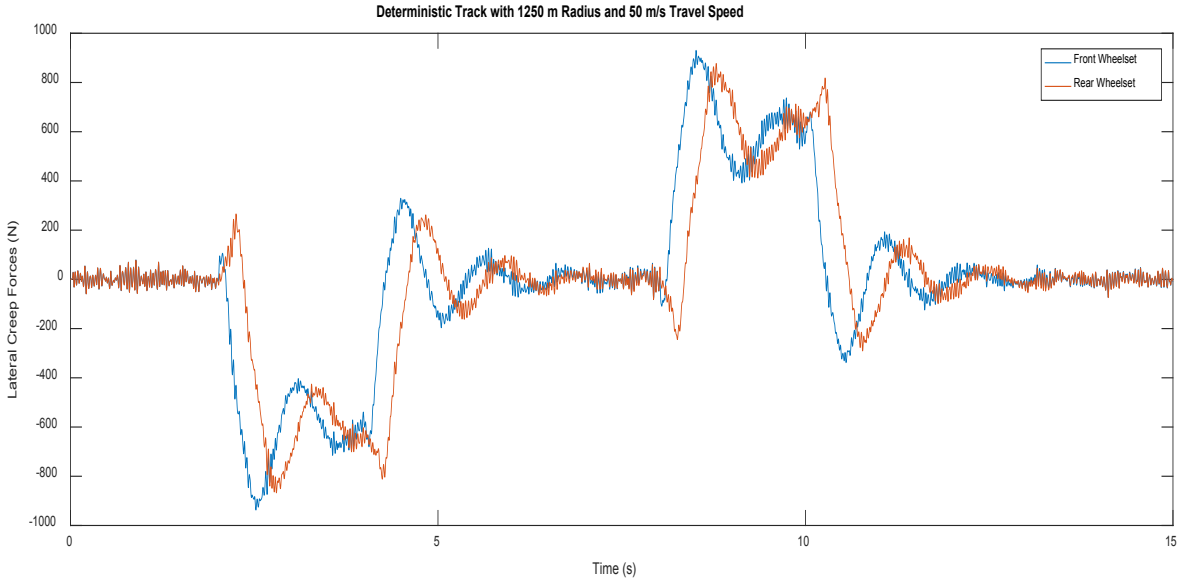

Figure 7. 27 – Longitudinal Creep Forces – Curved Track (1250 m / 50 ms^{-1}) (TAV)

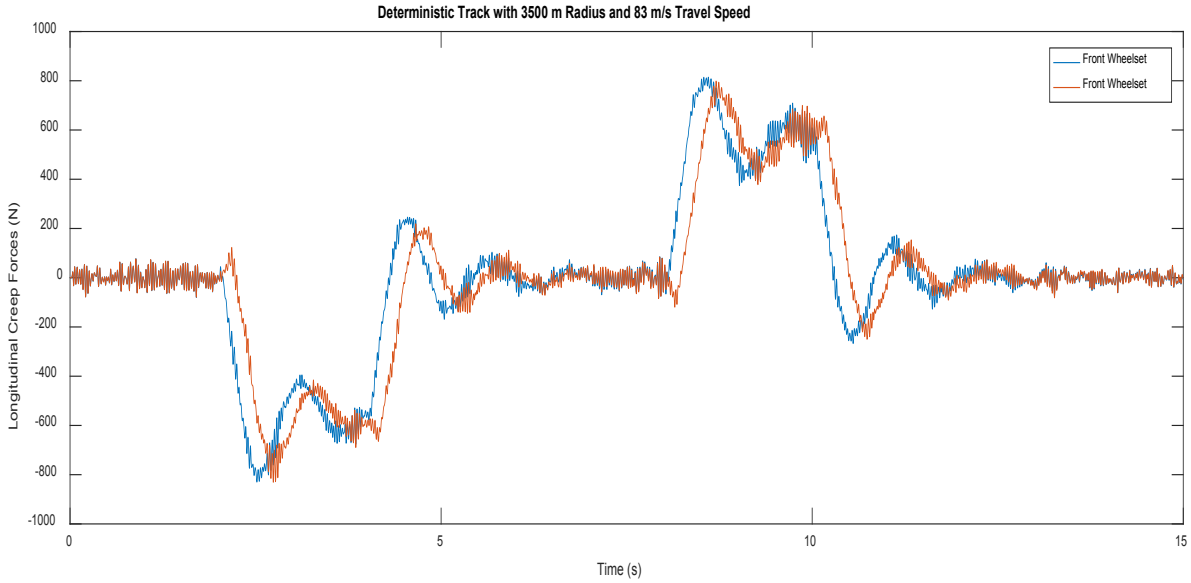

Figure 7. 28 – Longitudinal Creep Forces – Curved Track (3500 m / 83 ms^{-1}) (TAV)

In addition, from the Figure 7.28 shows that although travel speed is high, since the curvature radius of the track is low, longitudinal creep forces in the curve transition are low due to the inversely proportional relationship between curve radius and longitudinal creep forces.

Lateral Creep Forces

Similar analysis can be done on the lateral creep forces experienced by wheelsets when travelling on both measured and curved tracks. Figure 7.29 to Figure 7.35 depicts lateral creep forces of the wheelsets when exited by four measured tracks and three curved tracks.

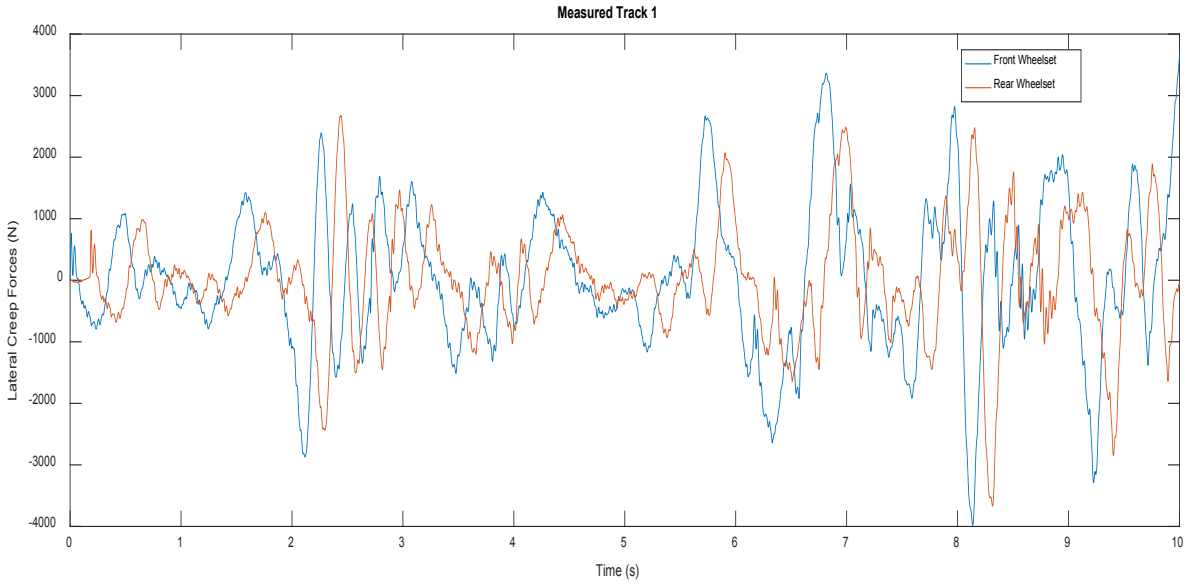

Figure 7. 29 – Lateral Creep Forces – Measured Track 1 (TAV)

With straight tracks with lateral irregularities, it can be seen from the lateral creep force values that both wheelsets are experiencing similar pattern of the forces as it can be expected due to the similarities in the wheelset lateral displacement and yaw behaviour.

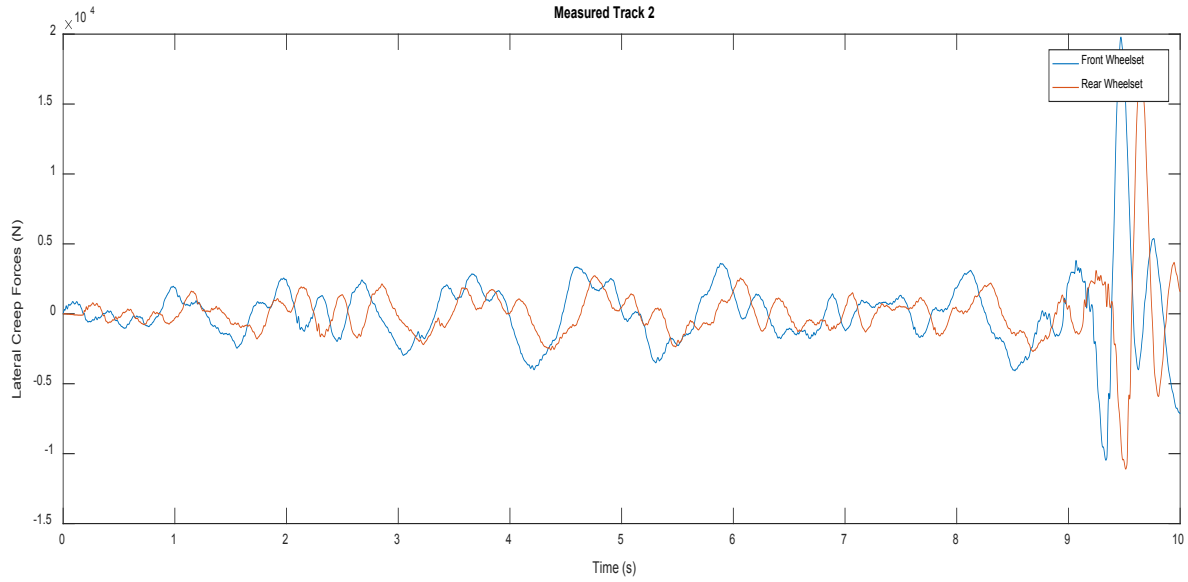

Figure 7. 30 – Lateral Creep Forces – Measured Track 2 (TAV)

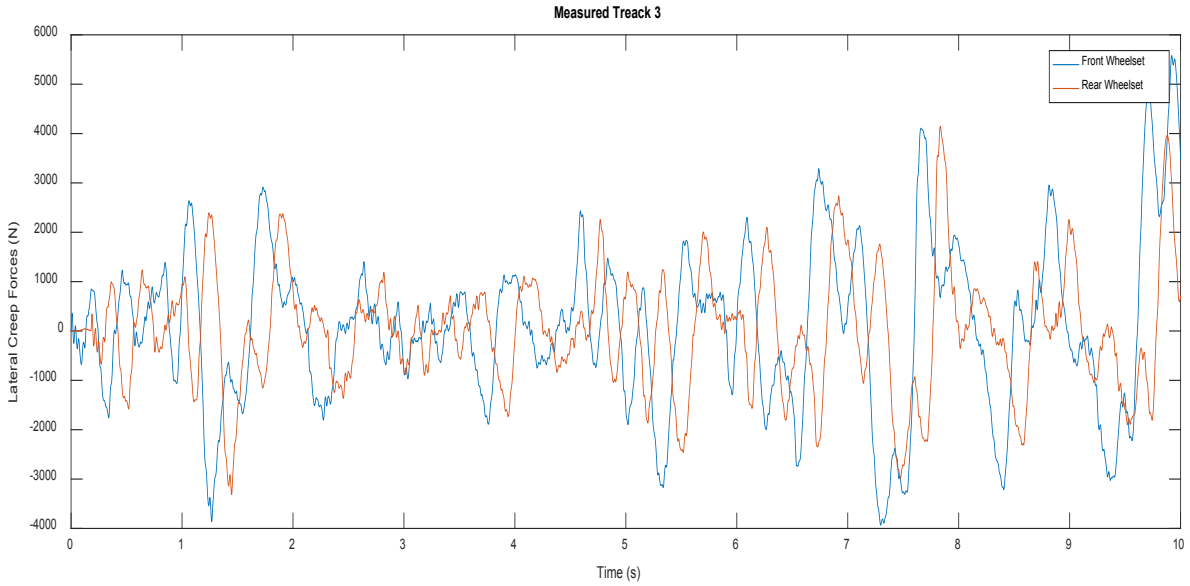

Figure 7. 31– Lateral Creep Forces – Measured Track 3 (TAV)

From the analysis of the Figure 7.33 to Figure 7.34, it can be seen that is expected active control is enabling the both front and rear wheelsets to have almost identical lateral creep forces for each curved track. This is an indication and creep forces required to counter the centrifugal forces caused by cant deficiency of the tracks are balanced between the wheelsets.

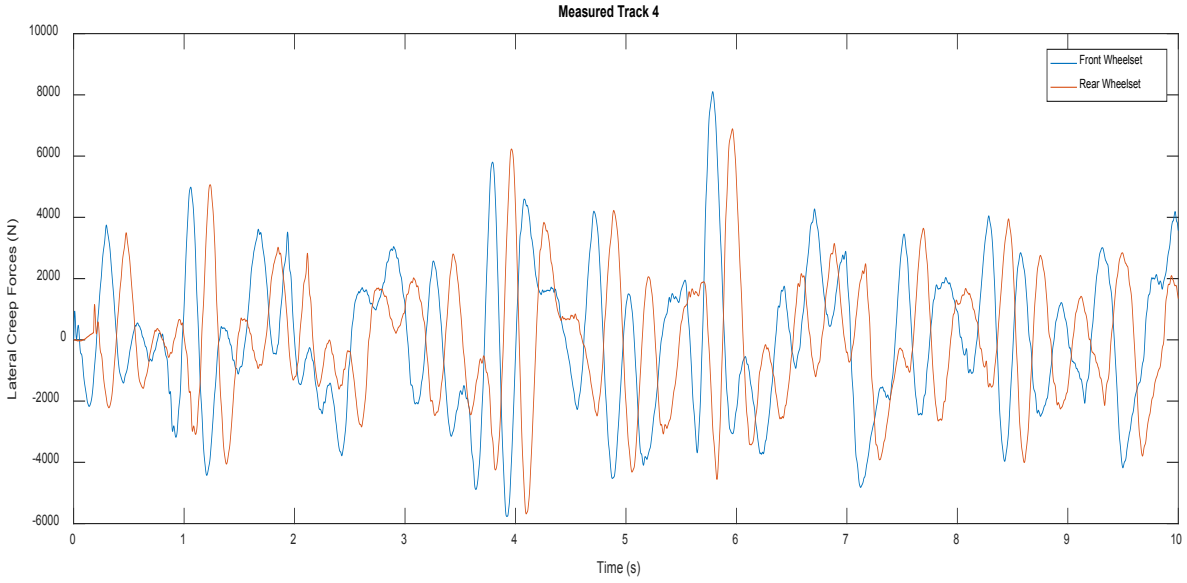

Figure 7. 32 – Lateral Creep Forces – Measured Track 4 (TAV)

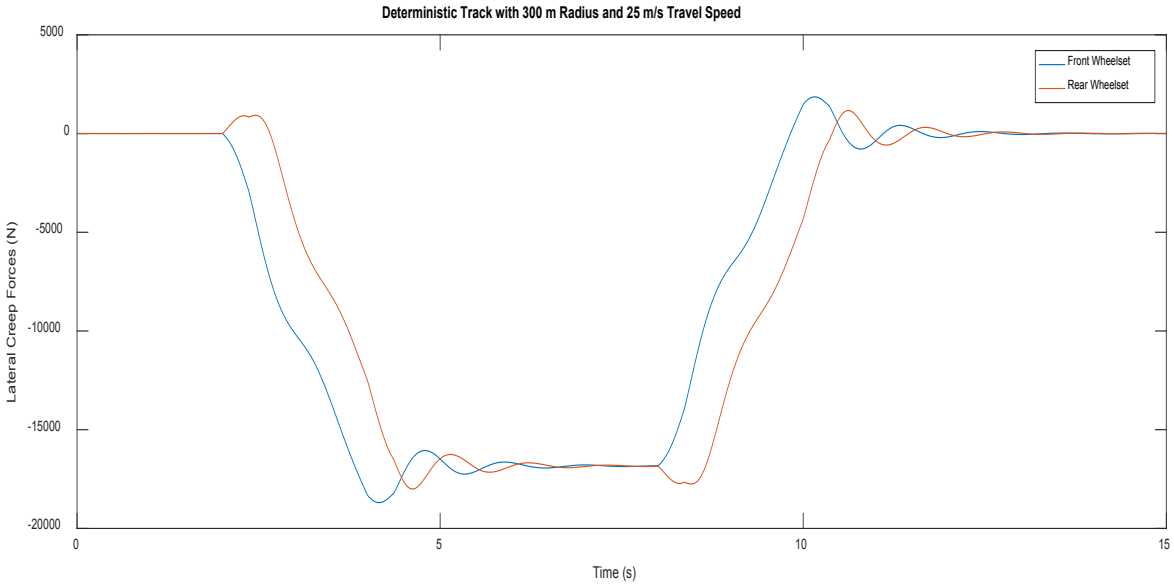

Figure 7. 33 – Longitudinal Creep Forces – Curved Track (300 m / 25 ms^{-1}) (TAV)

By comparing the values of the lateral creep forces, it can be seen that both travel speed and curvature radius have significant effect on the lateral creep forces since those factors proportionally affect the centrifugal forces which ultimately have an unfavourable affects the control torque demand and wheelset fatigue levels.

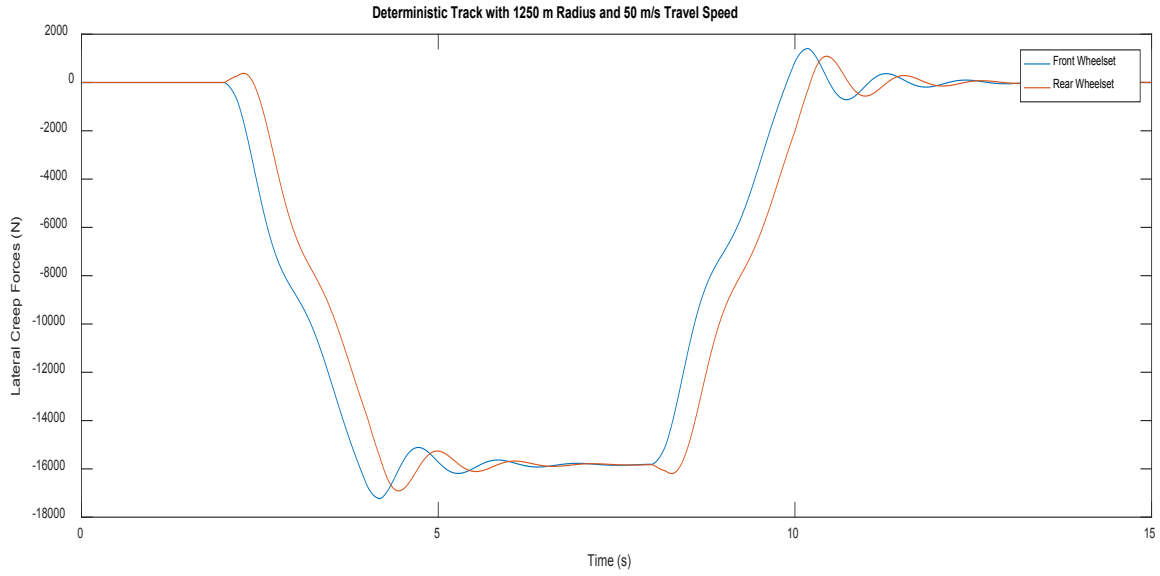

Figure 7. 34 – Longitudinal Creep Forces – Curved Track (1250 m / 50 ms^{-1}) (TAV)

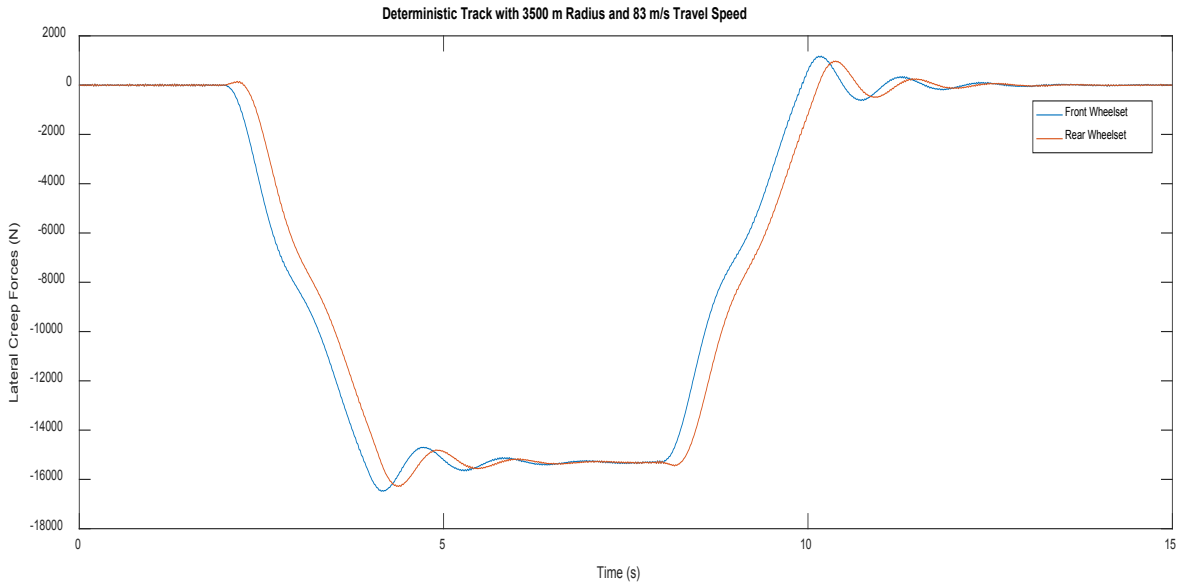

Figure 7. 35 – Longitudinal Creep Forces – Curved Track (3500 m / 82 ms^{-1}) (TAV)

However, when focusing on the actuator and model–based sensing technique used in this case, it is clear that they are operating in a satisfactory order.

7.3. Full Bogie Vehicle Model

Actuator Performances – FBV

Similar to the analysis done with the two–axle vehicle model, overall system can be assessed with the full bogie vehicle model while same measured straight tracks with lateral irregularities and curved tracks are used to excite the wheelsets. In order to conduct the assessment of the actuator performance with different track conditions, rms values of the key performance indicative parameters related to front wheelset in front bogie is depicted in Table 7.8 to Table 7.15. Results relating to only this particular wheelset is being used in this case since the purpose is to assess the actuator performance and other wheelsets depicts similar behaviours. Furthermore, in addition to actuator performance, wheelset dynamics can also be assessed similar to the evaluation done with two–axle vehicle.

Table 7. 8 – Performance Analysis of Measured Straight Track with Lateral Irregularities 1 – Wheelset 1 (FBV)

Measured Straight Track with Lateral Irregularities 1 – Wheelset 1	
Performance Indictor	RMS Value
Torque Demand (Nm)	3.364×10^3
Actuator Output Torque (Nm)	3.468×10^3
Difference Percentage (%)	3.09%
Motor Current (A)	8.75
Motor Voltage (v)	1.85
Motor Power (W)	23.25

Results show that torque demand is at its lowest with the measured track 1 compared with results from other measured random tracks. Thus, the of motor voltage, current and power are at its lowest with track 1. Another essential observation can be done by comparing the results obtained with two–axle vehicle and full bogie vehicle, as control effort demand is approximately 20% lower for the full bogie vehicle for the same track conditions. This behaviour can be expected since bogie vehicle has both secondary suspension and a lower wheelbase which cause the active control demand to be lower.

Table 7. 9 – Performance Analysis of Measured Straight Track with Lateral Irregularities 2 – Wheelset 1 (FBV)

Measured Straight Track with Lateral Irregularities 2 – Wheelset 1	
Performance Indictor	RMS Value
Torque Demand (Nm)	1.007×10^4
Actuator Output Torque (Nm)	1.051×10^4
Difference Percentage (%)	4.03%
Motor Current (A)	20.74
Motor Voltage (v)	3.76
Motor Power (W)	367.67

As it can be seen with the two–axle vehicle, with measured track 2, full bogie vehicle is experiencing the highest torque values compared to the other measured tracks due to higher irregularity levels.

Table 7. 10 – Performance Analysis of Measured Straight Track with Lateral Irregularities 3 – Wheelset 1 (FBV)

Measured Straight Track with Lateral Irregularities 3– Wheelset 1	
Performance Indictor	RMS Value
Torque Demand (Nm)	4.748×10^3
Actuator Output Torque (Nm)	4.963×10^3
Difference Percentage (%)	4.05%
Motor Current (A)	9.74
Motor Voltage (v)	2.12
Motor Power (W)	32.39

Table 7. 11 – Performance Analysis of Measured Straight Track with Lateral Irregularities 4 – Wheelset 1 (FBV)

Measured Straight Track with Lateral Irregularities 4 – Wheelset 1	
Performance Indictor	RMS Value
Torque Demand (Nm)	9.715×10^3
Actuator Output Torque (Nm)	9.862×10^3
Difference Percentage (%)	1.51%
Motor Current (A)	19.59
Motor Voltage (v)	3.58
Motor Power (W)	117.12

Results depicted in Table 7.8 to Table 7.11 shows that actuator is performing well for the straight tracks with lateral irregularities since it is evident that the error percentage is less than 5% in all the cases.

Same analysis is done with the three curved track conditions used with two–axle vehicle to evaluate the curving performance of the full bogie vehicle with the actuator developed in the study.

Table 7. 12 – Performance Analysis of Curved Track 1 – Wheelset 1 (FBV)

Curved Track with 300 m Radius and 25 ms^{-1} Travel Speed – Wheelset 1	
Performance Indictor	RMS Value
Torque Demand (Nm)	316.55
Actuator Output Torque (Nm)	330.21
Difference Percentage (%)	4.31%
Motor Current (A)	0.653
Motor Voltage (v)	0.109
Motor Power (W)	0.077

Table 7. 13 – Performance Analysis of Curved Track 2 – Wheelset 1 (FBV)

Curved Track with 1250 m Radius and 50 ms^{-1} Travel Speed – Wheelset 1	
Performance Indictor	RMS Value
Torque Demand (Nm)	255.98
Actuator Output Torque (Nm)	248.45
Difference Percentage (%)	2.92%
Motor Current (A)	0.511
Motor Voltage (v)	0.108
Motor Power (W)	0.059

Table 7. 14 – Performance Analysis of Curved Track 3 – Wheelset 1 (FBV)

Curved Track with 3500 m Radius and 83 ms^{-1} Travel Speed – Wheelset 1	
Performance Indictor	RMS Value
Torque Demand (Nm)	265.57
Actuator Output Torque (Nm)	273.28
Difference Percentage (%)	2.91%
Motor Current (A)	0.543
Motor Voltage (v)	0.171
Motor Power (W)	0.184

It is clear from the results of the Table 7.12 to Table 7.14 where three curved track conditions have been assessed, similar to the behaviour observed with the two–axle vehicle, that torque demand for all the curved tracks are somewhat similar. This can be expected since the active controller is effectively allowing the wheelsets to negotiate curves.

In addition to analysing the RMS values, below Figure 7.36 to Figure 7.42 depicts the instantaneous behaviour of the torque demand from the wheelset controller and output torques of the actuator when full bogie vehicle is assessed with both measured tracks and curved tracks. Results from the front bogie is presented here since the rear bogie depicts similar results.

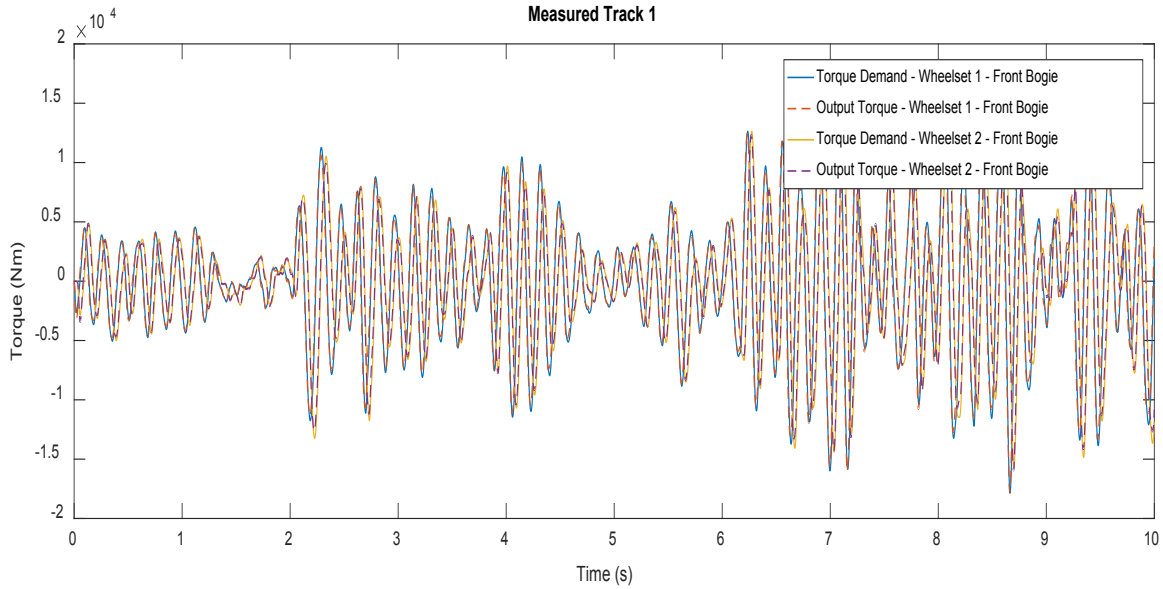

Figure 7. 36 – Torque Demand vs Output Torque – Measured Track 1 (FBV)

From analysing the results depicted in Figure 7.36, it is evident that the actuator is performing well to accurately match the control effort demand from the wheelsets. In addition, as it can be seen with the two–axle vehicle, measured track 1 is the relatively smoothest track since the control effort levels are low for this track. Furthermore, as discussed with the RMS value analysis, when comparing the Figure 7.1, full bogie vehicle requires slightly less amount of control torque to stabilise the wheelsets due to addition suspension and changes to the wheelbase.

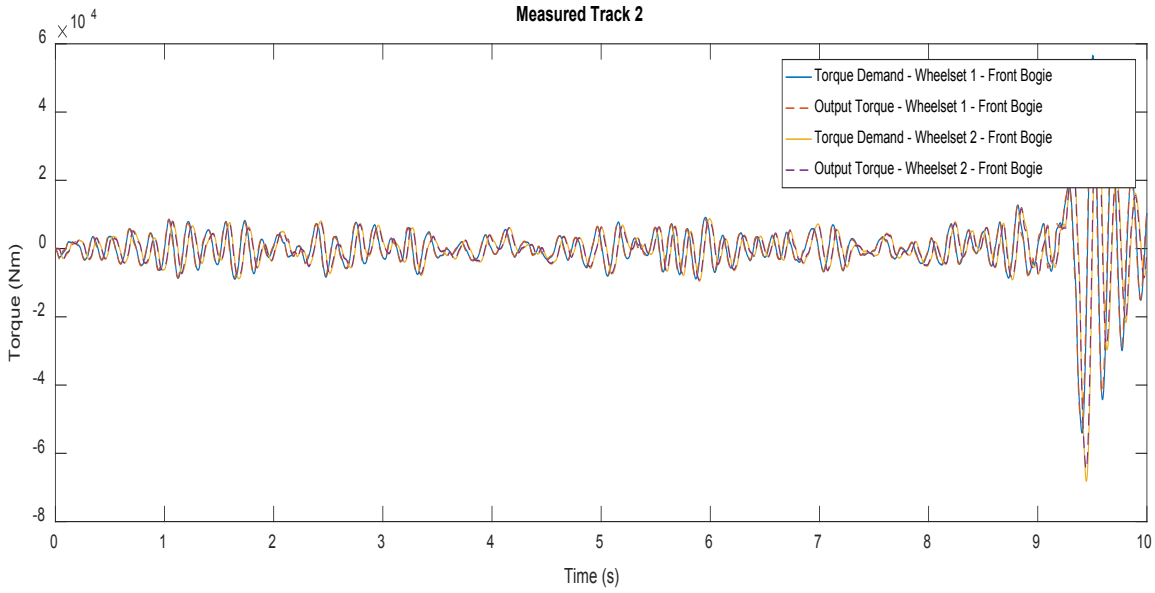

Figure 7. 37 – Torque Demand vs Output Torque – Measured Track 2 (FBV)

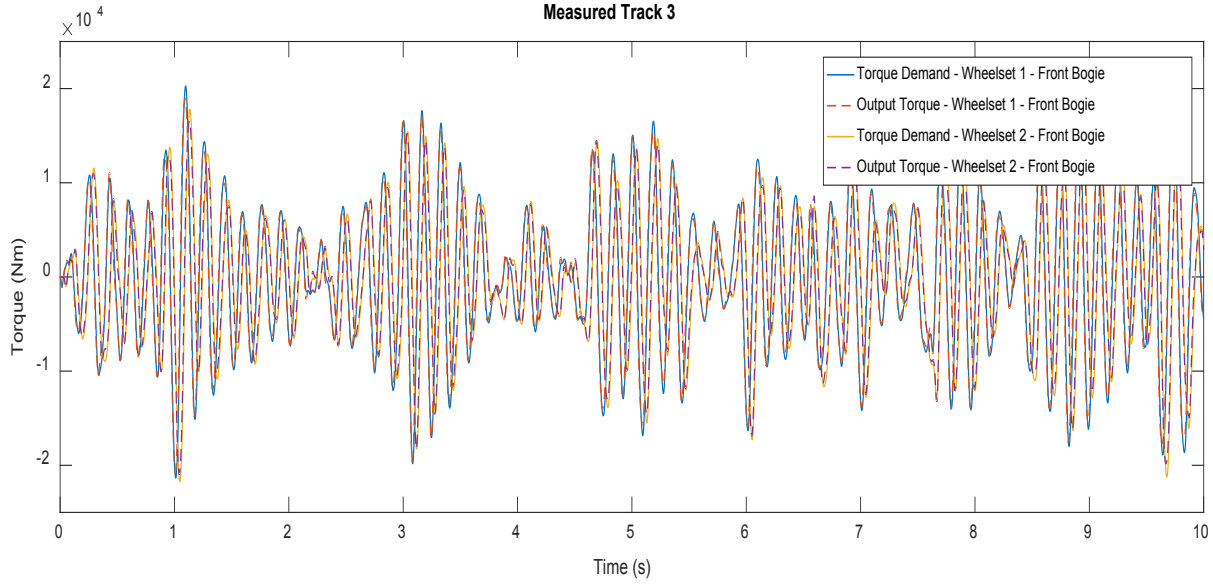

Figure 7. 38 – Torque Demand vs Output Torque – Measured Track 3 (FBV)

Similarly, results from Figure 7.37 to Figure 7.38 shows that the actuator is performing adequately to provide wheelset stabilising control effort.

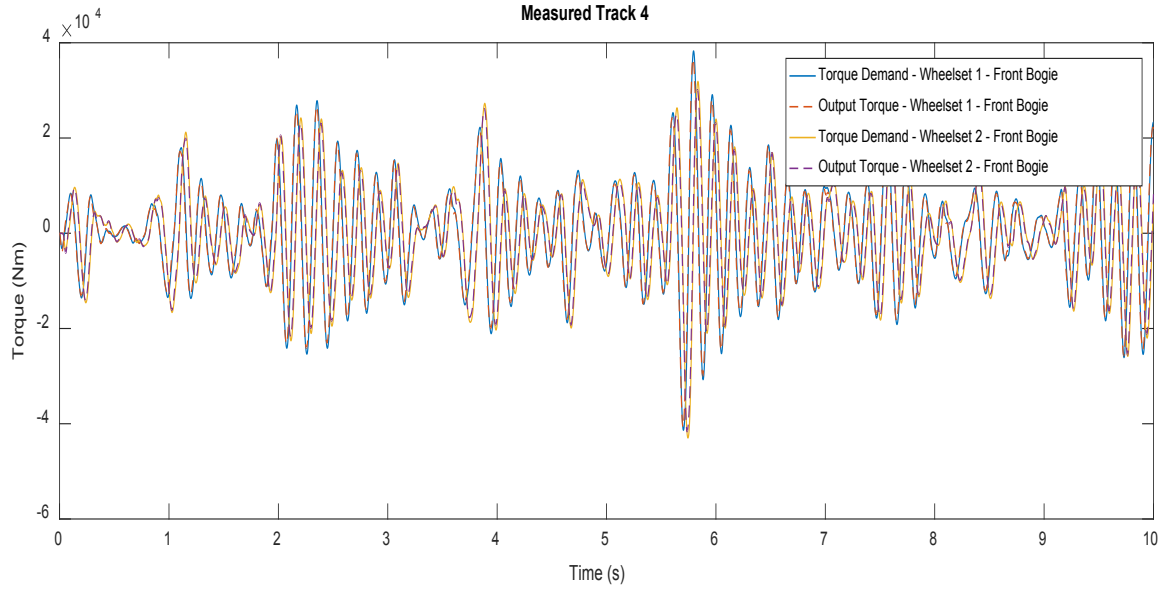

Figure 7. 39 – Torque Demand vs Output Torque – Measured Track 4 (FBV)

In addition to the straight tracks with lateral irregularities, same analysis is done with three curved track conditions to observe bogie vehicle wheelset's behaviour on curves.

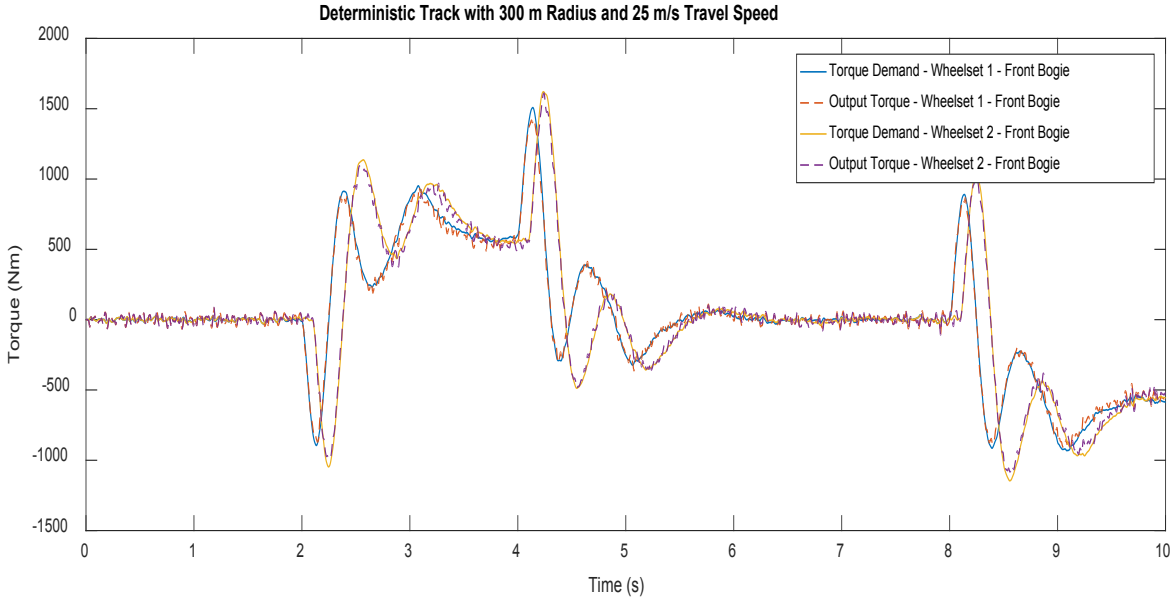

Figure 7. 40 – Torque Demand vs Output Torque – Curved Track (300m / 25 ms^{-1}) (FBV)

When comparing with the two–axle vehicle on the same track condition (Figure 7.5), similar control effort demand/supply can be seen on the wheelsets while overall control torque demand for wheelsets of full bogie vehicle is 20% lower.

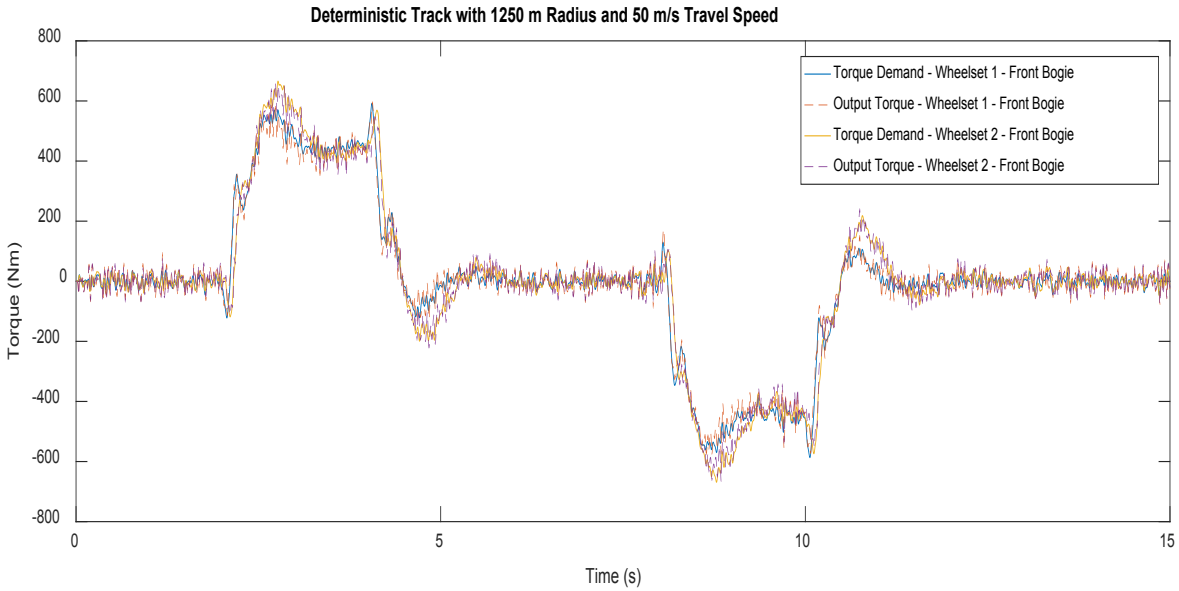

Figure 7. 41 – Torque Demand vs Output Torque – Curved Track (1250m / 82 ms–1) (FBV)

Figure 7.41 and Figure 7.42 both indicate that actuator is performing at an adequate level with the curved tracks to supply torque as demanded by the wheelset controller.

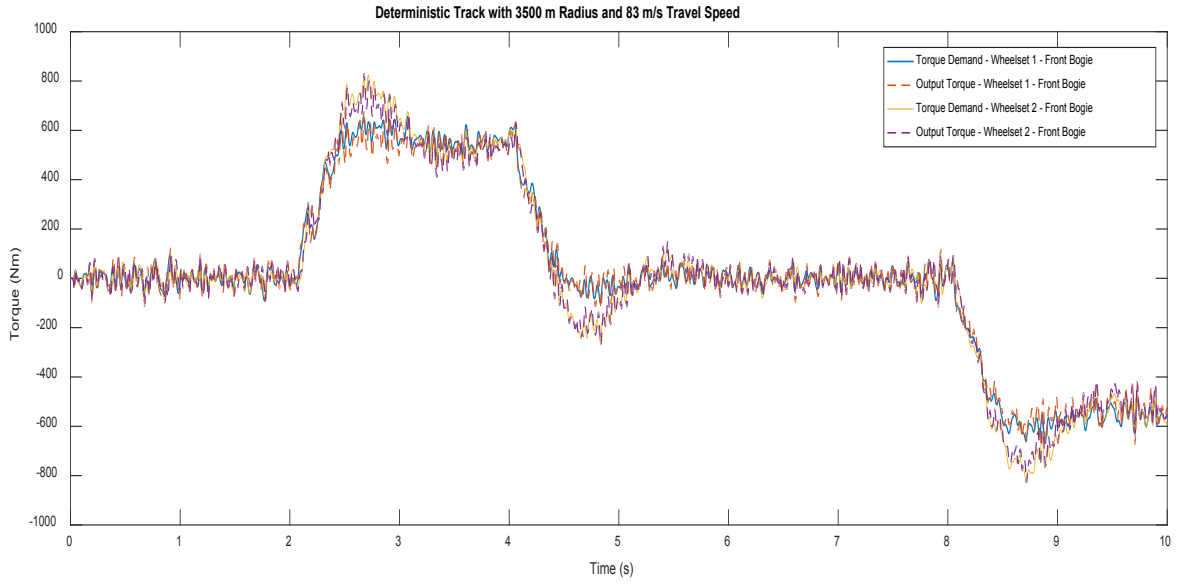

Figure 7. 42 – Torque Demand vs Output Torque – Curved Track (1250m / 82 ms^{-1}) (FBV)

Vehicle Dynamics Evaluation – FBV

In addition to the actuator performances, further analysis is done by evaluating the vehicle dynamics when integrated active control system is being utilised to stabilise the wheelsets of full bogie vehicle.

Wheelset Deflection

Wheelset deflections are used in this case to asses in order to assure that the values does not exceed 10 mm limit such that wheelset flanges are not contacted during measured random track travel while optimal lateral displacement of $5.685 \times 10^{-3}\, m$, for 300 m radius curve, $1.4 \times 10^{-3}\, m$ for 1250 m radius and $4.87 \times 10^{-4}\, m$, for the 3500 m radius curve, are reached on curved tracks.

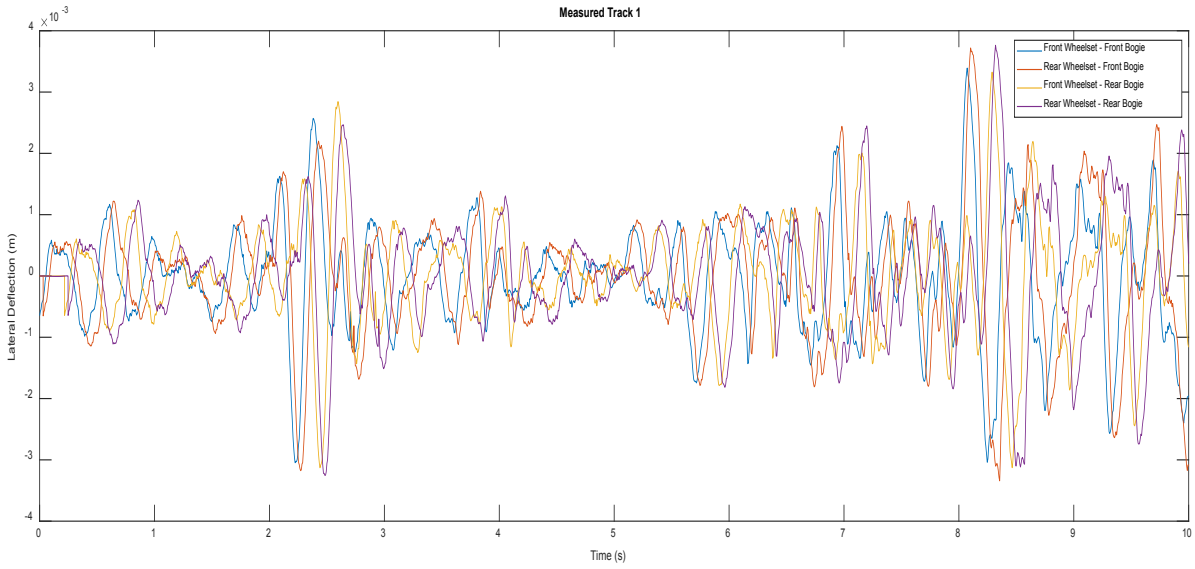

Figure 7. 43 – Wheelset Deflection – Measured Track 1 (FBV)

Figure 7.43 shows that wheelset deflection only reaches maximum of approximately 4 mm and it is clear the flanges are not contacted.

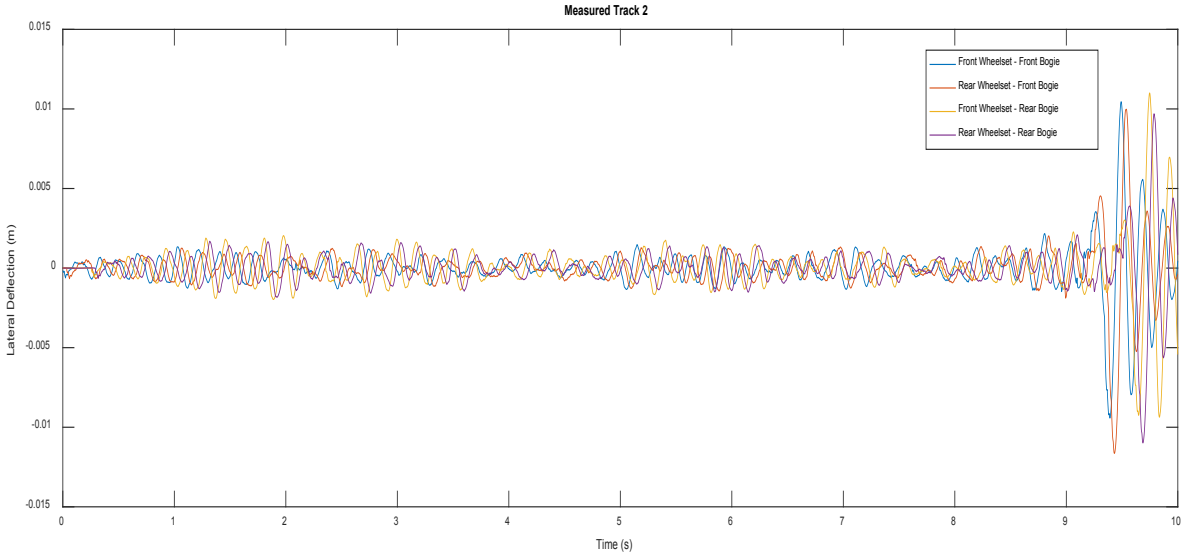

Figure 7. 44 – Wheelset Deflection – Measured Track 2 (FBV)

Similarly, Figure 7.44 shows even with the roughest part of the track (between 9th to 10th seconds), maximum wheelset deflection reaches approximately only up to 10 mm.

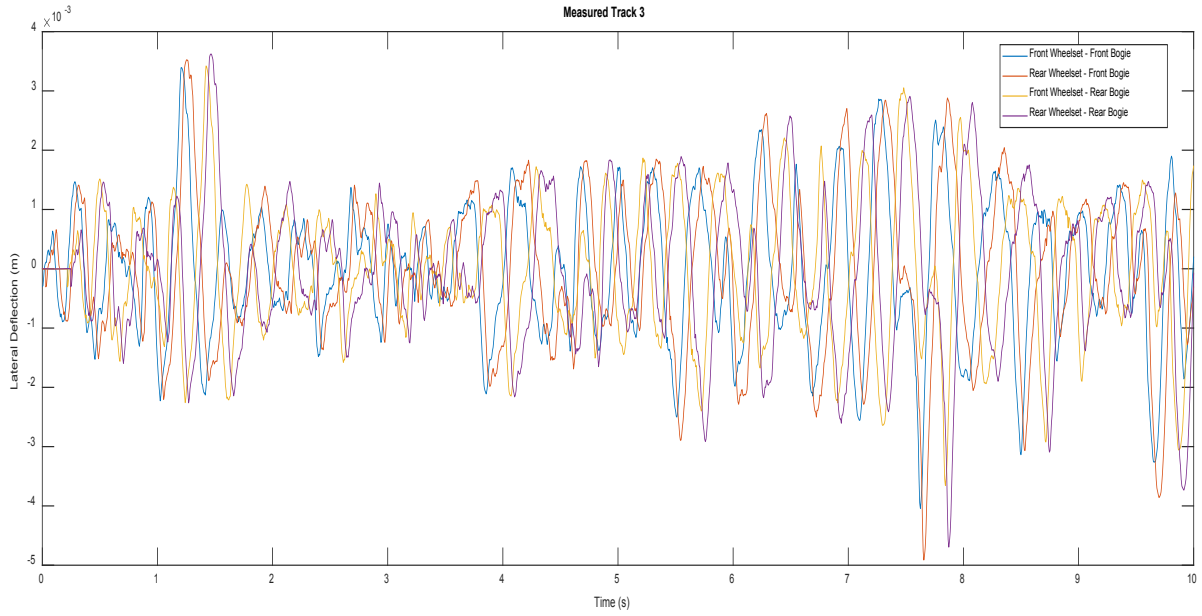

Figure 7. 45 – Wheelset Deflection – Measured Track 3 (FBV)

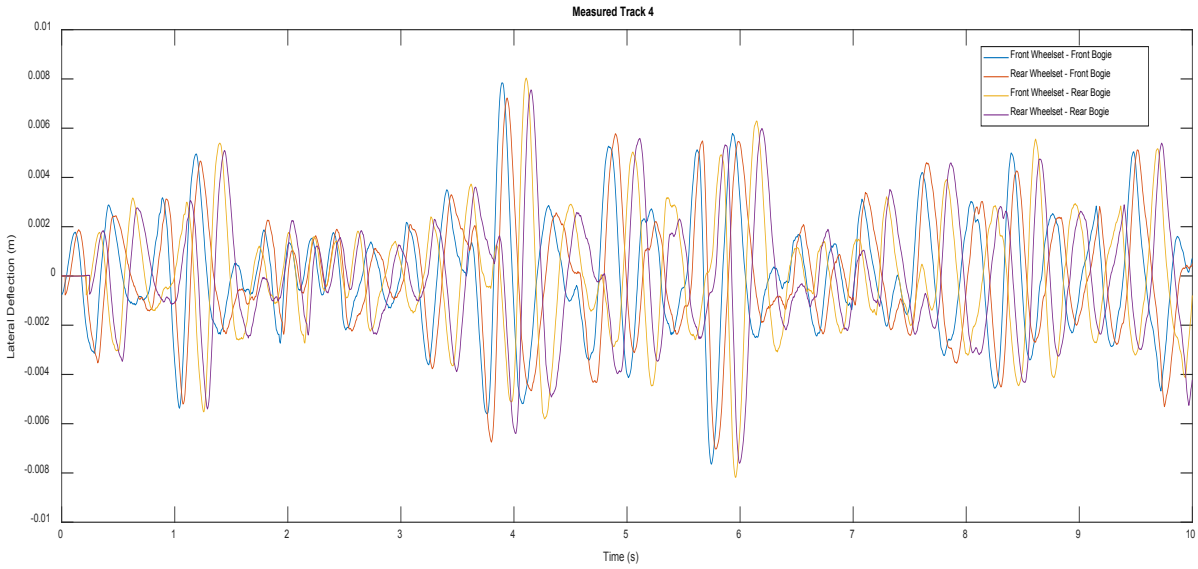

Figure 7. 46 – Wheelset Deflection – Measured Track 4 (FBV)

Figure 7.45 and Figure 7.46 shows that wheelsets are maintain lateral deflections less than 10 mm limit with measured track 3 and track 4.

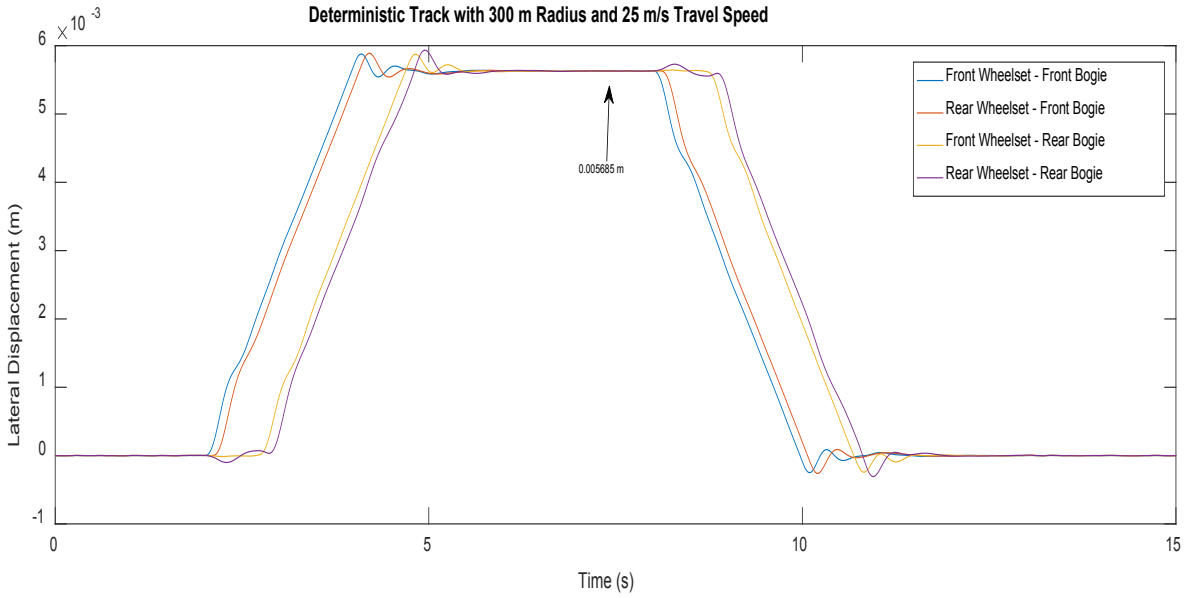

Figure 7. 47 – Wheelset Displacement – Curved Track (300 m / 25 ms^{-1}) (FBV)

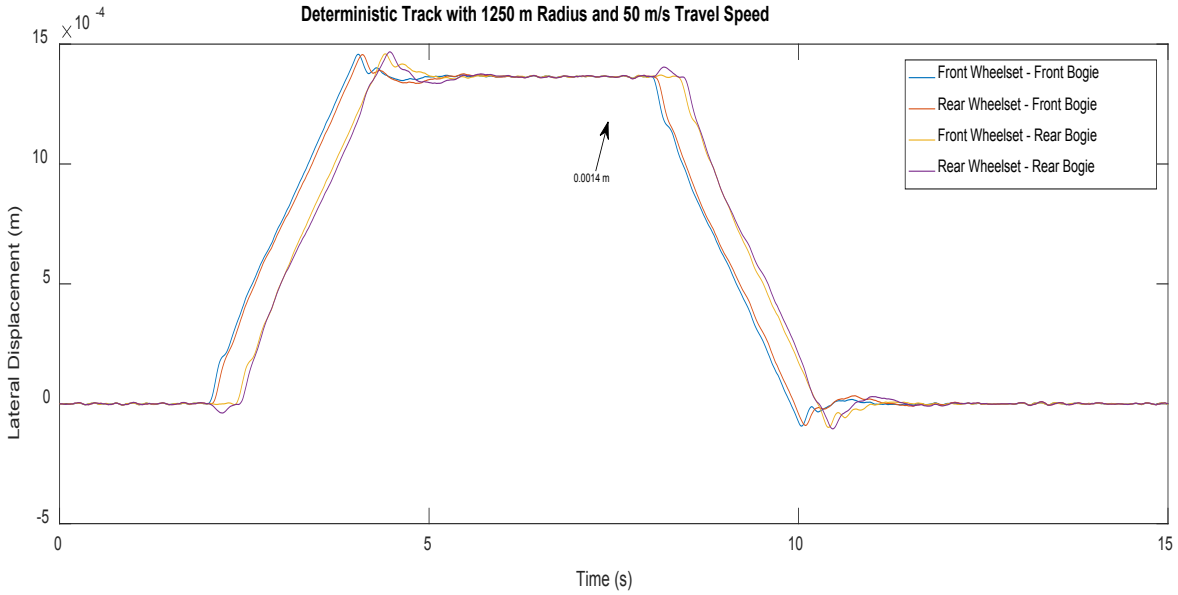

Figure 7. 48 – Wheelset Displacement – Curved Track (1250 m / 50 ms^{-1}) (FBV)

Similar to the behaviour seen with the two–axle vehicle, Figure 7.47 to Figure 7.48 indicates that active wheelset control system is stabilising the wheelsets effectively while allowing natural movements for the wheelsets such that optimal lateral displacement is achieved with the 300 m radius curve.

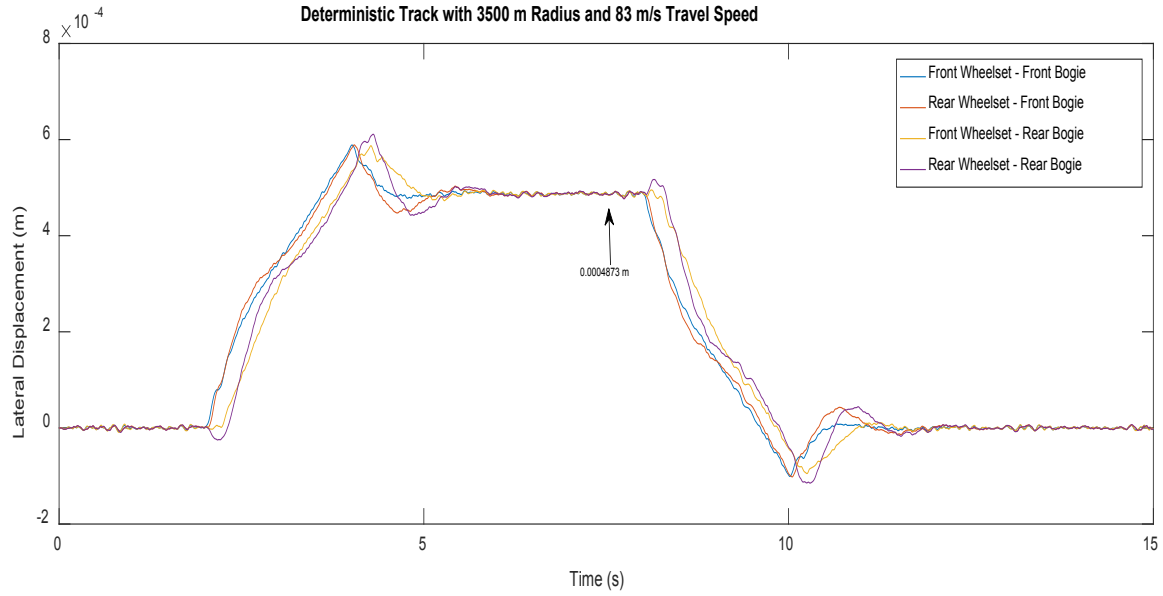

Figure 7. 49 – Wheelset Displacement – Curved Track (3500 m / 83 ms^{-1}) (FBV)

Furthermore, Figure 7.49 shows that for 3500 m radius curve with high travel speed, active controller is allowing the wheelsets to reach the optimal lateral displacement, which will reduce/eliminate longitudinal creep forces.

Yaw Angles

Wheelset yaw angles are also assessed to further observe insight to the wheelset dynamics and below Figure 7.50 to Figure 7.56 depicts the yaw angles of the front and rear wheelsets when traveling on measured tracks with integrated active wheelset control system.

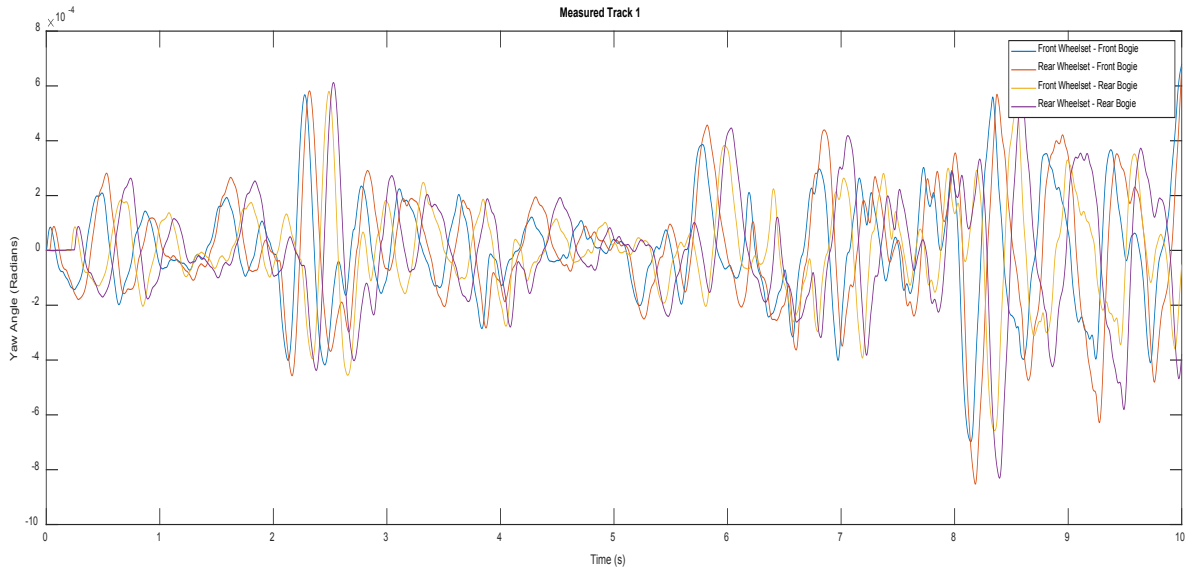

Figure 7. 50 – Wheelset Yaw Angle – Measured Track 1 (FBV)

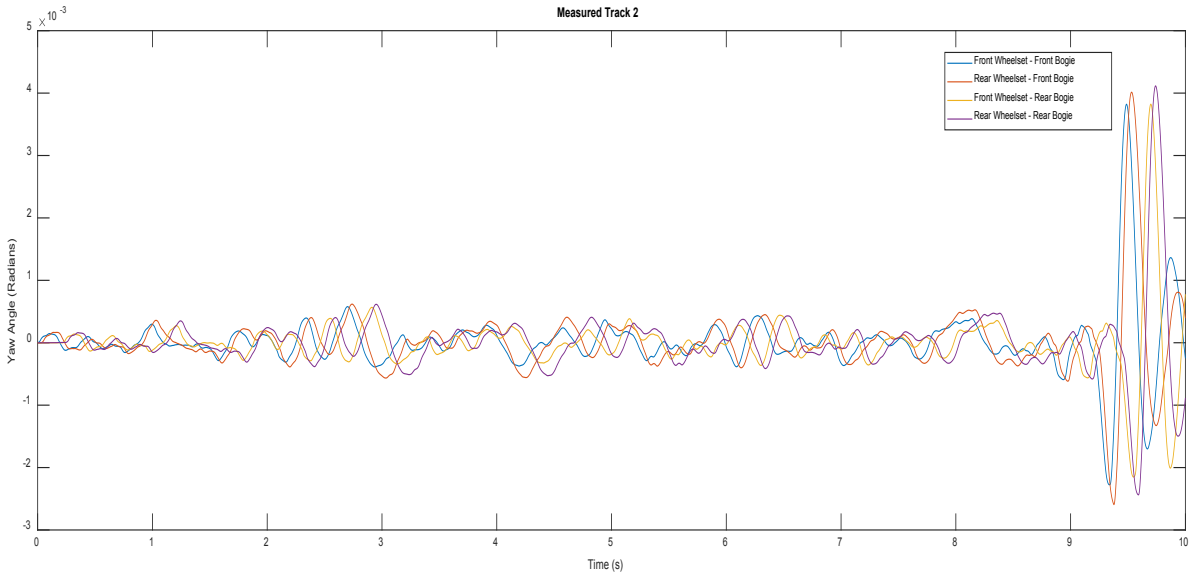

Figure 7. 51 – Wheelset Yaw Angle – Measured Track 2 (FBV)

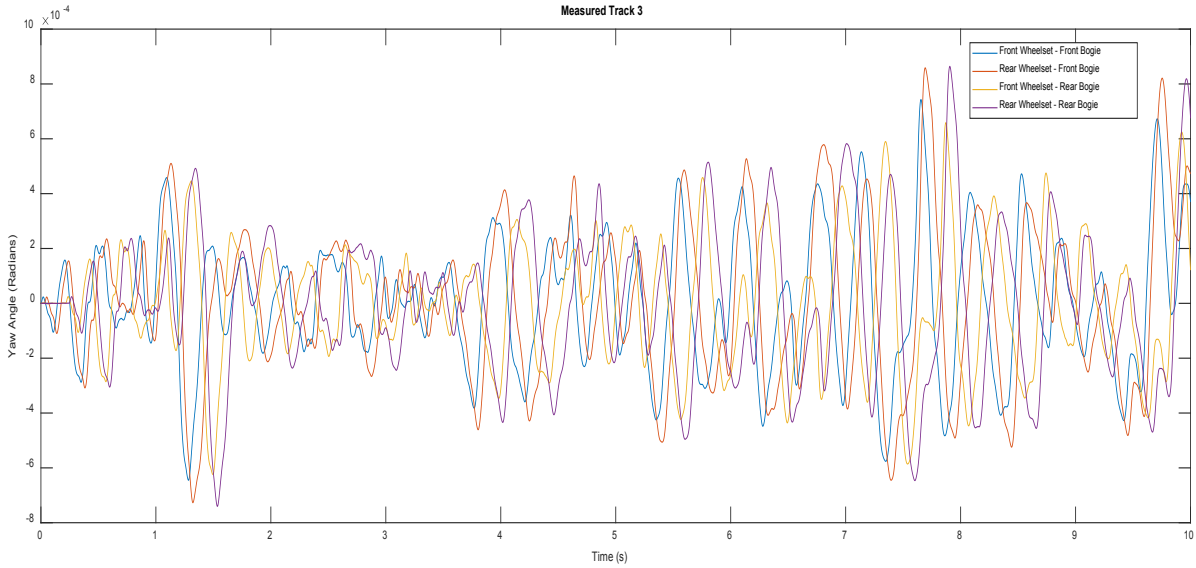

Figure 7. 52 – Wheelset Yaw Angle – Measured Track 3 (FBV)

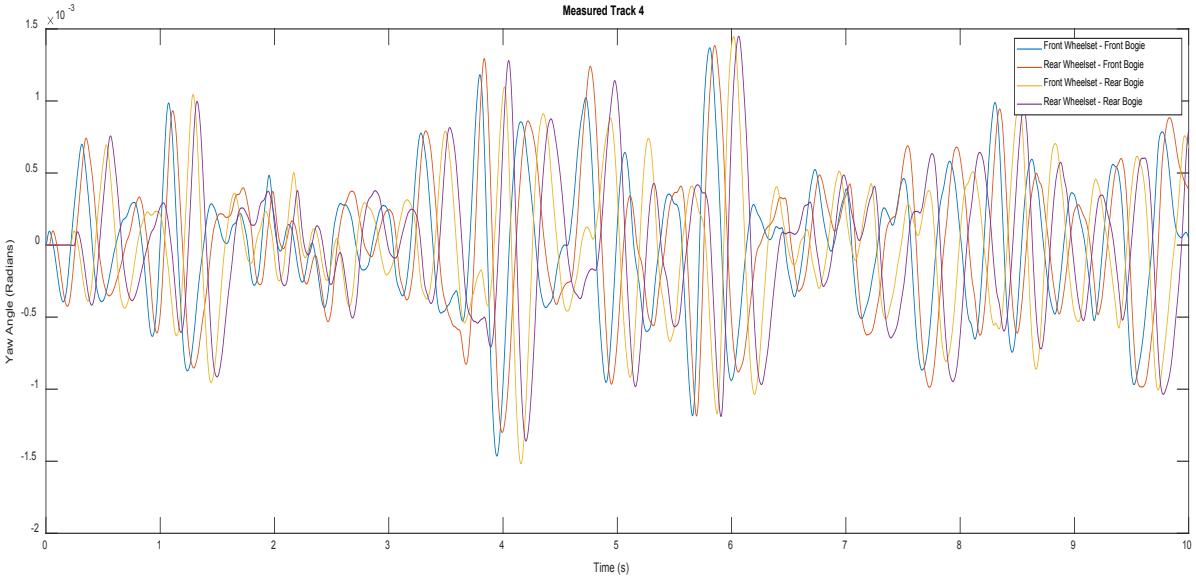

Figure 7. 53 – Wheelset Yaw Angle – Measured Track 4 (FBV)

It can be seen from the results that similarly with the two–axle vehicle, bogie vehicle is maintaining low yaw variations ($<1^0$) with the integrated active wheelset control system. Furthermore, these results indicate the all the four wheelsets are having similar of yaw angle variations. This is an indication of balanced lateral creep forces for all the wheelsets when travelling on measured straight tracks with latera irregularities.

In addition, Figure 7.54 to Figure 7.56 depicts angle of attack of the wheelsets in three curve tracks used in the analysis.

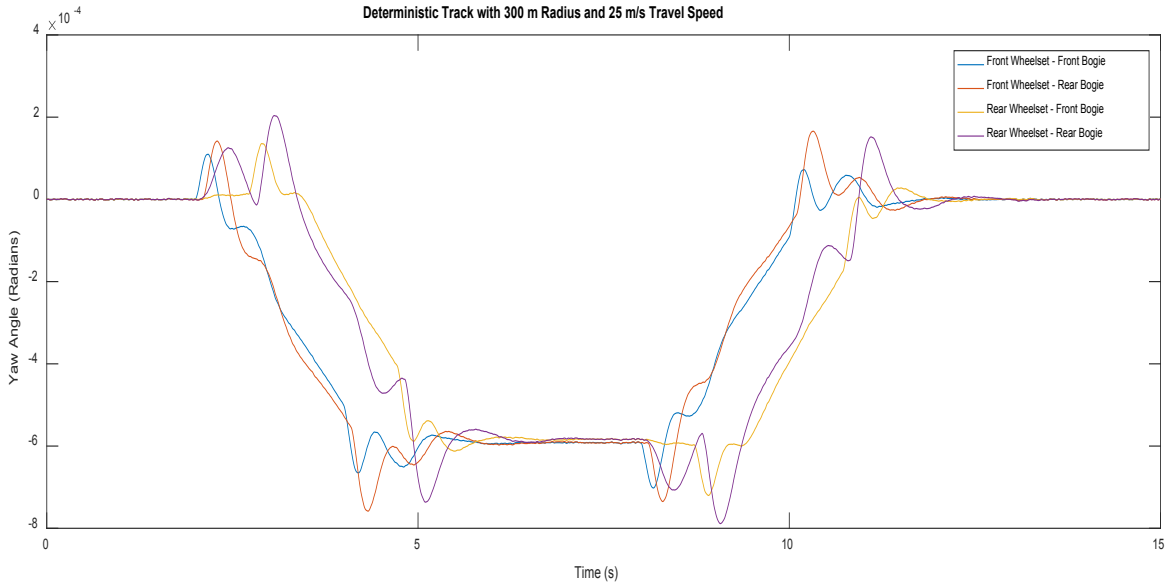

Figure 7. 54 – Wheelset Yaw Angle – Curved Track (300 m / 25 ms–1) (FBV)

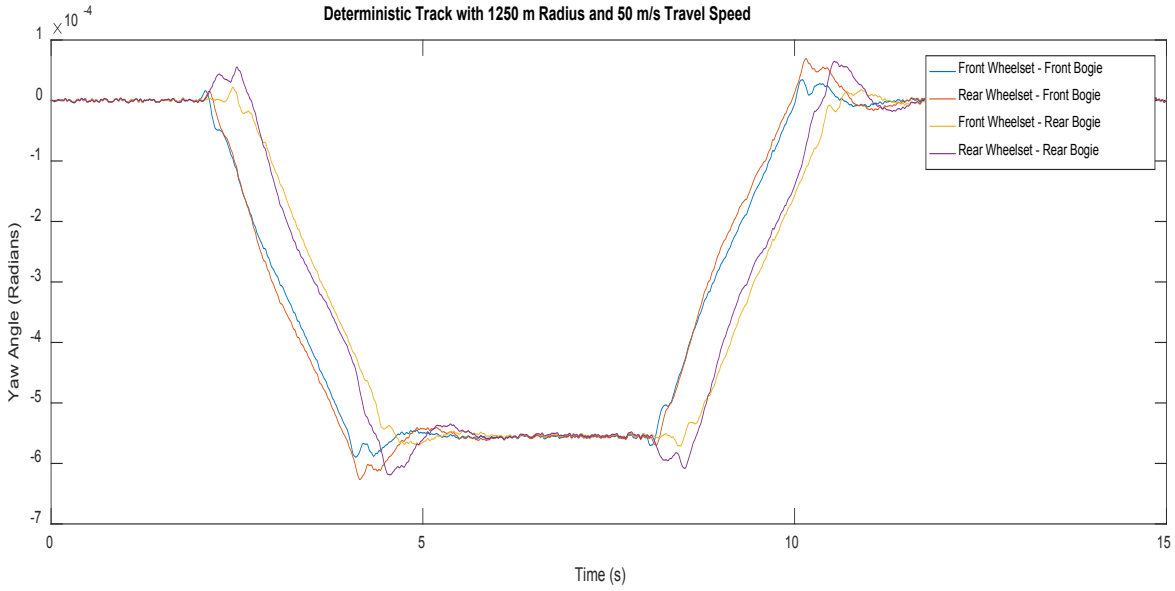

Figure 7. 55 – Wheelset Yaw Angle – Curved Track (1250 m / 50 ms^{-1}) (FBV)

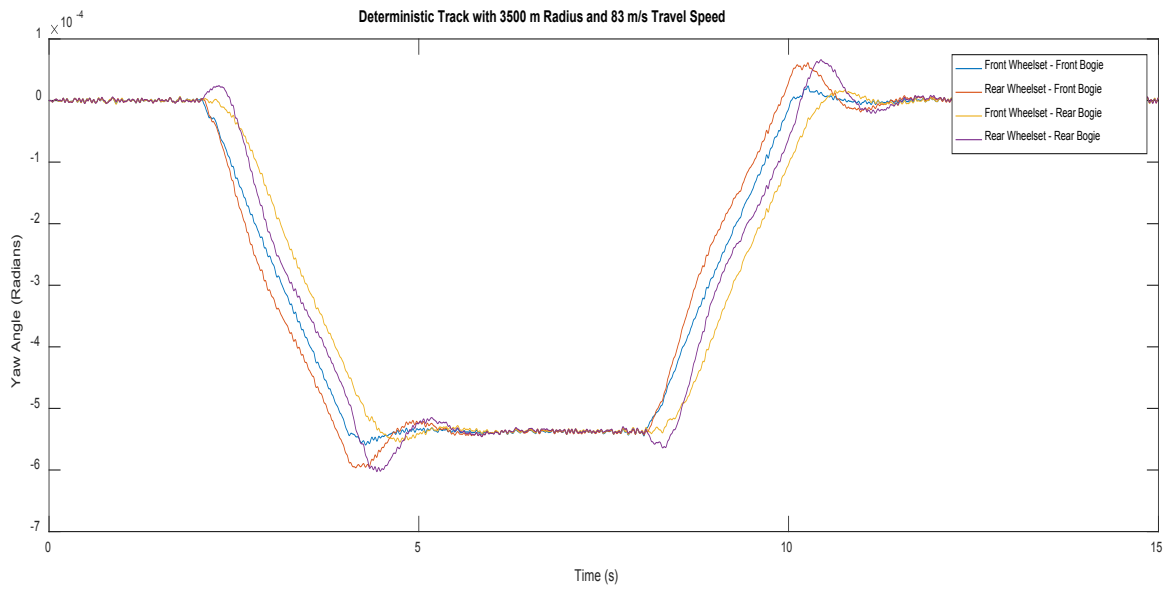

Figure 7. 56 – Wheelset Yaw Angle – Curved Track (3500 m / 83 ms^{-1}) (FBV)

It is evident from the result that as with the two–axle vehicle, wheelsets experience highest angle of attack in the 300 m curve radius with 25 ms^{-1} speed since that situation demands more lateral creep forces to counter the centrifugal forces occurred due to the tight curvature. On the other hand, 1250 m curve radius with 50 ms^{-1} track and 3500 m curve radius with 83 ms^{-1} track has relatively lower angle of attack since centrifugal forces are low in those conditions due to lower curvatures.

However, as with the measured tracks, results indicate that with the active control system developed in this case, it allows to wheelset's natural movements to reach optimal angle of attacks according to the track condition and all the four wheelsets are having almost similar values, which indicate balanced lateral creep forces.

Longitudinal Creep Forces

As a vital indication of the active control performances, longitudinal creep forces are observed with all the track conditions. Figure 7.57 to Figure 7.60 depicts the longitudinal creep forces encountered by the wheelsets with the measured tracks while Figure 7.61 to Figure 7.63 shows results with curved tracks.

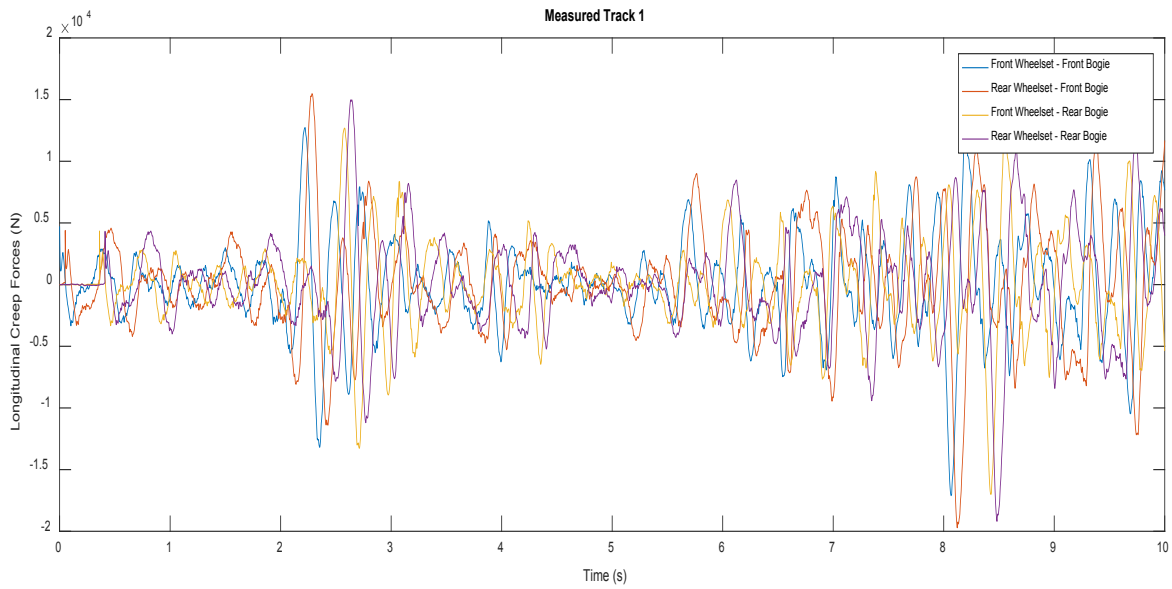

Figure 7. 57 – Longitudinal Creep Forces – Measured Track 1 (FBV)

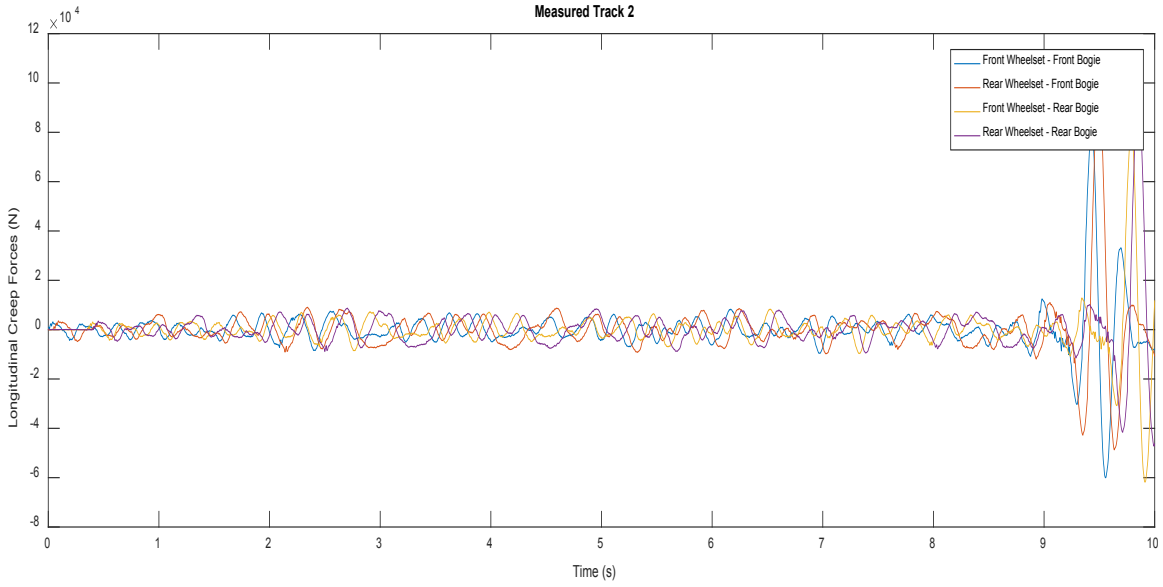

Figure 7. 58 – Longitudinal Creep Forces – Measured Track 2 (FBV)

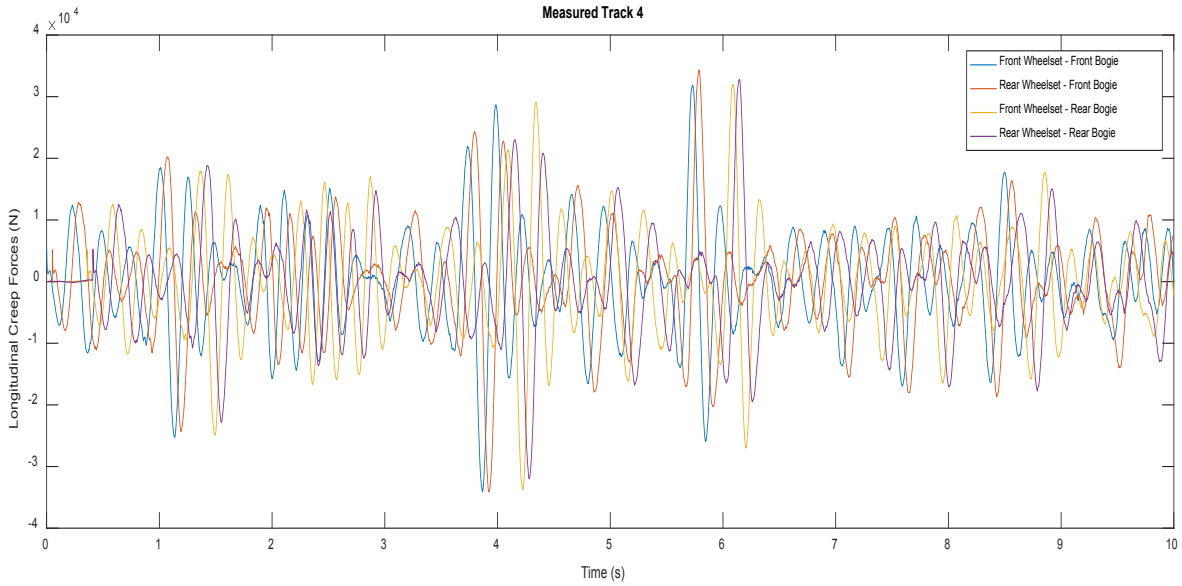

Figure 7. 59 – Longitudinal Creep Forces – Measured Track 3 (FBV)

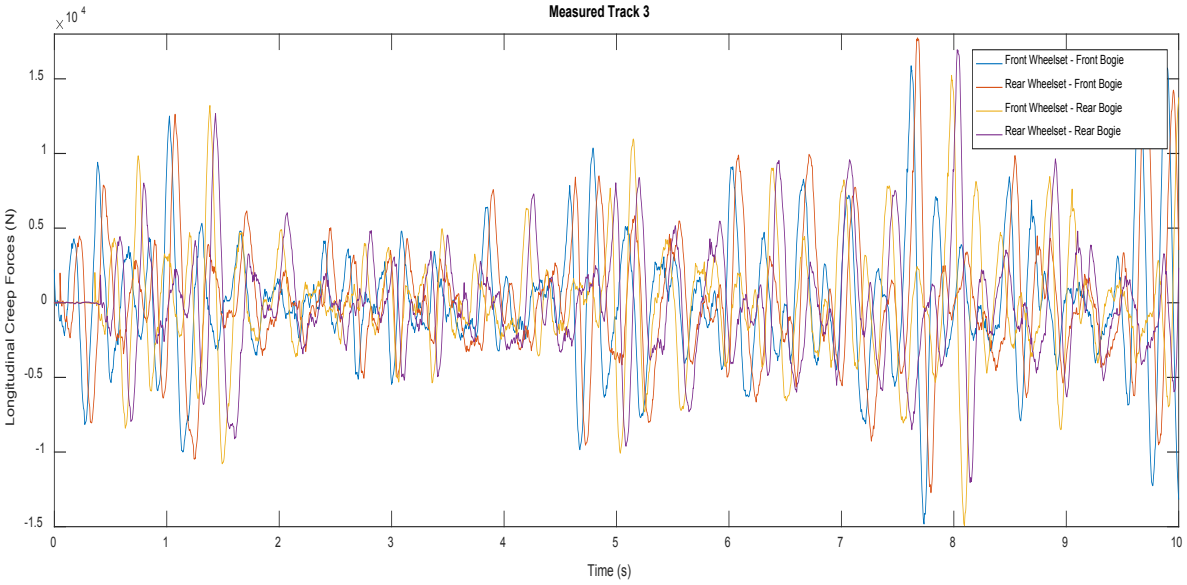

Figure 7. 60 – Longitudinal Creep Forces – Measured Track 4 (FBV)

It can be seen from results that with measured tracks, all four wheelsets are experiencing similar creep forces which can be expected due to the same behaviour observed with lateral displacement of wheelsets.

In addition, as expected/desired Figure 7.61 to Figure 7.63 shows that active control system developed in the study has managed to reduce/eliminate longitudinal creep forces when travelling on curves.

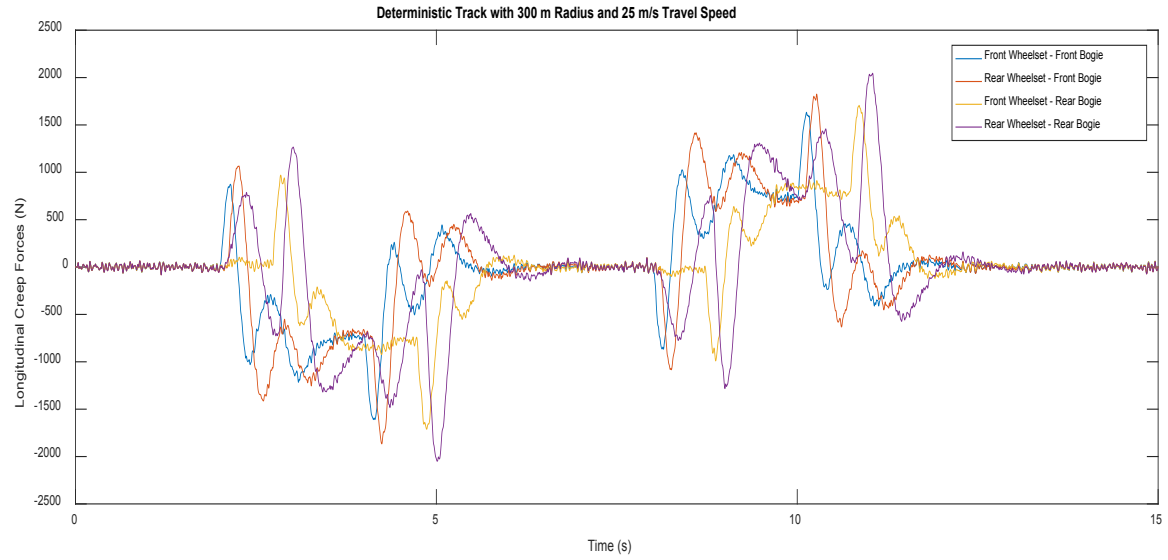

Figure 7. 61 – Longitudinal Creep Forces – Curved Track (300 m / 25 ms^{-1}) (FBV)

Results indicate that although there are minor variations (<10%) of the longitudinal creep forces experienced by wheelsets during the traversing period of the curve, all the forces are reduced/eliminated once the steady curve section has started.

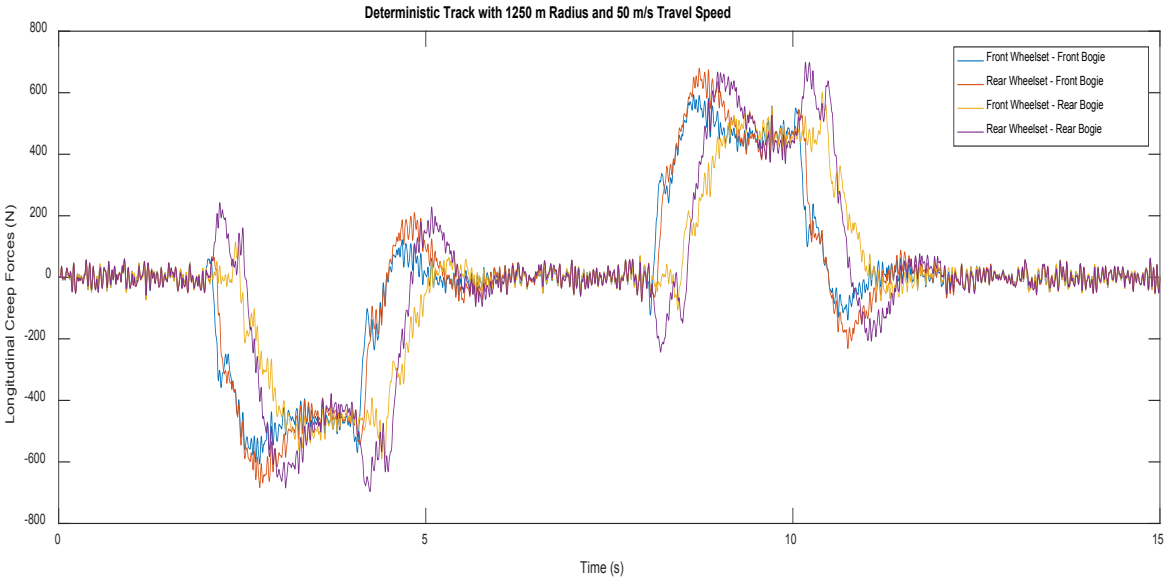

Figure 7. 62 – Longitudinal Creep Forces – Curved Track (1250 m / 50 ms^{-1}) (FBV)

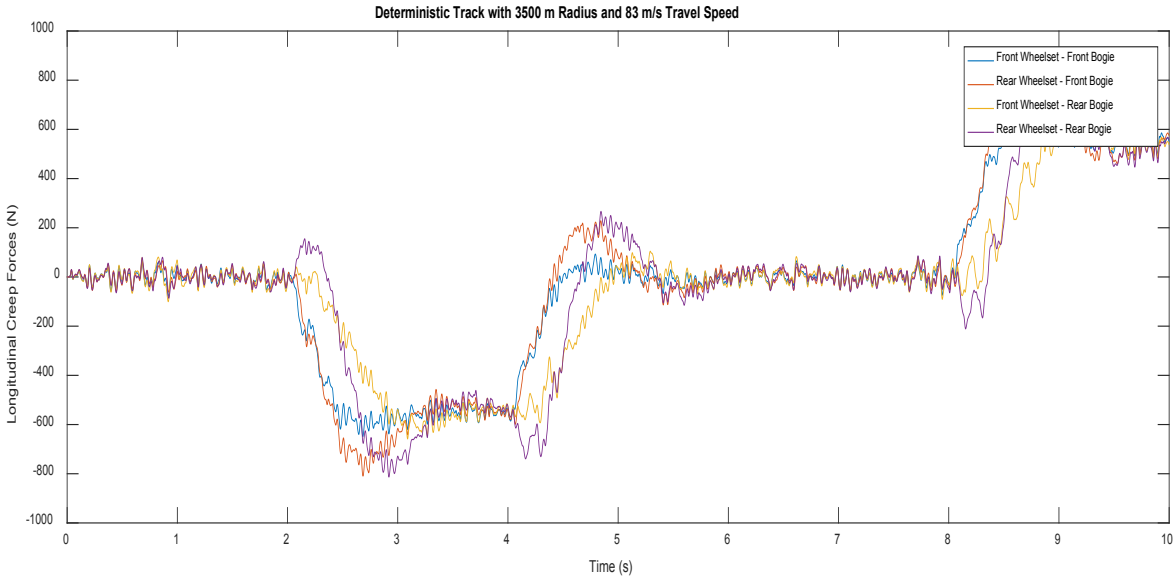

Figure 7. 63 – Longitudinal Creep Forces – Curved Track (3500 m / 83 ms^{-1}) (FBV)

It is evident from the results that curvature radius is a significant factor for the longitudinal creep forces, since lower curvature radius caused the wheelsets longitudinal creep forces to increase.

Lateral Creep Forces

Similar analysis is done with the lateral creep forces since it is essential for the wheelset stability in both measured tracks and curved tracks. Results indicate that active control system is allowing the wheelsets to maintain similar creep forces for all the wheelsets, and it will allow wheelsets to have balanced lateral creep forces in all the four wheelsets.

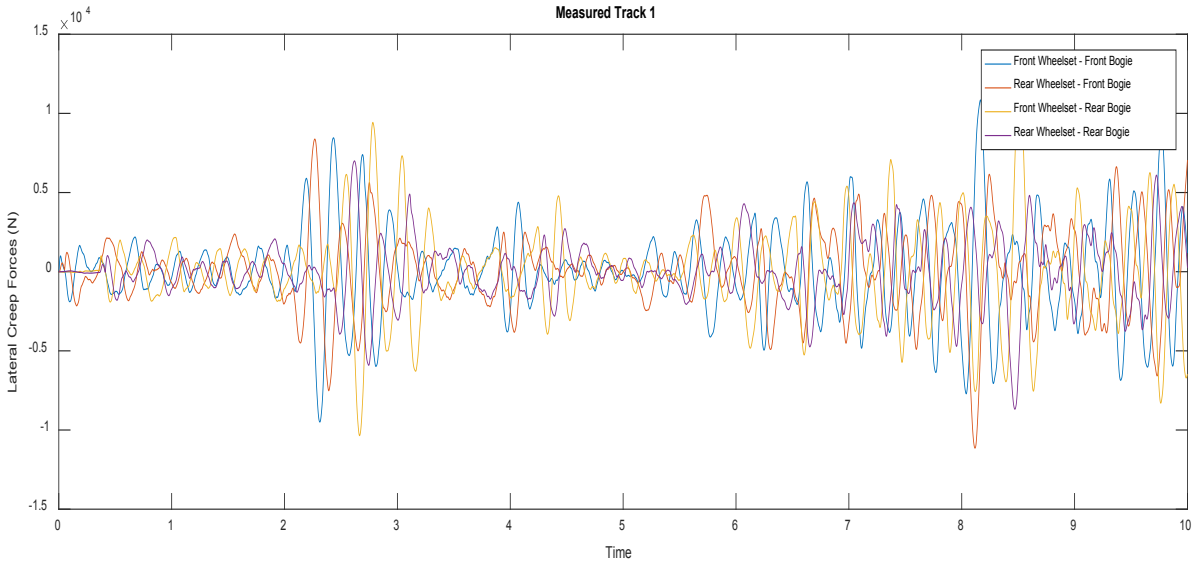

Figure 7. 64 – Lateral Creep Forces – Measured Track 1 (FBV)

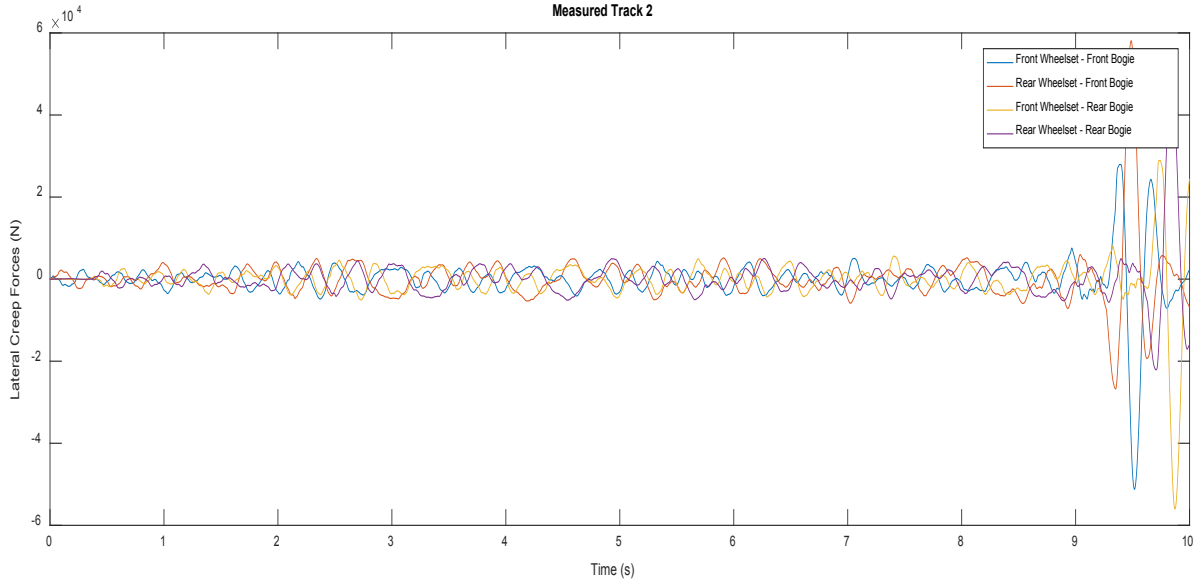

Figure 7. 65 – Lateral Creep Forces – Measured Track 2 (FBV)

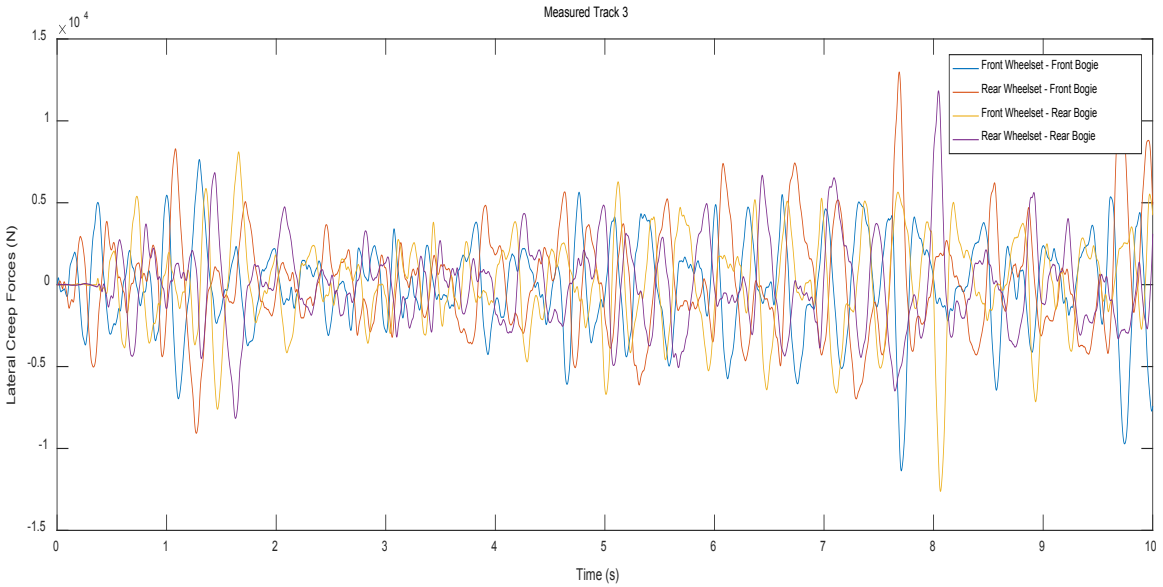

Figure 7. 66 – Lateral Creep Forces – Measured Track 3 (FBV)

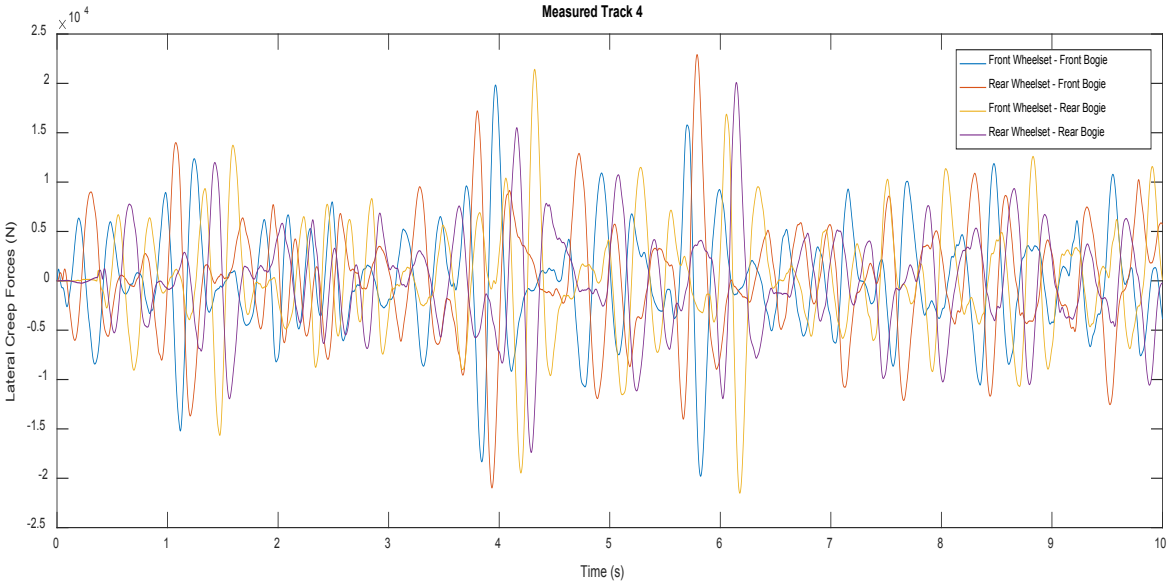

Figure 7. 67 – Lateral Creep Forces – Measured Track 4 (FBV)

Furthermore with the three determinstic tracks, it is evident that wheelsets are at the steady curve senction of the track, wheelsets are experiencing approximatly same lateral creep forces values and this is desirable behavior since it indicates that all wheelsets have natuarally streered themselves to counter the centrigual forces in a balanced way.

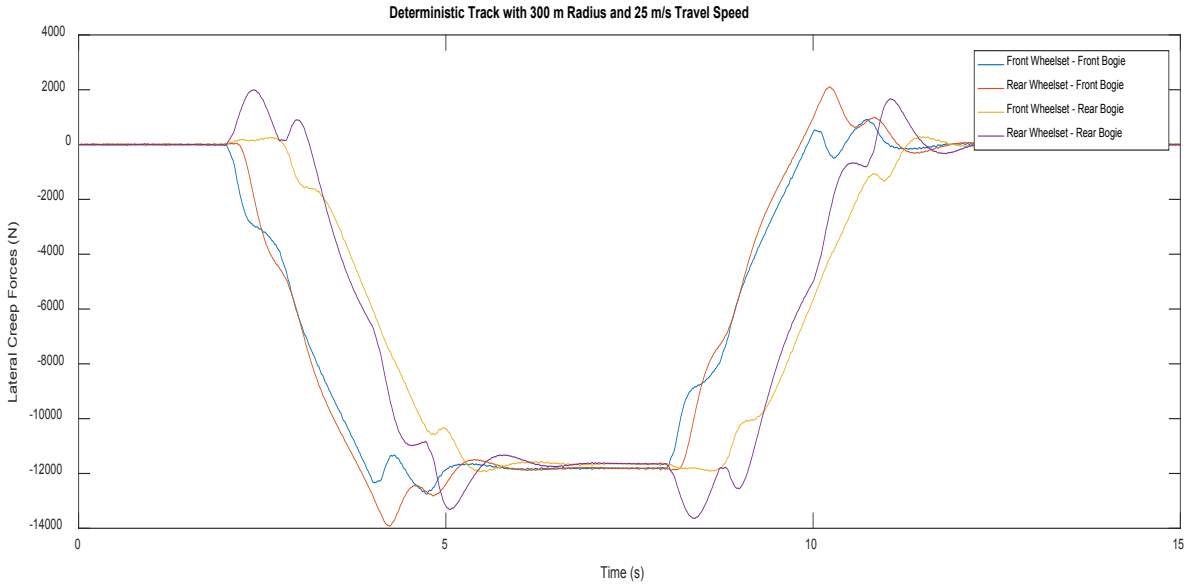

Figure 7. 68 – Lateral Creep Forces – Curved Track (300 m / 25 ms^{-1}) (FBV)

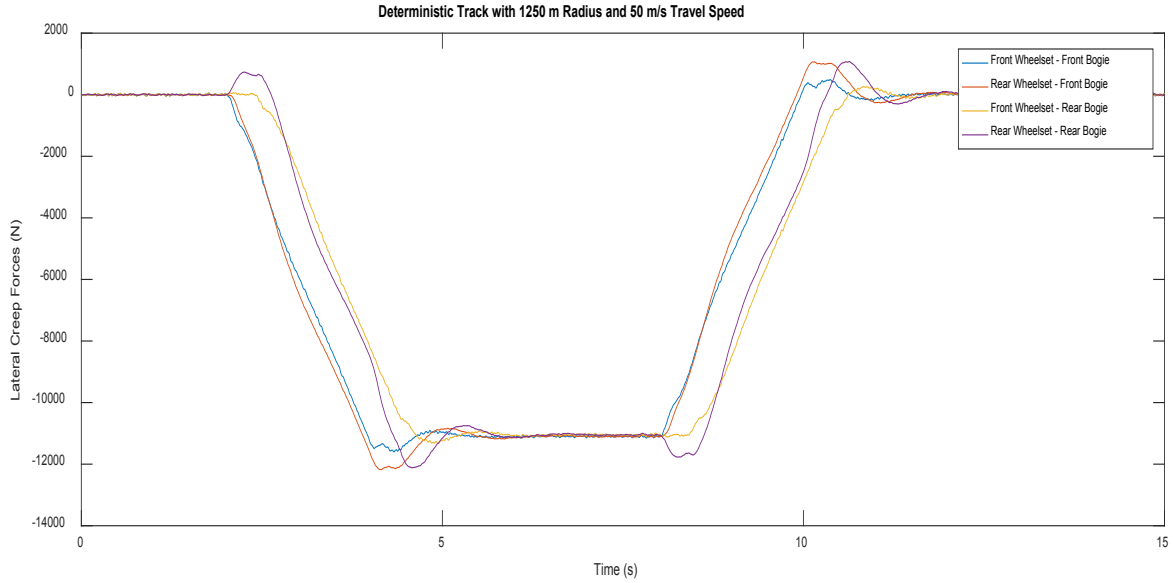

Figure 7. 69 – Lateral Creep Forces – Curved Track (1250 m / 50 ms^{-1}) (FBV)

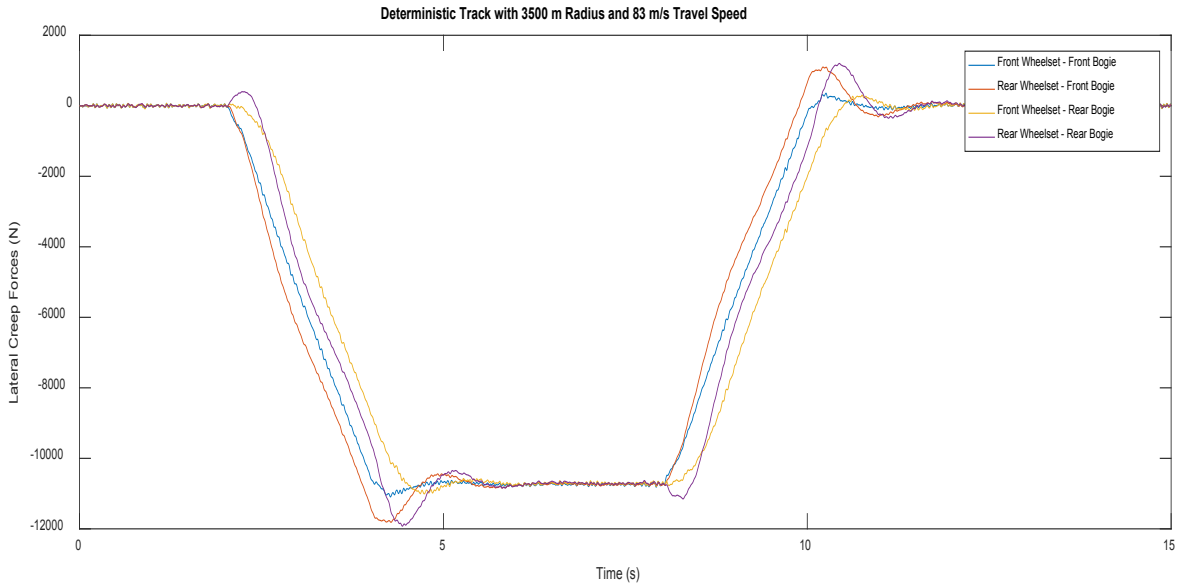

Figure 7. 70 – Lateral Creep Forces – Curved Track (3500 m / 83 ms^{-1}) (FBV)

Furthermore, as expected, higher curvature causes centrifugal forces to increase which subsequently cause lateral creep forces to increase.

Thus it can be stated that state observer based active control system with optimised actuator designed in the study is capable of improving curving performances of the full bogie vehicle while maintaing stability.

CHAPTER 8: CONCLUSION AND FURTHER WORK

8.1. Conclusions

This research has been conducted to study and optimise the performances of an EM actuator for the application of active wheelset control in primary suspension (ASW configuration) of both two–axle and conventional bogie vehicle with solid–axle wheelsets. Absolute yaw stiffness control scheme has been designed and implemented in the study for wheelset stability control while local feedback controllers, with model–based feedback estimators, have been studied to ensure that actuators respond to the demand in an accurate and rapid manner.

The study has evaluated the vehicle dynamics by modelling both the two–axle and conventional bogie vehicle models (linearized) with solid–axle wheelsets in MATLAB Simulink environment, in order to initiate the research by comparing between passive suspension and active control to assess the limitations in passive suspension, such as its restriction to the wheelsets to have natural movements in deterministic/curved tracks. Furthermore, through the comparison, the study investigates the improvements which can be realised by using active wheelset control with absolute yaw stiffness control scheme, which allows the wheelsets to have natural movements while providing stability. Since it is evident from the results and previous publications that active control can improve vehicle dynamics by eliminating/lowering creep forces, the focus of the particular study is on an actuator design, optimisation and control for the active wheelset control scheme.

Through actuator optimisation (for the active wheelset control application), it has been possible to obtain insight into the performances of an electro–mechanical actuator and its control. Optimisation is achieved by varying key actuator parameters such as gear ratio, material stiffness and damping at the connection (at actuator and wheelset), moment of inertial values of the gear wheel and motor rotor, while, observing important aspects of the actuator performances such as motor current, motor voltage, internal power loss and torque applied to the wheelset to identify optimal parameter values. Both two–axle vehicle and full bogie vehicle is being used for the analysis while using a generic straight track with lateral irregularities at high travel speeds.

It is found from the results that some of these parameters have a significant effect on the actuator performance than others and there is a trend to be followed when selecting these parameters. Results indicate that it is the gear ratio and stiffness of the connection (at actuator and wheelset) that has a significant impact on the actuator performances while effect of the damping at the connection and inertias of the gear wheel and motor rotor are minimal to a relatively larger range of values. From the analysis, it can be concluded that when selecting optimal values for the both gear ratio and material

stiffness at the connection (since they pose significant effect on actuator performances), higher (as practically possible) gear ratios for actuator is suitable as it improves actuator performances while material stiffness should be selected to closely resemble a solid connection (high stiffness). It is essential to follow these trends when selecting values for the gear ratio and stiffness at the connection when using an EM actuator for the active wheelset control application with the absolute stiffness approach in order to maintain the actuator performances optimal.

From further analysis of the behaviour of a DC motor, it is found during the gear ratio analysis that motor back–emf can have a significant effect on the performances and when increasing the gear ratio, after a threshold point that motor act as a generator by removing energy from the system to stabilise the wheelsets.

In addition, study focuses on designing a model–based technique (state observer) based on the dynamics of the EM actuator in order to avert difficulties of obtaining accurate/rapid feedback for the actuator controller. Thus, a state observer is being used to generate estimations of the actuator output torque, based on the motor speed and current inputs. Comparisons of the actuator performances with measured and estimated feedback control is done to assess the accuracy of the estimations and results provide evidence for high accuracy levels of the state predications and indicates this model–based technique is suitable for this application of active wheelset control. Further investigations are also done to evaluate the robustness of the state observer and found that it is capable of maintaining the stability within reasonable variation (approximately ± 20%) of defined parameter values such as motor damping, inertial values and motor constant value.

Through the evaluation of the fully integrated system (with optimised actuator parameters and estimated feedback) on both two–axle and full bogie vehicle with both curved and straight tracks with lateral irregularities, it can be seen that the active control system does not obstruct the natural curving of the solid–axle wheelsets as well it can stabilise the wheelsets. Results also indicate that with active control in curved track, longitudinal creep forces of the wheelsets have been significantly lowered/eliminated and subsequently control effort has also been reduced. On the other hand, with the straight track with lateral irregularities, results indicate that active control is effectively maintaining the stability of wheelsets such that flanges are not contacted.

Summary of key findings/contributions of the study:

- The study has revealed that optimisation of the EM actuators for the application of active wheelset control can help to substantially reduce the motor torque and motor power specifications. In addition, study also identifies gear ratio and material stiffness at the actuator–wheelset connection as key influential parameters of EM actuators in this application.

- More specifically, the gear ratio of the actuators has a significant effect to the motor back–emf and low gear ratios results in actuator operating in the motoring mode while high gear ratios results operating in the generating mode. In addition, higher gear ratios are preferable since actuator performances indicate that higher values result in higher effective torque to the load which subsequently reduce the current of the motor and internal power loss. Thus, selecting a gear ratio value high as possible within practical limitations is ideal.

- Similarly, since the material stiffness at the connection of actuator and wheelset plays a significant role when transferring torque between wheelset (load) and actuator, results indicate that it is essential that this stiffness is sufficiently high for efficient torque transfer. Thus, selecting a material stiffness value high as possible within practical limitations is ideal for the actuator–wheelset connection.

- Also, the study has developed a simplified approach for the use of a state observer to address issues of practical sensing for the actuator control and demonstrated that this model–based sensing technique is robust (within reasonable range) and performs adequately for the application.

8.2. Future Work

As future works, further research is needed to fully investigate the effect of gear ratio variation on the motor motoring/generating mode and its effect on the dynamics of the wheelsets. Further robustness evaluations will also be insightful for the developed overall system. Moreover, in order to make the system more realistic, nonlinearities such as realistic wheel and rail profiles can also be taken into account while time delays can be included in the models to represent more realistic actuators.

In addition to absolute stiffness control strategy, other full active classical control strategies such as active yaw/lateral damping as well as model–based active control schemes such as $H\infty$ control and H_2 optimal control (which are explained in the Chapter 2) can be evaluated while actuator dynamics are taken in to consideration such that practical implementations of these wheelset control strategies can be explored. However, model–based optimal controllers have an advantage over classical control strategies since model–based controllers can be developed to be more robust for track parameter changes than classical feedback controllers.

Furthermore, model–based sensing technique developed in this study can be evaluated with other active control strategies where EM actuators are used control the wheelsets.

Moreover, similar studies on actuator optimisation are valuable for the active control configurations for independently rotating wheelsets and active steering since it is field with very high potential to improve the vehicle performances.

When focusing more on sensing, conducting studies to address the issue of obtaining accurate feedback measurements for the controllers in independently rotating wheelsets is also a field with high research potential.

In addition, another major concern with active wheelset control is the safety aspect. Unlike with stiff passive suspension components which maintain the stability of wheelsets, when they are completely replaced with active suspension, wheelset stability is completely based on the sensing and actuation of the active control configuration. Thus, fault tolerant techniques and/or redundant/parallel sensing and actuation methods can be used to improve robustness of the active control which subsequently results in improved safety.

REFERENCES

[1] Goodall, R., 1997. Active railway suspensions: Implementation status and technological trends. *Vehicle System Dynamics*, *28* (2-3), pp.87-117.

[2] Mei, T.X. and Goodall, R.M., 1999. Wheelset control strategies for a two-axle railway vehicle. *Vehicle system dynamics*, 33 (sup1), pp.653-664.

[3] Vagheie, B.G. and Sheikhy, M., 2018. Design of Multivariable Controller PI for Propulsion Control System of a Maglev Train EMS. *Internal Journal Advance Technology*, 9 (209), p.2.

[4] Alfi, S., Bruni, S., Diana, G., Facchinetti, A. and Mazzola, L., 2011. Active control of air spring secondary suspension to improve ride quality and safety against crosswinds. Proceedings of the Institution of Mechanical Engineers, Part F: *Journal of Rail and Rapid Transit*, 225 (1), pp.84-98.

[5] Zolotas, A.C., 2002. Advanced control strategies for tilting trains (Doctoral dissertation, Argyrios C. Zolotas) – *Loughborough University*.

[6] Pratt, I., 1996. Active suspension applied to railway trains (Doctoral dissertation, Ian Pratt) – *Loughborough University*.

[7] Li, H., 2001. Measuring systems for active steering of railway vehicles (Doctoral dissertation, Hong Li) – *Loughborough University*.

[8] Abood, K.H.A. and Khan, R.A., 2011. Hunting phenomenon study of railway conventional truck on tangent tracks due to change in rail wheel geometry. *Journal of Engineering Science and Technology*, 6 (2), pp.146-160.

[9] Dukkipati, R.V., Narayana Swamy, S. and Osman, M.O.M., 1992. Independently rotating wheel systems for railway vehicles-a state of the art review. *Vehicle System Dynamics*, 21 (1), pp.297-330.

[10] Shen, S., Mei, T.X., Goodall, R.M., Pearson, J. and Himmelstein, G., 2003. Active steering of railway vehicles: A feedforward strategy. In 2003 European Control Conference (ECC) (pp. 2390-2395). IEEE.

[11] Iwnicki, S., 2006. Handbook of Railway Vehicle Dynamics. 1st edition, *CRC Press.*

[12] Kim M., Park J, You W, 2008. Construction of active steering control system for the curving performance analysis of the scaled railway vehicle. Proceedings of the 7th conference on *Circuits, systems, electronics, control and signal processing*, 223-227.

[13] Perez, J., Mauer, L. and Busturia, J.M., 2002. Design of active steering systems for bogie-based railway vehicles with independently rotating wheels. *Vehicle System Dynamics*, 37 (sup1), pp.209-220.

[14] Mei, T & Goodall, R 2003, Practical Strategies for Controlling Railway Wheelsets with Independently Rotating Wheels, Transactions of the ASME, *Journal of Dynamic Systems, Measurement and Control*, 125 (3), pp.354-360.

[15] Orvnäs, A., 2011. On active secondary suspension in rail vehicles to improve ride comfort (Doctoral dissertation, Anneli Orvnäs) – *KTH Royal Institute of Technology*.

[16] Kjellqvist, P., 2002. Experimental evaluation of an electromechanical suspension actuator for rail vehicle applications. *International Conference on Power Electronics, Machines and Drives* (Conf. Publ. No. 487) (pp. 165-170). IET.

[17] Persson, R., 2008. Tilting trains: technology, benefits and motion sickness (Doctoral dissertation, Rickard Persson) – *KTH Royal Institute of Technology*.

[18] Zhou, R., Zolotas, A. and Goodall, R., 2011. Integrated tilt with active lateral secondary suspension control for high speed railway vehicles. *Mechatronics*, 21 (6), pp.1108-1122.

[19] Li, H. and Goodall, R.M., 1999. Linear and non-linear skyhook damping control laws for active railway suspensions. *Control Engineering Practice*, 7 (7), pp.843-850.

[20] Foo, E. and Goodall, R.M., 2000. Active suspension control of flexible-bodied railway vehicles using electro-hydraulic and electro-magnetic actuators. *Control Engineering Practice*, 8 (5), pp.507-518.

[21] Goodall, R.M. and Kortüm, W., 1990. Active Suspensions for Railway Vehicles–An Avoidable Luxury or an Inevitable Consequence?. I*FAC Proceedings Volumes*, 23(8), pp.465-471.

[22] Bruni, S., Goodall, R., Mei, T.X. and Tsunashima, H., 2007. Control and monitoring for railway vehicle dynamics. *Vehicle System Dynamics*, 45 (7-8), pp.743-779.

[23] Goodall, R., Pearson, J., Prat, I., 1993. Actuator Technologies for Active Secondary Suspensions, *International Conference on Railway Speed-up Technology* (JSME), vol. 2,377.

[24] Garg, V.K & Dukkipati, R.V., 1984. Dynamics of Railway Vehicle Systems, 1st edition, *Academic Press*.

[25] Goodall, R.M., Bruni, S. and Mei, T.X., 2006. Concepts and prospects for actively controlled railway running gear. *Vehicle System Dynamics*, 44 (sup1), pp.60-70.

[26] Shen, G. and Goodall, R.M., 1997, Active yaw relaxation for improved bogie performance. *Vehicle System Dynamics*, 28, 273 – 289.

[27] Mei, T.X. and Goodall, R.M., 2000. Modal controllers for active steering of railway vehicles with solid axle wheelsets. *Vehicle System Dynamics*, 34 (1), pp.25-41.

[28] Pearson, J.T., Goodall, R.M., Mei, T.X. and Himmelstein, G., 2004. Active stability control strategies for a high speed bogie. *Control Engineering Practice*, 12 (11), pp.1381-1391.

[29] Tanifuji, K., Sato, T. and Goodall, R., 2003. Active steering of a rail vehicle with two-axle bogies based on wheelset motion. *Vehicle System Dynamics*, 39 (4), pp.309-327.

[30] Pearson, J.T., Goodall, R.M., Mei, T.X., Shen, S., Kossmann, C., Polach, O. and Himmelstein, G., 2005. Design and experimental implementation of an active stability system for a high speed bogie. *Vehicle System Dynamics*, 41, pp.43-52.

[31] Perez, J., Stow, J.M. and Iwnicki, S.D., 2006. Application of active steering systems for the reduction of rolling contact fatigue on rails. *Vehicle System Dynamics*, 44 (sup1), pp.730-740.

[32] Mei, T.X. and Lu, J.W., 2004, on the interaction and integration of wheelset control and traction system. *Vehicle System Dynamics*, 41 (suppl), 123–132.

[33] Gonzalez, F., Perez, J., Vinolas, J. and Alonso, A., 2007. Use of active steering in railway bogies to reduce rail corrugation on curves. Proceedings of the Institution of Mechanical Engineers, Part F: *Journal of Rail and Rapid Transit*, 221 (4), pp.509-519.

[34] Goodall, R. and Mei, T.X., 2001, July. Mechatronic strategies for controlling railway wheelsets with independently rotating wheels. In 2001 IEEE/ASME *International Conference on Advanced Intelligent Mechatronics*. Proceedings (Cat. No. 01TH8556) (Vol. 1, pp. 225-230). IEEE.

[35] Mei, T.X. and Goodall, R.M., 2001. Robust control for independently rotating wheelsets on a railway vehicle using practical sensors. *IEEE Transactions on control systems technology*, 9 (4), pp.599-607.

[36] Gretzschel, M. and Bose, L., 1999, A mechatronic approach for active influence on railway vehicle running behaviour. *Vehicle System Dynamics*, 33 (suppl), 418–430.

[37] Gretzschel, M. and Bose, L., 2002. A new concept for integrated guidance and drive of railway running gears. *Control Engineering Practice*, 10 (9), pp.1013-1021.

[38] Perez, J., Busturia, J.M., Mei, T.X. and Vinolas, J., 2004. Combined active steering and traction for mechatronic bogie vehicles with independently rotating wheels. *Annual Reviews in Control*, 28 (2), pp.207-217.

[39] Cheli, F., Corradi, R., Mapelli, F. and Mauri, M., 2002, Motion control of a bogie with independently motorised wheels. Proceedings of the IEEE 10th *International Power Electronics and Motion Control Conference* (EPEPEMC 2002), 132–138.

[40] Mei, T.X., Li, H., Goodall, R.M. and Wickens, A.H., 2002, Dynamics and control assessment of rail vehicles using permanent magnet wheel motors. *Vehicle System Dynamics*, 37 (suppl), 326–337.

[41] Aknin, P., Ayasse, J.B. and Devallez, A., 1991, Active steering of railway wheelsets. Proceedings of the 12th *IAVSD Conference*, 284–300.

[42] Wickens, A.H., 1994, Dynamic Stability of articulated and steered railway vehicles guided by lateral displacement feedback. *Vehicle System Dynamics*, 23 (suppl), 541–553

[43] Michitsuji, Y. and Suda, Y., 2006, Running performance of power-steering railway bogie with independently rotating wheels. *Vehicle System Dynamics*, 44 (suppl), 71–82.

[44] Diana, G., Bruni, S., Cheli, F. and Resta, F., 2002, Active control of the running behaviour of a railway vehicle: stability and curving performances. *Vehicle System Dynamics*, 37 (suppl), 157–170.

[45] Braghin, F., Bruni, S. and Resta, F., 2006, Active yaw damper for the improvement of railway vehicle stability and curving performances: simulations and experimental results. *Vehicle System Dynamics*, 44, 857–869.

[46] Zeng, J, Zhang,W.H., Dai, H.Y.,Wu, X.J. and Shen, Z.Y., 1998, Hunting instability analysis and H∞ controlled stabiliser design for high speed railway passenger car. *Vehicle System Dynamics*, 28 (suppl), 655–668.

[47] Matsumoto, A., Sato,Y., Ohno, H., Mizuma, T., Suda,Y.,Michitsuji,Y., Tanimoto, M.,Miyauchi, E. and Sato,Y., 2004, Research on high curving performance trucks – concept and basic characteristics of active-bogie-steeringtruck. *Vehicle System Dynamics*, 41 (suppl), 33–42.

[48] Lu, J. and Mei, T.X., 2003, September. Modelling and study of a railway wheelset with traction. In 2003 *European Control Conference* (ECC) (pp. 2401-2406). IEEE.

[49] Mei, T.X. and Goodall, R.M., 2003, Recent development in active steering of railway vehicles. *Vehicle System Dynamics*, 39(6), 415–436

[50] Mei, T.X. and Li, H., 2008. Control design for the active stabilization of rail wheelsets. *Journal of Dynamic Systems, Measurement, and Control*, 130 (1), p.011002.

[51] Mei, T.X. and Goodall, R.M., 2006. Stability control of railway bogies using absolute stiffness: sky-hook spring approach. *Vehicle System Dynamics*, 44 (sup1), pp.83-92.

[52] Goodall, R. and Li, H., 2000. Solid axle and independently-rotating railway wheelsets-a control engineering assessment of stability. *Vehicle System Dynamics*, 33 (1), pp.57-67.

[53] Qazizadeh, A. and Stichel, S., 2016. Improved curving performance for two-axle rail vehicles with actuated solid wheelsets using H∞ control. *ASME*, 5205-2412.

[54] Goodall, R.M. and Ward, C.P., 2002. Active control of railway bogies–assessment of control strategies. *Control Engineering Practice*, 1005-1012.

[55] Shen, G. and Goodall, R.M., 1997, Active yaw relaxation for improved bogie performance. *Vehicle System Dynamics*, 28, 273 – 289

[56] Mei, T.X., Shen, S., Goodall, R.M. and Pearson, J.T., 2005. Active steering control for railway bogies based on displacement measurements. *IFAC Proceedings Volumes*, *38* (1), pp.586-591.

[57] Qazizadeh A., Stichel S., and Feyzmahdavian H., 2018, Wheelset curving guidance using H∞ control, *Vehicle System Dynamics*, 56:3, 461-484.

[58] Perez, J., Busturia, J. and Goodall, R.M., 2002, Control strategies for active steering of bogie-based railway vehicles. *Control Engineering Practice*, 10, 1005–1012.

[59] Mousavi Bideleh, S.M., Mei, T.X. and Berbyuk, V., 2016. Robust control and actuator dynamics compensation for railway vehicles. *Vehicle System Dynamics*, 54 (12), pp.1762-1784.

[60] Mirzapour, M., Mei, T.X. and Xuesong, J., 2014. Fault detection and isolation for an active wheelset control system. *Vehicle System Dynamics*, *52* (sup1), pp.157-171.

[61] Selamat, H., Yusof, R. and Goodall, R.M., 2008. Self-tuning control for active steering of a railway vehicle with solid-axle wheelsets. *IET Control Theory & Applications*, 2 (5), pp.374-383.

[62] Lu, Z.G., Sun, X.J. and Yang, J.Q., 2017. Integrated active control of independently rotating wheels on rail vehicles via observers. Proceedings of the Institution of Mechanical Engineers, Part F: *Journal of Rail and Rapid Transit*, 231 (3), pp.295-305.

[63] Gysen, B.L., Paulides, J.J., Janssen, J.L. and Lomonova, E.A., 2009. Active electromagnetic suspension system for improved vehicle dynamics. *IEEE Transactions on Vehicular Technology*, 59(3), pp.1156-1163.

[64] Pollard M. G., 1983, Active Suspensions Enhance Ride Quality, *Railway Gazette International*, pp. 850-853.

[65] Sasaki, K., Kamoshita, S. and Enomoto, M., 1994, September. A design and bench test of multi-modal active suspension of railway vehicle. In Proceedings of IECON'94-20th *Annual Conference of IEEE Industrial Electronics*,Vol. 3, pp. 2011-2016.

[66] Hirata, T., Koizumi, S. and Takahashi, R., 1995. H∞ control of railroad vehicle active suspension. *Automatica*, 31 (1), pp.13-24.

[67] Hedrick J. K. and Wormley D. N., 1975, Active Suspensions for Ground Transport Vehicles - A State of the Art Review, *Mechanics of Transportation Systems*, ASME AMD, Vol. 15, pp. 21-40.

[68] Niksefat, N. and Sepehri, N., 2001. Designing robust force control of hydraulic actuators despite system and environmental uncertainties. *IEEE Control Systems Magazine*, 21 (2), pp.66-77.

[69] Shimamune, R. and Tanifuji, K., 1995, July. Application of oil-hydraulic actuator for active suspension of railway vehicle: experimental study. In SICE'95. Proceedings of the 34th *SICE Annual Conference*. International Session Papers, pp. 1335-1340

[70] Norinao H., 1997, Active and Semi-Active Suspensions Smooth 300 km/h Ride, *Railway Gazett International*, pp. 241-242

[71] Weerasooriya, L. and Mei, T.X., 2017. Active wheelset control—actuator dynamics and power requirements. *In Dynamics of Vehicles on Roads and Tracks* Vol 2 (pp. 735-740). CRC Press.

[72] Pacchioni, A., Goodall, R.M. and Bruni, S., 2010. Active suspension for a two-axle railway vehicle. *Vehicle System Dynamics*, 48 (S1), pp.105-120.

[73] Ji, Y., Ren, L. and Zhou, J., 2018. Boundary conditions of active steering control of independent rotating wheelset based on hub motor and wheel rotating speed difference feedback. *Vehicle System Dynamics*, 56 (12), pp.1883-1898.

[74] Shin, Y.J., You, W.H., Hur, H.M., Park, J.H. and Lee, G.S., 2014. Improvement of ride quality of railway vehicle by semi-active secondary suspension system on roller rig using magnetorheological damper. *Advances in Mechanical Engineering*, *6*, p.298382.

[75] Park, J., Shin, Y., Hur, H. and You, W., 2019. A practical approach to active lateral suspension for railway vehicles. *Measurement and Control,* p.202

[76] Brabie, D., 2002. Simulation of Active Lateral Suspension in Railway Vehicles: Parametric Studies on An Electro Mechanical Actuator. *TRITA-FKT*, 09.

[77] Grimm, J.J., 2009. Electromagnetic linear actuator-design, manufacture and control. Proceedings - 23rd *European Conference on Modelling and Simulation*, ECMS 2009. 708-713.

[78] Goodall R. M., Pearson J. T. and Pratt I., 1993, Actuator Technologies for Secondary Active Suspension on Railway Vehicles, Proceedings of the International Conference on Speedup Technology for Railway and Maglev Vehicles, *Japan Society of Mechanical Engineers*, pp. 377-382

[79] Pollard, M.G. and Simons, N.J.A., 1984. Passenger comfort—the role of active suspensions. Proceedings of the *Institution of Mechanical Engineers*, Part D: Transport Engineering, 198 (3), pp.161-175.

[80] Mei, T.X., Li, H. and Goodall, R.M., 2001. Kalman filters applied to actively controlled railway vehicle suspensions. *Transactions of the Institute of Measurement and Control*, 23 (3), pp.163-181.

[81] Ward, C.P., Goodall, R.M., Dixon, R. and Charles, G.A., 2012. Adhesion estimation at the wheel–rail interface using advanced model-based filtering. *Vehicle System Dynamics*, 50 (12), pp.1797-1816.

[82] Pal, D., 2016. Full order observer controller design for dc motor based on state space approach. *International Journal of science and research* (IJSR), 5 (2), pp.1752-1756.

[83] Pal, D., 2016, Minimum Order Observer Controller Design for DC Motor. Imperial Journal of Interdisciplinary Research (IJIR), 2.

[84] RUSU M. S., and Grama L., 2008, The Design of a DC Motor Speed Controller, *Fascicle of Management and Technology and Engineering*. pp. 1055-1060.

[85] Ren, H., Chen, S., Zhao, Y., Liu, G. and Yang, L., 2016. State observer-based sliding mode control for semi-active hydro-pneumatic suspension. *Vehicle System Dynamics*, 54 (2), pp.168-190.

[86] Lu, Z.G., Sun, X.J. and Yang, J.Q., 2017. Integrated active control of independently rotating wheels on rail vehicles via observers. *Proceedings of the Institution of Mechanical Engineers, Part F: Journal of Rail and Rapid Transit*, *231* (3), pp.295-305.

[87] Carquex, C., Rosenberg, C. and Bhattacharya, K., 2018. State estimation in power distribution systems based on ensemble kalman filtering. *IEEE Transactions on Power Systems*, 33 (6), pp.6600-6610.

[88] Mei, T.X. and Zhou, Y.J., 2013. Systems-on-chip approach for real-time simulation of wheel–rail contact laws. *Vehicle System Dynamics*, 51 (4), pp.542-553.

[89] Khaled E., Schwab A. L., 2009, Review Of Joost Kalker's Wheel-Rail Contact Theories And Their Implementation In Multibody Codes. Proceedings of the ASME 2009 *International Design Engineering Technical Conferences & Computers and Information in Engineering Conference*, 231-242.

[90] Sichani, M.S., Enblom, R. and Berg, M., 2014. Comparison of non-elliptic contact models: Towards fast and accurate modelling of wheel–rail contact. *Wear*, 314 (1-2), pp.111-117.

[91] Zong, L.H., Gong, X.L., Xuan, S.H. and Guo, C.Y., 2013. Semi-active H∞ control of high-speed railway vehicle suspension with magnetorheological dampers. *Vehicle System Dynamics*, *51*(5), pp.600-626.

[92] Farhat, N., Ward, C.P., Dixon, R. and Goodall, R.M., 2018. Benefits of mechatronically guided vehicles on railway track switches. *Proceedings of the Institution of Mechanical Engineers*, Part F: Journal of Rail and Rapid Transit, p.095

[93] Wang, P., Mei, T.X. and Zhang, J., 2014, July. Towards self-powered lateral active suspension for railway vehicles. In 2014 *UKACC International Conference on Control* (CONTROL) (pp. 567-572). IEEE.

[94] Zhou, Y.J., 2013. Systems-on-chip approach for real-time simulation of wheel–rail contact laws (Doctoral dissertation, Jin Zhou) – *University of Salford*.

[95] Hammood, H.F., 2018. Improvement of semi-active control suspensions based on gain-scheduling control (Doctoral dissertation, Hassam Hammood) – *University of Salford*.

[96] Hussain, I & Mei, T X & Ritchings, T., 2013, Estimation of wheel-rail contact conditions and adhesion using the multiple model approach, Vehicle System Dynamics: International Journal of Vehicle Mechanics and Mobility, 51(1), pp.32-53.

[97] Planetary Gearhead Catelog, 2019, SDP/SI - Stock Drive Products/Sterling Instrument (*www.sdp-si.com* accessed April, 2019)

[98] Iman Faridmehr, Mamood Md. Tahi, Tom Lahmer, 2016, Classification System for Semi-Rigid Beam-to-Column Connections, *Latin American Journal of Solids and Structures*, 13.

[99] Wang, W. and Gao, Z., 2003, June. A comparison study of advanced state observer design techniques. In Proceedings of the 2003 *American Control Conference*, 2003. (Vol. 6, pp. 4754-4759). IEEE.

[100] Abdelaziz, T.H., 2015. Pole placement for single-input linear system by proportional-derivative state feedback. *Journal of Dynamic Systems, Measurement, and Control*, 137 (4), p.041015.

[101] A Dictionary of Physics (6 ed.), 2009, *Oxford University Press*.

APPENDIX – A

List of Parameters – Actuator

Actuator Parameters

Symbol	Value	Unit	Definition
I_{motor}	$1.15 \times 10^{-3.2}$	kgm^2	Motor moment of inertia
I_{gear}	3.84×10^{-4}	kgm^2	
l_{arm}	9.04×10^{-4}	H	Motor armature inductance
r_{arm}	0.112	Ω	Motor armature resistance
k_t	0.537	$Nm\ A^{-1}$	Motor torque constant
k_e	0.435	-	Motor back emf constant
c_m	8.4×10^{-3}	$Nms\ rad^{-1}$	Motor-gearbox shaft Damping
n	1: 700	-	Gear Ratio
K_g	1.132×10^7	Nm^{-1}	Stiffness at the Connection
C_g	7540.7	Nsm^{-1}	Damping at the Connection

List of Parameters – Two–Axle Vehicle

Two–Axle Vehicle Model Parameters

Symbol	Value	Unit	Definition
C_s	37000	Nsm^{-1}	Double of Lateral damping per Wheelset
f_{11}	$10x10^6$	N	Longitudinal Creep Coefficients
f_{22}	$10x10^6$	N	Lateral Creep Coefficients
g	9.8	ms^{-2}	Gravity
I_v	558800	kgm^2	Vehicle yaw Inertia
I_w	700	kgm^2	wheelset Yaw Inertia
λ	0.2	-	Wheel Conicity
K_s	511000	Nm^{-1}	Double of Lateral Stiffness per Wheelset
L_v	4.5	m	Half Wheelset Spacing of the Vehicle
L_g	0.7	m	Half Gauge of Wheelset
m_v	30000	kg	Vehicle Mass
m_w	1250	kg	Wheelset Mass
r_0	0.45	m	Wheel Radius
θ_t	6^0	-	Cant angle of the Curved Track
y_t	-	-	Lateral Track Input
k	$6\ x10^6$	Nm^{-1}	Double of Longitudinal Stiffness per Wheelset
v	25, 50, 83	ms^{-1}	Vehicle Forward Speed
$R_1 - R_2$	300, 1500, 3500	m	Curvature Radius of Wheelset 1 and Wheelset 2

List of Parameters – Full Bogie Vehicle

Full Bogie Vehicle Model Parameters

	Symbol	Value	Unit	Definition
Wheelset	m_w	37000	kg	Wheelset Mass
	I_w	$10x10^6$	kgm^2	Wheelset Yaw Inertia
Bogie	m_b	$10x10^6$	kg	Bogie Mass
	I_b	9.8	kgm^2	Bogie Yaw Inertia
Car body	m_c	558800	kg	Vehicle Mass
	I_c	700	kgm^2	Vehicle Yaw Inertia
Primary suspension	K_{px}	$1.5x10^7$	Nm^{-1}	Double of Primary Longitudinal Stiffness
	K_{py}	511000	Nm^{-1}	Double of Primary Lateral Stiffness
	C_{py}	37000	Nsm^{-1}	Double of Primary Lateral Damping
Secondary suspension	K_{sx}	$3.4x10^5$	Nm^{-1}	Double of Secondary Longitudinal Stiffness
	K_{sy}	30000	Nm^{-1}	Double of Secondary Lateral Stiffness
	C_{sx}	1250	Nsm^{-1}	Double of Secondary Longitudinal Damping
	C_{sy}	0.45	Nsm^{-1}	Double of Secondary Lateral Damping
Lengths	a	0.7465	m	Half Gauge of Wheelset
	b	1.25	m	Half of Wheelset Contact Distance
	l	9	m	Half of Bogie Centre Pin Spacing
	r_0	0.45	m	Wheel Radius
Track	θ_t	6^0	-	Cant angle of the Curved Track
	f_{11}	$1.12x10^7$	N	Longitudinal Creep Coefficients
	f_{22}	$9.98x10^6$	N	Lateral Creep Coefficients
	λ	0.2	-	Wheel Conicity
	v	25, 50, 83	ms^{-1}	Vehicle Forward Speed
	$R_1 - R_4$	300, 1500, 3500	m	Curvature Radius of Wheelset 1 to Wheelset 4

APPENDIX – B

Academic Publications

(1) Weerasooriya L., Mei T X., 2016, Active Wheelset Control – Actuator Dynamics and Power Requirements, *First International Conference on Rail Transportation, International Journal of Rail Transportation,* 4:2, 130-133

(2) Weerasooriya L., Mei T X., 2017, Active Wheelset Control – Actuator Dynamics and Power Requirements, *Proceedings of the 25th International Symposium on Dynamics of Vehicles on Roads and Tracks* (IAVSD 2017)

(3) Weerasooriya L., Mei TX, Li H, Luo Y., 2019, Application of State Estimators for Sensing in Active Control of Railway Wheelsets *26th International Symposium on Dynamics of Vehicles on Roads and Tracks* (IAVSD 2019) (submitted)

Active Wheelset Control – Actuator Dynamics and Power Requirements

Lushan Weerasooriya[1] and Prof. T X Mei[1]
[1.] *School of Computing, Science and Engineering, University of Salford,*

Abstract: Active control mechanisms for railway vehicles have proven to provide better performances, improved operation efficiency and reduced track damages. Hence, based on absolute stiffness control [1] method, PD and PI controllers, this paper investigates the requirements of the actuators in implementation of active solid axle wheelset control systems. The research is based on the use of electric-mechanical (EM) actuators and two main issues are focused on. One is the effect of the active controller in stability and performance of the overall train suspension system when actuated. The other is the power and energy requirement of the actuators. Both of which will be affected by vehicle configurations, operational speed and track features such as curvatures and irregularities. During this study, optimum actuator parameters were also assessed.
Keywords: Active Primary Suspension; Actuator Dynamics; Actuator Power Requirements; Absolute Stiffness Control

1 Introduction

Trains have been the most commonly used mass transportation method since 19th century and continues to be even today (ex: metro tube trains). Due to the high usage and passenger's dependability on trains, developments in the aspect of speed and riding comfortability has taken place through the years. As a new trend, active control is being introduced in train suspension systems replacing the passive springs and dampers. Active control mechanisms for railway vehicles have proven to provide better performances, improved operation efficiency and reduced track damages through many of the previous studies. Those studies on the active control concept for primary suspensions for the controlling purposes of railway wheelsets have shown that the emerging steer-by-wire technology can provide a practical solution capable of removing the conflict in the design of railway vehicles using only the passive suspensions [2-5]. Many studies have focused on the development of control strategies that can stabilize the train body while not interfering with the natural curving dynamics of the wheelset [4]. However, more studies have to be done focusing on the development of the implementable active control strategies since their performances needs to be thoroughly analysed before replacing the traditional passive control methods due to the safety factors involved with passengers. There for, Even though, many methods can be introduced in theory, when implementing there occurs various difficulties and design limitations. In this research, actuators used in active control scheme are to be analyzed for their power consumptions and response times.

2 Dynamic Model

A two axle wheelset train body is modeled in this research focused on lateral and yaw movement of the trains. In the model, secondary suspension with a bogie has been omitted and it is taken that train body is coupled with two solid axle wheelsets as illustrated in Figure 1-2.
Only yaw and lateral dynamics of the wheelsets are taken into account in this model since the other dynamics such as vertical, pitch and roll movements will not have any effect in this case.

2.1 Solid Axle - Double Wheelset Model

Figure 1 illustrate the passive suspension springs and dampers while Figure 2 shows the active setup in the model and where the actuator has replaced the passive springs and dampers.

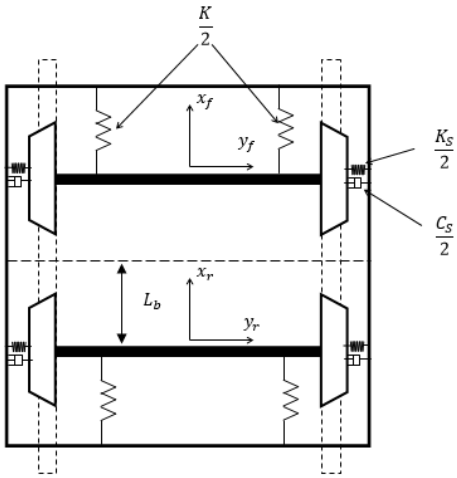

Fig. 1 Passive Primary Control

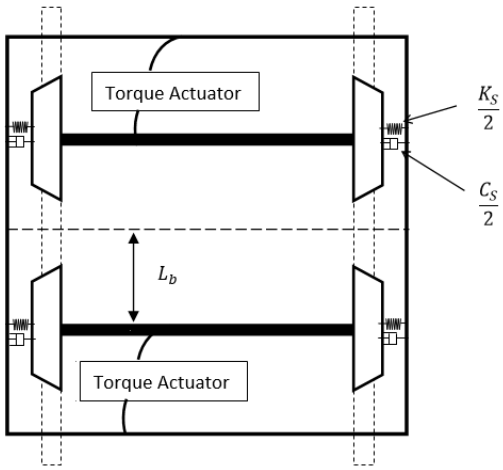

Fig. 2 Active Primary Control

2.2 Torque Actuator Model

Figure 3 depicts the model of the actuator with a AC motor and a gear box. This is to be coupled with the wheelsets to stabilize its movements while improving performances. Sensors to monitor the yaw of the wheelset have to be mounted to the wheelset. Monitored yaw angle of the wheelset is filtered using a high pass filter to differentiate the natural curving movements in the wheelset before being processed to generate the controller signal.

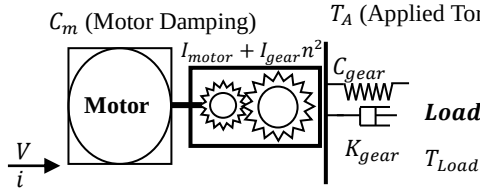

Fig. 3 Actuator Model

Based on the torque requirement to stabilize the wheelset, actuator controller (local controller) is used to generate the actuator's control voltage. Motor in the actuator is driven in accordance to the supplied control voltage.

2.3 Equations of motion for the Model

There are separate equations for the motion of both train model and actuator. 1 –6 Equations are for motion of vehicle model while equations 7 – 10 depicts motion equations for the actuator.

Wheelset 1:

$$m_w\,\ddot{y}_{w1} + \left(\frac{2f_{22}}{V_S} + C_S\right)\dot{y}_{w1} + K_S y_{w1} - 2f_{22}\psi_1 - C_S\dot{y}_v - K_S y_v - C_c L_v\dot{\psi}_v - K_c L_v\psi_v = m_w\left(\frac{{V_S}^2}{R_1} - g\theta_1\right) \quad (1)$$

$$I_w\,\ddot{\psi}_{w1} + \frac{2f_{11}{L_g}^2}{V_S}\dot{\psi}_{w1} + \frac{2f_{11}\lambda L_g}{r_0}y_{w1} = \frac{2f_{11}{L_g}^2}{R_1} + \frac{2f_{11}\lambda L_g}{r_0}y_{t1} + I_w V_S\left(\dot{1/R_1}\right) + T_{w1} \quad (2)$$

Wheelset 2:

$$m_w\,\ddot{y}_{w2} + \left(\frac{2f_{22}}{V_S} + C_S\right)\dot{y}_{w2} + K_S y_{w2} - 2f_{22}\psi_2 - C_S\dot{y}_v - K_S y_v - C_c L_v\dot{\psi}_v - K_c L_v\psi_v = m_w\left(\frac{{V_S}^2}{R_2} - g\theta_2\right) \quad (3)$$

$$I_w\,\ddot{\psi}_{w2} + \frac{2f_{11}{L_g}^2}{V_S}\dot{\psi}_{w2} + \frac{2f_{11}\lambda L_g}{r_0}y_{w2} = \frac{2f_{11}{L_g}^2}{R_1} + \frac{2f_{11}\lambda L_g}{r_0}y_{t2} + I_w V_S\left(\dot{1/R_2}\right) + T_{w2} \quad (4)$$

Train Body:

$$m_v \ddot{y}_v + 2C_S\dot{y}_v + 2K_S y_v - C_S\dot{y}_{w1} - K_S y_{w1} - C_S\dot{y}_{w2} - K_S y_{w2} = \frac{m_w {V_S}^2}{2}\left(\frac{1}{R_1}+\frac{1}{R_2}\right) - \frac{m_w g}{2}(\theta_1 + \theta_2) \quad (5)$$

$$I_v \ddot{\psi}_v + 2{L_v}^2 C_S\dot{y}_v + 2{L_v}^2 K_S y_v - L_v C_S\dot{y}_{w1} + L_v C_S\dot{y}_{w2} - L_v K_S y_{w1} + L_v K_S y_{w2} = \frac{I_v V_S}{2}\left(1/\dot{R}_1 + 1/\dot{R}_2\right) - (T_{w1} + T_{w2}) \quad (6)$$

Torque Actuator:

$$\dot{i_a} = -\frac{r_{arm}}{l_{arm}} i_a - \frac{k_e}{l_{arm}}\dot{\theta_m} + \frac{1}{l_{arm}} v_a \quad (7)$$

$$\left(I_m + I_g n^2\right)\ddot{\theta_m} = k_t i_a - c_m\dot{\theta_m} - nT_A \quad (8)$$

$$\left(I_m + I_g n^2\right)\ddot{\theta_m} = k_t i_a - c_m\dot{\theta_m} - C_g n^2\dot{\theta_m} - K_g n^2\, \theta_m \quad (9)$$

$$Torque\ (T_L) = K_g n\, \theta_m + C_g n\, \dot{\theta_m} - K_g\, \psi_m - C_g\dot{\psi_m} \quad (10)$$

3 Control Methodology

As mentioned earlier, there are two control loops to operate this for the full system. Main control loop for the train model is the PD controller (wheelset controller).

Control Torque / Force = -k ψ (11)

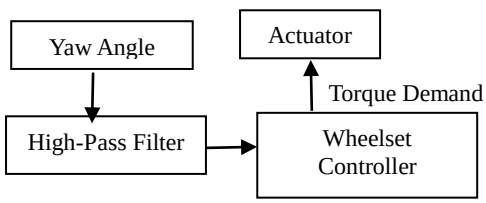

Fig. 4 Absolute Stiffness – Sky Hook

Mechanism for this controller loop is the "Absolute Stiffness – Sky Hook" approach, which is applying yaw stiffness to the wheel set to stabilize the yaw (ψ) as an effective stabilization control of the kinematic mode. Since the yaw angle is used in this case to compute the control force/torque, high pass filter is used attenuate the undesirable frequency components on the yaw angle signal occurred due to natural curving movements in the wheelset. Finalizing on a suitable cut-off frequency for this application is a trade-off.

Other control loop (actuator controller) is the PI controller to operate the actuator.

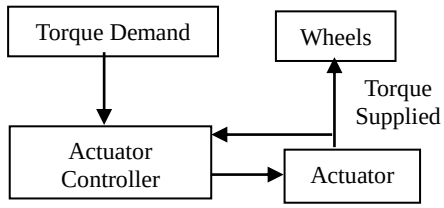

Fig. 5 Actuator Controller

In this control loop, voltage of the motor in the actuator is controlled by the actuator controller (PI) and it enhances the actuator dynamic response as well as power factors.

4. Track Inputs

In order to assess the model, both the curved track and irregularity track inputs were used to excite the model. Curved track was mostly used to test and verify the model while irregularity track was used to test the robustness of the system and to investigate in the actuator dynamics with its parameter changes. While focusing on the actuator performances on the irregularity track, dynamic behavior of the train body was also analyzed to maintain its stability and its response for vibrations.

In the study same track irregularities were used throughout all the actuator parameter changes since the focus is in to actuator dynamics with various parameter value changes while system model and inputs are constant.

5. Actuator Parameter Analysis

Actuator parameters were tuned to get the best energy performances. As the most practical changes to the actuator, gear ratio, Inertia of the gear wheel and inertia of the motor dynamic parts were compared. In order to observe the effect of the each parameter specifically on the actuator performances, only one tests were carried out by changing only one parameter at a time.

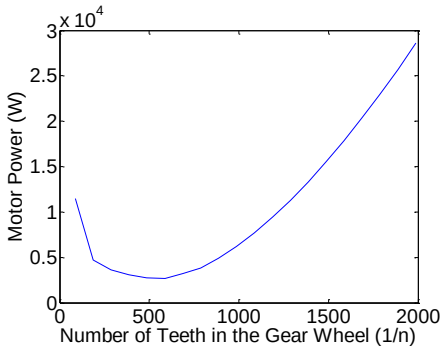

Fig. 7 Motor Power vs Gear Ratio

It can be seen that the gear ratio has significant effect in to the motor power and there is an optimum value range in the relative number of teeth in the gear wheel so that gear ratio reaches 1/500. Since the motor power is directly associated with voltage and current of the motor, lower power results in lower voltage and current consumptions.

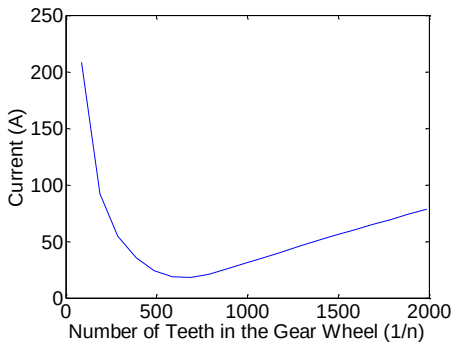

Fig. 8 Motor Current vs Gear Ratio

Motor current is significantly low in the range of optimum gear ratio while it increases as the gear ratio value decreases.

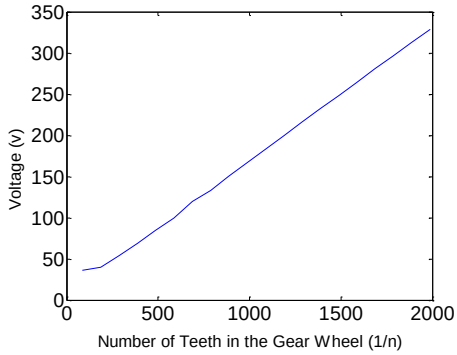

Fig. 9 Motor Voltage vs Gear Ratio

Unlike the motor current, motor voltage is at linear increase when the gear ratio value is decreasing. Increasing trends of current value after the optimum gear ratio range and continues increasing trend of the voltage values the motor results in the trend of the motor power.

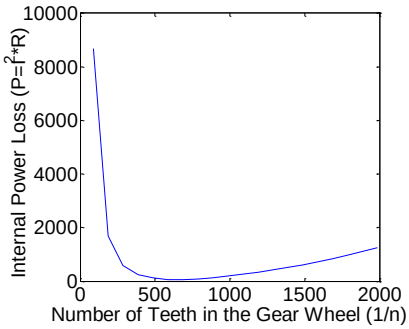

Fig. 10 Internal Power Loss vs Gear Ratio

As it can be seen from the relation between the motor current and the internal power loss, they are having a similar trend with the variation of the gear ratio.

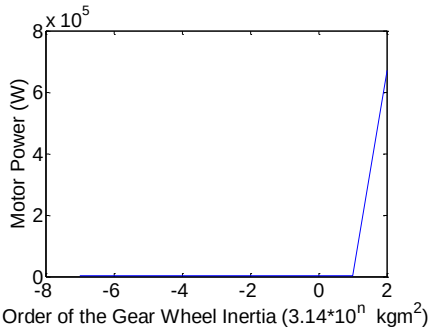

Fig. 11 Motor Power vs Gear Wheel Inertia

In order to assess the system with a larger range of values, power/order of the inertia value of the gear wheel was varied. It can be seen that system is well performing for lower inertial values and tend to provide unrealistic results when the power/order becomes positive. Since the effective inertia of the coupled gear wheel is $I_{gear}\ n^2$, its value is effected by gear ratio (n) value. Since the gear ratio is relatively smaller value (1/500), n^2 gets even smaller. Hence the effect of gear wheel inertia to system is less as long as its power/order kept negative.

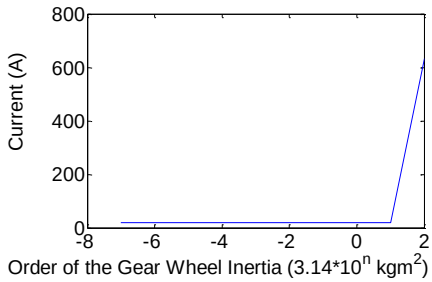

Fig. 12 Motor Current vs Gear Wheel Inertia

Current consumption trend is similar to the power consumption trend as gear wheel inertia is varied.

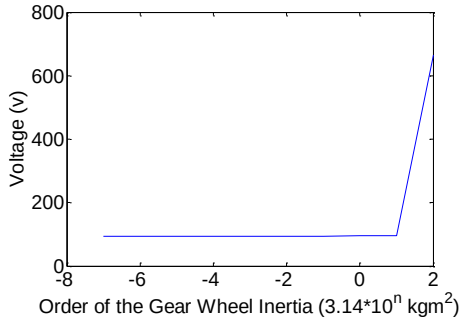

Fig. 13 Motor Voltage vs Gear Wheel Inertia

Voltage consumption trend is similar to the power consumption trend as gear wheel inertia is varied.

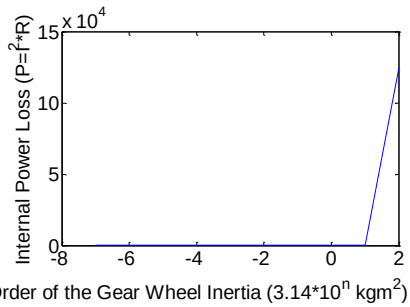

Fig. 14 Internal Power Loss vs Gear Wheel Inertia

Inter power loss is at very low level as the current consumption is low until the power/order of the gear wheel inertia value becomes positive.

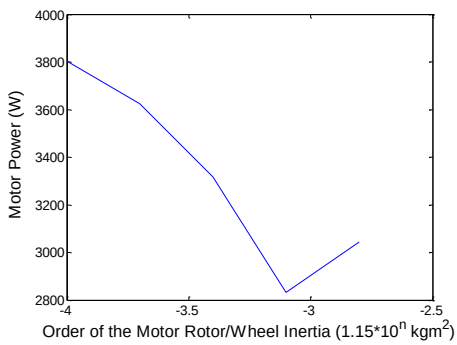

Fig. 15 Motor Power vs Motor Wheel/Rotor Inertia

It was found that unlike the gear wheel inertia, motor wheel/rotor inertia has a significant effect in the system and its value could not be varied much since using a lower or higher order/power for the motor wheel inertia value would make the system becomes unstable. When varied on the limited range of values, optimum order/power value can be seen as -3.2 for the motor wheel/rotor inertia.

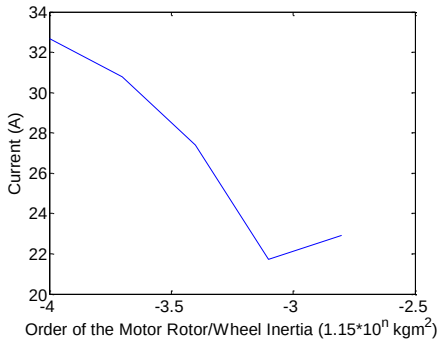

Fig. 16 Motor Current vs Motor Wheel/Rotor Inertia

Similar to the motor power variation, current consumption is at its lowest in optimum order/power range of the motor wheel/rotor value. But the current consumption is reduced only in approximatly1 A.

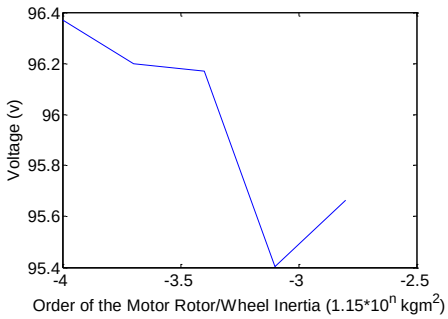

Fig. 17 Motor Voltage vs Motor Wheel/Rotor Inertia

Motor operational voltage has also similarly reduced in approximately 1 v.

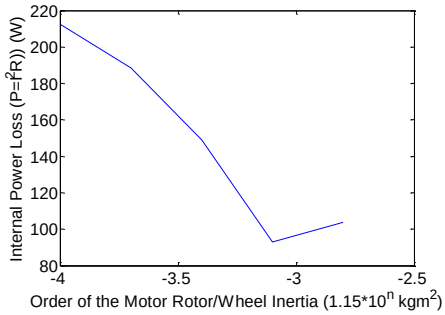

Fig. 18 Motor Current vs Motor Wheel/Rotor Inertia

Internal power loss depicts the same trend as the current consumption trend.

6. Conclusion

This research was conducted to study on the actuator power requirements in a solid – axle active primary control method. From observing all the important aspects (such as current, voltage, internal power loss and power at the wheelset end) of the actuator with respect to parameter changes, it could be concluded optimum parameters were found and this control method can be effectively used for solid-axle active primary controlling.

Absolute Stiffness – Sky Hook control mechanism also have proven to be effective for this active control method.

In addition, a separate study was conducted to identify the best type of actuators for this system and both a Linear Force Actuator to supply the force to a certain point in the wheelset body to control and a Rotational Torque Actuator was also compared. But due to the high energy consumption of Linear Force Actuator, It was concluded that Rotational Torque Actuator has the optimum power ratings and hence it was used in this study.

PD and PI controllers are very effective in this applications and when tuned they provided robust response with very fast response time.

References

1. T. X. MEI and R. M. GOODALL , 2006 , Stability control of railway bogies using absolute stiffness – skyhook spring approach.
2. Aknin, P., Ayasse, J. B., and Devallez, A., *Active Steering of Railway Wheelsets*, 12th IAVSD Conference, Lyon, France, 1991.
3. Anon, 1997, *A Powerful Lightweight Packed With Innovative Ideas - Single-Axle Running Gear*, BahnTech research journal of Deutsche Bahn AG, **3/97**, pp. 4–9, 1997.
4. Bruni, S, Goodall, R.M. Mei, T.X. and Tsunashima H, *Control and Monitoring of railway vehicle dynamics*, Vehicle System Dynamics, Vol 45 - Special Issue (7/8): the state of art, pp743-779, 2007.
5. Mei, T.X. and Li, H. *Controldesign for the active stabilisation of rail wheelsets*, Transactions of the ASME, Journal of Dynamic Systems, Measurement and Control. Vol. 130, Issue 1, 2008

Active Wheelset Control – Actuator Dynamics and Power Requirements

L. Weerasooriya & T. X. Mei
University of Salford, Salford, Lancashire, UK

ABSTRACT: The paper contains details of a research conducted to investigate the applicability and requirements of actuators in the implementation of active solid axle wheelset control and the effect of actuator dynamics on the whole control system. Research is based on the use of electric-mechanical (EM) actuators and it is focused on two main issues, both of which will be affected by vehicle configurations, operational speed and track features such as curvatures and irregularities. One is the effect of the active controller on the stability and performance of the overall train suspension system when actuated. The other is the power and energy requirement of the actuators. Furthermore, optimization of actuator parameters to achieve higher effectiveness is also addressed.

1 INTRODUCTION

Trains can be identified as the most commonly used mass transportation method since 19th century and continues to be so to this date. It has evolved from horse powered to steam engines and ultimately to present day technologies of electrical motor powered and equipped with sophisticated Electro - Mechanical systems to achieve high speeds, higher riding comfort, low ware and tare of equipment and etc. Due to high usage and passenger's dependability on trains, there have been continuous developments in those aspects of railway vehicles and active control is recently studied for suspension systems to replace or supplement the passive springs and dampers. Active control for railway vehicles in has been shown to provide better performances, improved operation efficiency and reduced track damages (for lateral irregularities of the track) through many of the previous studies. The studies on the active control concept for primary suspensions for the control of railway wheelsets have indicated that the steer-by-wire technology can provide a realistic solution capable of removing the conflict in the design of railway vehicles using only the passive suspensions (Aknin, Ayasse and Devallez, 1991; Anon. 1997). Many studies have focused on the development of control strategies that can stabilize the rail vehicles while not interfering with the natural curving dynamics of the wheelset (Bruni, Goodall, Mei and Tsunashima, 2007). Nevertheless, there is a need for more studies in order to address the practicalities in the development of implementable active control systems. In this research, actuators used in active control scheme are to be analyzed for their power consumptions and the dynamic effect on the performance of the overall control systems.

2 DYNAMIC MODELS

2.1 *Main Models*

In order to assess the performance of the actuator thoroughly, there are two models being used. Both the two axle wheelset vehicle and the two bogie full vehicle models are modeled in this research, with a focus on lateral and yaw movement of the vehicle as illustrated in Figures 1-4.

Only the yaw and lateral dynamics of the wheelsets are taken into account in this model since the other dynamics such as vertical, pitch and roll movements are largely dynamically decoupled from the plan view motions and therefore not expected to have any effect in this case.

2.2 *Two Solid Axle Wheelset Model*

This model is the most basic form of a train model. It only consists of a two solid axle wheelsets with the vehicle body. Passive springs of the primary suspension have been replaced by full active actuators as shown in Figure 1. This is used to analyze the dynamics of wheelsets and body for lateral track irregularities (Mei and Goodall, 2000).

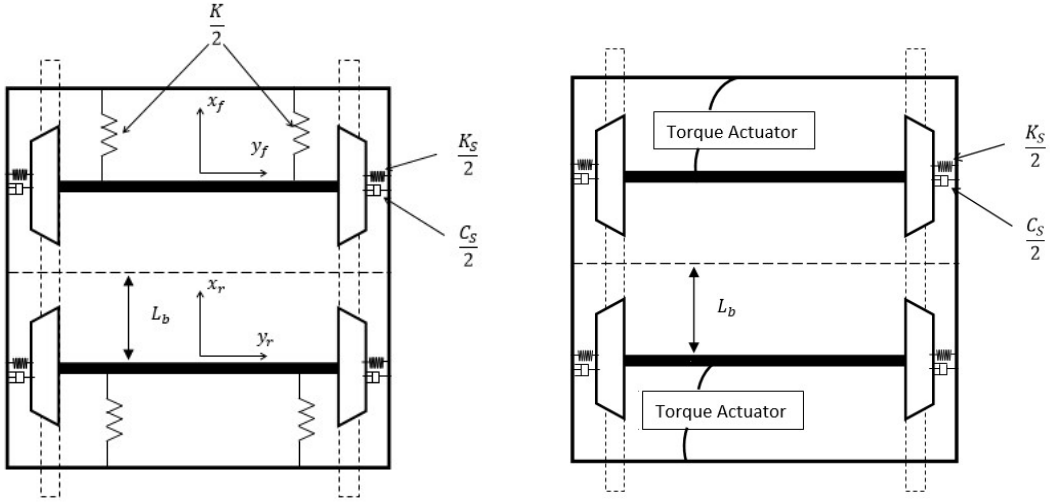

Figure 1. Passive Primary Suspension vs Active Primary Suspension – Two Axle Wheelset Model

2.3 *Two Bogie Model*

Secondary suspensions with bogies are introduced as an addition as shown in figure 2, to the above simple model to improve the performances. In this case the primary suspension is full active while the secondary suspension is passive. Analyzing this model gives more insight in to a more realistic scenario.

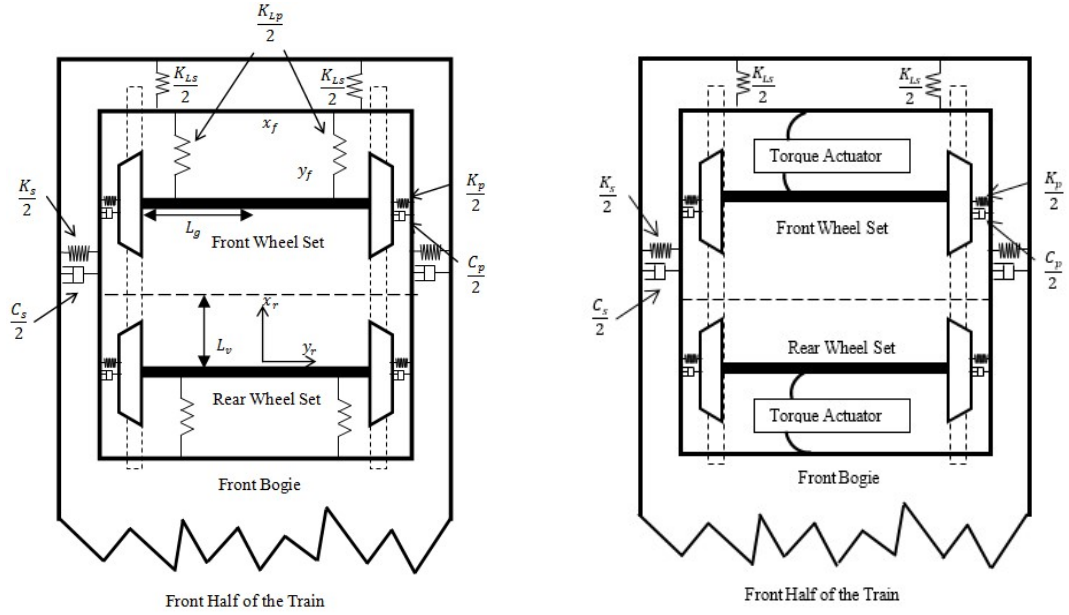

Figure 2. Passive Primary Suspension vs Active Primary Suspension – Two Bogie Full Vehicle Model

2.4 *Torque Actuator Model*

As Figure 3 depicts, the model of the actuator is consisted of a DC electrical motor and a gear box. This is capable of providing the necessary control effort to stabilize the wheelsets whilst maintaining the natural curving actions of the wheelsets. The feedback signals of the wheelset control system are from the sensors which will enable the controller to monitor the yaw motions of the wheelsets. Monitored yaw angle of the wheelset is filtered using a high pass filter to differentiate the natural curving movements in the wheelset before being processed to generate the control signal. Although the implementation of the actuator has not been concluded at this stage, it could be mounted between the wheelset and bogie/body frames in a setup similar to that in Active stability control strategies for a high speed bogie by J.T. Pearson, R.M. Goodall, T.X. Mei, G. Himmelstein, 2004.

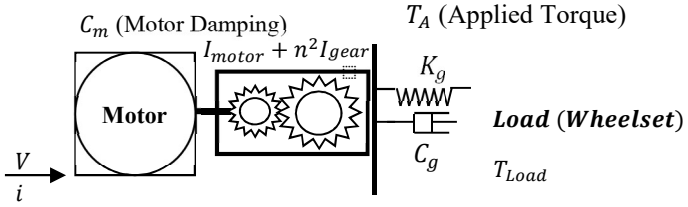

Figure 3. Actuator Model

Based on the torque requirement to stabilize the wheelset, an actuator controller (local PI controller) is used to generate the actuator's control voltage based on the torque feedback. Below equations 1-4 are the actuator operating equations.

Torque Actuator:

$$\dot{i_a} = -\frac{r_{arm}}{l_{arm}} i_a - \frac{k_e}{l_{arm}} \dot{\theta_m} + \frac{1}{l_{arm}} v_a \quad (1)$$

$$\left(I_m + I_g n^2\right) \ddot{\theta_m} = k_t i_a - c_m \dot{\theta_m} - n T_A \quad (2)$$

$$\left(I_m + I_g n^2\right) \ddot{\theta_m} = k_t i_a - c_m \dot{\theta_m} - C_g n^2 \dot{\theta_m} - K_g n^2 \, \theta_m \quad (3)$$

$$Torque\ (T_L) = K_g n \, \theta_m + C_g n \, \dot{\theta_m} - K_g \, \psi_m - C_g \dot{\psi_m} \quad (4)$$

3 CONTROL METHODOLOGY

3.1 *Wheelset Controller*

There are two control loops in this system and despite it's the two wheelset model or two bogie full vehicle model, same principle is applicable for both scenarios.

As mentioned earlier, wheelset controller operates as having a feedback of the yaw angle of the wheelset and this controller generates a torque output. This loop is based on the principle of the "Absolute Stiffness – Sky Hook" approach (MEI and GOODALL, 2006), which is to apply a yaw torque proportional to the yaw motion of the wheelset (ψ) as an effective stabilization control of the kinematic mode. As the yaw angle is being used in this case to compute the control force/torque, a high pass filter is used to attenuate the undesirable frequency components on the yaw angle signal which could occur due to natural curving movements in the wheelset.

$$\text{Control Torque / Force} = -k\,\psi \quad (5)$$

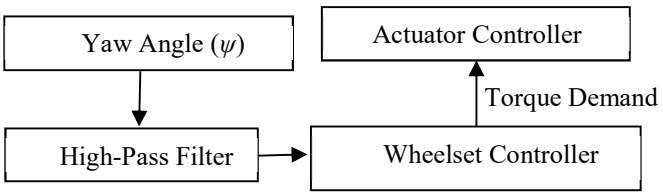

Figure 4. Wheelset Controller

3.2 *Actuator Controller*

Based on the torque demand of the above wheelset controller as well as the feedback of the supplied torque, operation of this actuator control (PI) loop is to control the voltage of the motor in the actuator to enhance the actuator dynamic response as well as power requirements.

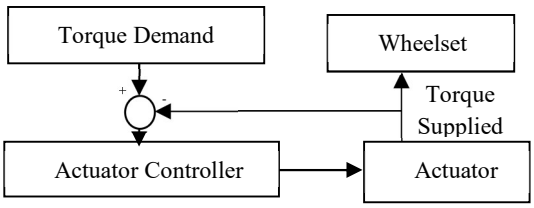

Figure 5. Actuator Controller

This second control loop (the inner loop) to ensure that the actuator will deliver the control effort accurately and timely as required for the outer control loop.

Gains for this local controller are assessed using bode plots and gains were selected to match the output to the input at best possible level for the bandwidth of 0-15 Hz since it was found that the wheelset have a natural frequency about 6-7 Hz.

4 TRACK INPUTS

In order to assess the performance and evaluate the key issues of actuator dynamics, both the curved track and irregularity track inputs were used in the study. The curved track is mainly used to verify the performance gains of the active control in terms of contact force reduction while the irregularity track is used to investigate the actuator dynamics with its parameter changes.

There are five different sets of irregularity track data used in the research. Apart from one computer generated lateral track irregularities, other four sets are from real-time measured data from sensors mounted on wheelsets.

In this case, computer generated track data was used for the tuning of controllers as well as identifying optimum parameter values for the actuator (which is discussed in below topics) and the finalized setup was evaluated with real track irregularity data.

5 ACTUATOR PARAMETER ANALYSIS

Selecting the most suited parameters for the actuator is a cruel importance since it affects its abilities as well as efficiency level. Hence, the key parameters of the electro-mechanical actuator are varied sequentially to observe the power consumption and the dynamic effect on the active control system to achieve optimum energy performances. The changes in the gear ratio, stiffness and dampness of the connection (at actuator and wheelset) the moment inertia of the gear wheel and the inertia of the electrical motor rotor are assessed in detail. Only one parameter is varied at a time in order to observe the effect of each parameter specifically on the actuator performances.

It has to be noted that, this analysis of the actuator parameters were initially done with setup of two axle wheelset on the computer generated irregularity track. When the same analysis was done with the full double bogie model on the computer generated irregularity track, it was found that

both results had similar patterns. Hence the discussions of these results are applicable for both models. These below results also prove an important aspect of on the robustness since it can be seen that the system is maintains its stability despite of the variation of its parameters within a reasonable range.

From the analysis of gear ratio, stiffness and dampness of the connection (at actuator and wheelset), the moment of inertia of the gear wheel and the moment of inertia of the electrical motor rotor, it was found that effect of the dampness of the connection and inertias of the gear wheel and motor rotor are minimal to a relatively larger range of value. It is the gear ratio and stiffness of the connection (at actuator and wheelset) that has a significant impact on the actuator performances.

Table 1. Actuator Performance vs Parameter Variation

Act Torque (kNm)	Current (A)	Volt-age (v)	Motor Power (kW)	Internal Power Loss (W)	Power at Gear (kW)	Power at Wheel-set (kW)	Variation Range	Parameter
24.24	190.25	857.83	200.96	6,643.79	132.52	7.46	1.13×10^3	stiffness of the connec-tion (at ac-tuator and wheelset)
26.34	205.98	930.87	229.04	7,523.24	151.49	8.55	1.13×10^4	
26.34	190.98	892.94	189.92	5,918.03	130.37	7.73	1.13×10^5	
18.20	58.69	273.59	18.74	593.30	19.18	2.14	1.13×10^6	
13.13	68.76	18.08	1.40	872.22	1.20	1.41	1.13×10^7	
13.12	409.89	47.50	31.49	31,107.47	1.09	1.32	1/100	Gear Ratio
12.99	205.61	25.03	8.07	7,816.09	1.12	1.34	1/200	
12.99	137.37	18.66	3.77	3,486.28	1.14	1.36	1/300	
13.03	103.16	16.77	2.32	1,965.00	1.16	1.37	1/400	
13.07	82.56	16.90	1.70	1,257.96	1.18	1.39	1/500	
13.13	68.76	18.08	1.40	872.22	1.20	1.41	1/600	
13.19	58.85	19.85	1.25	638.61	1.22	1.43	1/700	
13.26	51.37	21.97	1.16	486.31	1.24	1.45	1/800	
13.33	45.50	24.34	1.11	381.45	1.26	1.46	1/900	
13.41	40.77	26.87	1.09	306.14	1.28	1.48	1/1000	
13.48	36.87	29.55	1.07	250.21	1.30	1.50	1/1100	

6 PERFORMANCE OF ACTIVE CONTROL METHOD

As mentioned earlier, tests were conducted using both computer generated as well as measured empirical track irregularity data.

Lateral deflection, Lateral acceleration, Yaw acceleration and creep forces are mainly observed in both the models under different track inputs to assess performance of the control system since those factors directly affects the ware and tare of the surfaces as well as riding comfort. Below are the lateral deflections of both two axle wheelset and four axle full bogie models against to one of the four different measured real track data.

Figure 6 show that the full active method is maintaining the stability of wheelsets, bogies and vehicle against the track irregularities as expected. It can be seen that two axle wheelset model maintains lower level of overall deflection than the bogie vehicle model while having higher rate in change of deflection since its lacking any secondary suspension.

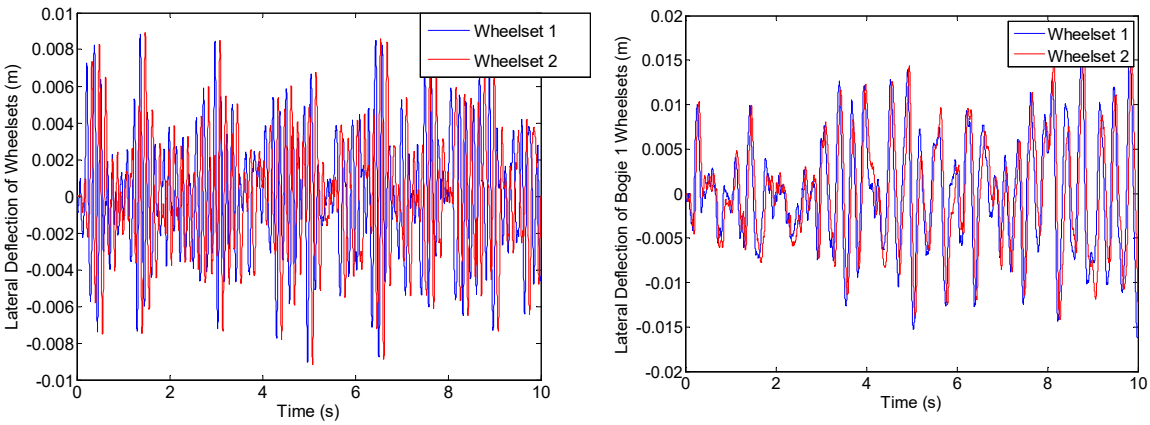

Figure 6. Lateral Deflections of Two Axle Wheelset Model (left) and Two Bogie Full Vehicle Model (right)

7 CONCLUSION

This research has been conducted to study the feasibility of a full active primary suspension system in a two-axle vehicle and for axle full bogie vehicle with the conventional solid axle wheelsets. It was also expected to get an insight of the power requirements as well as performances of the actuator being used.

After the analysis of all the important aspects (such as current, voltage, internal power loss and power at the wheelset end) of the actuator with respect to parameter changes, it could be concluded that the actuator design can have a significant impact on the system performance and power consumption and there appear to be optimal values for some of the key parameters such as the gear ratio, the moment inertia of the electrical motor and damping/stiffness constants of actuator. From the analysis of the Eigen values of the model, it is found that reason for this effect of optimal values occurs due to the internal damping of both wheelset and actuator controllers. It is seen that for some values has an effect on internal damping as well as natural frequency of those controllers.

Further studies will look into more details of the vehicle stability, different vehicle and wheelset configurations with different track inputs as well as the dynamic delays, energy consumptions of the actuators and its bandwidth conditions with variance of same parameters mentioned above including backlash of the gear box.

8 REFERENCES

1. T. X. MEI and R. M. GOODALL, 2006, Stability control of railway bogies using absolute stiffness – skyhook spring approach.
2. Aknin, P., Ayasse, J. B., and Devallez, A., Active Steering of Railway Wheelsets, 12th IAVSD Conference, Lyon, France, 1991.
3. Anon, 1997, A Powerful Lightweight Packed With Innovative Ideas - Single-Axle Running Gear, BahnTech research journal of Deutsche Bahn AG, 3/97, pp. 4–9, 1997.
4. Bruni, S, Goodall, R.M. Mei, T.X. and Tsunashima H, Control and Monitoring of railway vehicle dynamics, Vehicle System Dynamics, Vol 45 - Special Issue (7/8): the state of art, pp743-779, 2007.
5. Mei, T.X. and Li, H. Controldesign for the active stabilisation of rail wheelsets, Transactions of the ASME, Journal of Dynamic Systems, Measurement and Control. Vol. 130, Issue 1, 2008.
6. J.T. Pearson, R.M. Goodall, T.X. Mei, G. Himmelstein , 2004Active stability control strategies for a high speed bogie.

Application of State Estimators in Active Control of Railway Wheelsets

Lushan Weerasooriya[1], T. X Mei[1], Hong Li[2] and Y Luo[3]

[1] University of Salford, Salford M5 4WT, United Kingdom
[2] Manchester Metropolitan University, Manchester M15 6BH, United Kingdom
[3] Tongji University, Shanghai, P R China
L.Weerasooriya@edu.salford.ac.uk

Abstract. This paper presents the development of a state observer for the estimation of output torque of an electromechanical actuator in the application of active wheelset control for railway vehicles. The output from the state estimator is essential to ensure that actuator responds appropriately and deliver accurate and fast control effort as demanded to maintain the stability of wheelsets. The formulation and design of the observer is based on the use of the actuator model only, so that it reduces substantially the complexity and difficult uncertainties related to the model of a full rail vehicle. The performance and robustness assessments of the state estimator integrated active control system are carried out with the use of a full bogie vehicle model.

Keywords: Active Wheelset Control, Actuator Dynamics, State Estimators, Torque Sensing

1 Introduction

Active control for railway wheelset can help to substantially reduce wear and tear of wheels and track surfaces by lowering creep forces [1]. In the design of such active control systems, in addition to the main wheelset controller, local controllers for the actuators are also used to ensure a fast and accurate delivery of the control effort demanded by the wheelset control system. However, the feedback of the output torque of the actuators applied at the wheelset can be very difficult to measure reliably in practice due to the harsh working conditions. This study presents the development of a model based approach to provide the estimation of the output torque. The proposed solution does not involve the vehicle dynamics which can be very complex - the design is based on the local actuator dynamics only and the simple measurements of the actuator current and velocity are used.

There are many previous studies conducted on the use of model based estimation techniques on railway vehicles with actively controlled suspension systems in order to estimate measurements which are difficult/impractical to obtain with readily available sensors. A research has focused on the use of a kalman filter to estimate the cant angle

of a track using measurements from accelerometers and gyros mounted on the railway vehicle and wheelset accordingly [2] in both random and deterministic tracks. Another similar study has shown the application of using estimation techniques to obtain lateral displacement and yaw angle of wheelsets along with track condition such as curvature and cant angle [3]. In addition, a research has been done on use of multiple kalman filters to estimate creep coefficients and a kalman-bucy filter for the estimation of creep forces and interpretation of estimates through post-processing has enabled the detection of lateral and yaw creep forces [4]. Similarly, estimation techniques have been used in a semi-active control system to estimate torque and damping values of a vehicle suspensions [5] where an unscented kalman filter is used in the study to estimate vehicle suspension states such as vertical velocity of stiffness components while its vertical acceleration and stroke velocity are provided as measurable states which assist in developing a sliding mode controller.

In this study, a full active wheelset control scheme involving a wheelset controller and an actuator controller for each wheelset is developed for a full bogie vehicle model with the addition of having a state observer to provide the torque feedback to the actuator controller. The observer is developed based on the simple actuator model only, and it does not involve the dynamics of the vehicle which would result in a much more complex solution. The observer is formulated in such a way to consist of two states (the motor speed and toque applied to the wheelset). The measurements of the motor current and speed measurement used for correcting estimation errors in the observer are much easier to obtain accurately and reliably compared to the measurement of the torque output at the wheelset.

Performance of the state observer is assessed using a full bogie vehicle model with a number of different track inputs including the curves and straight track with irregularities. The robustness of the observer is also evaluated to account for the uncertainties and inaccuracies of the actuator parameters used in the observer.

2 Active Control

As illustrated in Figure 1, a conventional railway bogie vehicle model with solid-axle wheelsets and with an active wheelset control scheme is used in the study. Only the yaw and lateral dynamic motions [6] of the wheelsets and those of the bogie/body frames are taken into account in this model since the other dynamics such as vertical, pitch and roll movements are largely dynamically decoupled from the plan view motions and therefore not expected to have any substantial effect in this case.

In order to assess the performance and evaluate the performances of the observer estimations and its impact on actuator dynamics/controller, a number of different track conditions are used in the study, including a curved track with a curve radius of 300m and a cant angle of 6 degrees at a relatively low speed of 25 m/s and a straight track with generically generated irregularities at the high speed 83m/s.

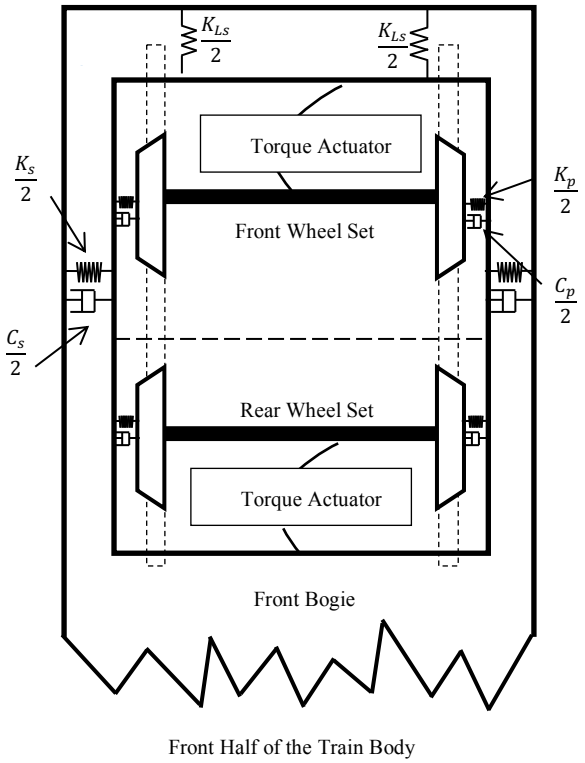

Fig. 1. Active Primary Suspension – Full Bogie Model

The actuation for each wheelset is provided by an electro-mechanical actuator. As depicted in Figure 2 below, a DC electrical motor and a gearbox is used as the actuator model in the investigation. Parameters of the actuator such as gear ratio (n), stiffness (K_g) and the damping (C_g) at the gear wheel-load connection is selected after a thorough comparison of the performance to obtain optimum results. Equations 1-4 represent the dynamics of the electrical motor and the mechanical coupling with the wheelset.

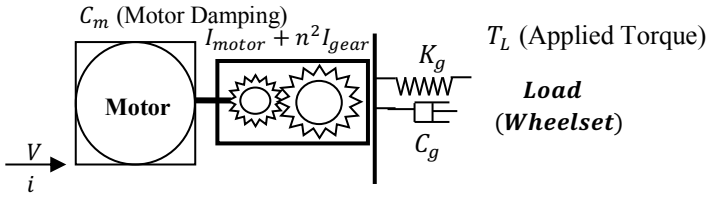

Fig. 2. The electro-mechanical actuator

$$\dot{i_a} = -\frac{r_{arm}}{l_{arm}} i_a - \frac{k_e}{l_{arm}} \dot{\theta_m} + \frac{1}{l_{arm}} v_a \quad (1)$$

$$\left(I_m + I_g n^2\right)\ddot{\theta_m} = k_t i_a - c_m \dot{\theta_m} - nT_L \quad (2)$$

$$\left(I_m + I_g n^2\right)\ddot{\theta_m} = k_t i_a - c_m \dot{\theta_m} - C_g n^2 \dot{\theta_m} - K_g n^2\, \theta_m + nK_g\, \psi_m + nC_g \dot{\psi_m} \quad (3)$$

$$Torque\ (T_L) = K_g n\, \theta_m + C_g n\, \dot{\theta_m} - K_g\, \psi_m - C_g \dot{\psi_m} \quad (4)$$

A number of different control strategies such as classical feedback controllers or model based optimal controllers have been previously proposed to provide stability control without interfering the natural curving of the solid axle wheelset [6-9], although there are also control schemes that are proposed to provide steering actions on curves to overcome the constraint on curving caused by passive suspensions [10]. In this study, the concept of absolute yaw stiffness method is applied to generate the torque required to stabilise the wheelsets as shown in Figure 3 while allowing the natural curving movements of the wheelsets [9].

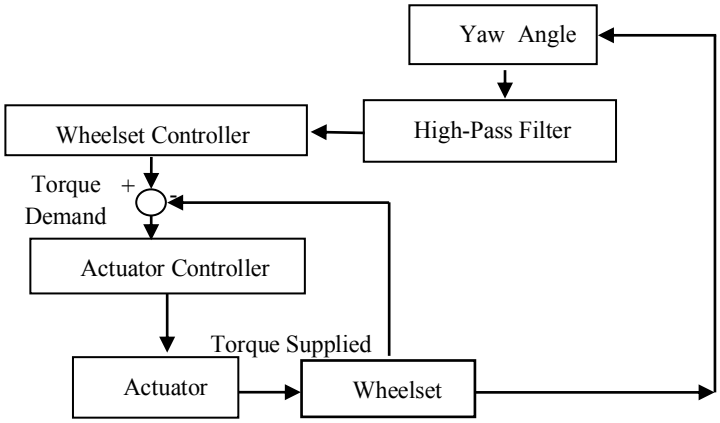

Fig. 3. Wheelset Controller and Actuator Controller

Two feedback control loops for each wheelset are used - the wheelset controller generates a torque demand for stabilising the wheelset whereas the local actuator controller ensures the motor to apply the required toque to the wheelset. Because the wheelset stability control is of high bandwidth in nature, the actuator controller is considered essential for the delivering of control efforts with fast and accurate responses.

3 State Observers

The actuator controller requires the feedback of the actuator output torque applied at the wheelset which is very difficult to measure reliably due to the harsh operating environments of wheelsets. This study develops a model-based approach to estimate the required feedback from sensors that are much more reliable and easier to install. The proposed approach for the design is based on the dynamic relationship between the actuator and the torque applied to the wheelsets using the readily available measurements such motor current, and motor speed. This is a much simplified approach compared with the full state estimation that would also need to include the vehicle dynamics that can be potential very complex.

The simplified observer is formulated to have only two states - the rotor speed of the electric motor $(\dot{\theta}_m)$ and the torque applied at the wheelset (T_L). The output measurement is the rotor speed and there is an additional input of the motor current that is also easily obtainable. The formulation and design process are shown in equations 5-9, where x is defined to be the two states and y is defined to be the system output while matrices A, B, C, D, G and H represent the dynamics of the system. Furthermore, w is considered as the process noise associated with the system, where w is represented as $\dot{T}_L$, while v is representing the noise associated with measurements. L is represents the observer gains which are designed using the pole placement technique and β is a parameter which is added to state space to maintain the full rank of the A matrix such that the system is observable. $(I_m - motor\ rotor\ inertia, I_m - gear\ wheel\ inertia, n - gear\ ratio, k_t - motor\ torque\ constant)$

$$\dot{x} = \begin{bmatrix} \frac{-c_m}{I_m + I_g n^2} & \frac{-n}{I_m + I_g n^2} \\ 0 & \beta \end{bmatrix} \begin{bmatrix} \dot{\theta}_m \\ T_A \end{bmatrix} + \begin{bmatrix} \frac{k_t}{I_m + I_g n^2} \\ 0 \end{bmatrix} [i_a] + \begin{bmatrix} 0 \\ 1 \end{bmatrix} [\dot{T}_L] \tag{5}$$

$$\dot{\hat{x}} = A\hat{\mathrm{x}} + Bu + Gw + L(y_t - \hat{y}_t) \tag{6}$$

$$\hat{y}_t = C\hat{\mathrm{x}} \tag{7}$$

$$C = [1\ \ 0] \tag{8}$$

$$L = \begin{bmatrix} 207.34 \\ -8.92 \end{bmatrix} \tag{9}$$

4 Performance Analysis

4.1 Estimation Assessment

An analysis is performed to compare the actual output torque and the estimated output toque of the actuator to assess the accuracy of the estimations using full bogie vehicles when simulated using both deterministic, random tracks and measured tracks. However, only the behaviour of the first wheelset of the vehicle model is shown since other wheelsets show very similar behaviour.

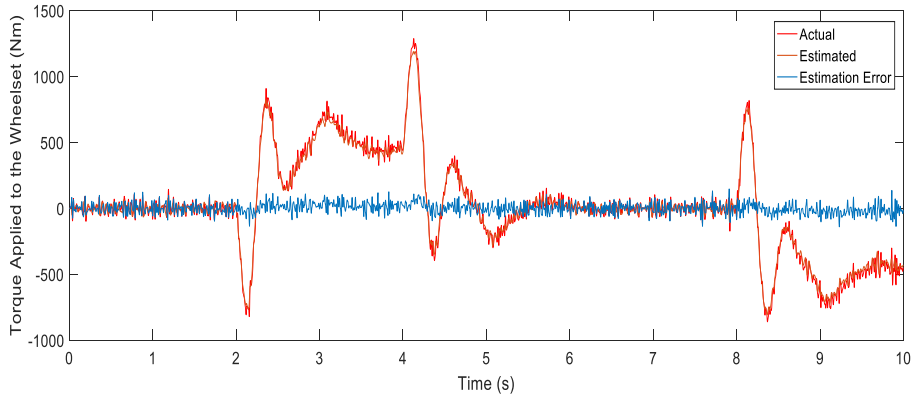

Fig. 4. Estimation Analysis for Deterministic Track – Full Bogie Vehicle

Fig. 4 shows that there are minor errors between the actual and estimated torques when full bogie vehicle is assessed. This can be clearly seen during the areas where the torque is zero and slight difference can be expected due to the process noise and noise associated with the measurement signals.

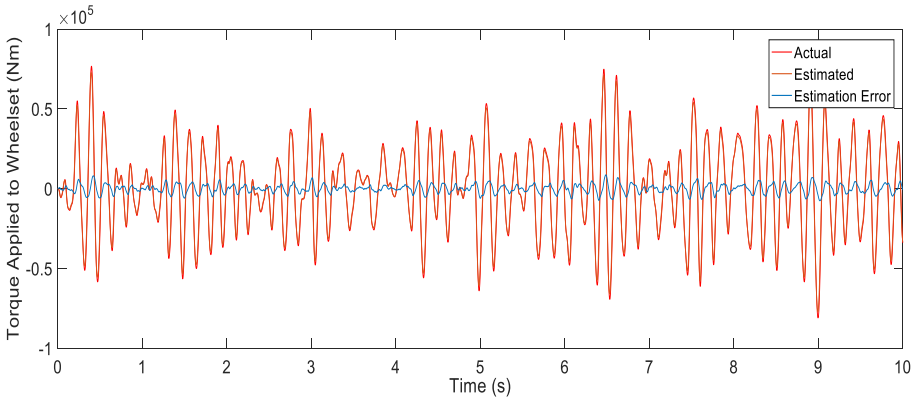

Fig. 5. Estimation Analysis for Generic Random Track – Full Bogie Vehicle

Similar analysis is done with the random track to evaluate the observer performances and there is an approximately 10% of error between the actual and estimated torques, as it can be seen in Fig 5.

4.2 Robustness Assessment

In order to assess the robustness of the observer, key parameters which are difficult to measure and define in a practical environment are varied while observing the performance of the observer. Thus, internal damping of the motor (c_m), motor constant (k_t) and the various inertias, such as gear wheel inertia (I_g) and motor rotor inertia (I_m), is being varied within a reasonable margin (±20%) to evaluate the observer performances. For this analysis, generic random track is being used while the travel speed is 83 ms^{-1}. It is evident from Fig. 6 that the internal damping of the motor does not affect the performance of the observer within a reasonable margin.

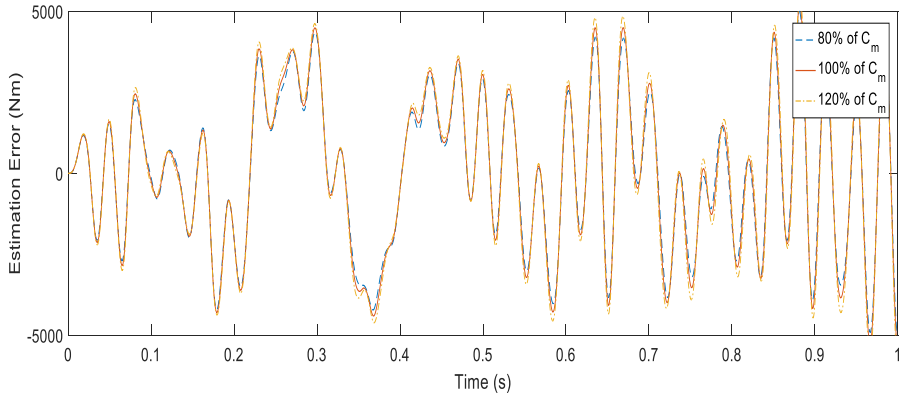

Fig. 6. Estimation Error vs. Robustness Assessment – Motor Damping

Similarly, the gear wheel inertia is varied by $\pm 20\%$ of the value, for which it is found that observer performance is not affected by this variation as it can be seen in Fig. 7. However, as it can be seen from Fig 8, the motor rotor inertia variation does have an effect though it does not result in any detrimental performance within the operational range.

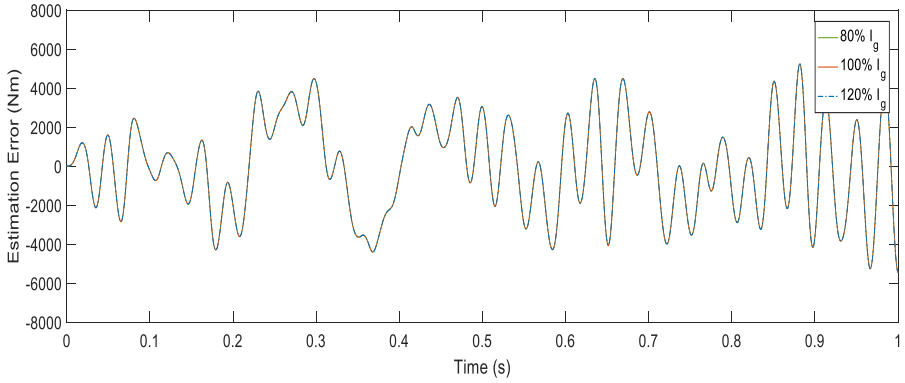

Fig. 7. Estimation Error vs. Robustness Assessment – Gear Wheel Inertia

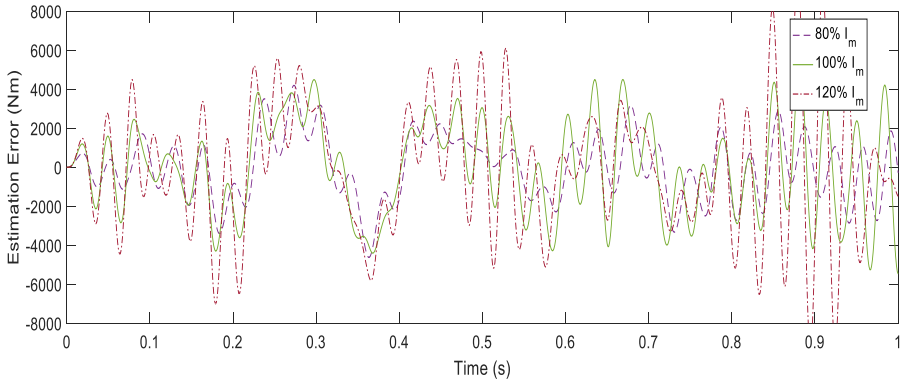

Fig. 8. Estimation Error vs. Robustness Assessment – Motor Rotor Inertia

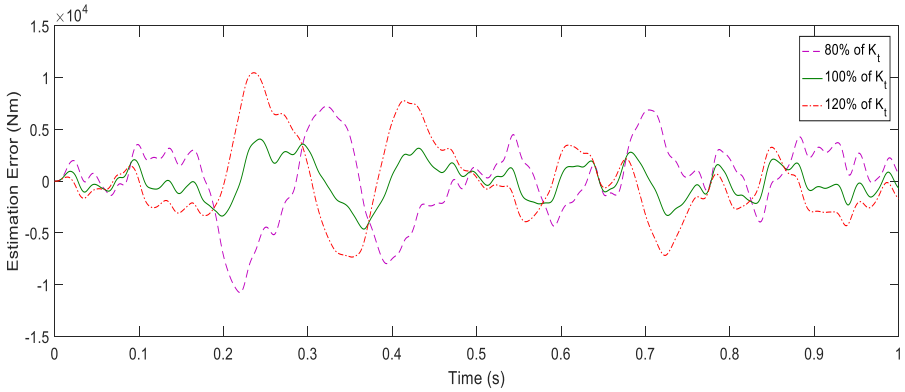

Fig. 9. Estimation Error vs. Robustness Assessment – Motor Constant - 1

It is evident from the Fig. 9 that changing of motor constant does pose some affect to the observer performance as the error is increasing significantly (error > 100%) as the effective value is 20% less than the original value. However, when the effective value is 20% higher, estimation error appears to rise approximately 70%. Thus, observer gains require to be tuned accordingly on the cases where observer performances are compromised due to motor constant variation.

Further analysis is done to assess the observer robustness while reducing the defined value of motor constant by 10% and it can be seen from Fig. 10 that the observer maintains its robustness. It is evident form the results that the there is only a minor error increase as the effective value is being reduced by 10%. Thus, it is evident that observer is robust motor constant values where it deviates -10% to + 20% from original/defined value.

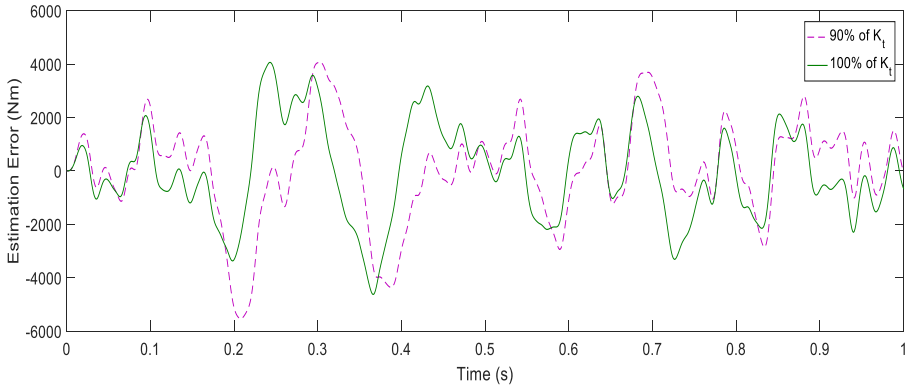

Fig. 10. Estimation Error vs. Robustness Assessment – Motor Constant - 2

These robustness assessments provides valuable insight in to the state observer performances, since, in a realistic environment, it is highly plausible that actuator parameters to be slightly different from the values used to design the sate observer. This could lead to inaccurate estimations and subsequent instability of the system. However, results of the tests are conducted indicate that the observer is capable of producing accurate estimations within a reasonable range of parameter variations since parameter variation can be expected to some extent in a realistic situation.

5 Discussions

As it is evident from all the results presented above, it can be concluded that the state observers can serve a significant role in this application since its capability to generate accurate estimations enables the overall system to be more practical and realistic. Analysis of the performance of the model also indicates that there is a high potential of using state estimators in active control of wheelsets with full bogie vehicle while it performed

well in both deterministic track and measured and generic (computer generated) and measured random tracks as well. Further reviewing elaborates that estimator has adequate frequency response for a similar type other applications which deal with DC motors.

Finally, the robustness analysis re-assures the functional capabilities of the estimator under different parameter conditions and provides insight into the effect of each individual parameter.

References

1. Mei, T.X. and Goodall, R.M., "Recent Development in Active Steering of Railway Vehicles", Vehicle System Dynamics Vol 39/6, (2003).
2. T.X. Mei, H. Li and R.M. Goodall, Kalman filters applied to actively controlled railway vehicle suspensions, Transactions of the Institute of Measurement and Control 23,3 pp. 163–181, (2001).
3. T.X. Mei, R.M. Goodall, H. Li, Kalman Filter for The State Estimation of A 2-Axle Railway Vehicle, European Control Conference (ECC) Germany, (1999)
4. C.P. Ward, R.M. Goodall, R. Dixon and G.A. Charles, Adhesion estimation at the wheel-rail interface using advanced model based filtering, (2012).
5. Hongbin Ren, Sizhong Chen, Yuzhuang Zhao, Gang Liu & Lin Yang State observer-based sliding mode control for semi-active hydro-pneumatic suspension, Vehicle System Dynamics, 54:2, 168-190, (2016).
6. Stefano Bruni, Roger Goodall, T. X. Mei and Hitoshi Tsunashima, Control and monitoring for railway vehicle dynamics - Vehicle System Dynamics International Journal of Vehicle Mechanics and Mobility, (2007).
7. Pearson, J.T., Goodall, R.M., Mei, T.X. and Himmelstein, G, Active stability control strategies for a high speed bogie. Control Engineering Practice, 12, 1381–1391 (2004).
8. T.X. Mei And R.M. Goodall, Modal Controllers for Active Steering of Railway Vehicles with Solid Axle Wheelsets, (2000).
9. T. X. Mei and R. M. Goodall, Stability control of railway bogies using absolute stiffness – skyhook spring approach, (2006).
10. Shen, G. and Goodall, R.M., Active yaw relaxation for improved bogie performance. Vehicle System Dynamics, 28, 273 – 289, (1997)